A STUDY OF THE APPLICATION OF LOW FREQUENCY OSCILLATIONS TO MULTI-TOOL DRAWING PROCESSES

by

G. R. Dawson, B.Sc.

Submitted in fulfilment of the requirements for the degree of Doctor of Philosophy, University of Aston in Birmingham,

September 1972.

Faculty of Engineering,
Department of Mechanical Engineering

Supervisor:
Dr. D.H. Sansome

Synopsis

Within the last decade a number of researchers have investigated the effects of applying vibrations to the tooling when forming metals. Results of these investigations indicate that vibrations may modify the state of stress in the body of the deforming metal and/or change the fricional boundary conditions between the tools and the workpiece.

The first part of this thesis describes and discusses the research so far conducted in this field of metalworking, and attempts to isolate the areas of possible benefit to industrial practice. The remainder of this thesis describes the progress, and presents and discusses the results of a two-part investigation into the application of low frequency axial vibrations (0 to 100 Hz) to the tandem wire and fixed plug tube drawing processes.

The investigation was conducted on a 2000 lbf horizontal bull block, the tools being oscillated by two electro-hydraulic vibrators. Mild steel wire and medium carbon steel tube were selected for the workpieces, and sodium stearate as the lubricant.

Results show that when wire is drawn through two dies in tandem which are oscillated axially and in anti-phase; or when tube is drawn through the annular gap between a die and a fixed plug which are oscillated axially in antiphase:

(a) The workpiece moves relative to the tools for a short period on every cycle.

(b) During the remainder of the cycle the drawn product is elastically off-loaded and loaded by the motion of the tooling.

(c) The workpiece moves alternately over each tool.

(d) The peak load in the drawn product is reduced by oscillations, since the product never experiences the force necessary for movement relative to both tools simultaneously.

(e) There is no indication of a reduction in yield stress or frictional coefficient produced by the application of oscillations.

(f) The reduction in peak drawing force is most marked for high frequencies and amplitudes, and low drawing speeds.

A theoretical analysis was conducted for single die oscillatory wire drawing to establish the basic mechanics of the process. This analysis was extended to cover the tandem wire drawing process which produced predictions of the upper and lower limits of the peak drawing force reductions. Experimental data was found to fall within these predicted limits.

The results of the investigation are discussed and suggestions for further work are presented.

Contents

Page No.

Synopsis
Contents
Nomenclature
Introduction 1

Part A: The Review 7

Section A1: The general review
A11: Fundamental aspects
(a) Effects on mechanical properties of metals
(b) Effects on interfacial friction
A12: Applications in metalworking processes
(a) The compressive deformation of metals
(b) Drawing of wire and bar
(c) Drawing of tube
(d) Extrusion
(e) Sheet metal working

Section A2: Review of published theories 36
A21: Volume effects
A22: Surface effects

Section A3: Discussion of published literature 51
A31: The volume and surface effects
A32: The volume and surface effects in metal working processes

Part B: Oscillatory wire drawing

Section B1: Introduction 61
Section B2: Equipment 64
B21: Drawing machine
B22: Vibrators
B23: Drawing dies
B24: Material
B25: Lubricant
B26: Die holders

Section B3: Instrumentation 68
B31: Loadcell design and construction
B32: Torquecell design and construction
B33: Loadcell on wire
B34: D.C. amplifiers
B35: Die and drum amplitude measurement
B36: Recording equipment
B37: Measurement of drawing speed

Section B4: Calibration of instrumentation 75
B41: Static calibration of loadcells
B42: Static calibration of torquecell
B43: Dynamic calibration of loadcells
B44: Calibration of vibration measuring equipment
B45: Measurement of effective mass of die assembly
B46: Moment of inertia of bull block drum

Section B5: Experimental procedure 80
B51: Non-oscillatory drawing tests
B52: Oscillatory drawing tests
B53: Analysis of loadcell and torquecell signals

Section B6: Results 89

Section B7: Investigation into the mechanics of Oscillatory drawing 91
Introduction
B71: Single die drawing with oscillations
(a) Simple theoretical considerations
(b) Derivation of the effective stiffness of the drawn wire
(c) Development of the analogue programme
(d) The experimental investigation
(e) The analogue investigation
B72: Tandem drawing with oscillations
(a) A discussion on the increase of the maximum load in the drawn wire
(b) Modification to the stiffness of the drawn wire
(c) Theoretical analysis of oscillatory tandem drawing

Section B8: Discussion of results 119
B81: Results of main tests
B82: Analogue investigation
B83: Tandem drawing analysis

Section B9: Appendices 138
B91: The drawing machine
B92: The vibrators
B93: Instrumentation
B94: Measurement of drawing speed
B95: Loadcell and torquecell calibration curves
B96: Derivation of the back tension drawing equation
B97: Measurement of the natural frequency of the drum
B98: Measurement of the damping coefficient of the drum
B99: Measurement of the constancy of drum rotational speed
B910: Measurement of the coefficient of friction between wire and drum
B911: Calculations for the tandem drawing theory
B912: Tensile test results for the wire
B913: Material compositions

Part C: Oscillatory tube drawing

Section C1: Introduction 155
Section C2: Equipment 158
C21: Drawing die
C22: Plug
C23: Plug bar and mount
C24: Material
C25: Lubricant
C26: Die holder and flange

Section C3: Instrumentation 162
C31: Die loadcell design and construction
C32: Plug bar loadcell design and construction
C33: Loadcell on tube
C34: Other instrumentation

Section C4: Calibration of instrumentation 166
C41: Static calibration of die loadcell
C42: Static calibration of plug bar loadcell
C43: Dynamic calibration of loadcells

Section C5: Experimental procedure 168

Section C6: Results 171

Section C7: Discussion of results 173

Section C8: Appendices 179
C81: Tensile test results for tube
C82: Loadcell calibration curves
C83: Determination of the back-pull factor for tube drawing
C84: Theoretical study
C85: Material compositions and properties

Part D 197
Section D1: Conclusions
Section D2: Suggestions for further work

Acknowledgements

References

NOMENCLATURE

A	cross sectional area
B	friction factor
C	back pull factor (relating die loads)
c	damping factor
D	diameter
E	Young's Modulus
F	Force in drawn product
ΔF	peak to peak force variation
$\tilde{F}$	cyclic component of force
f	force in coiled wire
h	thickness
I	moment of inertia
j	$\sqrt{-1}$
K	back pull factor (relating drawing loads)
L	die load
L_d	load in drawn product with minimum back tension
L_{nd}	load in drawn product with maximum back tension
ℓ	length
m	mass
N	normal force/unit length on coiled wire
n	amplitude ratio
p	normal pressure
R	radius of bull block
r	area ratio
S	stiffness of wire
s	torsional stiffness
T	torque amplitude
t	time
U	relative extension of coiled wire
U_{tot}	relative extension of free and coiled wire
V	mean drawing speed
X	displacement amplitude
x	instantaneous displacement, or linear co-ordinate
y	yield stress in uniaxial tension

$\alpha, \beta, \theta, \phi$	angular co-ordinates
ω	angular frequency
ω_n	natural frequency
θ	angular displacement
δ	relative extension
μ	coefficient of friction
α	$\frac{\mu L}{R}$
ϵ	strain
ξ	damping coefficient
τ	computer time, or shear stress
β	conputer time scale factor
ψ	coupling coefficient
σ	axial stress
ϕ	velocity ratio

Introduction

The application of oscillatory energy to the plastic deformation of metals has been widely investigated and several reviews have been published[1-4]. Claims have been made that oscillations reduce process stresses, and improve the metallurgical properties and surface conditions of the finished work piece.

Research has been concerned not only with the fundamental effects of oscillations on metal plasticity and surface friction, but also with applications to many industrial metal-forming processes. This has revealed the now generally accepted dual role of oscillations. The 'volume effect' deals with the influence of oscillations on the internal stresses during plastic flow of a metal, the 'surface effect' with interfacial friction.

The volume effect was first observed by Blaha and Langenecker[5] when testing zinc mono-crystals under tension with ultrasonic oscillations induced in the specimen. This resulted in an apparent reduction in the flow stress of up to 40%. Subsequent investigators have shown that in both tensile tests and metal deformation processes, this reduction in stress can be attributed to the superposition of mean and cyclic stress components, since the cyclic stress amplitude, where measured, was found to be equal to the apparent reduction in applied stress. Thus the peak force in the metal was unaltered. This has become known as the superposition mechanism, and has been found to apply to both ultrasonic and sonic oscillation frequencies. This behaviour offers no real benefit, since the metal deforms under its conventional stress, but does so intermittently.

The reduction of sliding friction forces by oscillations has been observed in fundamental investigations at both sonic and ultrasonic frequencies. These investigations consisted of a slider moving over the plane with oscillations applied in various directions to one of the members of the friction pair. In the majority of these cases, the mean friction force was said to be reduced by either a periodic separation of the surfaces, or a periodic variation in the direction of the friction force vector.

Similarly, oscillations have been said to reduce friction forces in metalworking processes. However, in many of these instances where a reduction in deformation load was attributed to a surface effect, insufficient experimental data was taken to justify such claims. Furthermore, the cyclic component of the applied stress was not measured, so that the syperposition mechanism cannot be discarded as a possible explanation for the observed effects.

There are situations, however, which indicate a real friction effect when oscillations are applied. When tube is drawn over an ultrasonically oscillated plug several beneficial effects have been observed:

(1) tubes may be drawn on a fixed plug which conventionally require a moving mandrel.

(2) drawing forces are reduced.

(3) diameter to thickness ratios of 500:1 can be drawn successfully with ultrasonic action, compared with a 50:1 limit for static loading.

(4) greater reductions in area are possible.

(5) the finish of the bore is brighter with the degree of roughness diminished.

(6) stick-slip, chatter and lubricant breakdown are virtually eliminated.

(7) more complicated sections may be drawn.

This process is now exploited commercially in the U.S.A. by Aeroprojects Inc., for which the above claims are made. Parallel work in the U.S.S.R. and at Aston in the U.K. point to similar effects. These benefits are claimed to be the result of a reduction in friction forces, and it has been proposed by Aston and Soviet researchers that this is produced partly by the periodic reversal of the plug friction vector.

At present, the majority of investigations have been concerned with the effects of ultrasonic oscillations. The purpose of this investigation is to study the effects of low frequency (0-100Hz) oscillations on drawing processes. The investigation is in two parts. The first is a study of the wire drawing process, in which wire is drawn through two dies which are oscillated axially. This is an investigation into the volume effect, studying the interaction of two applied low frequency oscillatory stresses to a deformation process. The second part is a study of the tube drawing process with axial oscillations applied to the die and plug. This is an investigation into the surface effect, again studying the interaction of two applied low frequency oscillatory stresses to the deformation.

The main variables studied in each investigation were:

(a) frequency of oscillation.

(b) amplitude of oscillation.

(c) phase relationship between oscillations.

(d) drawing speed.

This thesis describes and discusses the historical development of the technology of applying oscillations to metalworking processes, and details the research undertaken to investigate the interaction of two applied low frequency oscillatory stresses in the drawing processes.

PART A: THE REVIEW

A1: GENERAL REVIEW

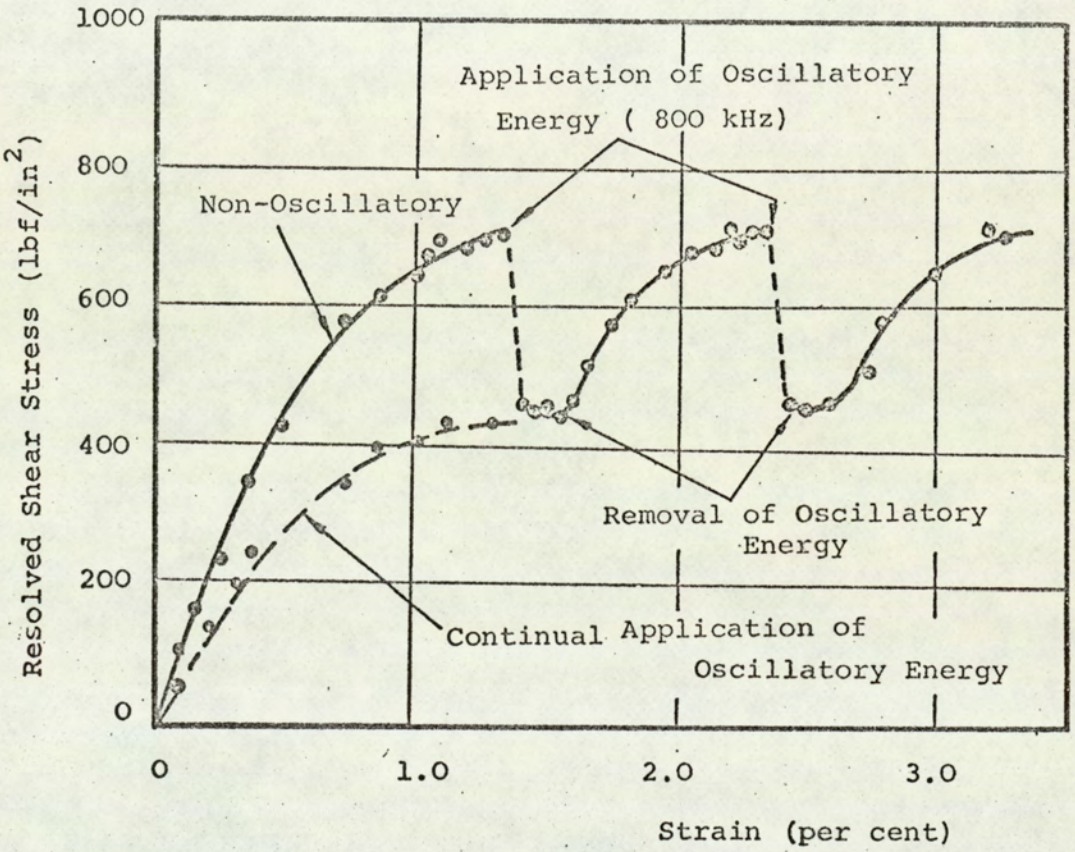

Fig No.1 Shear Stress-Strain Curve for a Single Crystal of Zinc

(Blaha and Langenecker 1955)

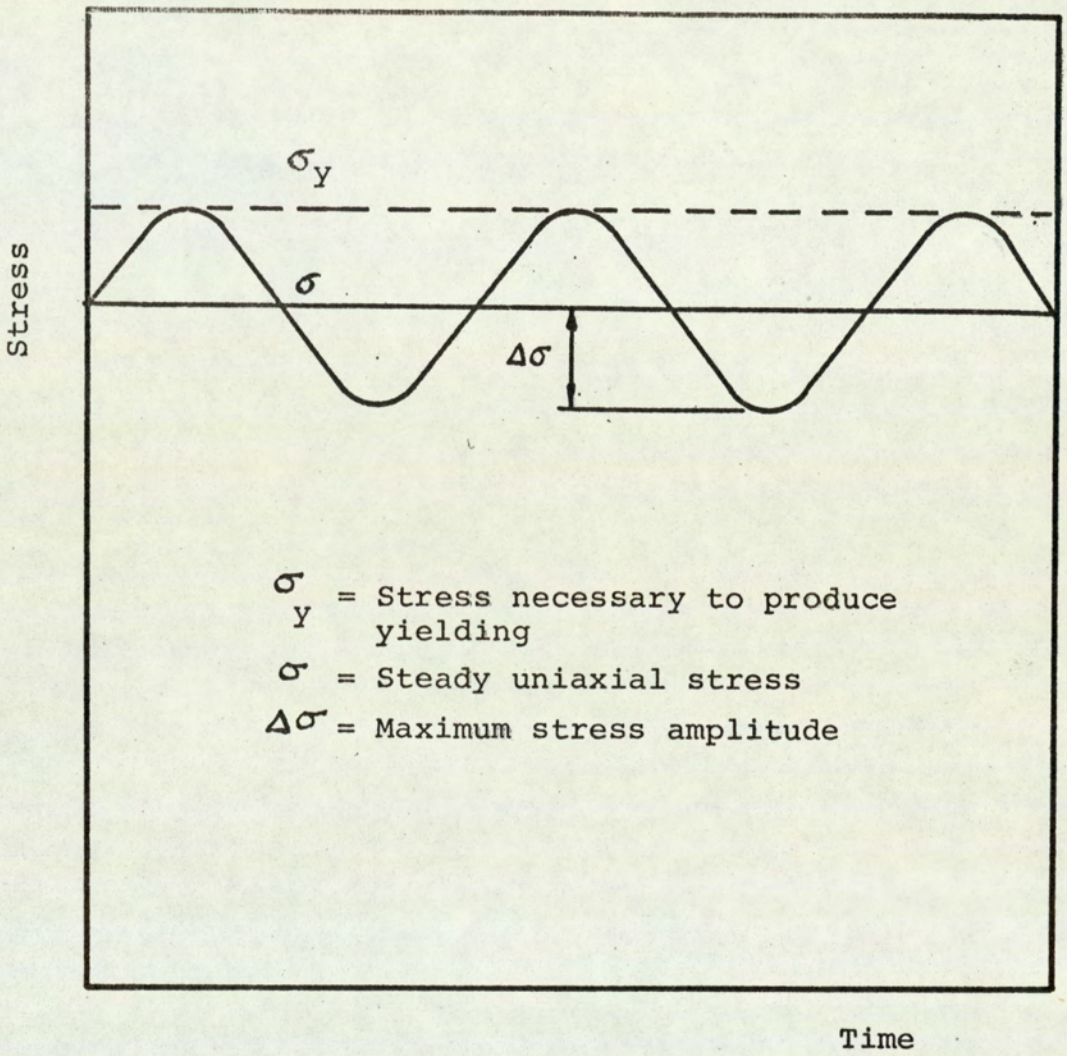

Fig No.2 Superposition of Steady and Alternating Stresses to Cause Yielding

(Nevill and Brotzen 1957)

A11: Fundamental Aspects

A11(a) Effects on the mechanical properties of metals

The first investigations into such effects were conducted some fifteen years ago by Blaha and Langenecker[5,6,7]. Monocrystals of aluminium, zinc, and cadmium were strained in tension whilst immersed in ultrasonically irradiated carbon tetrachloride. An ultrasonic energy density of $1 W/cm^2$ at 800 kHz was observed to apparently reduce the flow stress by 40%. Subsequent removal of the ultrasound caused the stress to return to its appropriate non-oscillatory value (fig. 1).

The irradiation was associated with an increase in the strain to fracture, and ultimate tensile stress, and a decrease in the rate of work hardening. Similar results were obtained in the frequency ranges $15\text{-}10^4$ Hz, and 0.8-1.0MHz. Since it appeared to them that ultrasonic energy was more effective in reducing stresses than thermal energy, they postulated that the ultrasound was absorbed perferentially at the dislocation sites where plastic flow was initiated. Similar results were obtained by Oelschlagel[8] for energy densities up to 29 W/cm^2.

Nevill and Brotzen[9] investigated the effect of ultrasonic standing waves on the yield strength of low-carbon steel and found the reduction in strength to be directly proportional to oscillation amplitude, and independent of prior strain and frequency in the range 15-80 kHz. By measuring the alternating stress level they were able to conclude that the maximum value of the superposition of mean and alternating stresses was equal to the static yield stress (fig. 2). Thus the metal was yielding at the conventional value of stress, but doing so intermittently once every cycle.

Subsequent investigations by Langenecker[10,11,12]

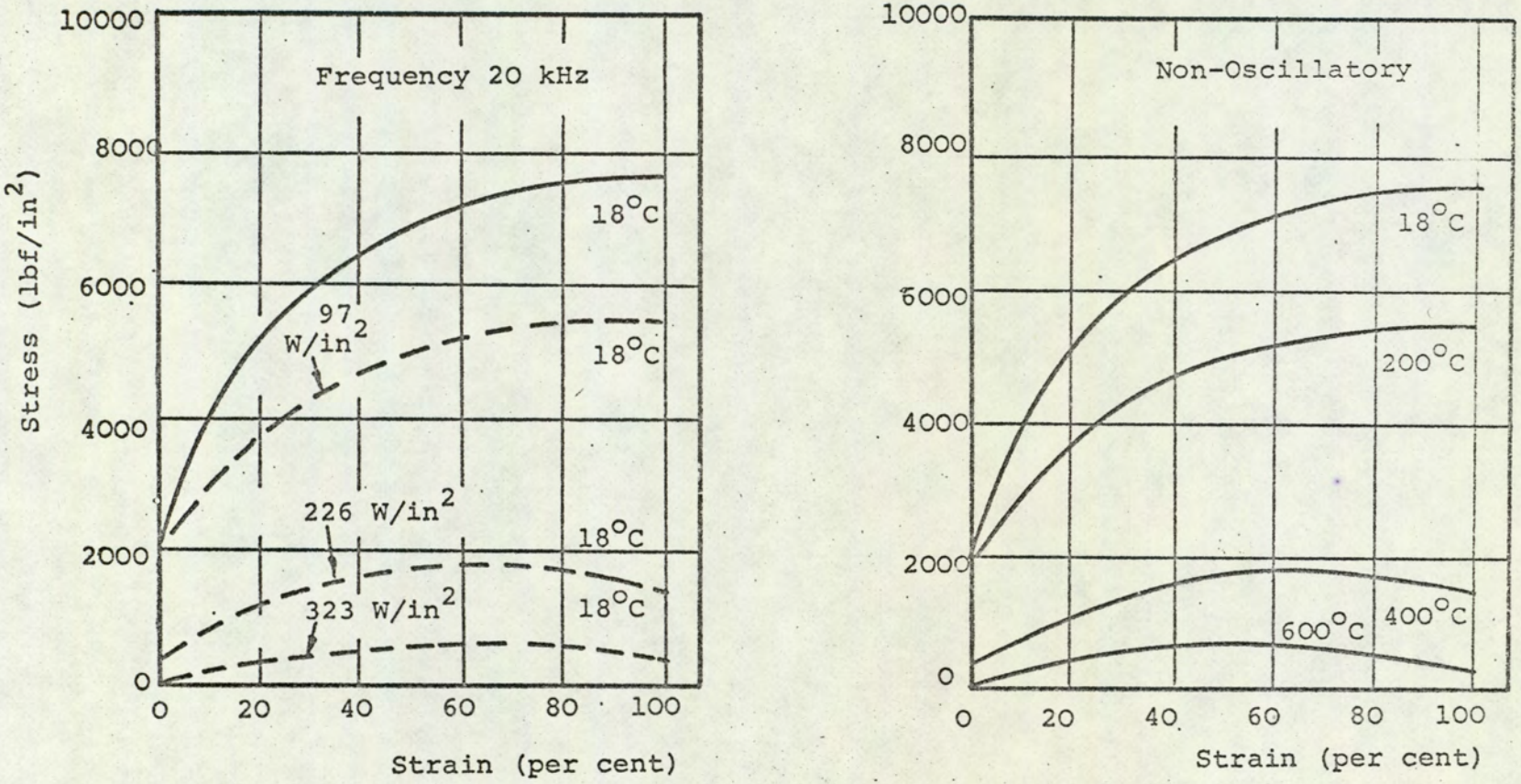

Fig No.3 Stress-Strain Curves for Aluminium Single Crystals Showing a Similarity Between the Effects Due to Oscillatory Energy and Temperature

(Langenecker 1959)

studied the effect of high-energy ultrasonic travelling waves on the tensile behaviour of metals, and similar results to his previous work were observed. Reductions in flow stress were greatest for the high-energy levels, and could even result in a zero stress. The shapes of the irradiated stress-strain curves were seen to correspond to those obtained at elevated temperatures (fig. 3).

Calculation of the acoustic stress levels revealed that, for the low-energy densities, the reduction in strength was attributable to superposition, thus agreeing with Nevill and Brotzen. However, for greater energy densities the stress reduction was much greater than that predicted by superposition. It was therefore proposed that the energy was absorbed preferentially at the dislocation sites, raising their temperature, and thus easing plastic flow.

During the investigations described above, research in the U.S.S.R. followed a similar line. Early work by Severdenko and Klubovich[13] showed that the effect of ultrasonic irradiation depended upon the length of test-piece, and therefore subsequent investigations employed standing waves to overcome this difficulty. A variety of metals and alloys were tested in tension[13-18] and torsion[15] with superimposed ultrasonic standing waves, and all exhibited a reduction in flow stress proportional to the amplitude of the applied oscillation. However, there was also a reduction in the ultimate tensile strength, elongation, and reduction of area i.e. these results conflicted with Langenecker's early findings.

Konovalov[16] observed the effects of ultrasound to be attenuated at the higher strain rates. Severdenko and Klubovich[13,17] in agreement with Langenecker, observed the

rate of work hardening to be reduced. They concluded that ultrasonic working was analogous to a rise in temperature. An extension of this hypothesis was provided by Skripnichenko,[18] who proposed that at low amplitudes stress superposition accounted for the apparent softening, whereas heating had a significant effect at the higher amplitudes.

Further work in the U.S.A. conducted by Baker and Carpenter[19] employed standing waves for the tensile testing of materials at power levels comparable with those used by Langenecker. They found that the flow stress reductions so obtained, were never in excess of the acoustic stress amplitude, thus conflicting with Langenecker's findings. They suggested that resonant bulld-up of stress and subsequent overheating could be the cause of the large-scale softening reported by Langenecker. However, neither investigation measured the acoustic stress in the test-piece directly, so either could be in error in their estimations.

A more direct measurement of stress variation was obtained by Pohlman and Lehfeldt[20] while tensile testing copper with superimposed ultrasonic standing waves. They found that the relatively small scale reduction in flow stress could be explained by the superposition mechanism, i.e. it was equal to the alternating stress amplitude. Friedrich, Kaiser and Peckhold[21] observed similar results but showed that the effectively increased strain rate caused the fall in the mean stress to be slightly less than the acoustic stress level.

In a later publication,[22] Langenecker stated that a resonant build-up of stress may occur when travelling waves are employed. He concluded that for low-energy densities the

superposition mechanism was sufficient to explain the stress reduction, but beyond a critical energy level, overheating occurs causing a further reduction in strength[23].

All(b) Effects on interfacial friction.

Most of the fundamental research concerned with this aspect of vibrations is related to friction under relatively low normal pressures. Although this is not representative of metalworking conditions, it is thought by the author that a qualitative assessment of the effectiveness of oscillations may be obtained from such research.

Several researchers have shown that when oscillations are applied to a plane, the interfacial friction between the plane and a slider is apparently reduced considerably. Fridman and Levesque[24] showed that when ultrasonic energy was applied at right-angles to an inclined plane, the coefficient of static friction was reduced proportionately, and in extreme cases to zero. They attributed this effect to the shearing of the welded junctions brought about by the induced motion of the particles in the plane.

Similar conclusions were reached by Pohlman and Lehfeldt[20] to explain observed reductions in sliding friction brought about by ultrasonic action. They applied oscillations to the slider both normal and tangential to the plane of motion, and in the latter case normal and parallel to the sliding direction. In all cases an apparent reduction in friction forces was observed, the most effective configuration being motion parallel to the direction of sliding. The reduction in friction was found to be less marked at the higher sliding velocities.

Low-frequency normal oscillations of a plane at 20, 100

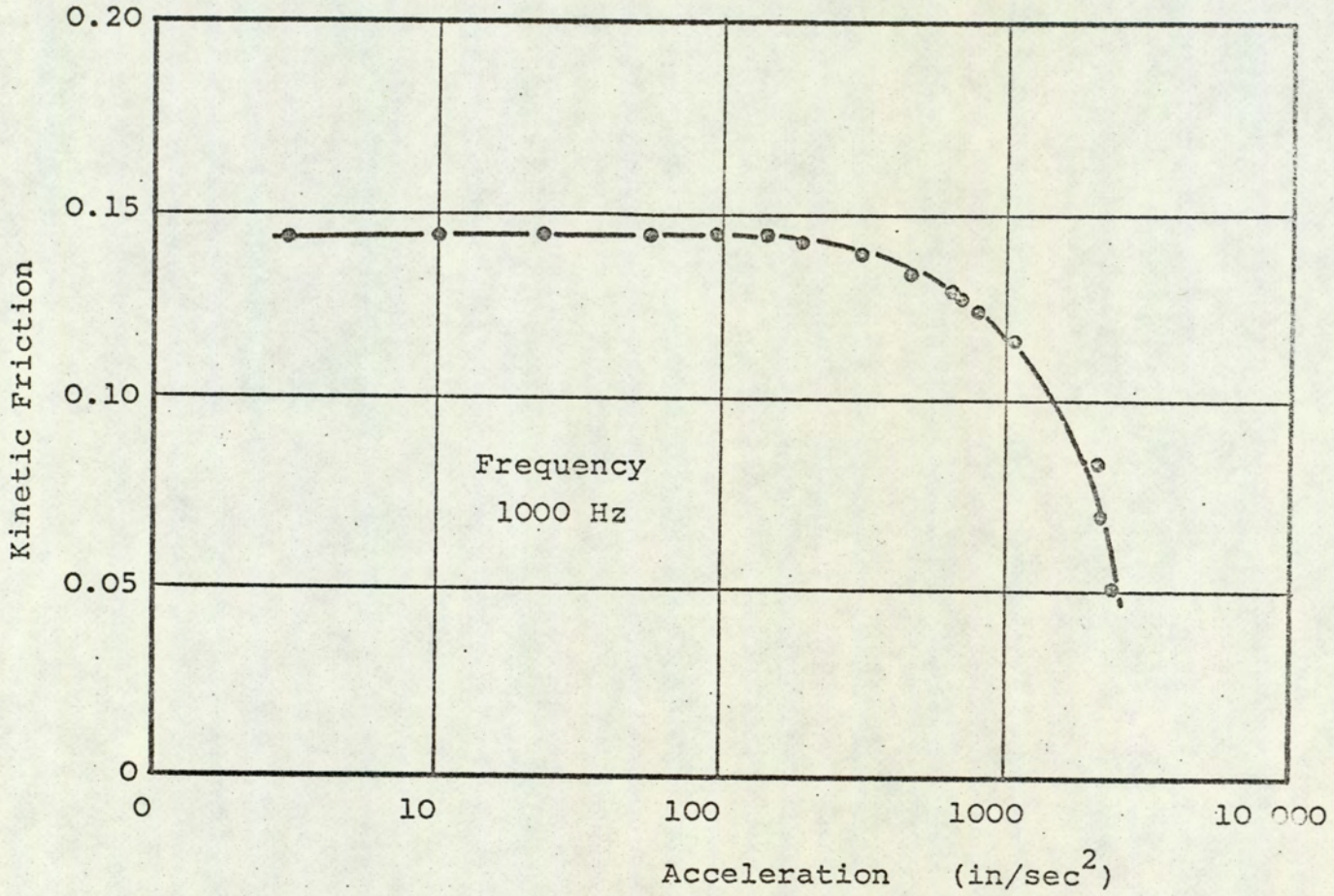

Fig No.4 Effect of Vibration on Coefficient of Kinetic Friction; Lubricated Steel Sliding on Steel

(Godfrey 1967)

and 1000 Hz have been observed to reduce sliding friction by Godfrey[25]. In this case friction was only seen to be reduced when separation of the mating surfaces occurred, i.e. there was a reduction in the period during which the friction forces acted (fig. 4). Balamuth[26] has suggested that separation is a mechanism for friction reduced at ultrasonic frequencies. Friction has been observed to be reduced under these conditions by Tolstoi[27]. He further noted that there was a resonant peak for friction reduction at 2 kHz and this he attributed to the natural frequency of the slider mass on the spring-like asperities in the contact zone.

Oscillations in the sliding direction have been observed to reduce static and sliding friction by Lenkiewicz[28]. At frequencies of 20-120 Hz reductions in friction of up to 80% were observed, the effect being most marked at high amplitudes and frequencies, and low sliding speeds. The phenomenon stick-slip was found to be eliminated by oscillations.

Similar observations were made by Mikhenl'man and Mashchinov[95]. They observed that when ultrasonic oscillations were applied to a steel plane in the sliding direction, the coefficient of sliding friction between the plane and a steel slider was reduced from 0.296 to 0.074.

A theoretical analysis of these effects was provided by Mitskevich[29] who showed that the friction force was periodically reversed, due to the periodic motion of one body relative to the other. Thus, if the magnitude of friction force remained unchanged, its mean value in the direction of sliding would be reduced. The analysis showed this reduction to be an increasing function of the ratio of oscillatory velocity to sliding velocity only, thus agreeing qualitatively

with the experimental work of Lenkiewicz, and Pohlman and Lehfeldt.

The situation where transverse oscillations are applied to the plane has been investigated theoretically and experimentally by Schneider[31]. The theoretical analysis assumed the friction force magnitude to be unaffected by oscillations, but that due to the relative motion, the line of action of the force swings periodically about the sliding direction. This results in a reduction in the mean friction force in the direction of motion. This reduction is shown to be solely a function of the ratio of oscillatory velocity to sliding velocity (cf. Mitskevich). The experimental work verified this analysis in the frequency range 15-53 Hz.

A12: Applications in metalworking processes

A12(a) The compressive deformation of metals.

The first investigation into this aspect of the oscillatory working of metal was conducted by Stankovic[34]. He forged lead test-pieces in closed dies with static, impulsive, and a combination of static and impulsive loading. For a frequency of 5.3 Hz the mode of operation which gave the optimum axial and transverse flow of metal was during the combined loading. It was suggested that this enhanced flow resulted from a reduction in friction forces.

Subsequently a considerable number of investigations have been carried out in the U.S.S.R. with low-frequency axial oscillation applied to the forging tools. The intial series of experiments was conducted on a hydraulic press, with the oscillatory force provided by rotating eccentric masses mounted on the upper platen[35-42]. The frequency range of force oscillations was 7-40 Hz, with displacement amplitudes up to 25 mm. Various materials were forged, hot and cold, with and without lubrication, in both open and closed dies.

The general observations were that the average pressures, hardness, degree of barrelling, and residual stresses were reduced, greater reductions were possible for the same static load, and the hardness, strain and residual stress distributions were more uniform. Reductions in the average pressures of 50% and increases in the degree of deformation of 50% were observed, the greatest benefits obtained when separation between the tool and work-piece occurred.

Investigations on a similar machine at frequencies up to 100 Hz were conducted by Polyakov et al.[43,44]. It was

found that the reduction in force for a given deformation, and the increase in attainable deformation for a given force was most marked at the higher frequencies. At 90 Hz a 50% decrease in force and a 300% increase in deformation was observed when upsetting lead by this method. In all these investigations the beneficial effects were said to be a result of decreased friction forces.

Golubev and Yavorovskii[45,46] found that the most uniform deformation was achieved when separation of the tool and work-piece occurred. The greatest improvement occurred when for static loading the uniformity was least, viz: dry surfaces, heated specimens. They concluded that the enhanced uniformity was a product of the impacting nature of the loading, and reductions in friction and heat transfer from the test-piece, all brought about by the reduced contact time. The effect of frequency in the range 37-150 Hz was minimal, so long as separation occurred.

Zaleskii and Volkov[47] measured both mean and alternating forces in vibratory upsetting, and observed that no reduction in peak load was achieved for small deformations. However, above a critical degree of compression reductions in the peak load of up to 30% were observed. The magnitude of this critical degree of compression was less for the higher diameter to height ratio and lower frequencies. For these conditions the reduction in load was greatest, and the degree of barrelling was reduced by 10-12%. The minimum force during the cycle was always positive, so separation of the tooling was not achieved.

To investigate the possibility of reducing friction forces by periodic offloading, Lee, Sata and Bakofen[48] conducted compression tests on various materials with a periodic release of stress at 1-5 cycles/min. They showed that pressures could

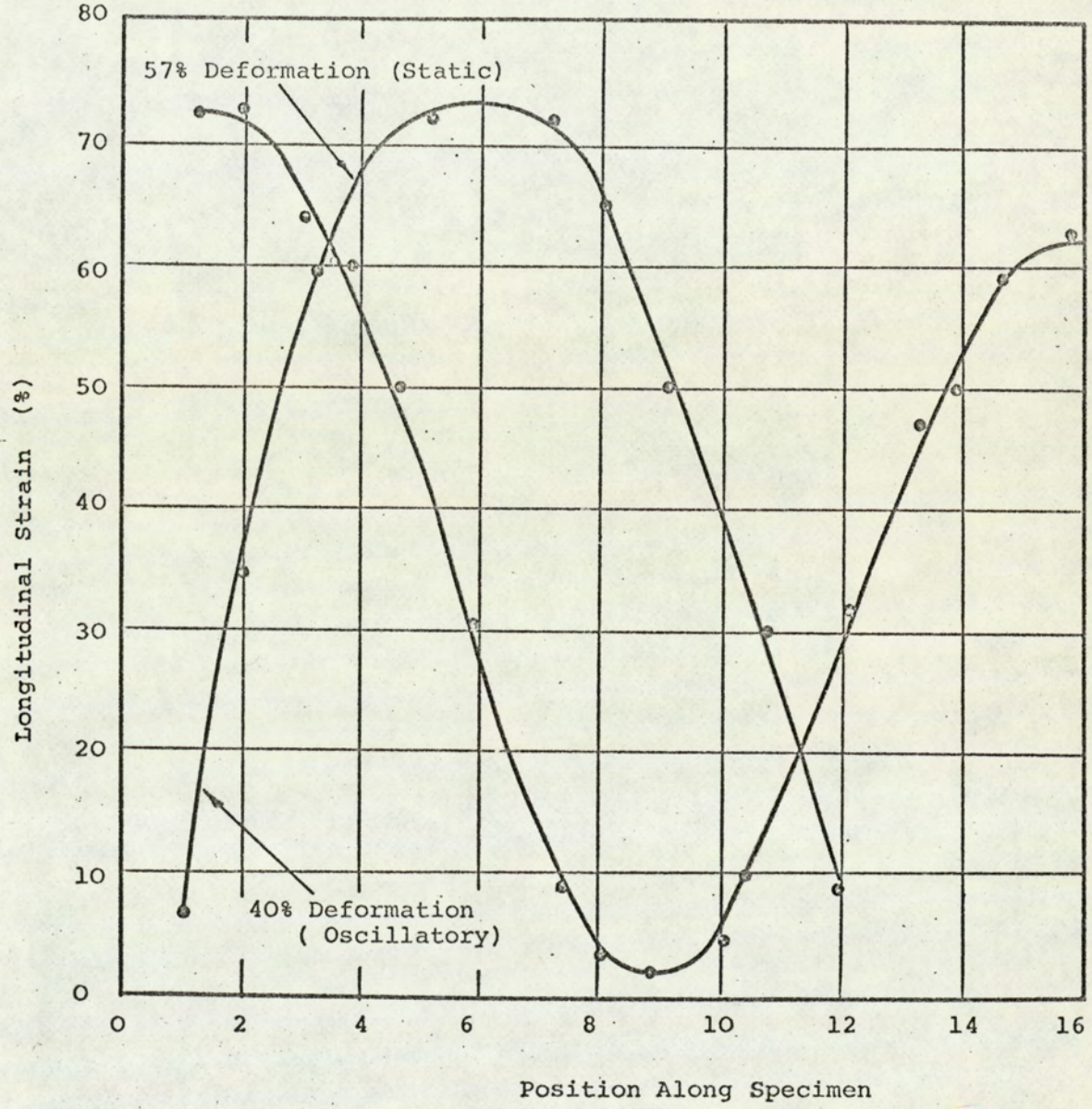

Fig No.5 Distribution of Longitudinal Strain Along the Specimen Axis for Two Copper Cylinders Showing Effect of Applied Vibration

(Severdenko and Klubovich 1965)

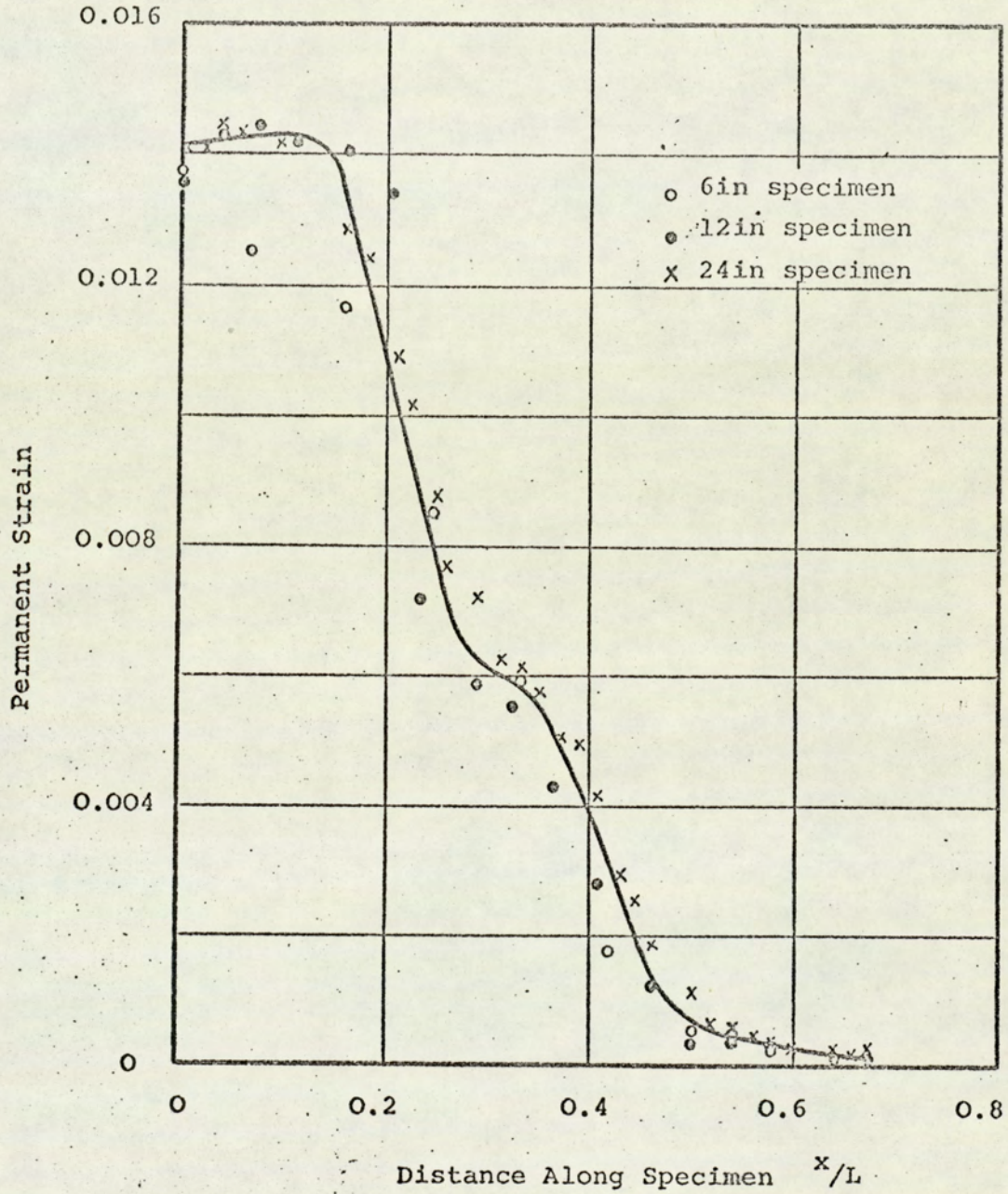

Figure 6: Strain Distribution in 6,12 and 24 in Aluminium Specimens

(Kolsky and Douch 1962)

only be reduced if a reactive lubricant was used, there was a strong tendency to weld, and if the load release was sufficient for the elastic recovery to break the welded junctions. However, it should be noted that the strain per cycle employed in these investigations was far in excess of that during the vibratory compression work described above, and was therefore not truly representative.

Concurrently with these very low-frequency investigations, forging has also been attempted with ultrasonically oscillated platens. Again, Russian investigators have been most active in this field. The aspects of forming forces and product shape have both been studied.

Initial work by Severdenko and Klubovich[49] showed that when ultrasonic oscillations were applied to the upper platen during forging aluminium, the forging force fell in proportion to the intensity of ultrasound, and could be reduced to zero. Barrelling was also reduced and could be virtually eliminated. Subsequently it was shown that the distributions of longitudinal strain,[50] radial strain,[51] microhardness[52] and residual stress[53] were reversed by ultrasonic action, being greatest at the end faces (fig. 5). In static compression these quantities have their greatest values in the centre.

To explain these results it was suggested that, in ultrasonic forging, friction was reduced[50]. Also, the impacting type of load was said to produce elasto-plastic waves which penetrated the specimen, causing non-uniform straining along their path[51]. Similar strain distributions have been observed due to impact loading of copper cylinders[94] (fig. 6). Finally, thermal softening, resulting from the absorption of ultrasonic energy, was said to be instrumental

in reducing flow stresses[50,51].

Severdenko and Labunov[54] showed that if the amplitude of oscillation remained constant throughout the compression the reduction in load was constant. For aluminium this amounted to 29% when the strain was 53% and only one platen was oscillated. This reduction in load reached 50% with both platens oscillated. Similarly, Zhadan[55] observed a small constant load reduction for steel deformed in an ultrasonic field. This he attributed to the superposition of mean and cyclic stresses. Severdenko and Petrenko[56] found the load reduction to be less at the higher strain rates.

A study of the effect of lubricants on ultrasonic upsetting has been made by Petrenko[96], who reports that the reduction in deformation load of aluminium specimens is uneffected by lubricant type for strains less than 36%. For strains above this figure, however, there was a greater reduction in load when oscillations were applied to specimens with surface active lubricants. (c.f. Lee, Sata, Bakofen (48)).

In the U.S.A. both Balamuth[57] and Kristoffy[58] succeeded in measuring the alternating component of stress during forging of aluminium with ultrasonic oscillations applied to the tooling. For low intensities both investigators found the drop in mean force to be equal to the alternating force amplitude. However, at high intensities, the drop in mean load observed by Balamuth was in excess of that predicted by a superposition mechanism. This was attributed to heating of the test-piece and its subsequent softening.

Similarly, Izumi et al.[59] have shown that the stress reduction is linearly proportional to amplitude for low intensities. For intensities above a critical amplitude,

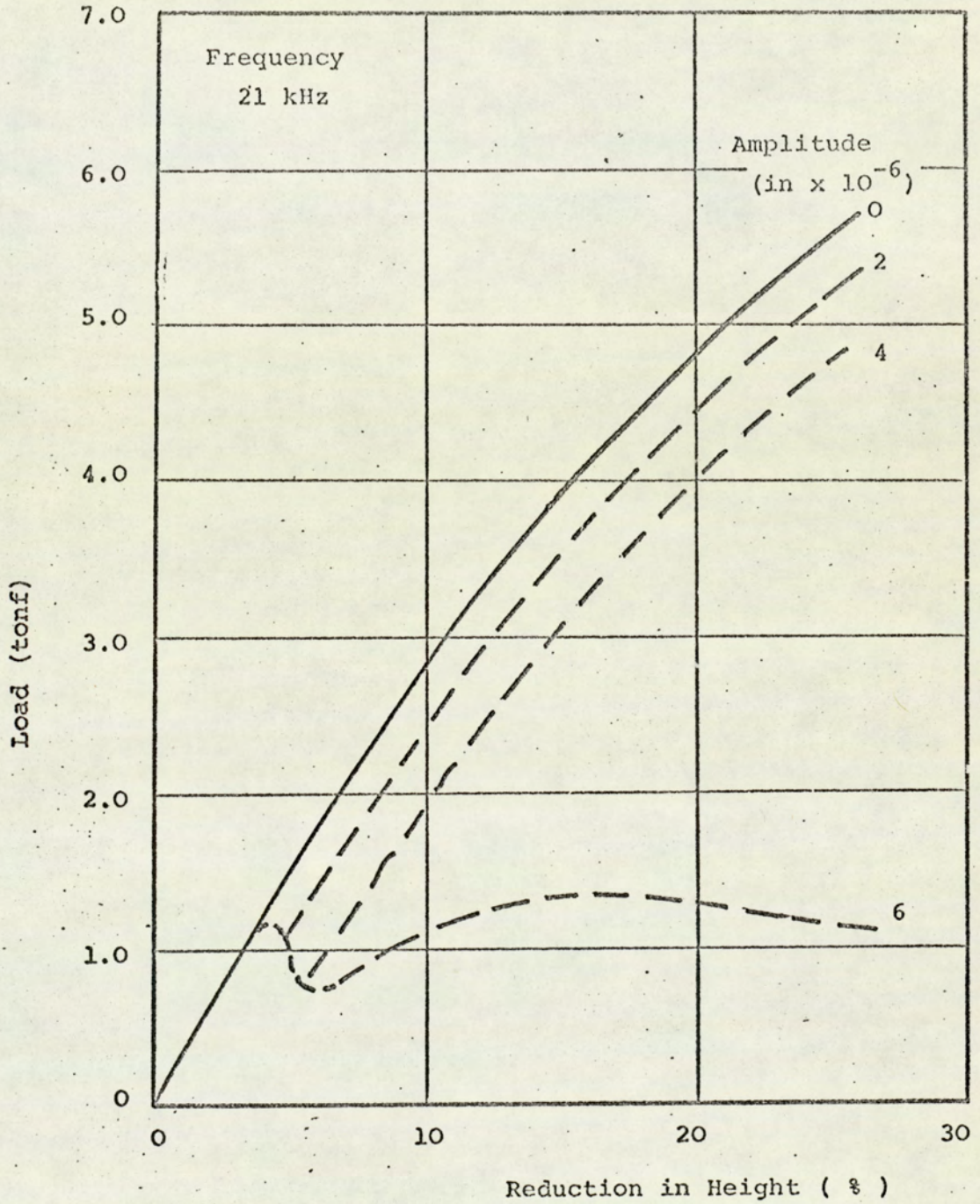

Fig No. 7 Compression Load-Reduction Curves for Copper Showing the Effect of Vibration

(Izumi et al 1966)

however, much greater reductions in stress were observed, and the shape of the stress strain curve was altered considerably (fig. 7). In such cases the temperature of the test-piece rose up to 300°C, and the hardness was reduced and more uniform. Similarly, temperature rises of up to 600°C have been reported by Severdenko and Petrenko[60]. However, the reversal of the distribution of deformation reported by Severdenko et al.[49-53] was not observed by Izumi, and at high intensities the degree of barrelling was seen to increase.

Both Izumi et al. and Kristoffy observed a lowering of the mean stress reduction with forming speed, thus agreeing with Severdenko and Petrenko. This was attributed by Kristoffy to the reduced alternating stress, caused by the tool velocity attenuating the degree of off loading by the cyclic component. Kristoffy pointed out that when the velocity of the tool exceeds the maximum oscillatory velocity, no stress variation will be induced, and therefore there will be no reduction in mean force.

A12 (b) Drawing of wire and bar

Since 1962, oscillations at low and ultrasonic frequencies have been applied in various modes to the die during wire drawing, and all researchers have observed an apparent reduction in drawing force. Golubev et al.[75] were the first researchers to apply low frequency oscillations to the drawing of wire rod. For oscillation frequencies in the range 25-312 HZ axial, transverse and torsional oscillations were all found to reduce drawing forces. For axial oscillations greater reductions in drawing force were observed at the higher frequencies reaching 70% at 312 Hz. This reduction in drawing

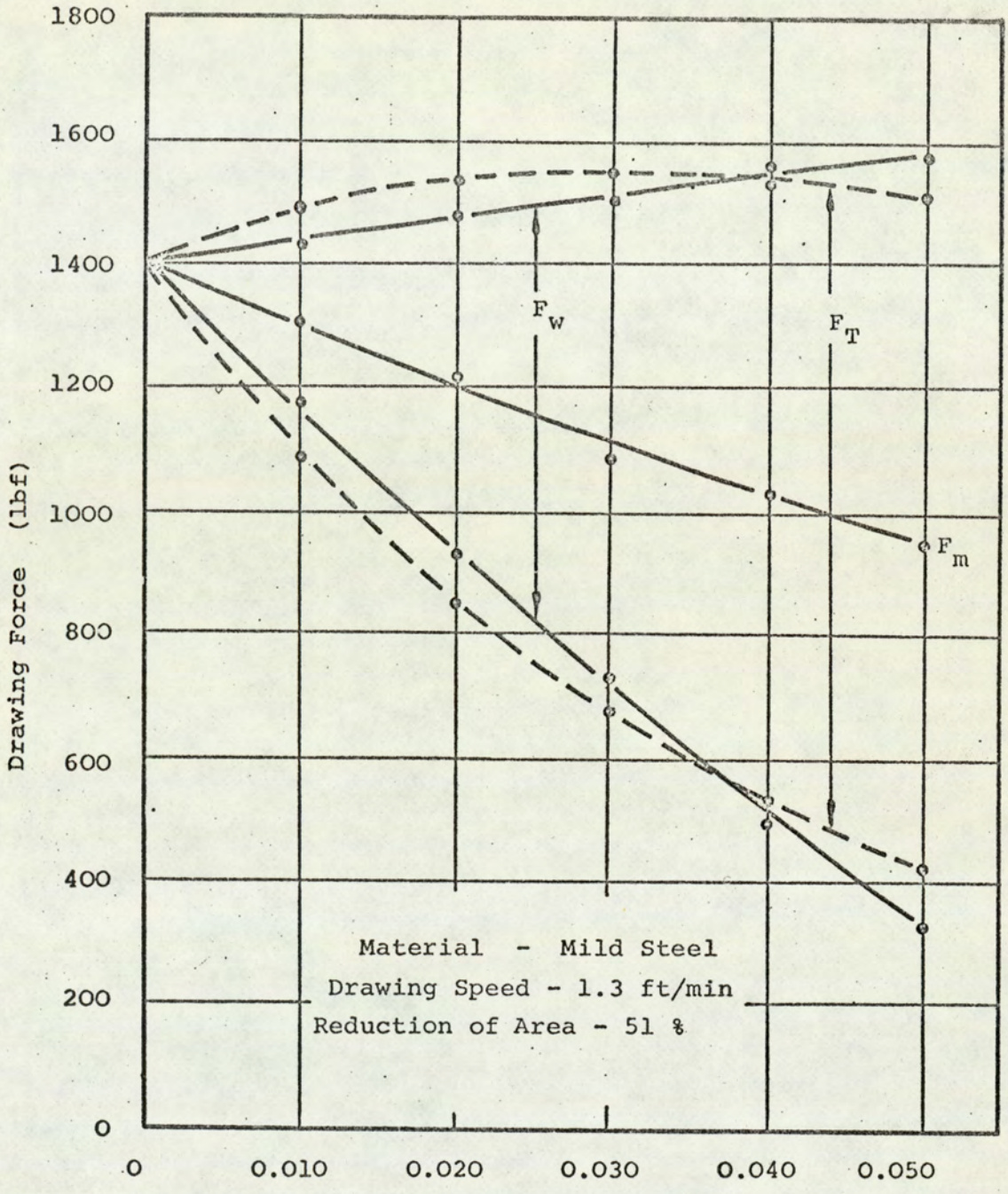

F_m= Mean drawing force; F_W= Actual force variation in wire;
F_T= Force variation in wire as recorded by the torquemeter

Fig No.8 Variation of Drawing Force With Amplitude of Die Oscillation (Winsper & Sansome 68)

force was unaffected by drawing speeds up to 477 ft/min. No figures for die amplitude were given. Oscillations were found to cause no increase in the temperature rise of the drawn product. Of the three modes of oscillation, torsional was said to be the most effective, but no figures were given. It was also noted that oscillations caused an improvement in surface finish, a reduction in residual stresses, and a more uniform distribution of micro-hardness across the cross section.

Severdenko and Klubovich[61] were the first to apply ultrasonic axial oscillations to the die during the drawing of copper wire. To avoid excessive overheating and fracture of the wire they found it necessary to make the tag length an odd number of quarter wavelengths, and thus minimize the acoustic stress amplitude. They observed a 50% reduction in tag load for drawing speeds up to 500 mm/min. Also, the ultimate tensile strength and microhardness of the drawn wire was found to be reduced by 15%.

Both Boyd and Maropis[62] and Robinson et al.[63,64] have observed similar drawing stress reductions for a variety of hard and soft metals and alloys. The reduction in stress was found to be proportional to ultrasonic power, and less at the higher drawing speeds, which reached 1000 ft/min. Both investigations showed that the stress reduction varied periodically with drawn length, the maximum effect occurring when the length was such that resonant standing waves were produced. Under these conditions Robinson noted that the wire temperature could rise by up to 870^{o}C, at the positions of maximum acoustic stress, which could result in fracture. Small-scale reductions in ultimate tensile strength and hardness were observed in the drawn wire. The use of ultrasonic die oscillation was generally

associated with excessive pick-up in the die and a poor surface finish. Boyd and Maropis suggested that the reduction in load was due to a combination of friction reduction and increase in plasticity brought about by the ultrasonic action. The reduced effect at higher drawing speeds was attributed to the reduced energy per unit volume imparted to the wire.

Both the Steel Company of Canada[65] and Aeroprojects Inc.[66,67] confirmed these general findings. However, the large-scale temperature rises reported by Robinson were not observed. The latter investigators also observed that the material properties were unaffected, stick-slip was eliminated, and the surface finish improved. Since the reduction in stress was greater for the higher surface to volume ratios, it was attributed mainly to a reduction in friction.

Similarly, Inoue and Mori[97] observed these general effects. The reduction in drawing load observed, (up to 80%), was attributed to an impact type of loading in the die.

The first investigators to measure the induced acoustic stress in the tag were Pohlman and Lehfeldt[20,68]. They observed that when ultrasonic axial oscillations are applied to the die, the apparent drop in drawing stress was equal to the acoustic stress amplitude, thus showing the process to be one of superposition. This explanation has been confirmed by Winsper and Sansome[69,70] for ultrasonic die oscillations and by Winsper and Sansome[71] and Solkowsky and Vilan[72] for low-frequency oscillations (fig 8). None of these investigators observed the large-scale heating reported earlier.

Both Winsper and Sansome[69,71] and Lehfeldt[68] observed the mean stress reduction to be less at the higher speeds, and attributed it to the reduced release of strain due to the increased speed of the wire. Winsper and Sansome derived a mathematical expression for the speed effect, which showed the induced stress to be a function of the ratios of oscillatory speed to drawing speed, and which was in close agreement with observed data (see section A21).

This superposition mechanism was found by Winsper and Sansome[70] to be further effective in reducing drawing stresses when the wire is drawn through several dies. It was found that if the back tension applied to the die had an alternating component, only its mean value was effective in raising the front tension. This resulted in a genuine reduction in final tag stress, as opposed to an apparent reduction, which the superposition mechanism provides. This explanation showed a close correlation with the observed mean and alternating stress levels (see section A21).

Other modes of ultrasonic die oscillation which have been investigated include transverse by Vatrushin[74] and radial by Oelschlagel and Weiss[73]. The former observed only small stress reductions of 5-9%, whereas Oelschlagel and Weiss obtained up to 62% reduction for maximum aplitudes. These modes were also investigated by Lehfeldt[68] and in both cases the stress was apparently reduced.

For the transverse mode it was found that the maximum reduction of stress was obtained when the length of the tag was matched for transverse resonance. Furthermore, the magnitude of stress reduction was equal to the induced stress amplitude for transverse oscillation.

Similarly, for the radial mode the magnitude of stress reduction was found to be equal to the induced cyclic stress in the deformation zone normal to the wire, and brought about by the motion of the die. This augmentation of the die pressure by the radial contraction of the die was found to reduce the non-uniformity after drawing. Similar results were obtained when a split die was used, with one half oscillated in the transverse mode.

A12 (c) Drawing of Tube

The drawing of tubes with ultrasonic axial oscillations applied to the tooling is the only process known to the authors to have achieved production status. The development of this technique has been carried out by Aeroprojects Inc. in the U.S.A. Their initial investigations[76,77] used an axially oscillated die in both tube sinking and plug drawing. As a result of this drawing rates were increased by up to 13-fold for a fixed drawing force, and drawing forces reduced by up to 80% for a fixed rate. These effects were most marked for softer materials, where greater area reductions were achieved using ultrasound. The surface finish and metallurgical properties were found to be unaltered.

Severdenko and Reznikov[78] confirmed these observations when sinking copper tubing, and by measuring the temperature rise were able to confirm that thermal softening was insufficient to explain the 30-35% reduction in stress observed.

Similarly Nosal and Rymsha[30] observed reductions of drawing force of up to 35% when sinking tube in an axially oscillated die at ultrasonic frequencies. This was attributed to a reduction in friction forces, brought about by the periodic reversal of the velocity of sliding, thus reducing

the mean component in the drawing direction (see section A22).

The effect of transverse ultrasonic die oscillations in tube sinking has been studied by Severdenko and Reznikov[98,99] where drawing forces were again reduced, but by smaller amounts (12-19%). This was attributed to a reduction in friction forces (see section A22).

Subsequent investigations at Aeroprojects were concerned with ultrasonic axial oscillation of the plug in fixed plug drawing of tube. This process is now used in production and the following advantages are claimed[79,80,105].

Tubes may be drawn on a fixed plug which conventionally require a moving mandrel.

Drawing forces are reduced by up to 10% for thin walled tubes.

Diameter to thickness ratios of 500:1 can be drawn successfully with ultrasonic action, compared with a 50:1 limit for static loading.

Greater reductions in area can be achieved.

The finish of the bore is brighter with the degree of roughness halved.

Stick-slip, chatter, and lubricant breakdown are virtually eliminated.

More complicated sections may be drawn.

It is suggested that these benefits result from a reduction in friction forces. Winsper and Sansome also observed reductions in drawing load and plug bar load when ultrasonic axial oscillations were applied to the plug, during the drawing of thin-walled stainless steel[81].

In this investigation both die load and drawing load were measured. Reductions in mean die, tube and plug loads

were observed to be proportional to plug amplitude. Furthermore, measurement of the cyclic component of force in the drawn tube revealed that the reduction in drawing force was considerably larger than the dynamic force amplitude, thus indicating that superposition alone could not explain the reduction in load.

Ultrasonic axial oscillations have been applied to the plug in tube drawing in the U.S.S.R. by Verderevskii et al.[100] in which reductions in the drawing load of 25-30% were achieved. This was attributed to the reduction of friction by its periodic reversal of direction (see section A22).

A12(d) Extrusion

Extrusion was one of the first metalworking processes to be attempted with oscillations applied to the tooling. The earliest investigations were conducted by Aeroprojects Inc. in the U.S.A.[82,83] Lead and aluminium billets were extruded with ultrasonic oscillations applied to the die, container and ram. Extrusion rates were increased by 88% for a fixed force, and the extrusion force reduced by 15% for a fixed rate. Oscillation of the die was found to be most effective in producing these results. Similar beneficial effects were observed when oscillations were applied to the inner tool during aluminium extrusion cladding of steel tubes. These effects were attributed to a reduction in die and container friction.

Similarly, Tursunov[84] in the U.S.S.R. observed reductions in force of 23% and 42% when extruding copper and brass respectively, with ultrasonic oscillations applied to the ram. The microstructure of the product was unaltered,

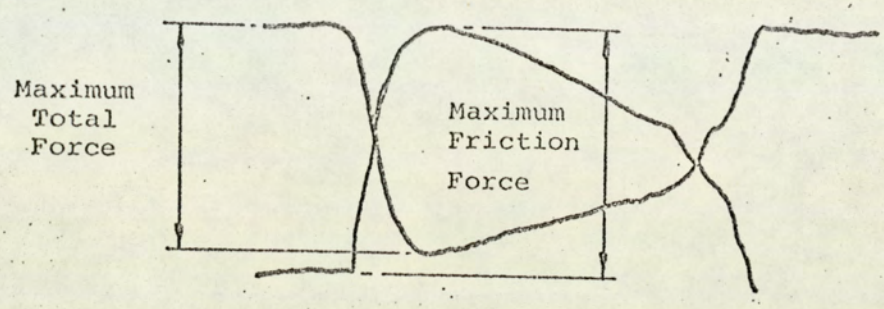

Non-Oscillatory Extrusion

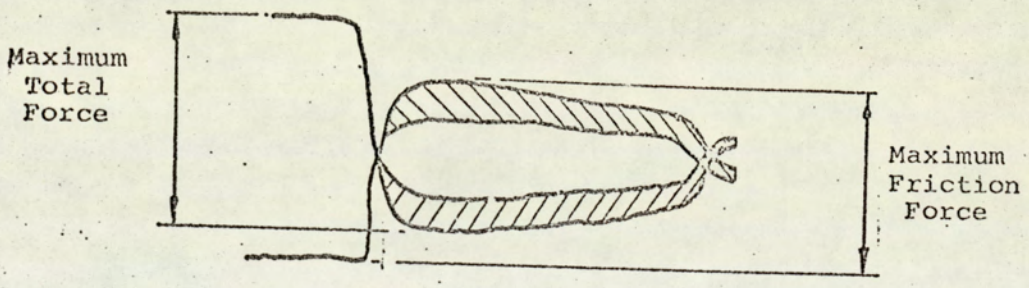

Oscillatory Extrusion

Fig No. 9 Oscillograms of the Forward Extrusion Process for Oscillatory and Non-Oscillatory Extrusion

(Zalesskii and Mendybaev 1967)

but a slight reduction in microhardness was noted. The effect was attributed to a reduction in yield stress brought about by the ultrasonic action.

Subsequently, Zaleskii and Mischenkov[85] have attempted to find the optimum method of supplying ultrasonic energy to the process. With the die and container forming part of a standing wave, two configurations were investigated. With the die at the displacement antinode it was found that lead could not be extruded, cracking and fragmentation of the product occurring. However, with the die at the displacement node, not only was cracking eliminated, but the deformation of the product was more uniform than for static extrusion. This enhanced uniformity was attributed to a reduction in container friction, brought about by the reversing velocity of the container relative to the blank.

Low-frequency oscillations have also been applied to the extrusion process. Zaleskii and Mendybaev[86] applied axial oscillations at 93 Hz to the moving die in backward extrusion. Measurement of the periodic and mean forces showed that the peak force was unaltered by oscillations, the mean force being reduced by the superposition effect.

Zaleskii and Mendybaev[87] also investigated the direct extrusion of lead with oscillations at 98 Hz applied to the ram. In this case the periodic and mean components of both the total force and the friction force on the container were measured. Oscillations were found to reduce the peak force on the container by 30-35% and the peak total force by 10% (fig. 9). The deformed grid pattern showed a more uniform straining with vibrations. The reduction in forces was less marked at the higher speeds. Again, friction reduction was the proposed explanation.

Such a reduction in forces was not observed by Spiers et al.[88] in the direct extrusion of lead and aluminium, with oscillations in the range of 20-200 Hz applied to the ram. Here the peak extrusion force during the cycle was found to be always slightly in excess of the corresponding force for static extrusion.

A12 (e) Sheet metal working

The use of ultrasonic energy in the rolling process was first reported by McKaig[89]. Copper, aluminium alloys, steel and zinc wire were rolled with ultrasonic oscillations applied to the rolls in an unstated mode. For the same roll-separating force an increase in the reduction per pass of between two- and five-fold was observed for all materials.

Cunningham[90] applied an ultrasonic standing wave to the test-piece in rolling. When a displacement node entered the rolls, reductions in roll separating force of 6% for aluminium, 2.5% for copper and 2% for steel were observed. At other positions in the standing wave the reduction in roll separating force was barely discernible. A stress superposition mechanism in which the acoustic stress acted as front and back tension, thus augmenting the stress state, was discounted since the change in load was directly proportional to roll separating force, and not acoustic power. However, the alternating stress magnitude was not measured, and therefore a superposition mechanism cannot be ruled out.

Subsequently, ultrasonic energy was fed into one of the rolls in a radial mode, which resulted in the roll separating force falling by 16% for lead rolled cold and 5% for aluminium at 500^{o}C. No effect was observed for the cold

rolling of aluminium, copper and steel, and was thought to be caused by the 'leaking' of ultrasonic energy to the un-activated rolls. The reductions in forces observed were attributed to a reduction in friction, brought about by the period separation of the rolls from the test-piece.

The application of low frequency oscillation to rolling has been studied in the U.S.S.R. by Burkhanov et al.[101,102] In this investigation the upper roll was oscillated transversely, such that there was a periodic variation in the roll gap, at a range of frequencies 0-100 Hz. In the rolling of copper strip reductions of 10-15% in specific pressure and 60-70% in roll torque were observed, these effects being most marked when the degree of off loading was greatest. A reduction in friction and yield stress was considered to be the explanation for these effects.

The effect of ultrasonic oscillations on the drawing of strip has been investigated by Rozner[103], where the die halves were oscillated normal to the direction of drawing. Reductions in the mean drawing load and die separating force were observed to result from oscillations. A superposition mechanism was said to be the explanation for the reduction in drawing load, whilst the die load was said to be reduced by decreased friction forces.

Sorokin[91] has shown that oscillations have beneficial effects on the stretch forming of double curvature shell segments. When the forming block was vibrated transverse and parellel to the direction of tensioning simultaneously at 45 Hz and 20 Hz respectively, a 30% reduction in force, or a 70% increase in the attainable deformation was achieved. It was also found that the number of stages and anneals could be

reduced by oscillations for a given final deformation.

McKaig,[89] when drawing aluminium sheet with ultrasonic oscillations applied to the die, observed an increase of the depth of draw 37% for a given load, with improved dimensional accuracy of the product. Similar results have been reported by Peacock[92] for dimpling of aluminium and titanium sheet with axial ultrasonic oscillations applied to the punch of die. The impacting nature of the load, producing high forces of short duration, together with a reduction in friction, brought about by the reduced contact time, were said to be the causes of the greater degrees of deformation.

A 65% reduction in the forming force was reported by Langenecker et al.[93] for the ironing of copper cups with ultrasonic axial oscillations of the die. Greater reductions per pass were also achieved using ultrasound. A reduction in the yield stress was said to account for these effects.

Similar force reductions have been observed by Kristoffy[58] when ultrasonic axial oscillations were applied to the punch, or radial oscillations were applied to the die, in the deep drawing and ironing of aluminium and steel. Axial punch oscillations and torsional die oscillations, both at 20 Hz had the same result for ironing of aluminium and steel. Measurement of the periodic and mean punch loads revealed that both ultrasonic and low frequencies, the reduction in forces when the punch was oscillated was due to superposition, the peak stresses were unaltered.

However, with radial and torsional oscillations of the die a real reduction in load was observed. It was concluded that the radial oscillations reduced the force by the superposition of a periodic normal stress in the die, resulting from its radial oscillation, thus augmenting its static

pressure. Torsional oscillations were said to produce a real reduction in force, by causing the line of action of the friction force in the die to swing periodically about the axial direction. This results in a reduction in the mean value of friction force in the axial direction.

Friction forces have been measured in the wedge test analogue of deep drawing by Young[104]. When ultrasonic oscillations of the dies in the direction of the punch were applied, a considerable reduction in the blankholder friction force was observed. Furthermore, this effect was diminished at the higher drawing speeds. This reduction in friction was found to correlate closely with the friction reversal mechanism described in A22.

A2: REVIEW OF PUBLISHED THEORY

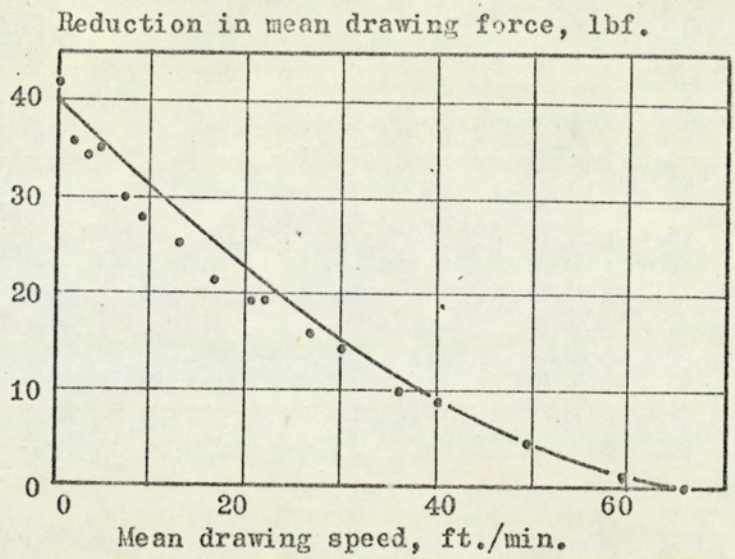

Curve - theoretical; points - experimental.

Figure(10): Model for ultrasonic drawing with increasing drawing speed.

Winsper and Sansome 1969.

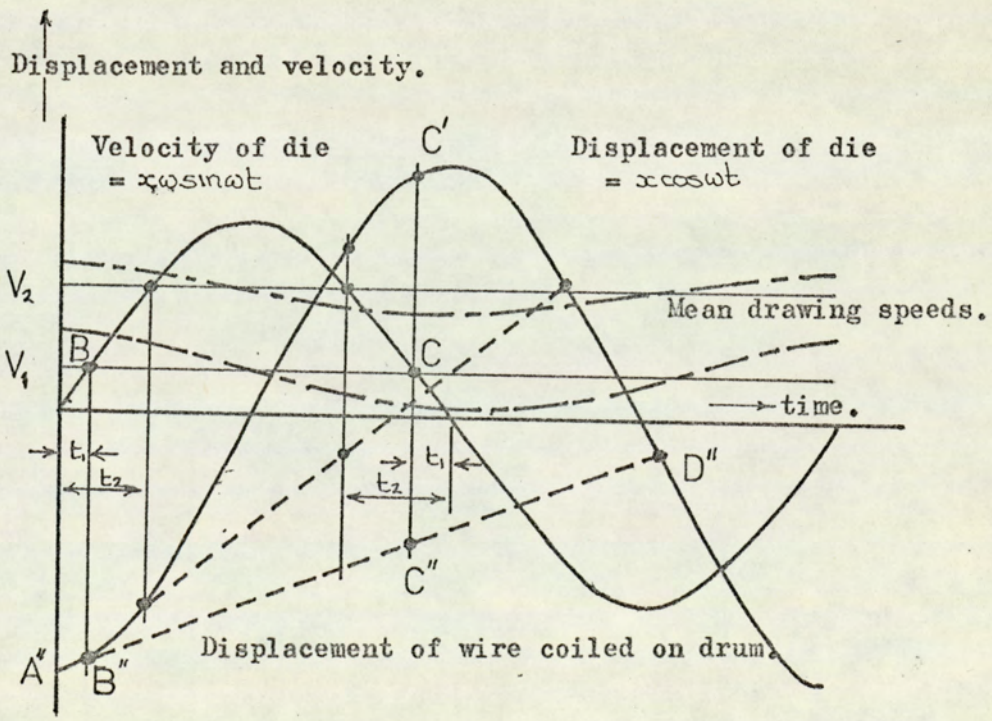

This review is concerned with theoretical, quantitative studies of oscillatory drawing, which have attempted to predict the effect of oscillations on the deformation loads.

A21: Volume Effects

To the author's knowledge, the only comprehensive theory on the volume effect is the superposition mechanism of Winsper and Sansome[69]. These authors investigated the wire drawing process with axial ultrasonic oscillations applied to the die. They observed that the apparent reduction in drawing force was equal to the cyclic force amplitude in the wire at the die (i.e. superposition), and that the cyclic force diminished with increasing drawing speed. The following is a presentation of the theory proposed to account for these effects.

Consider the wire being drawn by a bull block at a mean velocity V through a die that is oscillating longitudinally with an amplitude x (figure 10). The position of the die at A" thus represents the furthest position of the die from the drum. After time t_1 (point B) the die and the wire are travelling at the same speed and it is postulated that at this instant drawing ceases. As a result of the elastic extension in the drawn wire, after time t_1 has elapsed, the particle of wire at point B" follows the die movement. At the same time the bull-block drum coils the wire at a constant speed, as represented by the broken line B" C" D". When the die velocity again equals the mean velocity of the wire (point C) an elastic extension has been released in the wire that is equal in magnitude to C'C". This extension is then "taken

up" partly by the drum and partly by the die on its return cycle, until at point D" drawing commences again. The length C'C" represents the peak to peak amplitude of movement in the drawn wire and hence the magnitude of the reduction in drawing force. This analysis can be described in mathematical terms as follows:

The amplitude of die oscillation = $x\cos\omega t$ and therefore the velocity of the die = $x\omega \sin\omega t$. It is postulated that drawing ceases when $V = x\omega \sin\omega t$.

i.e. when $$t_1 = \frac{1}{\omega} \sin^{-1} \left(\frac{V}{x\omega}\right) \qquad (1)$$

If the periodic time = $2\pi/\omega$, then after $\pi/\omega - t_1$ has elapsed, the peak to peak displacement amplitude in the drawn wire is a maximum. At this interval in time the die and wire will have travelled a distance:-

$$= x\cos\omega t_1 + x\sin\omega\left(\frac{\pi}{2\omega} - t_1\right)$$

$$= 2x\sin\left(\frac{\pi}{2} - \omega t_1\right) \qquad (2)$$

and the drum will have coiled a length of wire:-

$$= V\left|\frac{\pi}{\omega} - 2t_1\right| = \frac{V}{\omega}\left|\pi - 2\omega t_1\right| \qquad (3)$$

The peak to peak oscillatory elastic movement induced in the wire is then obtained by subtracting equation (3) from equation (2).

$$2X = 2x\sin\left(\frac{\pi}{2} - \omega t_1\right) - \frac{V}{\omega}\left|\pi - 2\omega t_1\right| \qquad (4)$$

Now the maximum acoustic stress amplitude in a standing wave is related to the maximum displacement amplitude by the equation:

$$\hat{\sigma} = \frac{\omega \hat{X} E}{C} \qquad (5)$$

and therefore, knowing the position of the die in the standing wave, the cyclic stress amplitude at the die may be computed, and compared with the observed reduction in drawing stress (figure a).

It should be noted here that the authors appear to have taken equation (5) to relate stress amplitude at a point in a standing wave to the displacement amplitude at the same point, since the displacement amplitude computed in equation (4) is substituted directly in (5) to obtain stress amplitude at the die, and therefore the reduction in drawing force.

i.e. $$2\Delta F = \frac{\omega EA}{C} \quad 2x\sin\left(\frac{\pi}{2} - \omega t_1\right) - \frac{V}{\omega} \left|\pi - 2\omega t_1\right| \qquad (6)$$

However, when the results given are checked with the correct use of equation (5), it does appear that the authors have indeed correctly applied this equation and the theoretical curve presented is not in error.

This theory can be seen to correlate well with experimental data, (< 15% error.) especially at the higher drawing speeds. At the lower drawing speeds the theory overestimates the cyclic stress and therefore the apparent reduction in drawing force. The authors attribute this to the assumption that during the period when drawing occurs the velocity of the wire at the die is the steady drawing speed, V. They suggest that, in reality there is a cyclic component of drawing speed superimposed on the steady value, represented by the chain-dotted line in figure (10), which will result in a delay in the cessation of

drawing and a subsequent reduction in the amplitude of induced oscillation of the wire. Furthermore, this cyclic component, and hence error, will be greatest at the lower drawing speeds, where the induced stress levels are highest.

The velocity variation indicated in figure (10), however, is not compatible with theory, since it is assumed that while drawing is not occurring the wire moves with the die, i.e. the velocities of wire and die are equal. Thus through most of the cycle the cyclic component of velocity of the wire is the die velocity. During the period when drawing occurs, the wire is not forced to oscillate, but inertia forces may cause the oscillation to continue to some degree. The cyclic velocity indicated in figure (10) is therefore 90^{o} out of phase with the theoretical one. However, a cyclic component of velocity as described above will have the same effect of reducing the induced oscillation amplitude in the wire, especially at the lower drawing speeds.

Inherent in this theory is the assumption that the drawing force is unaltered by oscillations. However, at low frequencies (0-500 Hz), Winsper and Sansome[71] observed an increase in the peak load with oscillations, which was attributed to a combination of sticking friction and a transient, non-equilibrium deformation pattern. This effect was most marked for high cyclic stress levels. It is possible that at ultrasonic frequencies a similar increase of the drawing force would result from oscillations, and thus diminish the reduction of mean drawing force, as observed.

Inspection of equation (4) will reveal that the coupling coefficient (X/x) between the die and wire is a function of

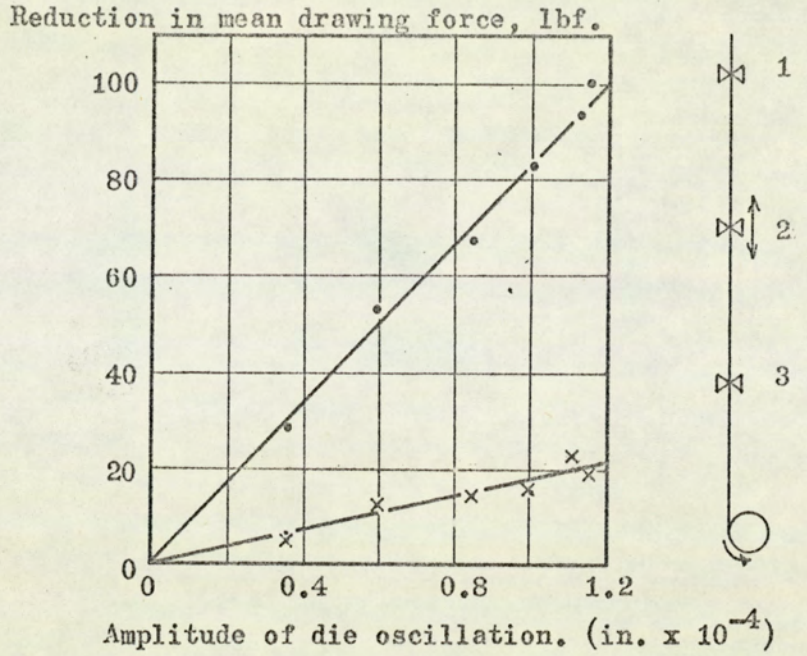

Figure (11) Correlation between theoretical and observed values of load reduction.

Winsper and Sansome 1970

(Upper curve - total drawing force, lower - second fixed die)

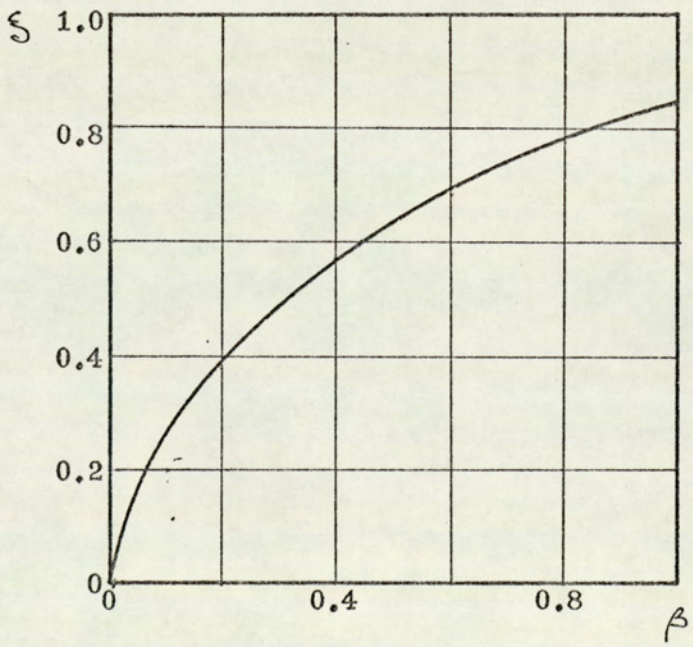

Figure (12) Decrease in friction force with velocity ratio.

Golubev and Dyadechko, 1965.

the ratio of mean drawing velocity to the peak die velocity only. Furthermore no oscillation is induced into the wire for a drawing speed greater than the peak die velocity.

In their study of multi-die drawing with ultrasonic axial oscillations applied to one die, Winsper and Sansome[70] found that the superposition theory described above did not predict all of the drop in drawing force observed experimentally. It was found that in those dies that had an oscillatory back tension applied to them, the deformation only responded to the mean component of that back tension and therefore resulted in a genuine reduction in final drawing load (see figure (11)).

When wire is drawn through a die with an applied back tension, the drawing load P, is given by:

$$P = P_o + (1 - b)Q$$

where P_o = drawing load without back pull.

Q = back pull.

b = back pull factor.

Thus, in conventional drawing, for the situation shown in figure (11), the following equations apply.

$$P_2 = P_{2o} + (1 - b_2)P_1$$

and

$$P_3 = P_{3O} + (1 - b_3)P_2$$

Substituting for P_2

$$P_3 = P_{3O} + (1 - b_3)\ P_{2O} + (1 + b_2b_3 - b_2 - b_3)P_1$$

If now the second die is oscillated axially an ultrasonic oscillatory force of magnitude dF' will be induced in the lengths of wire between the dies, and between the second fixed die and the coiling drum. The effect of this oscillatory

force is to reduce the forces P_1, P_2 and P_3 by an amount equal in magnitude to the applied oscillatory force. Therefore the equations for P_2 and P_3 given above will be modified as follows:

$$P_2 = P_{20} + (1 - b_2)(P_1 - dF^1) - dF^1$$

and

$$P_3 = P_{30} + (1 - b_3)\ P_2 - dF^1$$

The total mean drawing force under oscillatory conditions can be written as follows:

$$P_3 = P_{30} + (1-b_3)P_{20} + (1+b_2b_3-b_2-b_3)P_1 - (3 - 2b_3-b_2+b_2b_3)dF^1$$

Thus the reduction in total mean drawing force is given by:

$$\Delta P_3 = (3-b_2-2b_3+b_2b_3)\ dF^1$$

The reduction in peak drawing force is obtained by subtracting the amplitude of induced cyclic force from the reduction in mean force computed above.

A comparison between theoretically predicted and experimentally observed reductions in mean drawing force is shown in figure (11). As may be seen from this graph there is close agreement between theory and observed data, thus validating the theory.

Thus there may be seen to be an essential difference between the effects of oscillatory front tension and oscillatory back tension at ultrasonic frequencies. The deformation in the die responds to the instantaneous value of the former, as illustrated by the superposition mechanism, since it is the peak instantaneous value which equals the non-oscillatory drawing force, whereas it does not respond to the latter, merely feeling the average value. There is as yet no clear indication why this should be so.

A22: Surface Effects

Investigators in the U.S.S.R. have proposed three theoretical explanations in terms of friction to account for the observed reductions in drawing force when oscillations are applied to the die during drawing.

Golubev[75] observed that low frequency torsional oscillations of the die in bar drawing produced a reduction in drawing force. This he explained in terms of the displacement of the vector of friction force from its axial direction, since with oscillations the velocity of the wire relative to the die has both axial and transverse components.[32]

i.e. $$v_c = \sqrt{v_k^2 + v_t^2}$$

where v_c = resultant velocity of sliding of wire relative to die

v_k = velocity of sliding towards the apex of the die

v_t = velocity of sliding normal to the die axis

Thus $$v_c = \sqrt{v_k^2 + \phi^2 r^2 \omega^2 \cos^2 \psi}$$

Where r = average radius of die.

ω = angular frequency of vibrations

ϕ = angular amplitude of vibrations

$\psi = \omega t$

t = time

The inclination of the resultant sliding direction to the conventional direction (that of v_k), is γ given by:

$$\cos \gamma = \frac{v_k}{\sqrt{v_k^2 + \phi^2 r^2 \omega^2 \cos^2 \psi}}$$

Thus the average friction force in the direction of drawing throughout one oscillation period is given by:-

$$N_1 f_1 = \frac{NF}{T} \int_0^T \cos\gamma \, dt$$

where $N_1 f_1$ = average friction force in direction of drawing

N = normal force on an elemental area of the contact surface

f = coefficient of friction

Thus $$N_1 f_1 = \frac{2}{\pi} \frac{\nu k}{\phi r \omega} \cdot Nf \int_0^{\pi/2} \frac{d}{\sqrt{(\frac{\nu k}{\phi r \omega})^2 + \cos^2\psi}}$$

and for $\beta = \frac{\nu k}{\phi r \omega}$,

$$N_1 f_1 = \frac{2}{\pi} \cdot Nf \, \beta \int_0^{\pi/2} \frac{d\psi}{(\beta^2 + \cos^2\psi)^{1/2}}$$

$$= \frac{2}{\pi} \cdot Nf \cdot \frac{\beta}{(1 + \beta^2)^{1/2}} \cdot k$$

Where $k = \int_0^{\pi/2} \frac{d\psi}{(1 - c^2 \sin^2\psi)^{1/2}}$; $\quad c = \frac{1}{1 + \beta^2}$

Thus the proportional reduction of the mean frictional force in the direction of drawing is given by:

$$\xi = \frac{N_1 f_1}{Nf} = \frac{2}{\pi} \frac{\beta}{(1 + \beta^2)^{1/2}} \cdot k$$

The authors solve k using elliptical integrals, the resulting variation of proportional reduction of friction force ξ, with velocity ratio β, being shown on figure (12).

Several assumptions are inherent in this analysis, though not stated by the author. It is assumed that the torsional oscillations of the die do not induce forced torsional

oscillations in the wire. However, since the direction of the friction vector is swinging about the axial direction, there must be a transverse component in the form of an applied torque to the wire. This will cause an elastic rotation of the drawn wire, thus reducing the effective transverse component of velocity. This effect will be most marked for wire with a low torsional stiffness, i.e. small diameter, large free length. Thus it is thought that the greatest effect will be achieved in the drawing of bar.

Secondly it is assumed that the friction force magnitude is unaltered by oscillations. The effect of oscillations is to increase the sliding speed v_c, thus for torsional velocities the coefficient of friction may indeed be altered by the increased rate of shear of the lubricant film. However, for small torsional velocities the assumption is less erroneous.

The analysis yields the effect of oscillations on the mean friction force. During those instants in the cycle when the torsional velocity is zero, no reduction in friction in the drawing direction will be achieved, and therefore the maximum friction force is unchanged. At low frequencies it is thought that the deformation will respond to these cyclic fluctuations in the friction component, resulting in a fluctuating drawing force, the mean of which is reduced by an amount determined by the theory, but the peak of which is unaltered. Thus no real benefit is achieved. However, there is evidence that at ultrasonic frequencies the deformation does not respond to fluctuation friction stresses[100,104], but merely feels the mean. In this case real reductions in drawing force may be achieved.

Finally it should be noted that the above analysis is for

an elemental plane in the deformation zone. To compute the effect on drawing force it must be integrated over the whole deformation zone.

Transverse oscillations of the die have been observed to reduce drawing forces by Golubev[75] for low frequency wire drawing, by Vatrushin[74] and Lehfeldt[68] for ultrasonic wire drawing, and by Severdenko and Reznikov[98,99] for ultrasonic tube sinking. These last authors have presented a possible mechanism of friction reduction with transverse oscillations. They state that since the direction of the velocity vector of a particle in the die is generally not inclined to the drawing direction by the die angle, due to the transverse oscillatory velocity component, then the friction force vector is similarly not inclined to the drawing direction by the die angle. Thus only a component of the friction force is in the conventional direction, and the effective friction force is reduced. However, this argument is in error, since no matter what transverse velocity the die has, it still has the same cone angle, and the friction force is still along the surface of the cone, and is thus unaltered in direction. It is most likely that the observed reduction in drawing force is due to the induced transverse oscillations of the drawing wire producing a cyclic stress in it, which will then give rise to a conventional superposition mechanism, as observed by Lehfeldt[68].

A mechanism for the reduction of friction when axial oscillations are applied to the die in drawing has been described by Verderevskii et al.[100] The basis of this is the periodic reversal of the friction vector brought about by the periodic reversal of the sliding direction, thus reducing the mean friction force throughout the cycle.

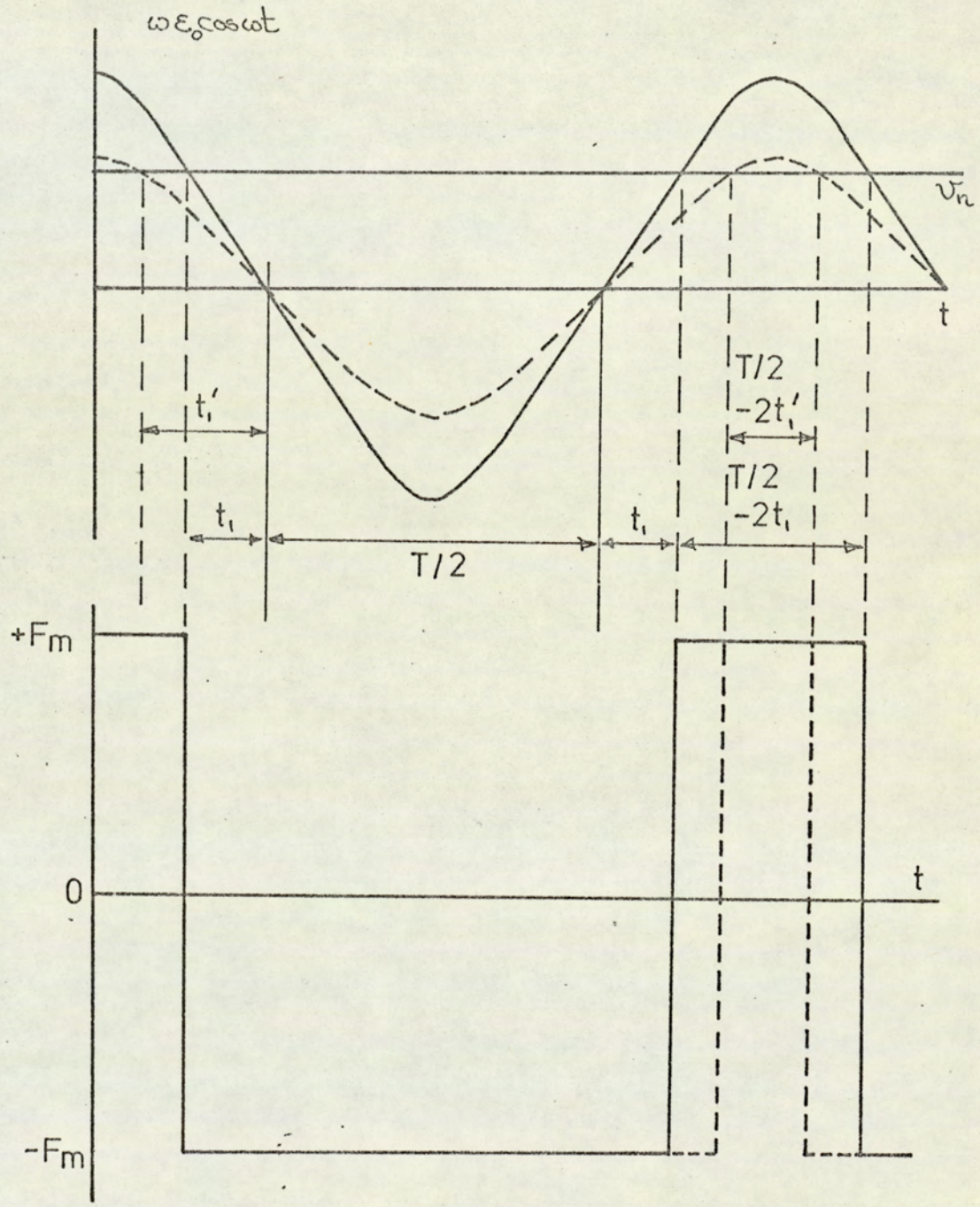

Figure (13) Decrease in mean friction force with oscillations.

Verderevskii et al., 1964.

Consider wire or tube being drawn through a die at a velocity v_n whilst the die has an oscillating velocity $v_k = \omega\xi_o$ where ω is the angular frequency and ξ_o is the die displacement amplitude. If $v_n > v_k$, then over the period of time when v_k coincides with the direction of v_n and exceeds it (i.e. when $\omega\xi_o \cos\omega t > v_n$), the die will "pull" the body, with a force equal in magnitude to the friction force, F_m, but opposite in direction.

Figure (13) shows the die oscillating velocity and the constant velocity of the body varying with time. The lower curve shows the attendant variation of friction force, from the assumptions adopted. As seen, in the time interval $T/2 - 2t_1$, when $v_k > v_n$ the die motion assists the body motion. As the oscillatory velocity amplitude decreases, (broken curve), there is a decrease in $T/2 - 2t_1$. When $v_n = v_k$, $2t_1 = T/2$, and throughout the period the friction force F_m acts on the body. As the constant body velocity v_n is decreased, the period $T/2 - 2t_1$ during which the body motion is assisted, is increased. The period $T/2 + 2t_1$ during which motion is hindered by friction is consequently decreased. The ratio of the oscillation period to the difference these time intervals, n 2 $T/4t_1$ shows by what factor the friction force is reduced.

Now $$n = \frac{\pi}{2} \cdot \frac{1}{\sin^{-1}\left(\frac{v}{\omega\xi_o}\right)}$$

and if $v_n << \omega\xi_o$

$$n = \frac{\pi\omega\xi_o}{2v_n}$$

Thus friction is more effectively reduced for large ω and ξ_o.

The above analysis, whilst it is considered to give a possible mechanism of reduction of the mean friction force in the general case of a body sliding with constant speed over an oscillating body, it is thought inapplicable in the case given of drawing through an oscillating die. In this case when drawing is taking place the velocity of sliding is determined; the product may only move forwards relative to the die. Thus, when drawing is occurring the friction force is unaltered. An enlarged theory of this type has been used by Nosal and Rymsha[30] in an attempt to explain the reduction in drawing force in tube sinking with axial oscillations applied to the die. However, this theory is also inapplicable for the same reason.

In the application of this theory, however, Verderevskii et al. investigate a situation where this problem does not arise; the drawing of tube with ultrasonic axial oscillations of the plug. In this case friction is reversed on the plug, and drawing may occur when the friction force is in either direction. Experimentally reductions in drawing load of 25-30% were observed, whereas the theory predicted reductions of 20-25%. However, since plug loads were not measured, only an estimation of the effect of these on drawing loads could be achieved and therefore the predicted values must be approximate. The author of this thesis has published independently a similar theory for friction reduction in this case[33].

This theory predicts a reduction in the mean friction force applied by the plug on the bore of the tube. It is thought that at low frequencies the deformation will respond to these reversals of friction and thus during some portion of the cycle drawing will occur with friction in the conventional direction, and therefore with the conventional drawing load.

Thus in this instance no benefit is achieved. However, at ultrasonic frequencies experimental evidence suggests that the deformation only responds to the mean component of friction force[104], and thus in this instance real reductions in drawing force may be achieved.

The theory assumes that the friction force remains unaltered in magnitude by oscillations. However, since the velocity of sliding is increased and thus the lubricant film is sheared more rapidly this may not be so. Also more friction work is done in the bore of the tube, and this may affect the surface condition of the bore, thus altering the friction coefficient.

Finally it is assumed that no oscillatory component of velocity is induced in the drawn tube. However, Winsper and Sansome[81] have observed that when ultrasonic oscillations are applied to the plug, cyclic stresses are induced in the tube, which will not only give a cyclic component to the drawing speed, but also give rise to a reduction in the mean drawing stress due to superposition.

A3: DISCUSSION OF PUBLISHED LITERATURE

A31: The Volume and Surface Effects

The effectiveness of applying oscillatory motion to a metal deforming plastically is generally considered from two aspects. It can be said that the volume effect deals with the influence of oscillations on the internal stresses during plastic flow, while the surface effect is concerned with the external friction on the metal. Fundamental research into these aspects is described in part A1 of this review.

Since in a tensile test there are no external friction forces, research in this area has revealed the nature of the volume effect. Early work searched for an understanding of the mechanics of ultrasound propagation in a yielding metal. It suffered from the difficulty of assessing accurately the periodic stresses induced and confusion arose from the approaches adapted. Consequently, the reduction in force observed was considered to be real; ultrasonic energy was thought to be absorbed by the dislocations, which assisted their motion (6,7).

However, difficulties arose when attempting to discover the means by which such energy could be so absorbed. Once it became possible to measure accurately the periodic stress it became apparent that the reduction in mean force was equal to the periodic force amplitude, and thus the peak stress during the cycle was equal to the current yield stress[9]. This implies the material yields intermittently when the applied stress equals the yield stress, and during the remainder of the cycle the test-piece undergoes elastic off-loading and loading.

Although this superposition mechanism is sufficient to

explain the majority of experimental data, the large-scale reductions in stress observed when intensive ultrasound is imparted to the test-piece,[11,57,59] is not so explained. Similarly, superposition does not account for reductions in hardness, rate of work hardening and residual stress.[52,6,7,53] It now seems that these are the result of heating of the test-piece, brought about by internal friction.

There are conflicting reports about the effects of ultrasound on the strain to fracture. In some cases travelling waves cause an increase,[6,7] which may be the result of heating, whereas standing waves result in a decrease in strain to fracture.[13-18] However, with standing waves the maximum value of acoustic stress varies along the length of the test-piece, being greatest at the displacement node and zero at the displacement antinodes. Therefore, the majority of straining will occur at the node, resulting in an effective reduction in the active length of the test-piece. Thus, not only may the strain of the test-piece be apparently reduced, but, because the geometry of the active portion of the test-piece is altered, the reduction in area and ultimate tensile stress may similarly be reduced.

Thus there are now thought to be two components of the volume effect. At low intensities the mean stress is reduced by superposition, while thermal softening becomes progressively more apparent as the intensity of oscillation is raised.

The surface effect is not so readily explained, but fundamental investigations have shown several possible mechanisms for friction reduction. The most common claim is that separation of the surfaces gives an apparent reduction in friction, by reducing the time during which the force acts.[25]

This, however, does not necessarily change the effects of friction, since during the period of contact, when deformation occurs, the friction forces will still be felt. However, it is thought that separation may result in a reduction of the friction forces by the breaking of weldments,[24] and by the redistribution of lubricant when used.[48]

Another possibility for the reduction of friction forces is periodic changing of the line of action of the friction vector. Tangential oscillations in the direction of sliding may produce a periodic reversal of friction forces,[29] and normal to the sliding direction a swinging of the friction vector about its static position.[31] Neither of these modes necessarily reduces the magnitude of friction forces, but both result in a reduction of its mean component in the sliding direction.

A32: The Volume and Surface Effects in Metalworking Processes

Most of the early attempts to apply oscillations to metalworking processes were hampered by a lack of understanding of the nature of ultrasonic stress waves, and the inability to measure accurately their magnitude. Consequently, at ultrasonic frequencies only mean forces were measured. Furthermore at low frequencies, no mention was made of allowing for the high inertia forces involved, when relatively massive tooling is oscillated with high accelerations. Hence, the universal claims of reduction in deformation forces are not reliable, since the peak instantaneous stresses in the deformation zones are not known.

Any assessment of the kind of mechanisms involved in these apparent effects is further hampered in many cases by insufficient details of equipment, technique or results being given.

In those later investigations, however, where periodic stresses were measured,[9,20,21,58,68-72,86] the universality of the superposition mechanism has been demonstrated, i.e. when the applied stress has a cyclic component, then the mean applied stress will be reduced by the cyclic stress amplitude. Furthermore this has been shown to be true at ultrasonic and sonic frequencies.[70,71] Thus, even if other mechanisms of force reduction are active, superposition will always account for some reduction in forces, when the forming force has a cyclic component. Thus, in the absence of a heating or friction effect, it is thought that for the majority of instances where a reduction in load, increased deformation, or increased strain rate were observed, these effects were the result of superposition.

Whilst in many early investigations the temperature rise of the workpiece was not recorded, there is no doubt that at high intensities of ultrasonic energy, heating of the workpiece becomes an important factor. The temperature rises reported by Izumi,[59] Severdenko[60] and Robinson[63] were sufficient to produce thermal softening of the material being formed.

From the published data it is difficult to assess the effects of oscillations on friction in metal-working processes. Many claims of friction reduction have been made which were largely unsubstantiated. It is considered that, in the light of more recent research, the majority of reductions in force observed and attributed to a reduction in friction, were more likely due to a combination of superposition and heating.

However, there are cases which are not so readily explained by these mechanisms. The barrelling of a forged test-piece is due to the frictional constraint at the end faces. Oscillations of the platens have been shown to reduce this non-uniformity of deformation at low frequencies,[34-47] and even reverse it at ultrasonic frequencies.[50,51] Similarly, the virtual elimination of stick-slip and chatter in wire and tube drawing[79,80] and the improved product in extrusion[85] point to ultrasonic oscillations improving friction conditions. Low frequency axial oscillations have been shown to reduce friction forces in extrusion,[87] and low frequency torsional oscillations are thought to reduce frictional forces in ironing[58] and bar drawing[75].

At present, the underlying mechanisms are not definitely known, but research reveals several possibilities. Low frequency oscillations are most effective in reducing barrelling

in upsetting when the tools periodically separate from the surface. Thus, the welded functions are being broken continually, and if a lubricant is being used, the specimen may be effectively relubricated once every cycle. The importance of lubricants has been demonstrated by Lee et al.[48] at low frequencies, and Petrenko[96] at ultrasonic frequencies. The former showed that under cyclic loading, the peak force was reduced only when active, i.e. reactive, lubricants were used. The latter showed reductions in mean load of a higher magnitude when an active lubricant was used.

However, it has been suggested that the loading is of an impacting nature,[45,51] resulting in the production of elasto-plastic waves which penetrate the specimen. Research into the impacting of finite bodies has revealed that the permanent strain produced by such loads has a similar distribution to that observed after forging with ultrasonic oscillations of the platens.

The most probable mechanism for friction force reduction in drawing and extrusion is the reduction of its mean component in the axial direction by periodic variations in the direction of the friction vector. Periodic reversal of the plug friction force in tube drawing, with ultrasonic axial oscillations of the plug, has been suggested as an explanation of the apparent reduction in drawing force.[100,106] Winsper and Sansome[81] have observed that superposition alone cannot account for the load reductions in this case. Furthermore Young[104] has demonstrated this mechanism to be active in deep-drawing. Periodic swinging of the friction vector produced by torsional oscillations of the die has been proposed as a means of reducing friction in bar drawing[75,32] and in ironing.[58]

Oscillations have been applied to metalworking operations in such a manner that the above mechanisms of superposition and friction reduction cannot be applied. In these cases the application of oscillations results in a changing of the process itself. In the case of wire drawing with ultrasonic radial die oscillations studied by Lehfeldt,[68] the process becomes a combination of drawing and swaging, since cyclic radial pressures are induced at the die to wire interface. Evidence of this change of deformation pattern is provided by the radically changed deformed grid pattern. Furthermore, the low frequency transverse oscillations of the roll gap in strip rolling, studied by Burkhanov et al.,[101,102] changes the process to a combination of rolling and plane strain forging. In both these cases plastic work is done in the transverse direction, reducing that required axially.

Thus, there are four main areas of effectiveness when oscillations are applied to metal deformation, and these will now be discussed in turn.

If the oscillations are applied to the process in such a manner as to produce a cyclic component of the applied stress, then this will result in a reduction of the mean applied stress equal to that cyclic component. Thus, the maximum value of the applied stress in unaltered. Furthermore, deformation will occur intermittently, when the load is a maximum. This has been shown to be true for both ultrasonic and sonic frequencies. Such a mechanism means that no effective load reduction is achieved, and therefore when the applied loads are tensile, no greater reductions in area are possible. Also, superposition is only effective for drawing speeds less than the

peak oscillatory velocity. However, the power requirement on the forming machine is less, since the mean forces are reduced. The residue of power is provided by the oscillator. Thus, the capacity of existing machines may be increased.

When the level of oscillatory energy imparted to the workpiece is high, it will result in a rise in temperature. This may result in thermal softening of the material, resulting in a reduction in forming load. However, since conventional methods of applying heat are readily available, and generally more efficient, it is considered that this mechanism has little commercial significance.

If the oscillations are applied in such a manner as to do work on the workpiece in the direction normal to the applied work, then the applied work will be reduced. In the situation where the applied forces are tensile, e.g. drawing with radial die oscillations, real benefits are possible, since greater reductions in area are possible. Also, the conventional limit on the maximum reduction of area does not apply since with sufficiently powerful oscillations all the work could be transferred to the transverse direction, and the process becomes one of swaging only. In the case of rolling with transverse oscillations of the rolls, however, there will still be a limit on the reduction due to roll flattening. The choice of frequency is important when this mechanism is used, since if the throughput of material per cycle is large, it may produce a rippled product as observed by Burkhanov[101] in the case of rolling. However, the reduction of applied forces by this mechanism is not dependent on the ratio of product speed to oscillatory velocity, as in the case of the superposition mechanism.

The major friction reduction mechanisms which have been proposed are those relating to a reduction in the mean component in the direction of applied stress, by means of a periodicity in the direction of the friction vector. By these mechanisms the mean friction component can be reduced, in the limiting condition of zero deformation speed, or infinite oscillation velocity, to zero. Thus the most that can be achieved is the elimination of the mean friction force on the oscillated tool. If, however, the cyclic velocity is less than the drawing velocity, then with axial oscillations no reduction in mean friction is achieved. However, with torsional oscillations, no such limitation occurs, and the mean friction force will be reduced by some degree for all velocity ratios.

Whilst the mean friction force will be reduced at all frequencies by these mechanisms, it is not yet clear how the applied stress is affected. At ultrasonic frequencies it appears that the deformation only feels the mean component of friction. This has been shown to be the case when radial oscillations are applied to the blank-holder in deep drawing.[104] Also, it has been shown that the deformation in wire drawing only responds to the mean component of back tension.[70] The effects of a low frequency oscillatory frictional stress, or back tension, has not yet been studied, but it is thought that in this case the deformation will respond to the cyclic component, and thus little benefit will be achieved. This possibility will be studied as part of this present investigation.

Finally, it is thought that when deforming metal over an oscillating tool, the increased relative mention, and hence

frictional work, will result in a 'burnishing' of the product, thus improving the surface finish. When tube is drawn over an ultrasonically oscillated plug, a marked improvement in the surface finish has been reported.[79,80,81,105] Such an improvement in the surface condition will result in a changed friction force, thus invalidating the assumption in the theories of friction reduction of a fixed magnitude of friction force.

PART B: OSCILLATORY WIRE DRAWING

General view - wire drawing.

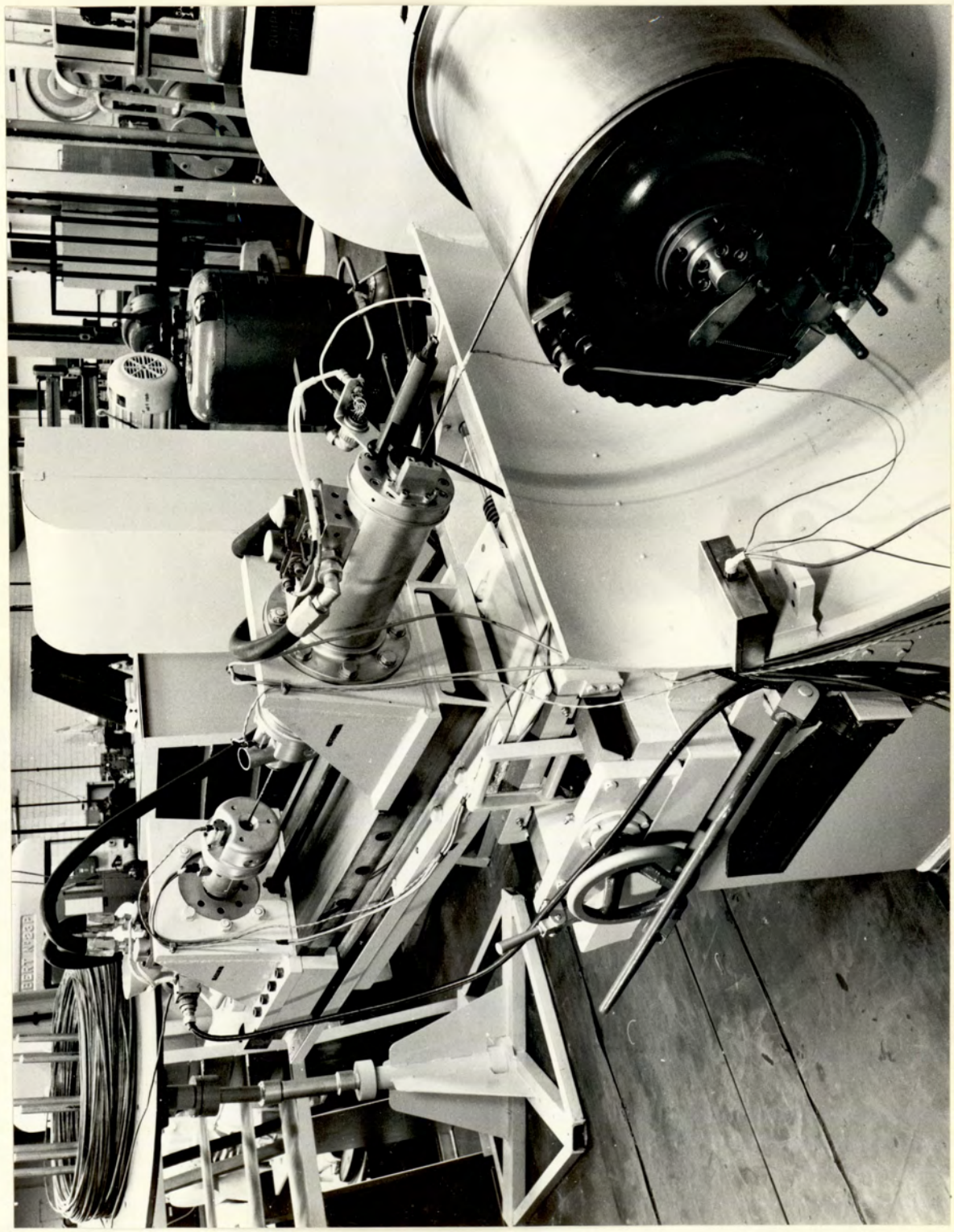

B1: Introduction to Oscillatory Wire Drawing

B1: Introduction to Oscillatory Wire Drawing

Prior to the initiation of this research programme, axial oscillations had been applied to the die in single die wire drawing only. At both ultrasonic and sonic frequencies, the reduction in mean drawing stress was shown to be the result of the superposition of the cyclic stress upon the mean stress. Thus the peak force during the cycle was unaltered by oscillations, and therefore no greater reductions in area were possible. This behaviour infers that wire is being drawn intermittently at the peak stress, while in the remainder of the cycle the motion of the die causes elastic offloading and loading of the drawn wire.

It was therefore proposed that if wire was drawn through two axially oscillated dies in succession, and the dies were oscillated in anti-phase, the wire would be drawn alternately through each die. Thus the drawing machine would never be subject to a load attributable to reducing wire in both dies simultaneously, and consequently the drawing load would be reduced. It was further proposed that the peak load in the first die would be unaltered by oscillations, but its mean load would be reduced by superposition. The motion of the two dies would induce a cyclic force in the wire between them, due to elastic off-loading, providing the cyclic component for this superposition mechanism. This would constitute a cyclic back tension applied to the second die. It was considered that at low frequencies the deformation would respond to the cyclic component of this back tension. By oscillating the dies in anti-phase, drawing would occur in the second die when the applied back tension was minimum. Thus the maximum load in the final wire would be reduced by

virtue of a reduced back tension in the second die.

The purpose of this research programme was to investigate the possibility of such a mechanism, and to determine the underlying mechanics of the process. It was therefore decided to investigate the effects of the following variables.

(1) Frequency of oscillation

(2) Amplitude of oscillation

(3) Stiffness of wire between the dies

The drawing machine used was a 2000 lbf bull block, converted to take two drawing dies. The axial oscillations were imparted to the die by two electro-hydraulic vibrators. Strain-gauge load cells were inserted between the die-holders and the vibrator rams to measure the die loads, and strain-gauges on the drum shaft measured the torque in the drum. Seismic mass velocity transducers measured the amplitude and phase relationship of the two dies, and the torsional amplitude of the induced drum oscillations. Drawing speed and die separation were also measured.

Initial tests revealed that the friction forces in the drum bearings rendered the drum torque cell measurements inaccurate, and its use was discontinued. Drawing loads were determined by the algebraic addition of the two die loads, and checked for various conditions with strain-gauges bonded directly to the wire.

In view of the mechanical nature of the superposition mechanism as revealed by prior research, it was thought unnecessary to investigate the effects of various reductions of area, material, or lubricant. Accordingly, these were held constant for the whole investigation.

In order to develop an understanding of the underlying mechanics of the process, it became necessary to study the mechanics of drawing wire through one axially oscillated die, since the process was less complex. Therefore a series of drawing tests were conducted, studying the effects on the magnitude of induced cyclic stress of such variiables as,

Amplitude

Frequency

Drawing Speed

The results of this investigation were compared with those obtained from an electrical analogue of the process. The insight gained from this investigation was then utilised in formulating a theoretical analysis for the initial case.

B2: Equipment

Die holders, loadcells, and friction slider.

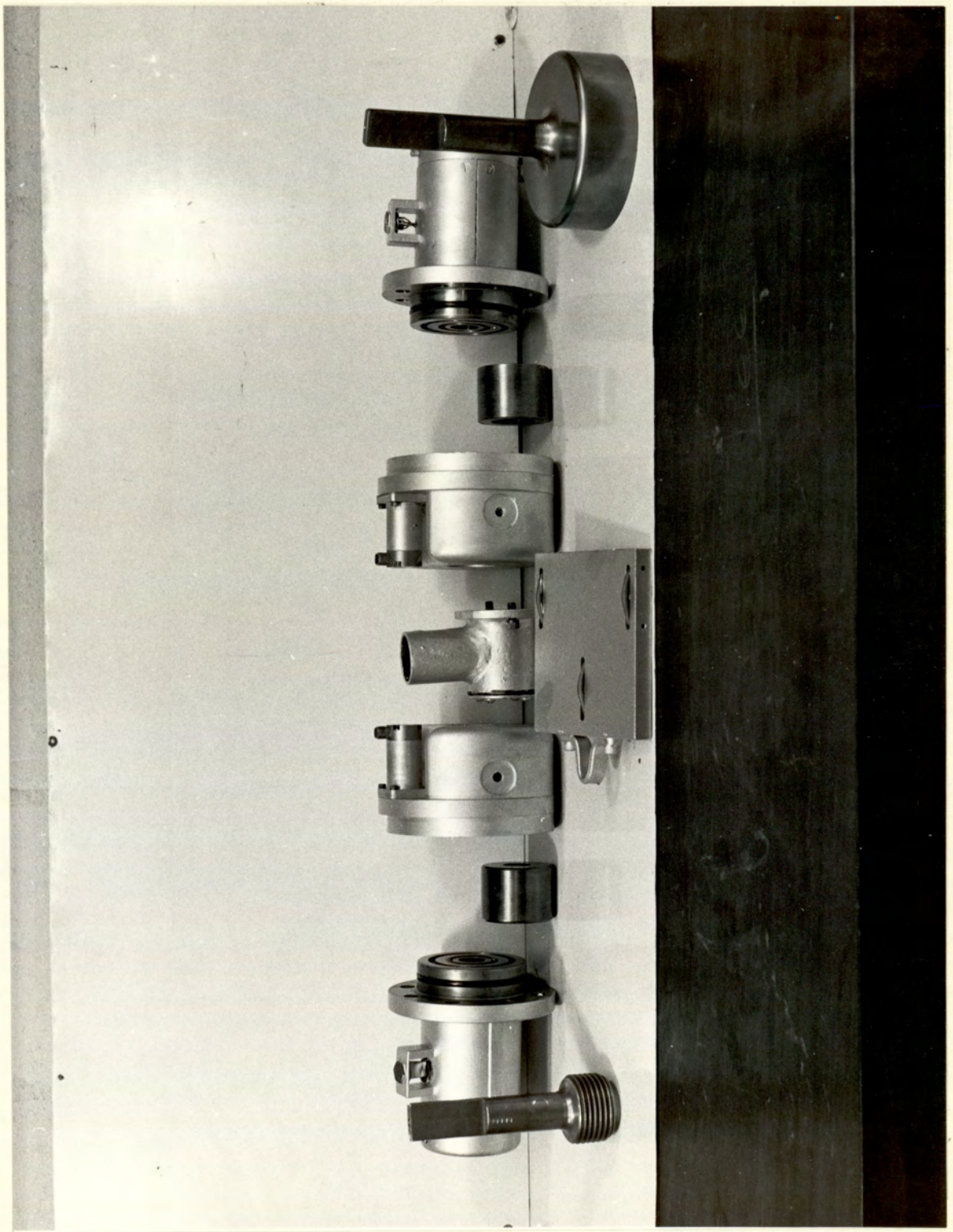

B2: Equipment

For the purposes of identifying the positions assigned to the various units, the following convention is used throughout this investigation. The position at which the wire receives its first reduction is designated 2, and the position of the second reduction as 1. Thus vibration transducer 2 is attached to the die-vibrator unit performing the initial reduction.

B21: Drawing machine

The drawing machine used was a horizontal bull-block of conventional design, but with extensive use made of plane bearings and close tollerances to ensure maximum rigidity. This was done to ensure the minimum loss of oscillatory energy to the machine. This type of machine was originally selected since it ensures a fixed free length of drawn wire. In order that the machine could accommodate two vibrators and dies, a rigid cantilever assembly was mounted on the die box table, upon which the vibrator holding flanges were mounted. The flange for die vibrator 1 was permanently attached to the root of the cantilever, whilst the position of vibrator flange 2 could be varied along the beam by means of a leadscrew.

A full specification of the drawing machine and detailed drawings of the modifications are given in appendix 1.

B22: Vibrators

The oscillations were imparted to the drawing dies by means of electro-hydraulic vibrators. These were essentially double acting jacks powered by hydraulic oil under pressure. The oscillations of the vibrators were controlled by servo

amplifiers driving hydraulic control valves. The controlling signals were generated by a low-frequency electronic oscillator, coupled with a phase shifting adaptor. These signals were fed into the servo amplifiers together with the outputs of displacement transducers mounted on the vibrator ram.

Complete specifications of the above items are given in appendices 2 and 3.

B23: Drawing Dies

A range of drawing dies were available for use on the drawing machine. Since previous investigators had shown that reduction of area was not an important parameter in determining the effectiveness of applied oscillations on the drawing process, it was decided to limit these investigations to one reduction of area in each stage. The previous investigations by Winsper[71] on this machine revealed that the cyclic forces induced in the drawn wire set up forced oscillations of the drum, rendering the analysis of the system more complex. It was therefore decided to use the smallest diameter die in the second reduction stage, thus minimising the stiffness of the drawn wire, and hence the magnitude of the cyclic forces. However, in order to ensure the largest possible range of die amplitudes before the dies separated from the wire, the overall reduction in area was made as high as possible with the existing dies, this creating the maximum stresses in the drawn wire.

The dies used were of radius profile, manufactured from tungsten carbide pellets, brazed into mild steel cases. Details of their geometry are given in[71]. Their throat diameters were 0.185 ins and 0.158 ins, giving, for wire of initial diameter 0.213 ins, reductions of 25% and 26.3% respectively, and an overall reduction of 44.8%.

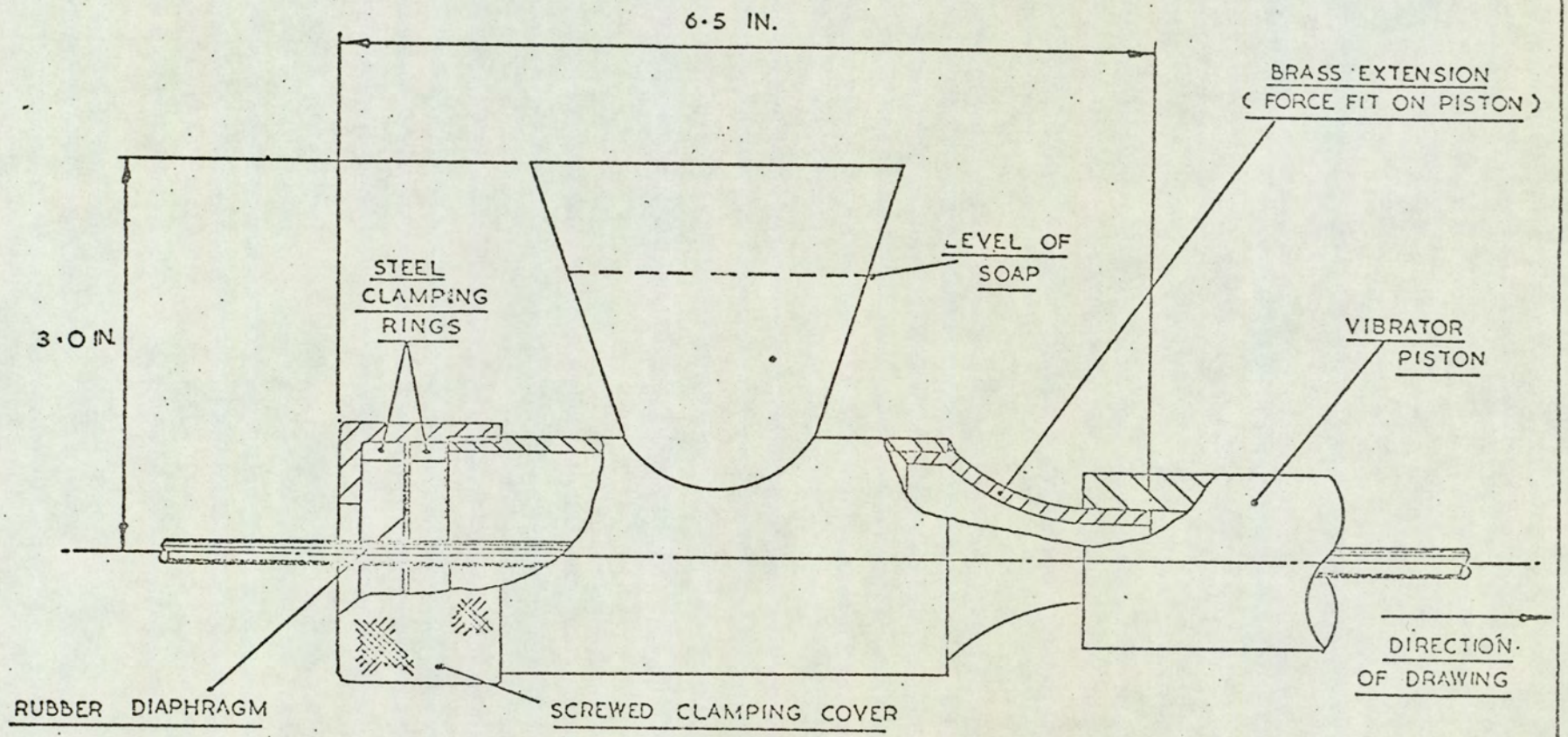

FIG. NO. 46. DETAILS OF SOAP CONTAINER

Figure 14 (from Winsper).

B24: Material

In view of the mechanical nature of the process evidenced by previous investigators, it was decided to limit the investigation to one material only. Mild steel EN2B was selected because of its commercial implications. A specification of this steel is given in appendix 13.

The wire was supplied in coils, taken from the same cast to minimise variations in drawing load, fully annealed and lubricated with a phosphate coating, with a diameter of 0.213 ins. Stress-strain curves for this wire in the undrawn and drawn state are presented in appendix 12.

B25: Lubricant

Since lubricants have generally been shown to have little influence on the effects of oscillations on metalworking processes, it was decided to use dry soap (sodium stearate) throughout the investigation. This choice was made partly because of the wide industrial application of this lubricant, and also because of its consistent lubricity, its ease of application, and cleanliness in use.

The soap was applied to the wire at die 2 by a soap bath shown in figure 14. A similar bath of smaller dimensions was attached to the end face of die-holder 1. The dimensions of this unit were minimised to ensure that the dies could be brought as close together as possible, when investigating the effects of wire length between dies.

B26: Die holders

During the course of the previous investigation two die-holders of identical design were manufactured. The materials used were alloy steel, Vibrac 45, and aluminium alloy, Duralumin.

These units were also used in this investigation, the steel unit with die 1 and the aluminium unit with die 2. Facilities for applying cooling water to the dies were provided in these units, but since the previous investigation has shown no tendency for over-heating when low frequency oscillations were applied, no cooling was applied in this investigation. The die-holders were designed to accept the attachment of seismic mass velocity transducers to their end face. Detailed drawings of the design are given in appendix 1.

B3: Instrumentation

Instrumentation.

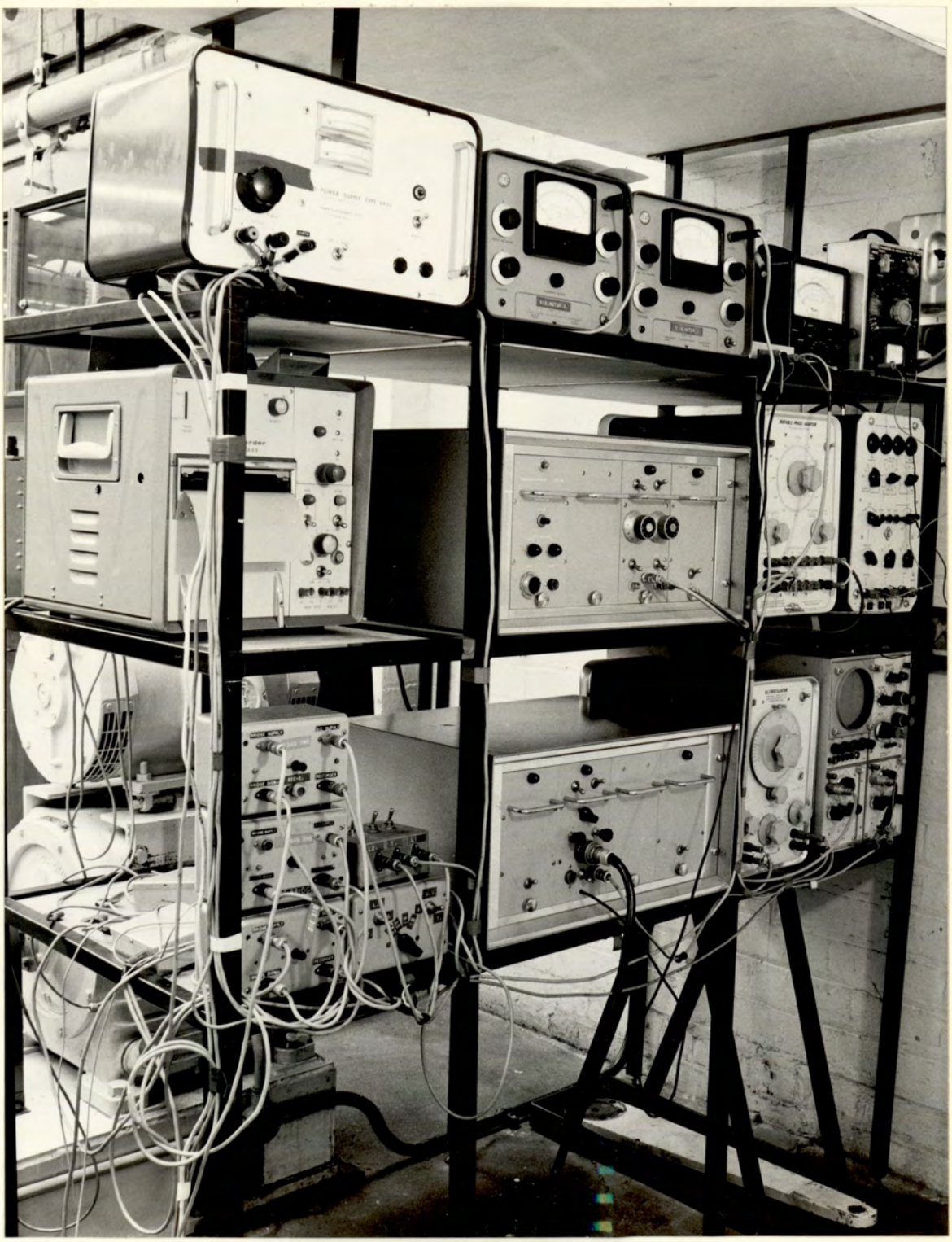

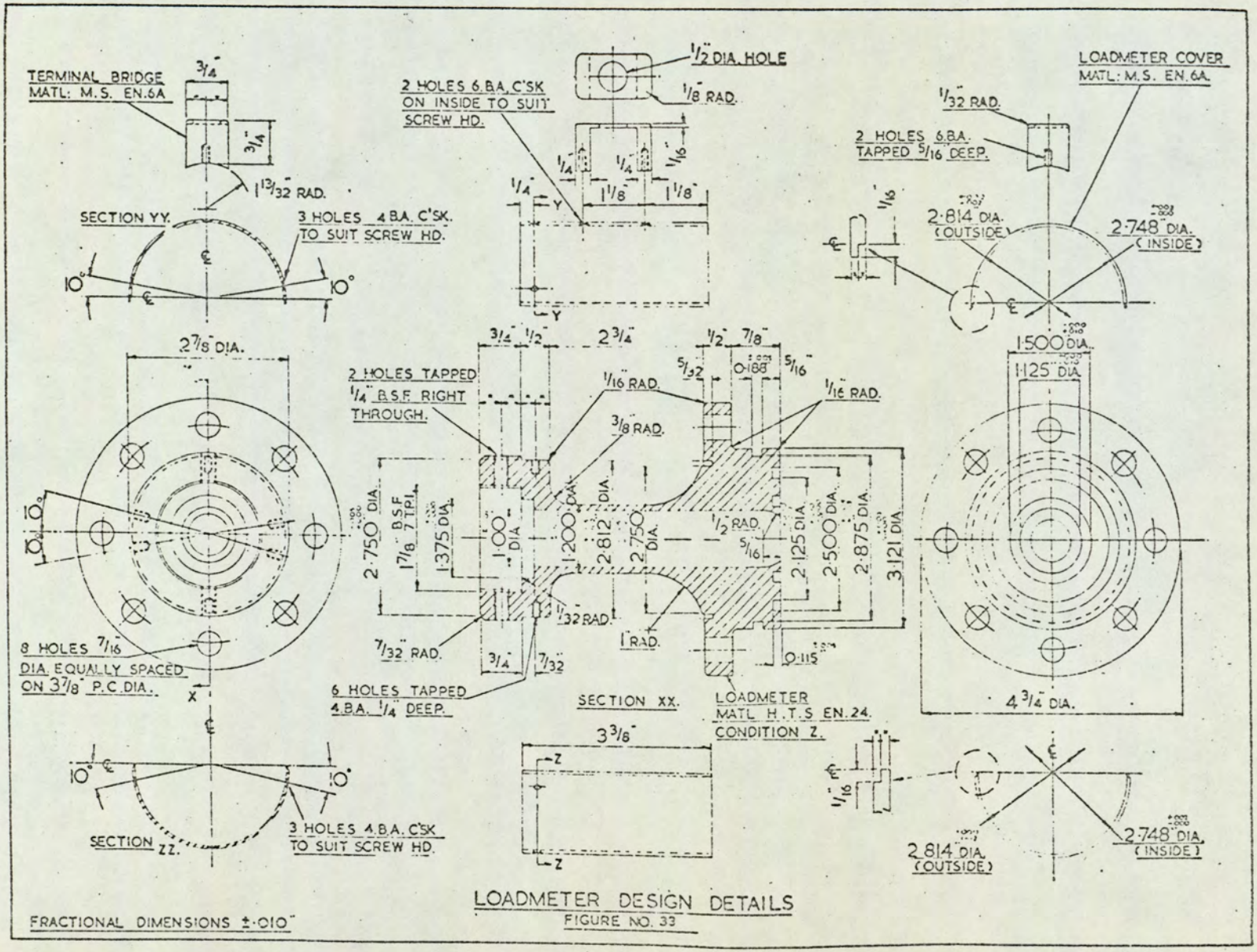

LOADMETER DESIGN DETAILS

FIGURE NO. 33

FRACTIONAL DIMENSIONS ±.010"

Figure 15 (from Winsper).

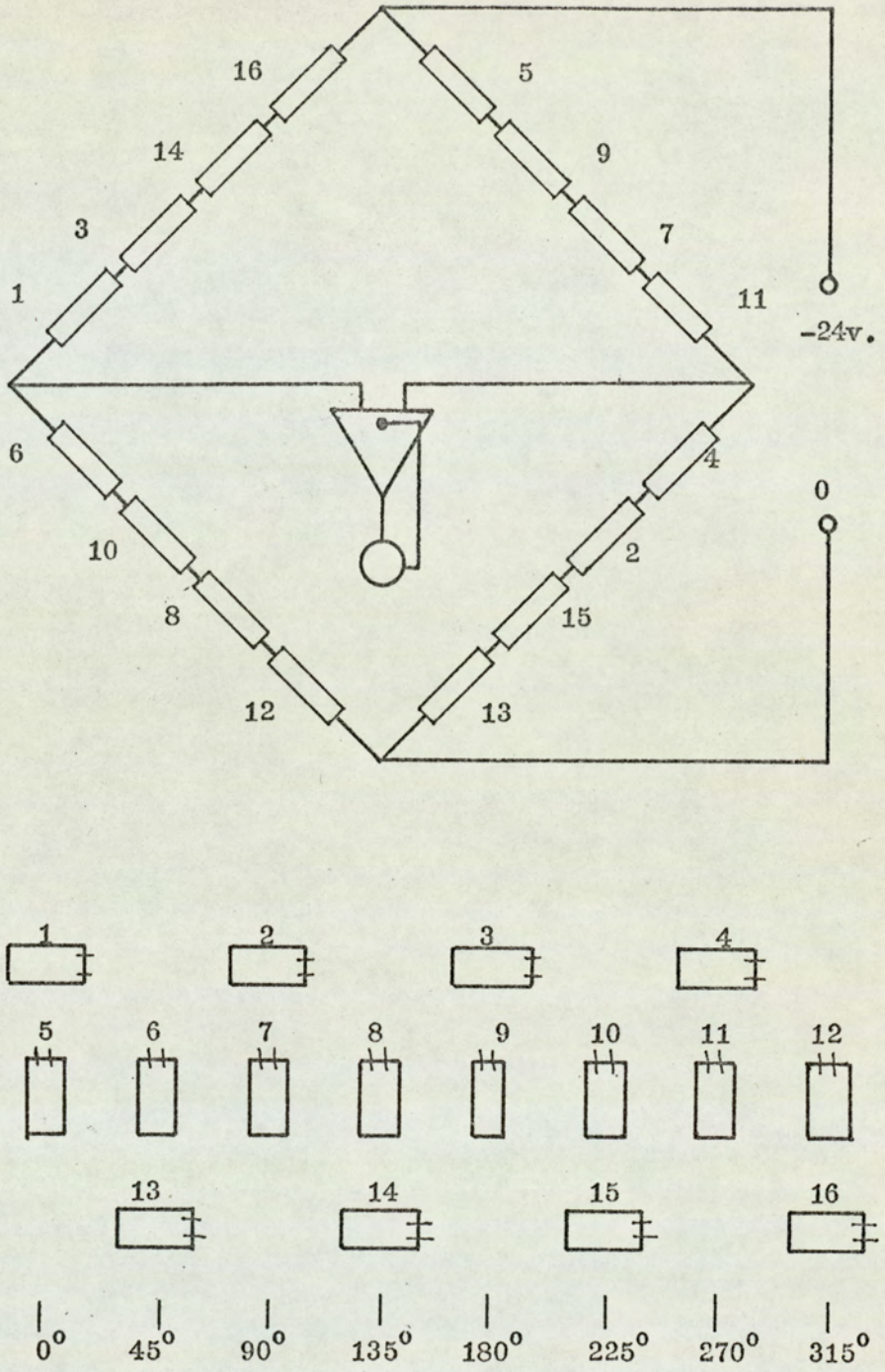

Figure 16: Disposition of gauges on die loadcell column and bridge circuit details.

B3 Instrumentation

B31: Loadcell design and construction

The load imparted to the die during drawing was measured by a loadcell placed between the vibrator ram and the die-holder. The loadcell was attached to the vibrator ram by means of screw threads, 1⅞ in B.S.F., and to the die-holder by eight ⅜ in B.S.F. bolts on a 3⅞ in diameter pitch circle.

One loadcell was available from the previous investigation, the design details of which are given in figure 15. This was manufactured from Vibrac 45 alloy steel, heat treated to a tensile strength of 120 tonf/in^2, the analysis of which is given in appendix 13.

The loadcell consisted essentially of a cyclinder 1 in. internal diameter and 0.1 in thick designed to strain 0.02% at the maximum load of 2,000 lbf. The cylindrical section was ground to size, and sixteen 75 ohm strain gauges were bonded to it in the manner described in Ref.[71], the configuration of the bridge being shown in figure (16). This loadcell was employed in position 1.

A second loadcell of identical design was manufactured from carbon steel, EN24, heat treated for a tensile strength of 80 tonf/in^2. The analysis of this material is given in appendix 13.

In this case the gauges had a resistance of 120 ohms each, since manufacture of the 75 ohm gauges had been discontinued. The construction of the bridge was identical to that described in[71]. This loadcell was employed in position 2.

B3a: Torque-cell

Facilities for the measurement of drawing load on the drum of the drawing machine were available from the previous

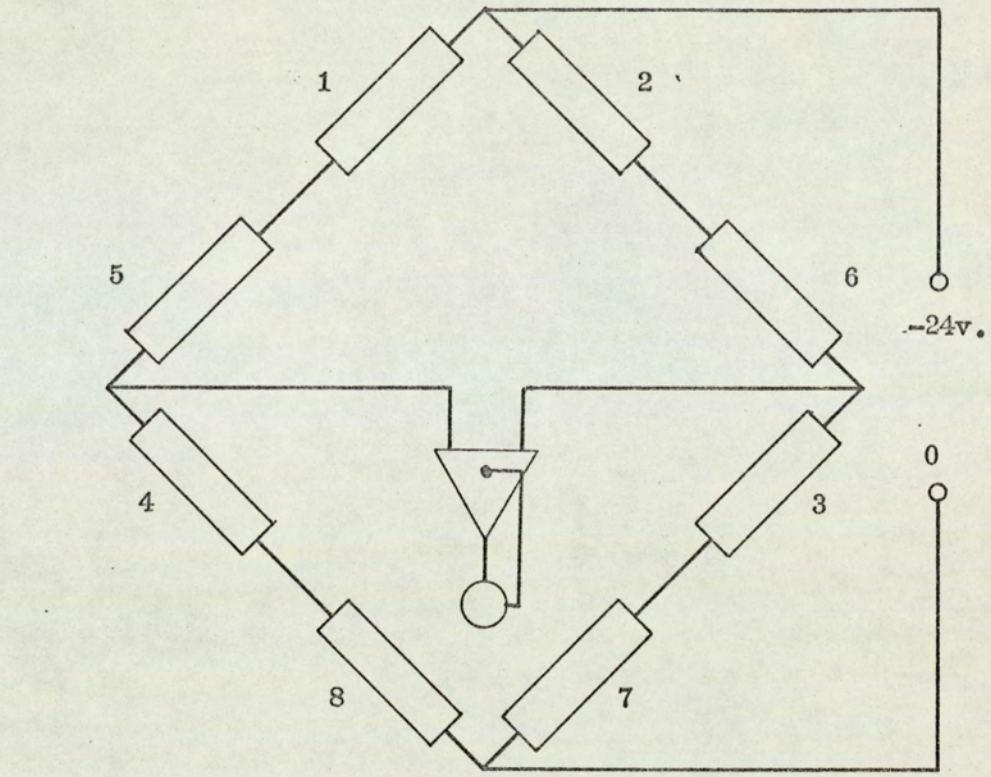

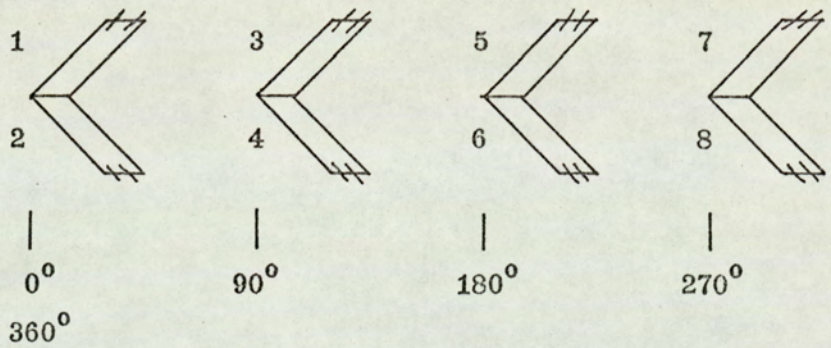

Figure 17: Disposition of torque gauges on drum drive shaft and bridge circuit details.

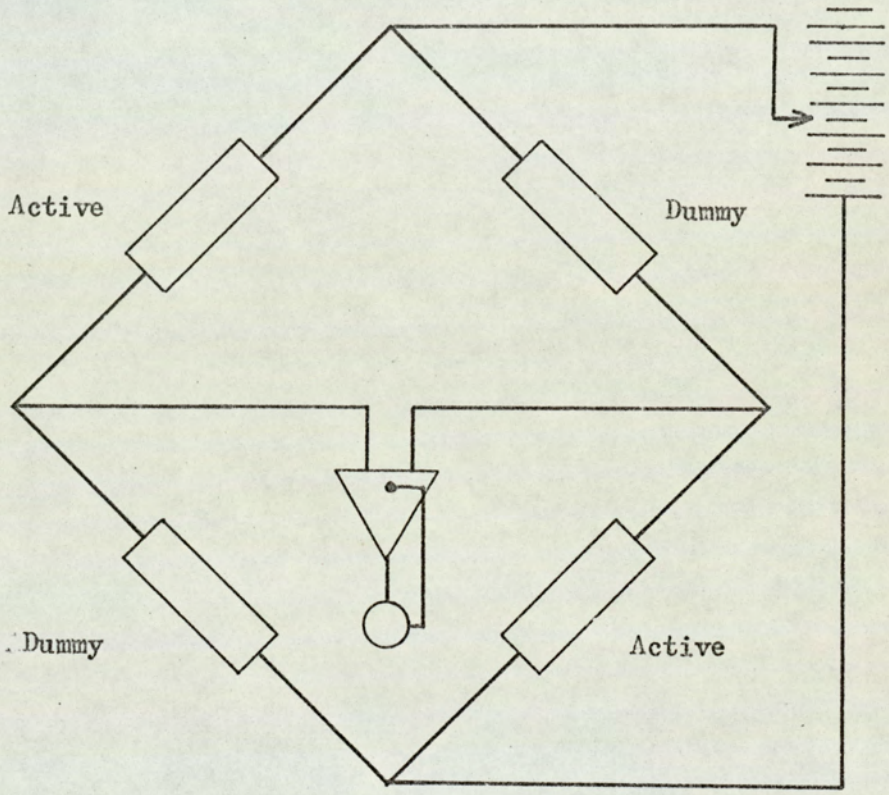

Figure 18 : Bridge circuit details for loadcell on wire.

investigation. A torque cell had been constructed on the drive shaft of the drum incorporating four foil torque gauges.

A poor junction in the connections of this bridge circuit had developed necessitating the rebuilding of the bridge. To this end four foil torque gauges, resistance 50 ohms were bonded to the drive shaft, equally spaced around the circumference. The method of preparation and attachment was identical to that described in[71]. The resin was allowed to cure for 8 hours under an infra-red lamp and the gauges were interconnected in the form of a wheatstone bridge, as shown in figure 17, thus ensuring the most effective compensation for temperature changes and bending. The bridge was encased in di-gel to ensure adequate moisture proofing.

The leads from the bridge were fed through the centre of the shaft to its free end, and connected to a slip ring assembly; the specification of this appears in Appendix 3. Both the loadcells and the torquecell were designed to operate with a 24v a.c. supply (see Appendix 3).

B33 Loadcell on Wire

In order to check the accuracy of the derivation of total drawing load from the die loads, it was necessary to measure directly the load in the drawn wire. This was achieved by bonding two foil gauges, resistance 100 ohms, along the axis of the wire, and diametrically opposed, in the manner described above. Two similar gauges were bonded to a length of previously drawn wire in an unstressed condition. These four gauges were interconnected in the manner shown in figure 18, producing a wheatstone bridge with compensation for both bending of the wire and temperature. Due to the greater strains experienced by the

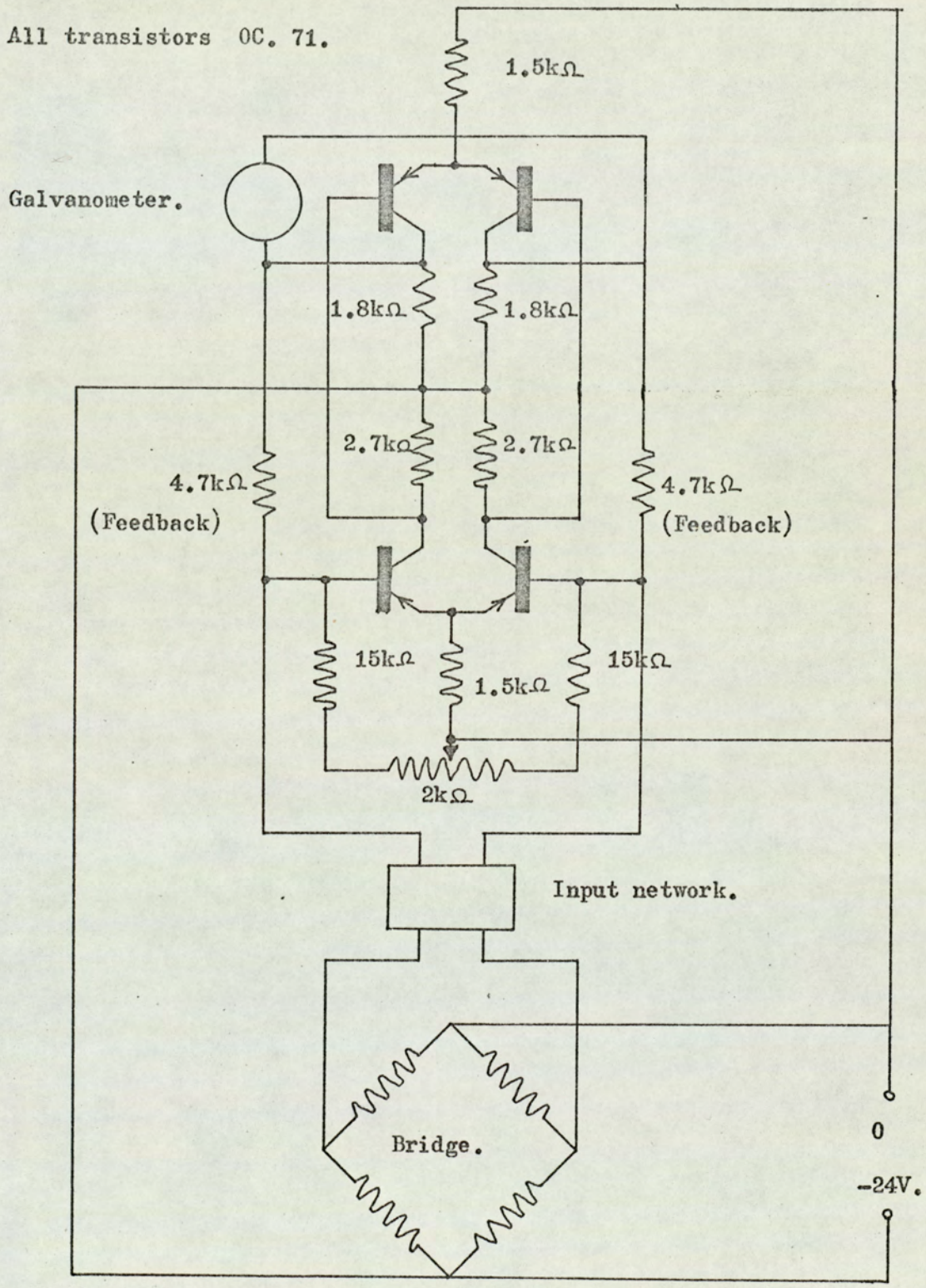

Circuit diagram for D. C. amplifier.

Figure 19.

drawn wire a reduced voltage was required for this bridge. This was provided by a variable d.c. supply, which was set to give a convenient deflection of the galvanometer under test conditions.

B34 D.C. Amplifiers

In order to obtain a flat frequency response in the recording equipment for the range 0-100 Hz. investigated, it was necessary to use galvanometers with a high natural frequency, and therefore low sensitivity. It was thus necessary to amplify the output of the bridges in order to obtain sufficient deflection on the galvanometers. For this purpose, a two-stage differential d.c. amplifier had been designed for use in the previous investigation, and this type of amplifier was used in this investigation also (figure 19).

The amplifiers were designed to operate with a 300 ohm bridge, using the same 24v supply as employed in the bridges. A balancing network was incorporated in the input of the amplifier using a variable resistance of 2000 ohms, thus eliminating the necessity to balance the bridge itself, and also providing some means of drift compensation. The overall gain of the amplifier was primarily dictated by the value of feedback resistance employed. With a 300 ohm bridge, a feedback resistance of 4.7×10^3 ohms produced a gain of approximately 100. In order to minimise zero drift, produced by either a small change in supply voltage, or temperature variations, the components in each stage were carefully matched, and the transistors in each stage were placed in a double heat sink. Furthermore, the design of the amplifier was such that the drifts caused by each transistor in a stage were self-cancelling. In order to produce a flat frequency response in the galvanometers,

a capacitance was inserted across the input to the amplifier, thus matching the frequency response of the amplifier to one galvanometer. The necessary value of capacitance was derived experimentally and is detailed later.

Preliminary testing of these amplifiers revealed that the gain of the amplifier used for loadcell 2 was low. This was the result of using a 480 ohm bridge in an amplifier designed to work with a 300 ohm bridge. To compensate for this, the gain of the amplifier was increased by changing the feedback resistances from 4.7×10^3 ohms to 6.3×10^3 ohms.

B35 Die and drum amplitude measurement

The instantaneous displacements of the dies were measured using linear seismic mass velocity transducers mounted on the end face of the die holders. The signals generated by these transducers, which is proportional to the instantaneous velocity, were fed into individual vibration meters, the impedances of which were matched to the transducers. These units incorporated amplification and integration facilities, such that the meter deflection could register the peak to peak velocity or displacement amplitude. An output socket on the instrument provided a signal proportional to the instantaneous velocity or displacement, suitable for displaying on an oscilloscope.

The periodic rotary displacement of the drum was measured using a torsional seismic mass velocity transducer, (Torsiograph) mounted on the free end of the drum. The signal generated from this was fed into the second input channel of the vibration meter 1, and processed in the same way. The meter deflection in this case registered the zero to peak amplitude of displacement or velocity.

The full specification for these items is given in Appendix 3.

B36 Recording Equipment

The outputs of the three bridge amplifiers and the vibration meter oscilloscope sockets were fed into a junction box. The signals from the bridge amplifiers passed through the junction box and onto their respective galvanometers in the ultraviolet recorder, via individual switches. The purpose of the junction box was to select from the five inputs combinations of two of these for display on the oscilloscope. The possible selections were:-

Any combination of two bridge signals.

The outputs of both vibration meters.

The output of vibration meter 1 with any bridge signal.

The aim of this facility was to provide an immediate display of the bridge signal waveforms, to set the correct phase relationship between the die oscillations, and to observe the phase relationships between the die oscillations and the various loads measured. The purpose of the switches in the ultraviolet recorder circuit was to identify each trace.

The oscilloscope was fitted with two vertical displacement amplifiers (Y1 and Y2) and one horizontal displacement amplifier (X), all of which would accept external signals. Thus, by inserting one output of the junection box into Y1 and the other into both Y2 and X, it was possible to have both signals displayed as time varying quantities, or one variable displayed as a function of the other. This latter facility provided an easy means of accurately setting the vibrations of

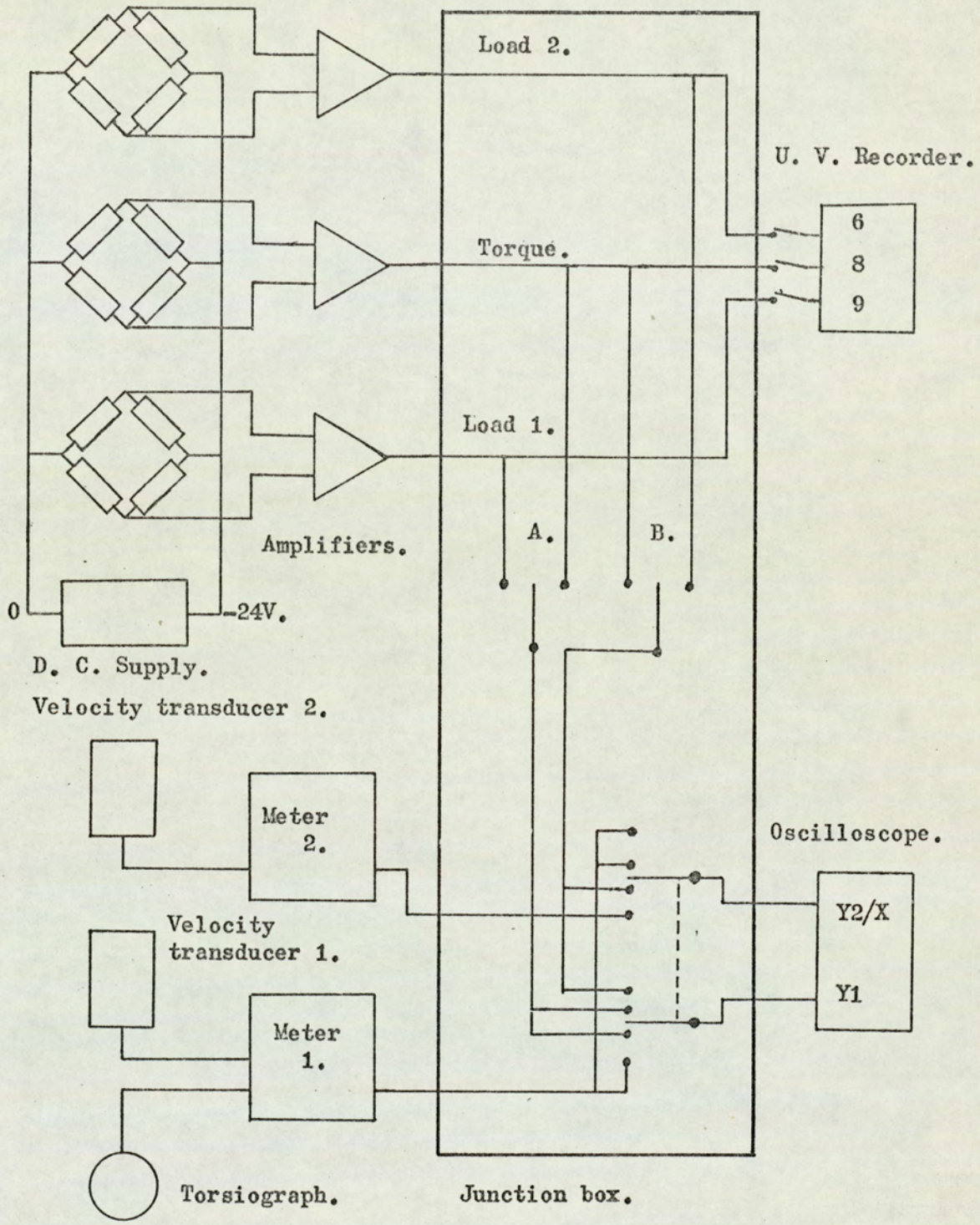

Instrumentation circuits.

Figure 20.

the dies in anti-phase. Since the alignment of one velocity transducer was in the reverse direction to the other, the signals from the vibration meters were in phase, when the dies oscillated in anti-phase. This resulted in a straight line of positive slope displayed upon the screen. Thus, to set the phase relationship between the dies it was simply necessary to adjust the phase shifting adaptor until such a figure was obtained.

All leads used in the transmission of transducer signals were carefully screened to minimise noise, and gold plated plugs were used wherever possible to reduce contact resistance. By these techniques the level of electrical noise on the recordings taken was undetectable.

A circuit diagram of the whole transducer system is shown in figure 20, and specifications of the ultraviolet recorder are given in Appendix 3.

B37 Measurement of Drawing Speed

A facility for measuring drawing speed was available from the previous investigation. Measurement was achieved by a determination of the period of time for the worm shaft driving the bull block drum shaft to turn through one quarter of a revolution, this period was recorded on a digital counter, details of which are given in Appendix 3. The counter was triggered in the following manner:-

Two circular cam plates were attached to the free end of the worm shaft, each with two diametrically opposed circular projections. The plates were attached such that the projections were 90^{o} apart. These cams operated two micro-switches, which activated the digital counter. When the cam

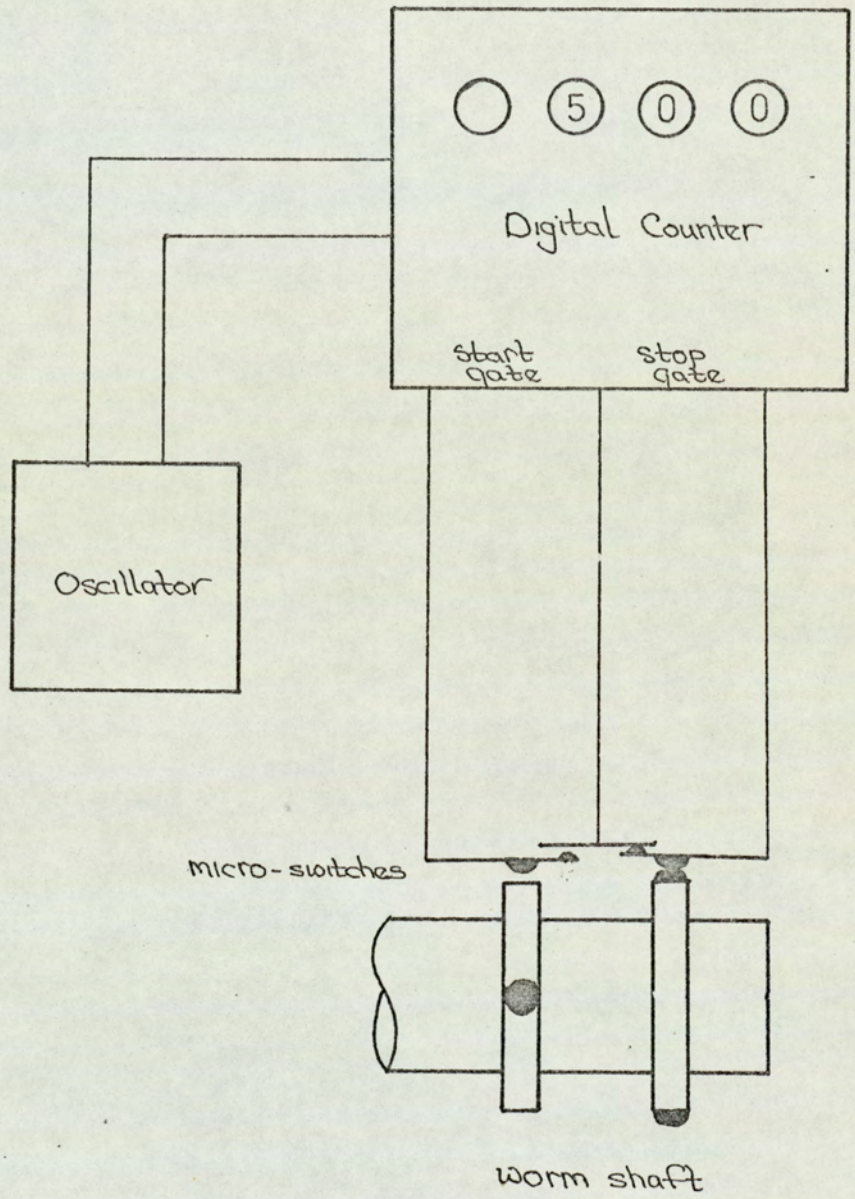

Measurement of drawing speed. Figure 21.

closed the micro-switch in circuit B (figure 21) an electrical pulse flowed in the circuit, putting the counter in the operate mode. The instrument then counted the number of pulses supplied by an external oscillator. Counting was arrested by the closure of the microswitch in circuit A. The instrument displayed the total count for a short period, and then automatically reset, ready for the next measurement cycle. The frequency of the external oscillator was set such that the reading on the counter was equal to the reciprocal of the drawing speed in ft/min. The setting of this frequency is detailed in Appendix 4.

B4: Calibration of Instrumentation

B4: Calibration of instrumentation

B41: Static calibration of loadcells

Both loadcells were calibrated in tension using a Denison dead-weight testing machine. In order that the load could be applied to the loadcells, two mild steel adaptors had been manufactured for use in the previous investigation. Both terminated in a flat tongue which could be gripped in the jaws of the testing machine, one being bolted onto the dieholder mounting flange, and one screwed into the female thread for attachment to the vibrator ram.

The amplifiers were allowed to warm up and stabilise for one hour prior to each test. The load was applied in increments of 200 lbf. up to a maximum of 2000 lbf., and reduced in a similar manner to zero. At each load increment a a record was taken of the galvanometer deflection. Several such tests were performed to check the repeatability of the measuring system. Typical calibration curves for both load cells are shown in Appendix 5.

When in use, loadcell 1 experienced a compressive load. However, it was considered acceptable to calibrate under tension, since the maximum strains were low (0.02%), and the equipment for testing under tension was more readily available.

B42 Static calibration of torquecell

Again, this was achieved using equipment already available from the previous investigation. The torque was applied by dead weights suspended on the end of a 24 in. torque arm mounted on the free end of the drum. To prevent rotation of the drum during loading, the drive pinion to the drum was locked in position with the torque arm horizontal.

After allowing sufficient time for the amplifiers to

stabilise, the loads were applied in increments of 100 lbf., up to a maximum of 800 lbf. This was equivalent to a torque of 1600 lbf ft., or a drawing load of 2120 lbf. The loads were decreased to zero in a similar manner. For each load increment a record was taken of the galvanometer deflection.

Initial calibration curves revealed an unacceptably high hysteresis loop, considered to be due to friction in the drum bearings. In an effort to overcome this, an extra load was applied manually after each load change, and then removed gradually. Thus the torquecell always approached the load from the same direction. This technique considerably reduced the hysteresis in the calibration curves. Several such calibration tests were conducted, and the mean taken to further reduce these effects. At this time it was still planned to employ the torquecell, since it was hoped that the induced oscillations of the drum would serve to reduce the magnitude of the friction drag on the drum under test conditions to an acceptable level.

The torque applied during these calibration tests was in the opposite sense to that experienced during drawing, the geometry of the machine prohibiting the application of torque in the correct sense. However, this was considered acceptable since the strains experienced by the torquecell were small.

This method of calibration applied both torsion and bending to the drum. However, the direct load on the drum was taken by the drum bearings, relieving the drive shaft of any bending stresses. Furthermore, the torquecell was constructed to compensate for bending stresses.

A typical calibration curve for the torquecell is given in Appendix 5.

B43 Dynamic calibration of loadcells

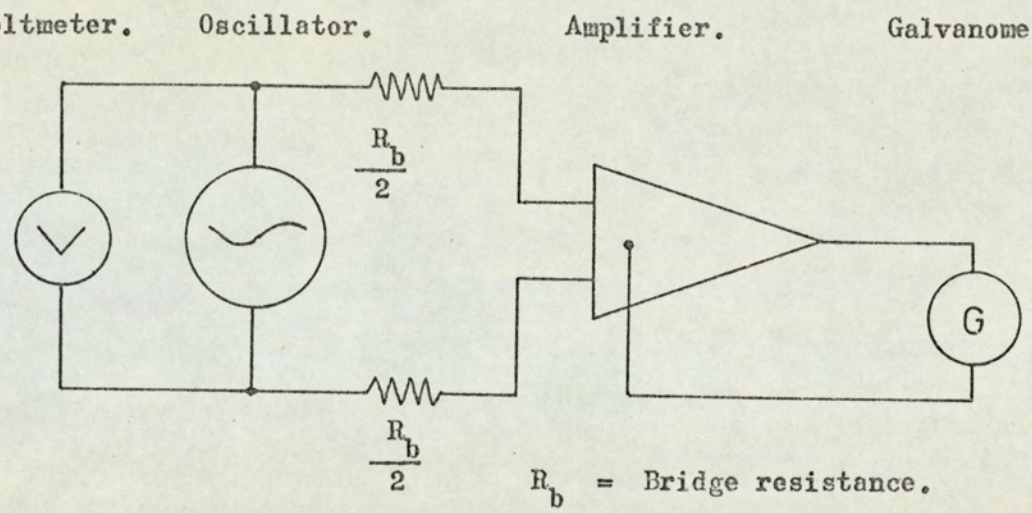

Circuit for dynamic calibration of load cells.

Figure 22.

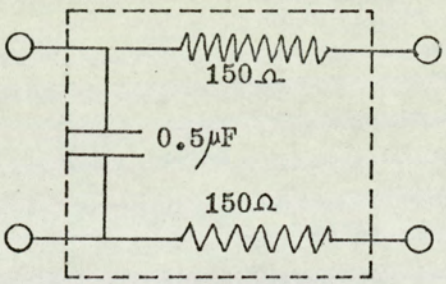

Load cells

From bridge.

To amplifier.

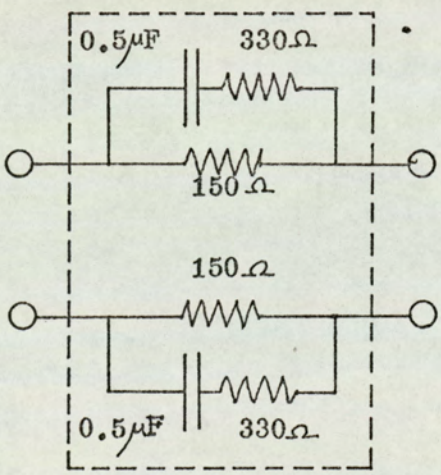

Torque cell

Amplifier input networks.

Figure 23

The purpose of these tests was to determine the requisite input network to each amplifier to produce a flat frequency response of the amplifier/galvanometer system in the range 0 - 200 Hz. This was achieved by applying an alternating voltage of variable frequency to the input of the amplifier, and recording the galvanometer peak to peak deflection. A diagram of the circuit is shown in figure 22. In order to reproduce the output impedance of the bridge circuit, represented by the oscillator, a resistor of half the bridge resistance was placed in series with the oscillator in both leads to the amplifier.

The input network requirements for each amplifier - galvanometer unit was determined by trial and error. The amplifier was allowed to stabilise over one hour, and the amplifier output balanced to zero. The oscillator was switched on, and a record taken of the galvanometer oscillations for coarse frequency increments in the range 1.5 - 200 Hz. The applied voltage was held constant for each test using the integral voltmeter of the oscillator, which previously had been calibrated. These tests were repeated for various capacitances placed across the input terminals of the amplifier, until a flat response (±2%) was obtained in the whole range of frequencies. A check was made using fine increments of 20 Hz. over the whole range, to ensure that the tolerance of 2% was not exceeded. This procedure was repeated for all three amplifier/galvanometer units. Figure 23 shows the type of input network which was adopted for each unit.

To ensure that there was no phase shift in the amplifier/ galvanometer system, the input signal to the amplifier also was fed to a second galvanometer with a natural frequency of

1000 Hz. Comparison of the phases of the two galvanometer traces revealed a phase lag of less than 2^{o} at the highest frequency.

B44: Calibration of vibration measuring equipment

Both linear velocity transducers and the Torsiograph were supplied with calibration charts. In the previous investigation the Torsiograph and velocity transducer 1 were recalibrated, and found to be accurate within the stated tolerances. It was therefore decided to accept the calibration data as supplied.

In order that a permanent record could be made of the die or drum displacement, the low impedance output of a vibration meter was fed to a galvanometer in the ultra-violet recorder. The connection to the vibration meter was via a coaxial plug, which could be quickly transferred to the other meter, thus providing the facility for recording any of the velocity transducer outputs.

B45: Measurement of referred inertia of die/loadcell assembly

As had been shown in the previous investigation, the inertia of the die, die holder, and loadcell resulted in a cyclic force in the loadcell when the die was oscillated. The effective mass of these elements was measured in the following manner:

The loadcell, die, and dieholder were assembled on the vibrator ram, and the vibrator oscillated at various frequencies and amplitudes, readings being taken of the forces induced in the loadcell. Considerable distortion of the loadcell signal was observed, especially at the higher frequencies. This was thought to be due to the natural oscillations of the complete

assembly, since there was a distinct periodicity in the distortion. To check this, the dieholder was struck with a soft hammer, and the resulting force induced in the loadcell recorded. The frequency of oscillation of this force was found to be approximately equal to the frequency of distortion.

To overcome this, the area under a half-period of these traces was measured using a planimeter, and the amplitude of an equivalent sine wave computed. The amplitude of this force was related to the acceleration amplitude of the die, computed from the die displacement and frequency. From this an effective mass for the system was obtained for each amplitude and frequency, and a mean taken. The effective mass of die assembly 1 was found to be 21.4 lb., and that of die assembly 2 13.8 lb., these figures being in close agreement with those obtained in the previous investigation.

B46: Moment of inertia of drum

In order to calculate from the torquecell signal the load applied to the drum, it was found necessary in Winsper's investigation to take account of the inertia force due to drum oscillations. To achieve this, the moment of inertia of the drum was measured experimentally by a trifiliar suspension technique. The value of the moment of inertia obtained, 53.77 lbf in. s^2., was adopted in this investigation.

B5: Experimental Procedure

B5: Experimental Procedure

B51 Non-oscillatory Drawing Tests

Prior to the main series of oscillatory tests, wire was drawn without die oscillation to determine the correlation between the die loads and the drum torque, and to obtain a value for the back pull factor of die 1.

Prior to the tests, the amplifiers were switched on and allowed to stabilise for one hour. A coil of wire was placed on the decoiler and a length was swaged to a diameter less than that of die 1. The wire was threaded through the two dies, which were at their maximum separation, and gripped in the drawing jaws of the bull block. The lubricant baths were filled with dry soap and the vibrators switched on to shake down the soap to the die orifices. The lubricant baths were refilled with dry soap. Prior to balancing the amplifier outputs, the drum was rotated in the drawing direction a short distance to ensure that the static friction torque in the drum bearings was in the correct sense for drawing. Also the wire was checked for slackness, so that no load was on the drum or the dies.

The compressors for the vibrators wer switched on and the actuator rams centralised. This was done to ensure that the drawing load was carried by the oil pressure, and not the oil seals of the actuator ram. A short length of wire was drawn at 2 ft/min, and a record taken of the die loads and drum torque. After drawing was stopped the drum was reversed a short distance, and then rotated a short distance in the drawing direction. Die 2 was moved forward a small distance by means of the centralising control. This was done to

release all loads in the system, and to set the friction torque on the drum in the required sense. A record was taken of the loadcell and torquecell galvanometer deflections to ensure that no drifting of the amplifier balance had occurred.

The ingoing wire to die 2 was cut and drawing recommenced, and records taken of the loads experienced. After a brief period the end of the wire passed through the orifice of die 2, and the load in the wire between the dies released. This caused a sudden increase in the load in die 1, and a drop in the drawing torque. Recordings were made of these new load levels, until the wire was completely drawn. The drum was stopped and the balance of each amplifier recorded.

Several such tests were conducted. Measurements were taken of the galvanometer deflections for both situations at random points along the trace. The results of a typical test are shown in table 24(a).

The back pull factor was calculated from the following equation, the derivation of which is given in Appendix 6,

$$L_1 = L_{10} - CL_2,$$

the symbols being defined in figure 24. The back pull factor C, has been shown by Sachs [106] to be theoretically a function of reduction of area, die geometry, and the coefficient of friction only, and therefore constant for a given pass. Experimental verificatioon of this has been provided by Baron and Thompsen [107], for example. Therefore, it was considered that the back pull factor could be considered constant for all values of back tension, and could be determined using one value of back tension only.

From the results of these tests the following observations were made.

The correlation between loadcell and torquecell loads was found to be poor. The load felt by the torquecell was consistently 8% to 10% higher than the sume of the die loads. Since during calibration the measuring systems were found to be repeatable and free from faults, and under test conditions they returned to their balanced settings, a fault in the measuring systems was discounted. It was therefore concluded that there must be an extra load on the system not accounted for. The back tension applied by the decoiler was dismissed since the bearings were checked and found to be free running.

Similarly the bending moment necessary to coil the wire round the drum was dismissed due to its low magnitude in relation to the discrepancy. It was therefore concluded that the dynamic friction in the drum bearings was the source of the extra applied force. To check this, the drum was rotated in the drawing direction without an applied load and a recording made of the friction torque. This was found to be equivalent to an average force of 40.2 lbf tangential to the drum surface. It was therefore concluded that in the loaded condition, the friction torque was most likely the source of the error in the load correlations. It was therefore decided not to use the torquecell in the non-oscillatory tests.

It was also noted that there was a variation of up to ±10% in the die loads recorded. Since the surface condition in the undrawn wire was not uniform, having sections with a phosphate coat and sections which were uncovered and rusty, it was considered that variations in the friction conditions

were a contributary factor in the fluctuating drawing loads. The wire was therefore returned to the manufacturers for a fresh phosphate coat to be applied.

When the wire was returned with a uniform phosphate coating, a similar drawing test was performed, the results of which are given in table 24(b). It was noted from these results that the friction conditions had been improved considerably, as evidenced by a fall in the drawing load in the intial die of approximately 7%, and a reduction in the back pull factor of 24%. However, no detectable improvement in the variation of drawing load was observed. It was therefore concluded that these variations were due to inconsistencies in the properties of the undrawn wire, and it was therefore decided to accept them.

During the subsequent test with die oscillations it was found that a considerable build-up and compaction of the soap lubricant had occurred in the interior of the vibrator ram, and the lubricant at the die orifice had fused. It was thought that this was evidence of the establishment of hydrodynamic lubrication, since the vibrator ram acted as a Christopherson tube building up high lubricant pressures at the die inlet and thus dragging a thick lubricant film into the deformation zone. In order to maintain consistent lubrication conditions during the investigation, this build-up of lubricant was periodically removed. However, to test the effect of this, at the end of the investigations when the lubricant had built up to some degree, a second non-oscillatory test was performed. The results of this test are given in table 24(c). A small decrease in drawing loads and back pull factor was observed, consistent with an improvement in friction conditions. Average

Drawing speed 2 ft./ min.

Load at Die 2. (L2). lbf.	Load at Die 1. (L1). lbf.	Load at Drum. (T). lbf.	Sum of Die loads. ($\leqslant$L). lbf.	Back pull factor. C.
654	445	1159	1099	0.601
690	431	1205	1121	0.590
665	431	1172	1096	0.613
654	445	1172	1099	0.601
654	445	1188	1099	0.601
Average values.				
663	449	1179	1103	0.601

Load in die 1 without back tension; ($L1_o$).

Average. $L1_o$ 838 lbf.

Maximum. $\hat{L1}_0$ 861 lbf.

Minimum. $\check{L1}_0$ 806 lbf.

Non-oscillatory drawing tests: Initial series. Figure 24(a).

Drawing speed 2 ft./ min.

665	403	-	1068	0.457
581	445	-	1026	0.459
629	417	-	1046	0.463
605	445	-	1050	0.442
629	431	-	1060	0.447
641	417	-	1058	0.460
605	431	-	1036	0.464
Average values.				
625	425	-	1051	0.456

$L1_0$ (average) = 712 lbf; $\hat{L1}_0$ = 750 lbf; $\check{L1}_0$ = 681 lbf.

Non-oscillatory tests: After new phosphate coat. Figure 24(b).

Drawing speed 2 ft./ min.

L2. (lbf).	L1. (lbf).	$\lesssim$L. (lbf).	C.
605	417	1022	0.436
593	417	1010	0.446
635	403	1038	0.438
630	410	1040	0.430
617	417	1034	0.428
630	396	1026	0.452
617	403	1020	0.450
Average values.			
618	409	1027	0.440

$L1_0$ (average) = 381 lbf; $\hat{L1}_0$ = 695 lbf; $\check{L1}_0$ = 674 lbf.

Non-oscillatory tests: With compacted lubricant. Figure 24(c).

Averaged values from last two series:

L2 = 621 lbf.

L1 = 415 lbf.

$\lesssim$L = 1039 lbf.

C = 0.448.

L2. (lbf).	L1. (lbf).	ΣL. (lbf).	C.
556	389	945	0.404
550	382	932	0.421
556	382	938	0.417
556	382	938	0.417
539	389	928	0.404
550	382	932	0.421
556	382	938	0.417
550	382	932	0.421
562	375	937	0.425
556	389	945	0.404
Average values.			
383	553	936	0.415

$L1_0$ (average) = 614 lbf. $L1_0$ = 625 lbf. $L1_0$ = 598 lbf.

Non-oscillatory tests: 5 ft./ min. Figure 24(d).

values of loads and back pull factor were taken from the two tests in order that the values were most representative of all lubrication conditions.

A similar series of test were conducted for a drawing speed of 5 ft/min, the results of which are given in table 20(d). A further decrease in die loads and back pull factor was observed here, which was again attributed to enhanced friction conditions, resulting from the increased strain rate of the lubricant film.

During the non-oscillatory tests it became apparent that it was not possible to maintain the drawing speed constant at 2 ft/min. Consequently, this figure is merely nominal (±10%). This inaccuracy was thought to be due to setting the reduction in the variable speed drive to below its rated range. This problem was not so severe at 5 ft/min drawing speed.

B52 Oscillatory drawing tests

Before the commencement of each oscillatory test the loadcell amplifiers and electronic equipment were switched on and allowed to stabilise for one hour. At the end of this period the outputs of the loadcell amplifiers were balanced with the loadcells in the unloaded state, and the torquecell feeling the static friction torque set up by rotating the drum a short distance in the drawing direction.

The hydraulic compressors were switched on, and the vibrator rams centralised. The frequency of oscillation was selected on the oscillator, and the vibrators switched on. The requisite amplitude was set for each vibrator, and using the oscilloscope, the phase angle between the vibrators was set at 180°, in the manner described previously.

The vibrators were switched off, the balance of the

amplifiers checked, and a record taken of the unloaded galvanometer deflections. A short length of wire was drawn under non-oscillatory conditions, and a record taken of the new galvanometer deflections. With drawing still proceding, the vibrators were again switched on and adjustments made to the amplitude, phase, and drawing speed, where necessary. (With high amplitudes of oscillation the reduction in drawing load caused an increase in the drawing speed, which was corrected.) A record was taken of the load cell, torquecell, and torsional amplitude signals. At the end of each test the load and torquecells were checked in the unloaded state to ensure that no change in the amplifier balance has occurred.

In the early stages of these tests it became apparent that the force variation in the final drawn wire obtained from the torquecell was unacceptable, since it was consistently higher than that obtained from the sum of the die loads. This error was attributed to friction in the drum bearings. Consequently, use of the torquecell was discontinued for the remainder of the tests. In order to check the derivation of the force in the drawn wire, it was therefore necessary to mount a strain gauge bridge on the wire itself. This was done at selected frequencies and amplitudes.

The signal from this bridge was calibrated using the die loadcell signals. With the wire in the unloaded state, the amplifier outputs were balanced and a record taken of the galvanometer null positions, a short length of wire was drawn and a record taken of the new galvanometer deflections. The loadcell was released and the amplifier balance checked. From the die loadcell signals, the force in the drawn wire was computed. A calibration coefficient for the bridge on the

wire was obtained by dividing the computed load by the galvanometer deflection. The assumption that the calibration curve for this bridge was a straight line, was checked in the following manner. After a length of wire had been drawn as described above, the recorder was left running, and the load in the wire was gradually released by moving the dies slowly in the direction of the drum. In this way a calibration curve was constructed for a range of loads up to the total drawing load. It was found that as expected the calibration curve for the bridge was linear.

Once calibrated, the bridge was used under oscillatory conditions to record the fluctuating total drawing load directly.

B53 Analysis of loadcell and torquecell signals

A result of the high inertia forces generated when the dies and drum were set into oscillation was that the forces detected at the loadcells and torquecells were not those applied by the wire alone, but the vector sum of the applied loads and inertia forces. Therefore it was necessary to calculate the latter component of force, and subtract vectorially from the observed value.

Computation of the inertia force felt by the loadcells was achieved using the effective mass of the die assembly, which was determined experimentally, in the equation:-

$$\text{Inertia force amplitude} = \text{effective mass} \times \text{acceleration}$$

$$= mX\omega^2$$

In using the experimental value of effective mass, it was assumed that the relative amplitudes of each particle in

the die assembly were identical in the drawing situation, and in the test conditions when the effective mass was determined. However, in the drawing situation, a further cyclic load is applied to the assembly by the wire. This will result in a second component of cyclic straining of the assembly, producing a different distribution of particle amplitude, and hence a different effective mass. However, it was considered that the assembly was sufficiently stiff to ensure that any change in amplitude along the length of the assembly, and resulting from elastic strain, would be minimal.

The phase relationship between the die motion, (and hence acceleration), and the induced die load was checked at several amplitudes and frequencies. In cases it was found that the die load was at a peak when the die was at the furthest position from the drum. Hence to obtain the load in the die applied to the wire, the inertia force amplitude was added to the maximum die load, and subtracted from the minimum die load.

The cyclic force in the drawn wire, $\tilde{F}$, was determined from the equation of oscillatory motion for the drum:

$$I\ddot{\theta} + c\dot{\theta} + s\theta = -\tilde{F}R$$

θ here is considered positive in the direction of drawing. Since the drum motion was sinusoidal, the equation was transformed to relate the amplitudes of force and rotational displacement.

$$s\hat{\theta} - I\omega^2\hat{\theta} + jc\hat{\theta} = \frac{-\Delta FR}{2}$$

The first term in this equation represents the amplitude of torque measured at the torque cell, the second the amplitude of inertia torque, the third the amplitude of damping torque,

and final term the amplitude of torque applied to the drum by the wire. An initial calculation showed that the damping torque was insignificant and therefore was not included. Thus the torque amplitude in the drawn wire was taken to be the difference between the observed torque amplitude and the computed inertia torque amplitude.

B6: Results of Oscillatory Tests

B6: Results of Oscillatory Tests

The experimental data obtained from the oscillatory tests are presented in graphical and tabular form at the end of this section.

The initial series was conducted with the dies separated by a maximum distance of 18 in., with both dies oscillating in anti-phase with the same amplitude and frequency. Graphs 1 to 4 relate to this series, showing the effect of increasing die amplitude, up to die separation from the wire, on the maximum and minimum die loads, and the computed total drawing force. They corresponded to oscillation frequencies of 40, 60, 80, and 100 Hz respectively. The continuous curves refer to results obtained at 2 ft/min drawing speed whilst the broken curves in graphs 2 to 4 correspond to a drawing speed of 5 ft/min.

The results of a similar series of tests, but with the dies at their minimum separation of 10 in., are shown in graphs 5 to 8. These similarly correspond to oscillation frequencies of 40, 60, 80 and 100 Hz respectively. The drawing speed in this and subsequent tests was 2 ft/min.

To investigate the effects of oscillating one die only, two tests were conducted at a frequency of 60 Hz and a die separation of 10 in. Graph 9 shows the effect of increasing amplitude up to die separation from the wire when die 1 only is oscillated. Graph 10 shows the effect of increasing amplitude when die 2 only is oscillated.

Finally, a test was conducted at a frequency of 60 Hz and die amplitudes of 5×10^{-3} in. peak to peak, to investigate the effects of varying the separation between the two dies.

Graph 11 shows the maximum and minimum forces observed when the die separation was varied from 18 in to 8 in.

The results of the tests incorporating a strain gauge bridge bonded directly onto the drawn wire and conducted to check the validity of the derivation of the total drawing force, are presented at the end of the tabulated results.

The subsequent graphs in this section were constructed from the data obtained from the above mentioned tests.

The relationship between back tension and die load at the instant of drawing in die 1 is shown in graphs 12 to 14. The instant of drawing corresponds to the condition when the back tension is minimum and the die load maximum. The continuous lines on these graphs represent the relationship between back tension and die load for steady state drawing, assuming a constant back pull factor. Graphs 12 and 13 relate to die separations of 18 in and 10 in respectively. Graph 14 shows this relationship for one die oscillating only, and for a variable separation of the two dies.

The magnitudes of the cyclic components of die loads and total drawing loads are shown in graphs 15 and 16. They correspond to 18 in. and 10 in. die separation respectively, with frequencies of oscillation of 40, 60, 80 and 100 Hz.

The effects of amplitude and frequency on the maximum total drawing force are shown in graph 17.

Finally, the effects of amplitude, stiffness of wire between dies, and frequency on the magnitude of the cyclic component or force in the wire between the dies, is shown in graph 18.

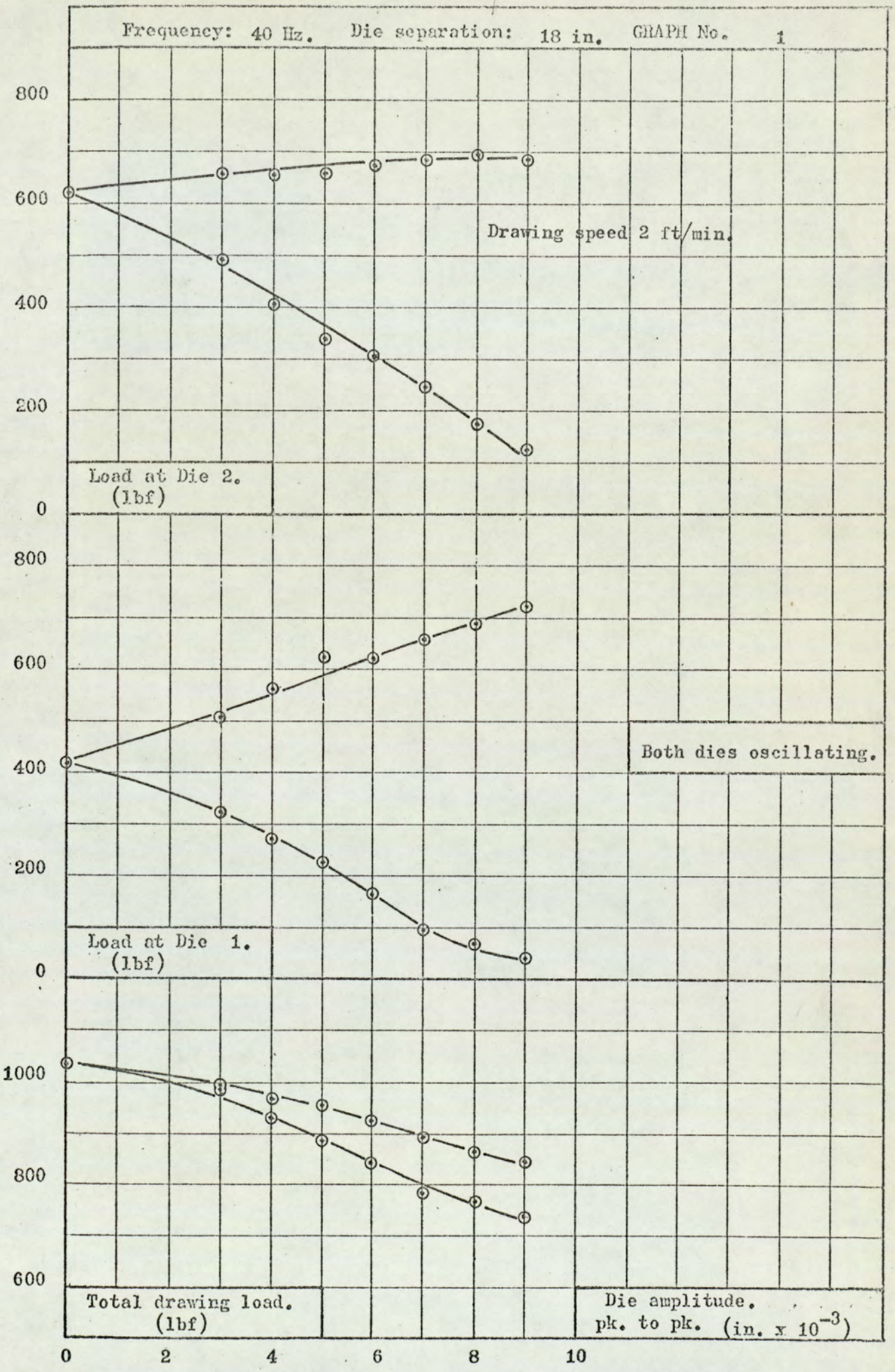
Frequency: 40 Hz. Die separation: 18 in. GRAPH No. 1
800
600
400
200
0
Drawing speed 2 ft/min.
Load at Die 2. (lbf)
800
600
400
200
0
Both dies oscillating.
Load at Die 1. (lbf)
1000
800
600
Total drawing load. (lbf)
Die amplitude. pk. to pk. (in. x 10^{-3})
0
2
4
6
8
10

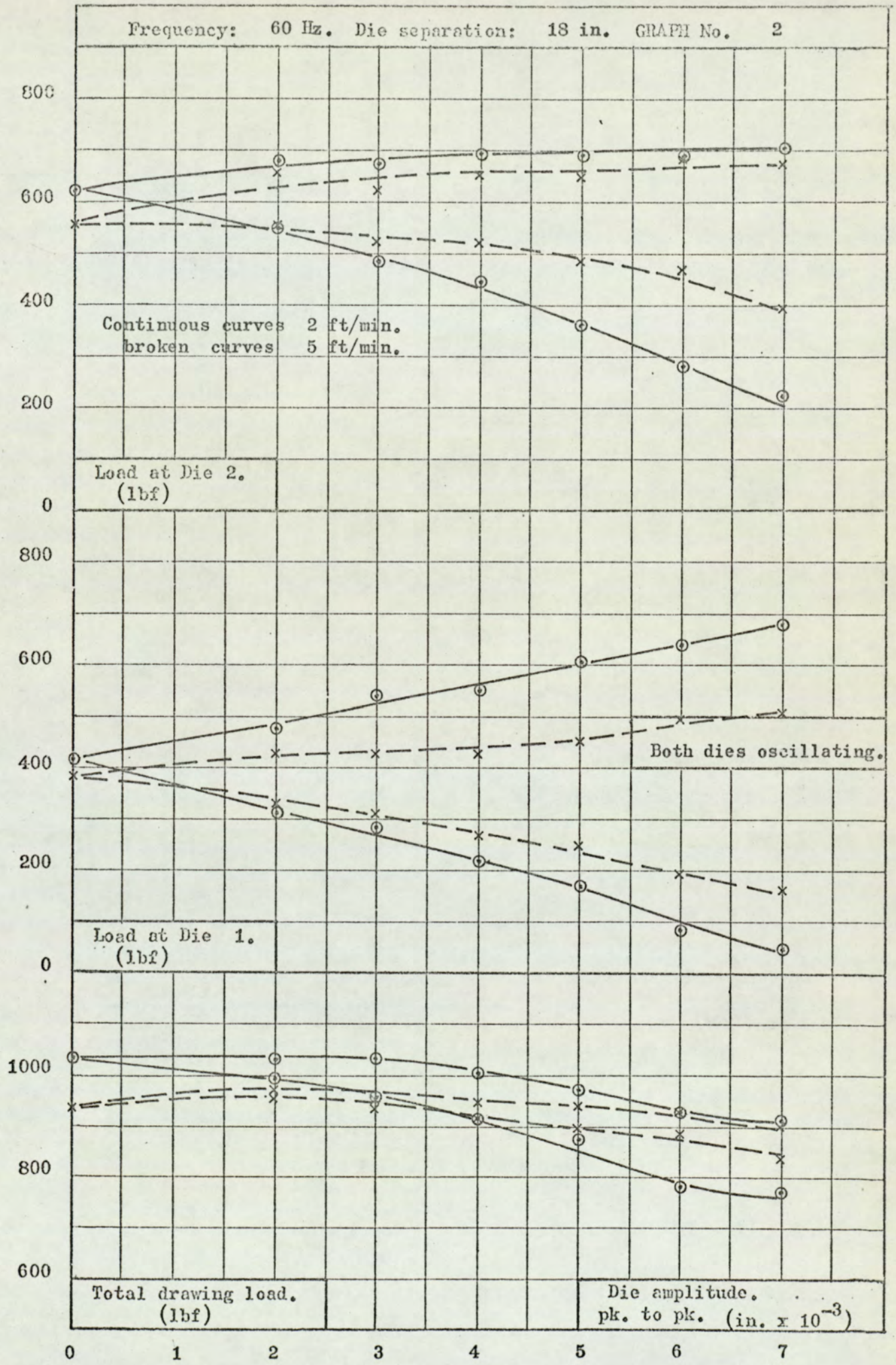
Frequency: 60 Hz. Die separation: 18 in. GRAPH No. 2
800
600
400
200
0
Continuous curves 2 ft/min.
broken curves 5 ft/min.
Load at Die 2.
(lbf)
800
600
400
200
0
Both dies oscillating.
Load at Die 1.
(lbf)
1000
800
600
Total drawing load.
(lbf)
Die amplitude.
pk. to pk. (in. x 10^{-3})
0
1
2
3
4
5
6
7

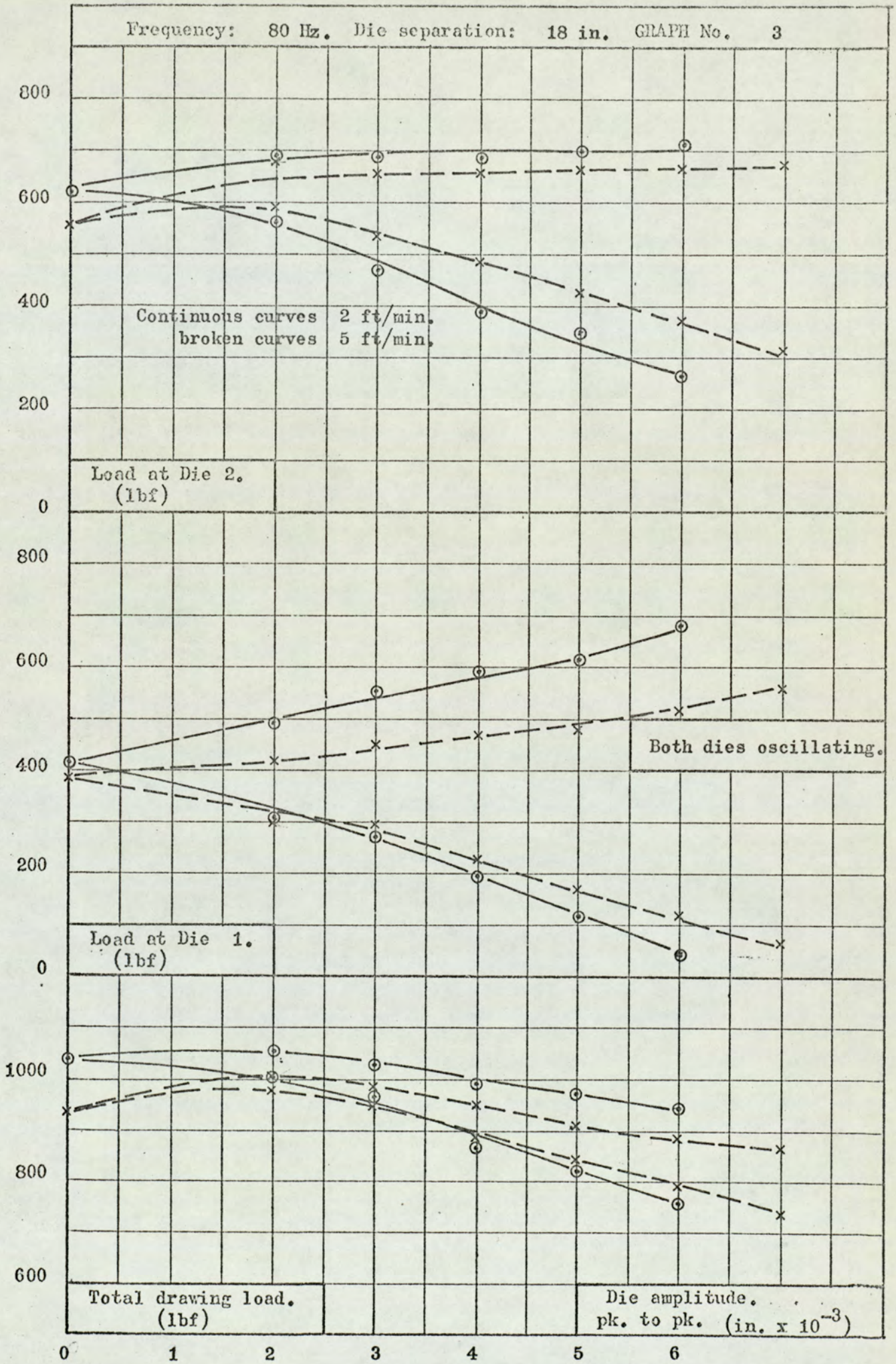
Frequency: 80 Hz. Die separation: 18 in. GRAPH No. 3
800
600
400
200
0
Continuous curves 2 ft/min.
broken curves 5 ft/min.
Load at Die 2.
(lbf)
800
600
400
200
0
Both dies oscillating.
Load at Die 1.
(lbf)
1000
800
600
Total drawing load.
(lbf)
Die amplitude.
pk. to pk. (in. x 10^{-3})
0
1
2
3
4
5
6

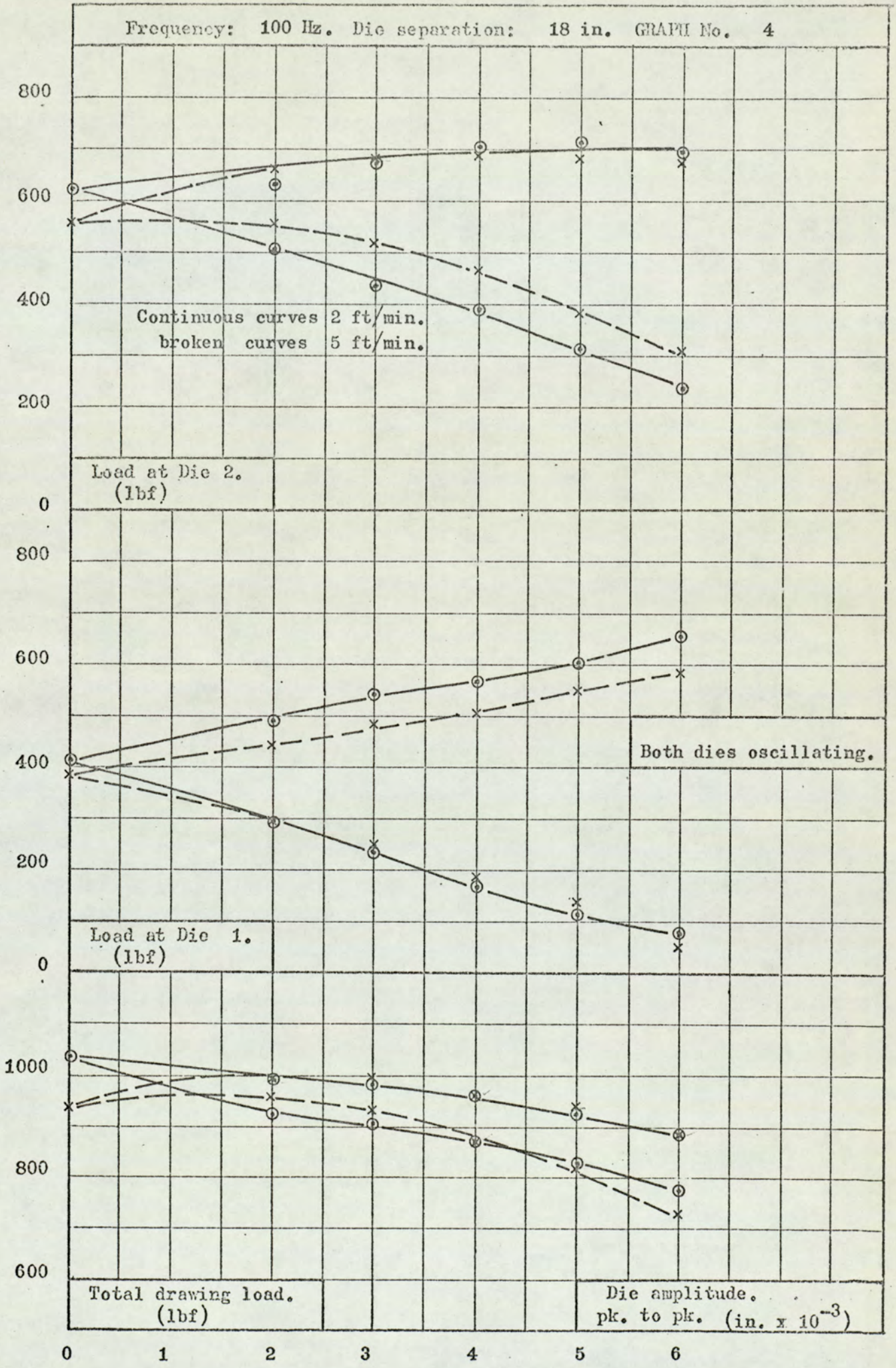
Frequency: 100 Hz. Die separation: 18 in. GRAPH No. 4
800
600
400
200
0
Continuous curves 2 ft/min.
broken curves 5 ft/min.
Load at Die 2.
(lbf)
800
600
400
200
0
Both dies oscillating.
Load at Die 1.
(lbf)
1000
800
600
Total drawing load.
(lbf)
Die amplitude.
pk. to pk. (in. x 10^{-3})
0
1
2
3
4
5
6

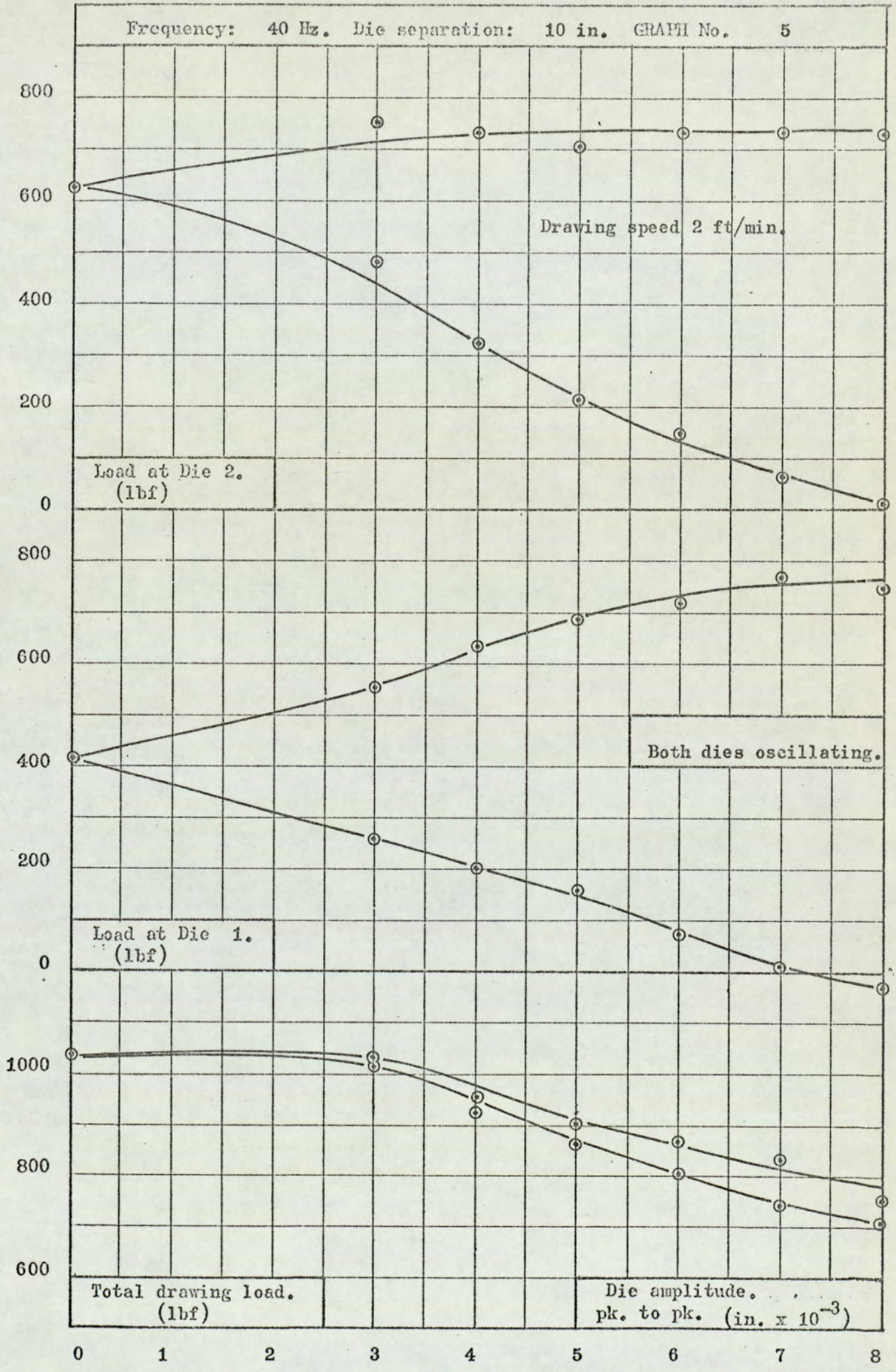
Frequency: 40 Hz. Die separation: 10 in. GRAPH No. 5
800
600
400
200
0
Drawing speed 2 ft/min.
Load at Die 2. (lbf)
800
600
400
200
0
Both dies oscillating.
Load at Die 1. (lbf)
1000
800
600
Total drawing load. (lbf)
Die amplitude. pk. to pk. (in. x 10^{-3})
0
1
2
3
4
5
6
7
8

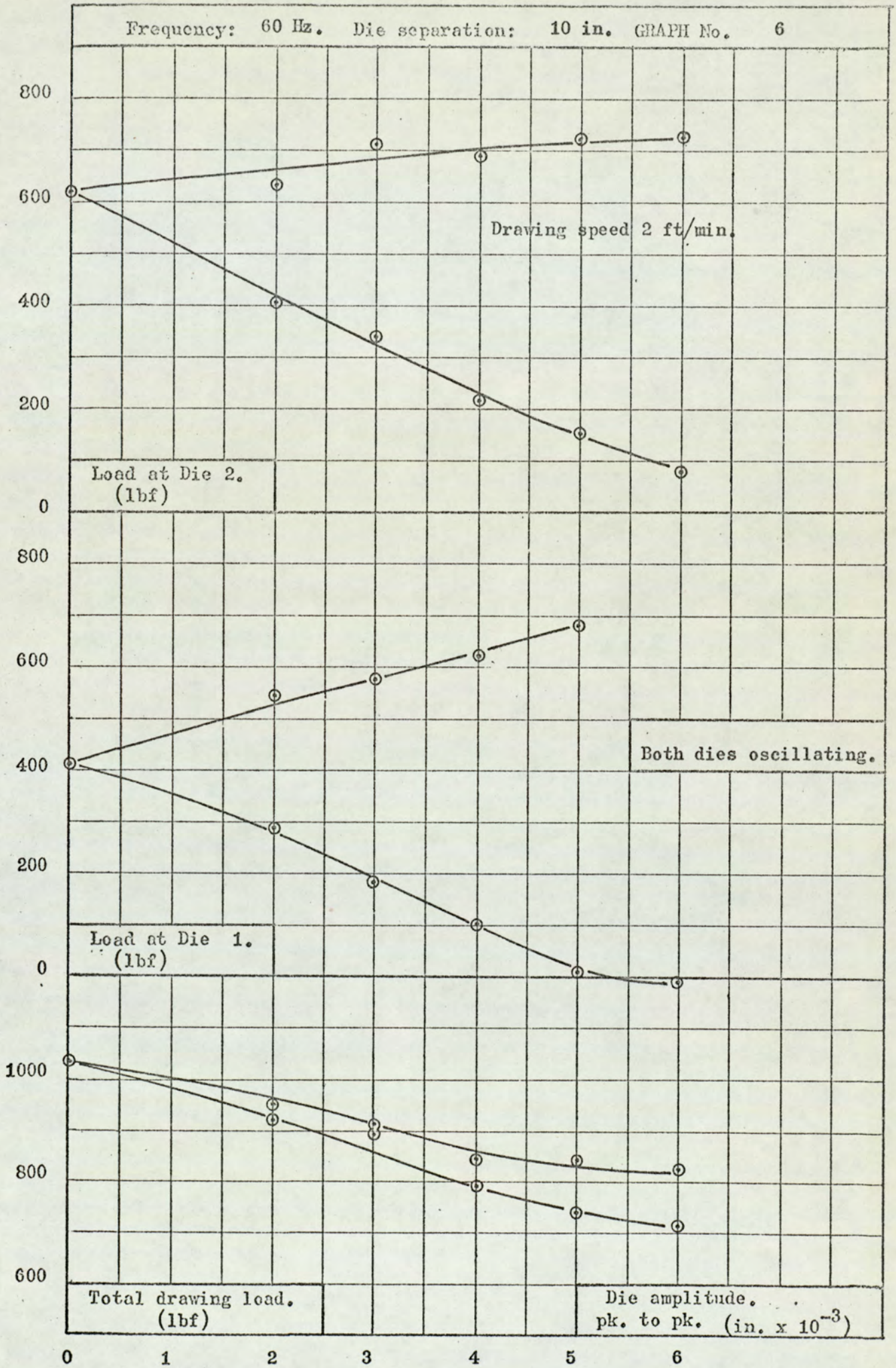
Frequency: 60 Hz. Die separation: 10 in. GRAPH No. 6
800
600
400
200
0
Drawing speed 2 ft/min.
Load at Die 2. (lbf)
800
600
400
200
0
Both dies oscillating.
Load at Die 1. (lbf)
1000
800
600
Total drawing load. (lbf)
Die amplitude. pk. to pk. (in. x 10^{-3})
0
1
2
3
4
5
6

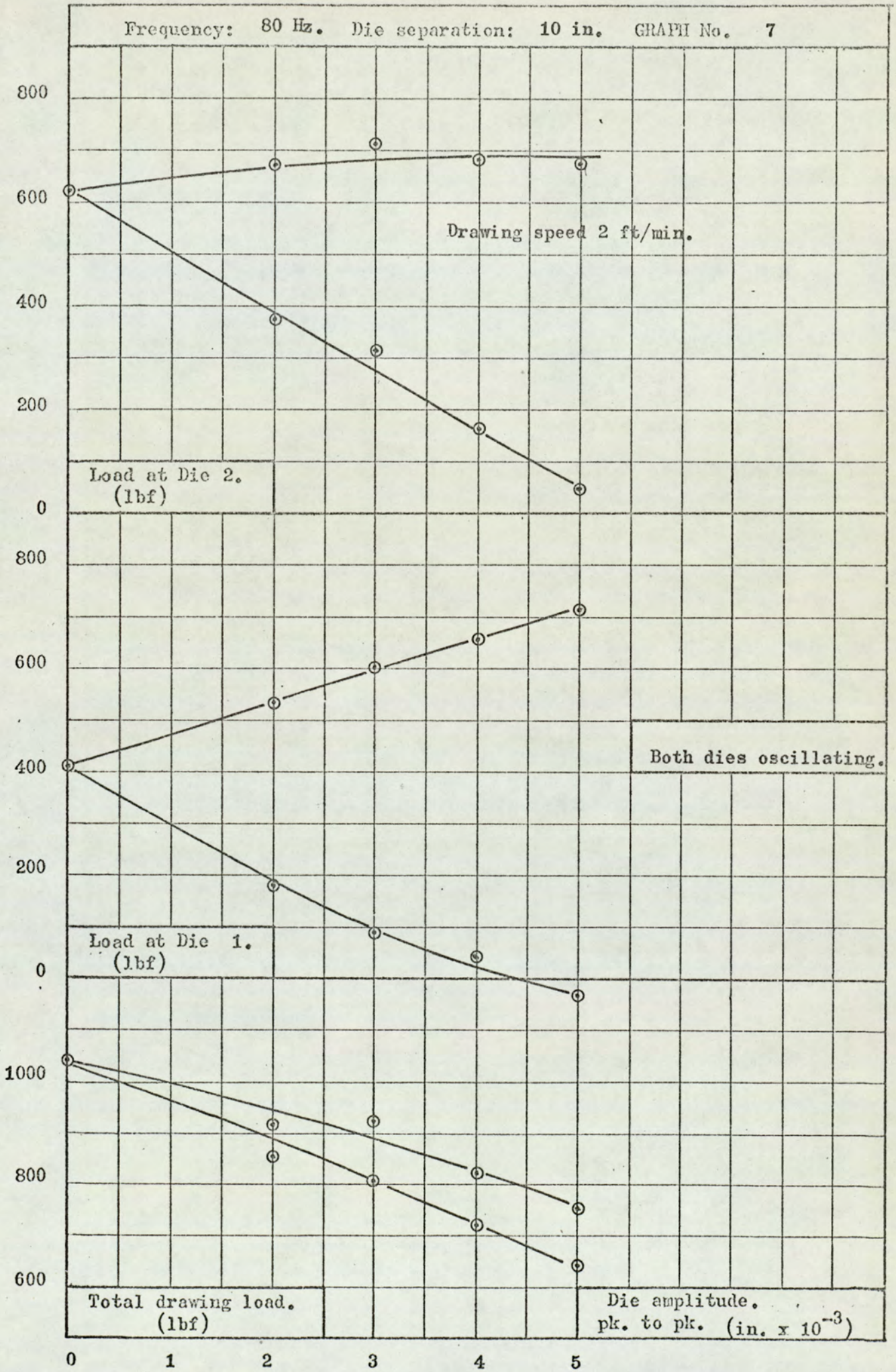
Frequency: 80 Hz. Die separation: 10 in. GRAPH No. 7
800
600
400
200
0
Drawing speed 2 ft/min.
Load at Die 2. (lbf)
800
600
400
200
0
Both dies oscillating.
Load at Die 1. (lbf)
1000
800
600
Total drawing load. (lbf)
Die amplitude. pk. to pk. (in. x 10^{-3})
0
1
2
3
4
5

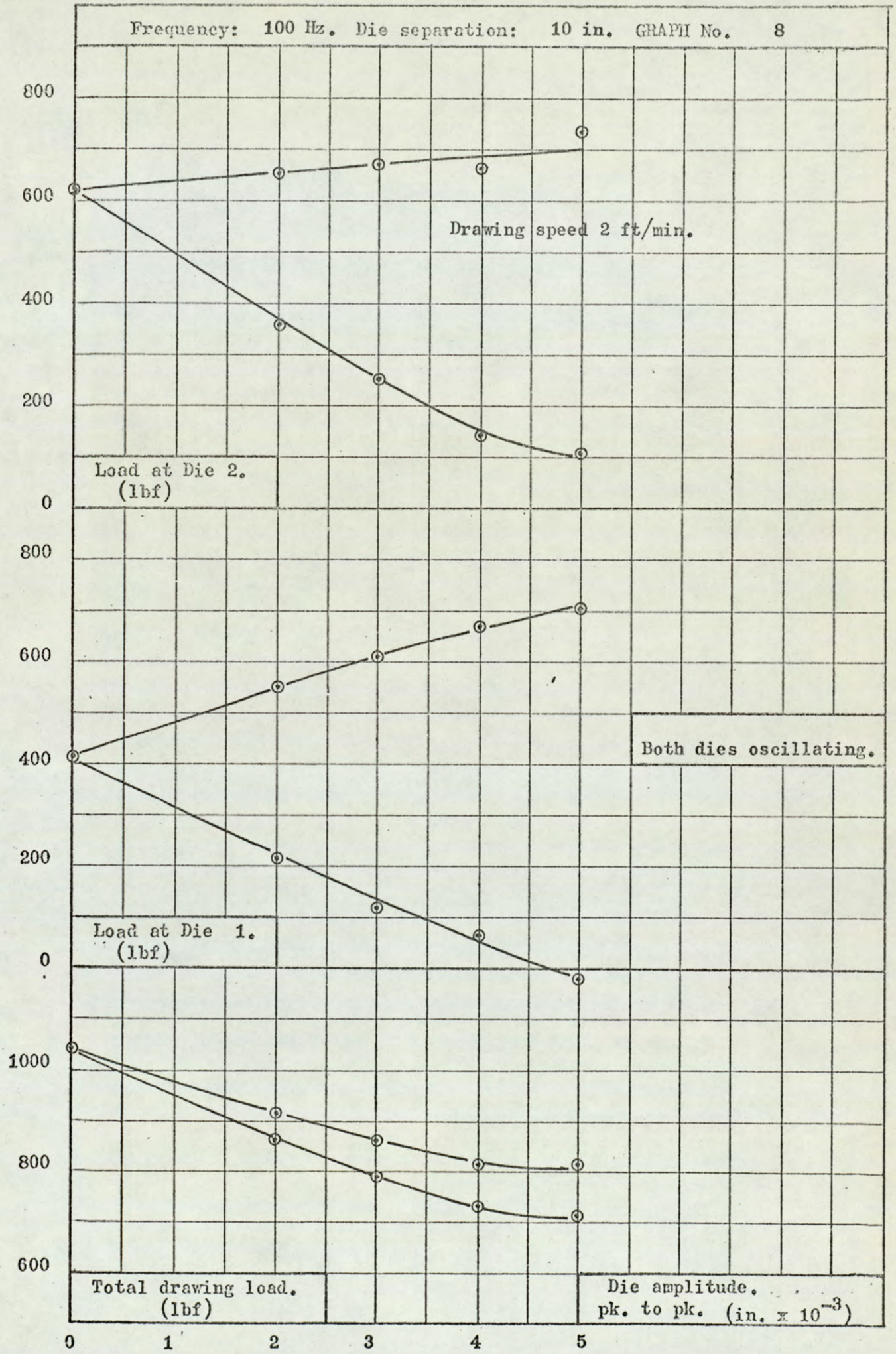
Frequency: 100 Hz. Die separation: 10 in. GRAPH No. 8
800
600
400
200
0
Drawing speed 2 ft/min.
Load at Die 2. (lbf)
800
600
400
200
0
Both dies oscillating.
Load at Die 1. (lbf)
1000
800
600
Total drawing load. (lbf)
Die amplitude. pk. to pk. (in. x 10^{-3})
0
1
2
3
4
5

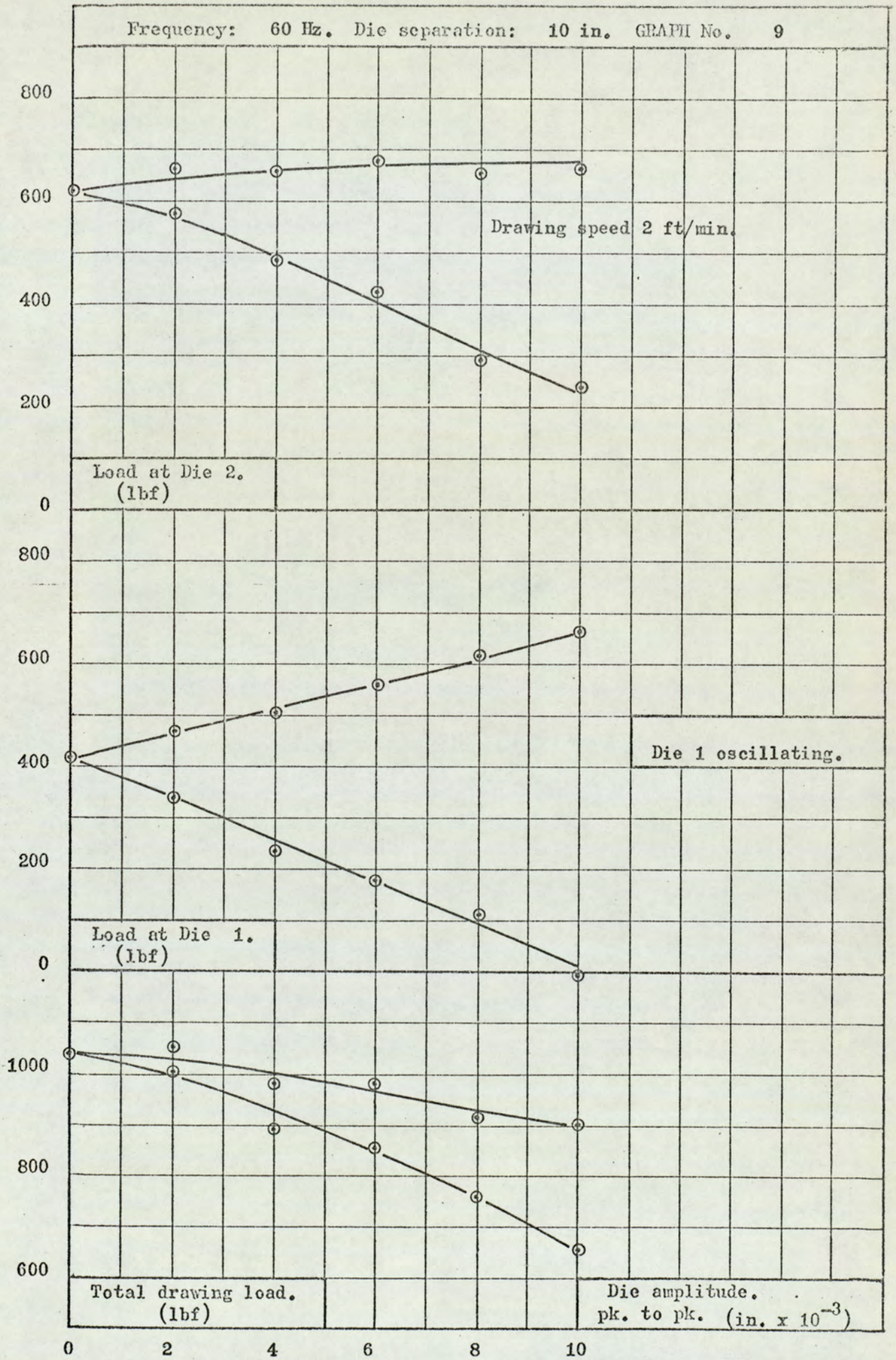
Frequency: 60 Hz. Die separation: 10 in. GRAPH No. 9
800
600
400
200
0
Drawing speed 2 ft/min.
Load at Die 2. (lbf)
800
600
400
200
0
Die 1 oscillating.
Load at Die 1. (lbf)
1000
800
600
Total drawing load. (lbf)
Die amplitude. pk. to pk. (in. x 10^{-3})
0
2
4
6
8
10

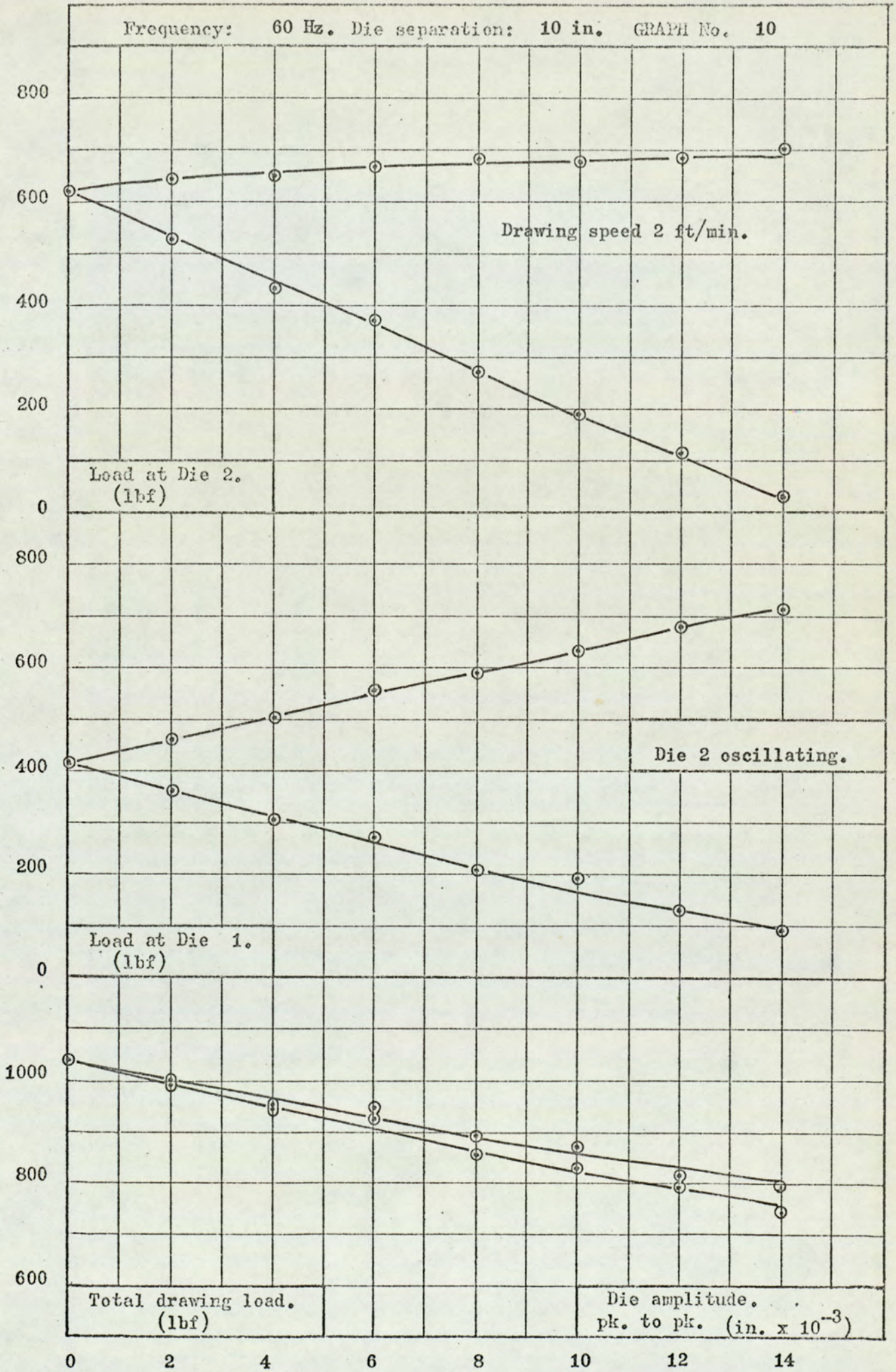
Frequency: 60 Hz. Die separation: 10 in. GRAPH No. 10
800
600
400
200
0
Drawing speed 2 ft/min.
Load at Die 2.
(lbf)
800
600
400
200
0
Die 2 oscillating.
Load at Die 1.
(lbf)
1000
800
600
Total drawing load.
(lbf)
Die amplitude.
pk. to pk. (in. x 10^{-3})
0
2
4
6
8
10
12
14

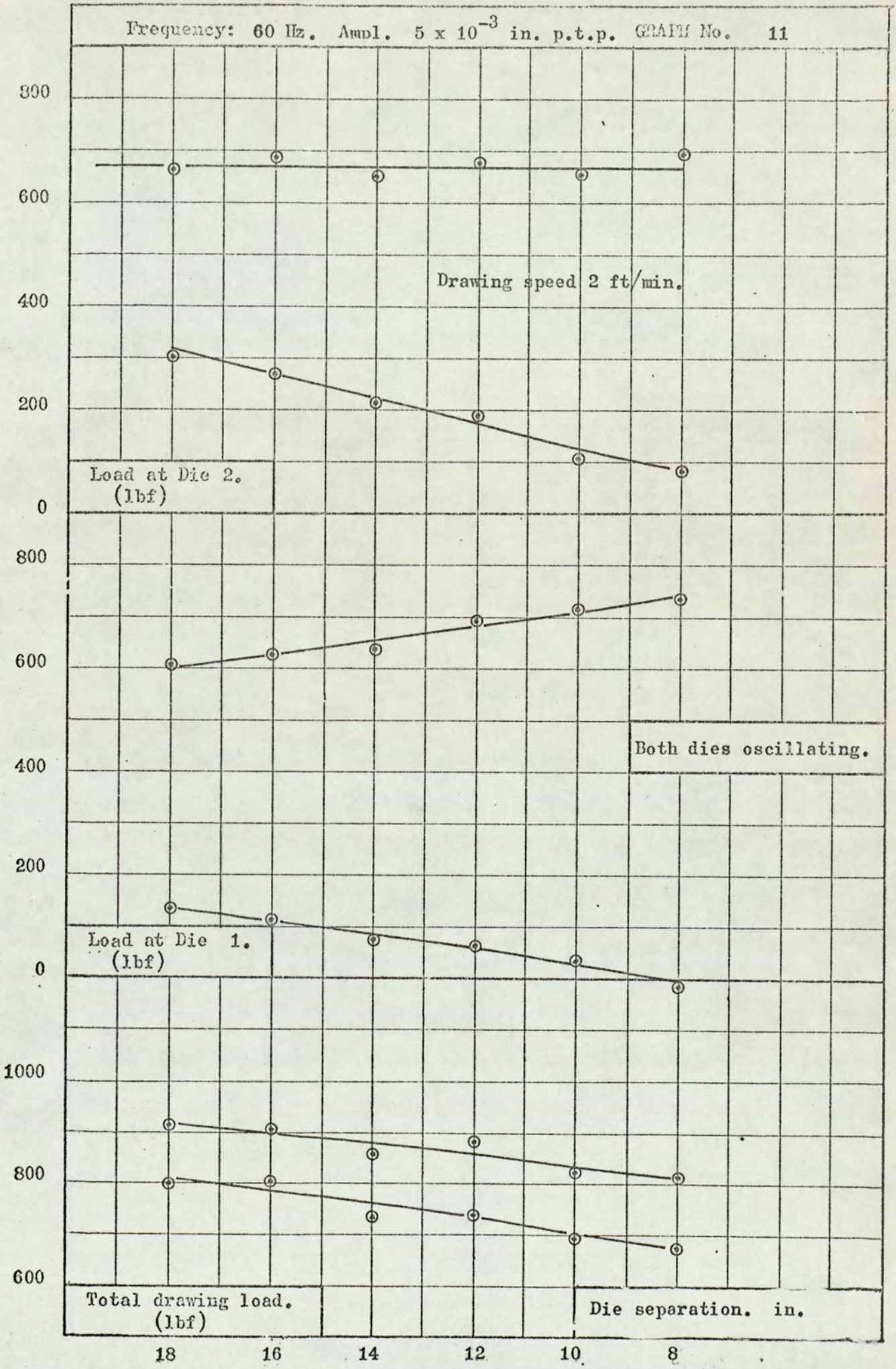
Frequency: 60 Hz. Ampl. 5 x 10^-3 in. p.t.p. GRAM No. 11
800
600
400
200
0
Drawing speed 2 ft/min.
Load at Die 2. (lbf)
800
600
400
200
0
Both dies oscillating.
Load at Die 1. (lbf)
1000
800
600
Total drawing load. (lbf)
Die separation. in.
18
16
14
12
10
8

Die load vs. back-pull at instant of drawing.

Die separation 18 in. Graph No. 12

Drawing speed 2 ft/min.

Both dies oscillating.

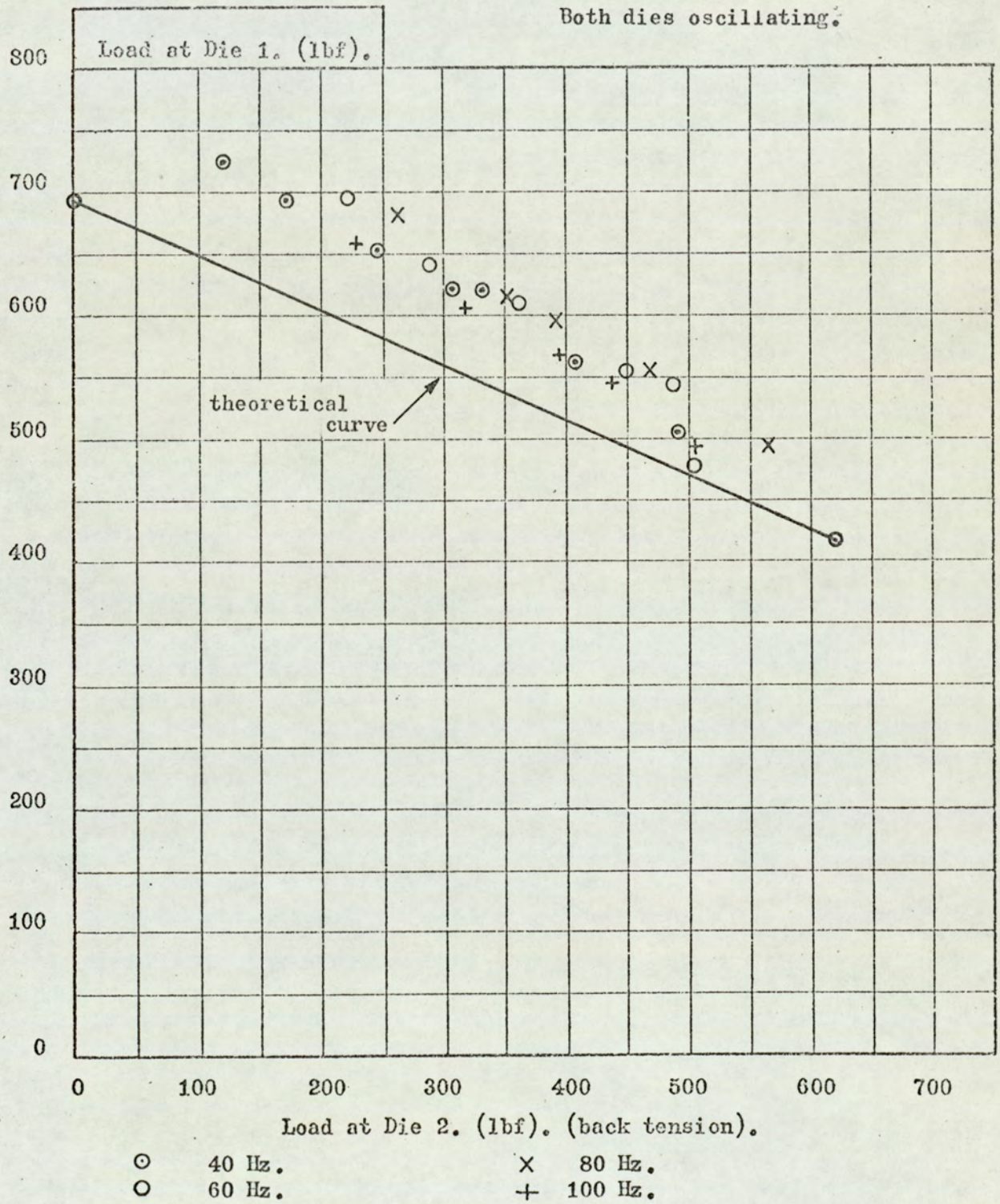

Die load vs. back-pull at instant of drawing.

Die separation 18 in. Graph No. 12(a).

Drawing speed 5 ft/min.
Both dies oscillating.

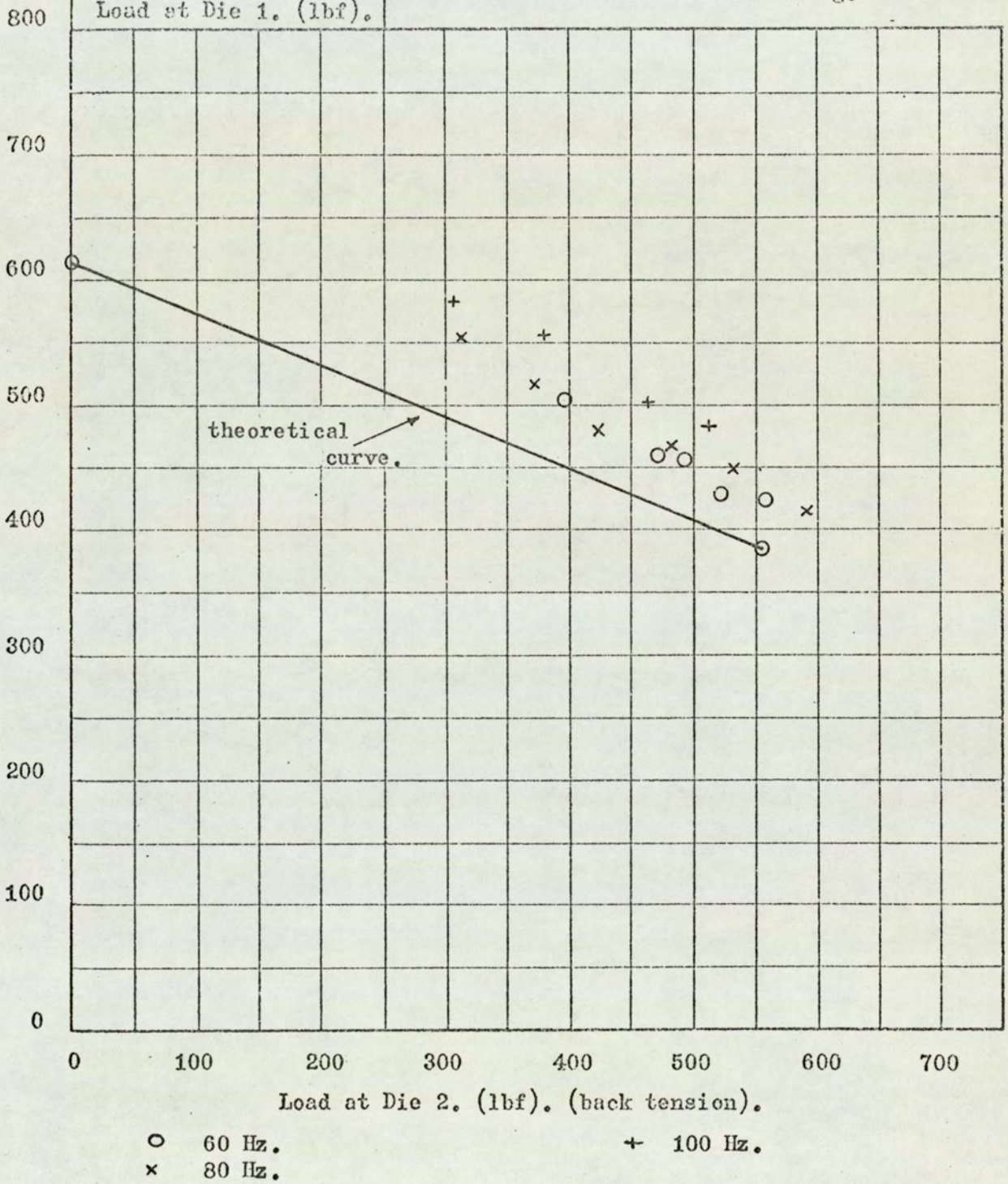

○ 60 Hz. + 100 Hz.
× 80 Hz.

Die load vs. back-pull at instant of drawing.

Die separation 10 in. Graph No. 13

Drawing speed 2 ft/min.

Both dies oscillating.

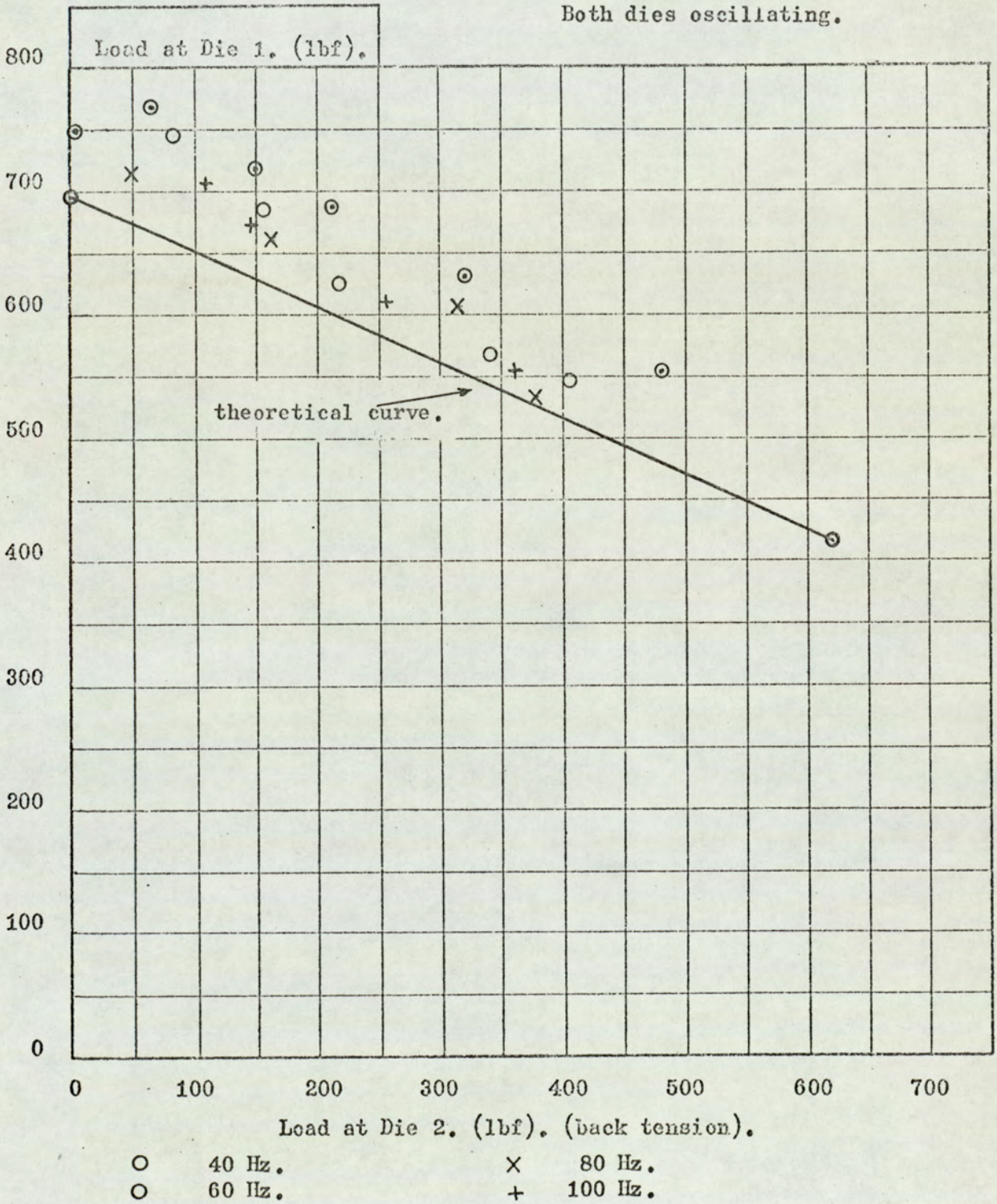

○ 40 Hz. × 80 Hz.

○ 60 Hz. + 100 Hz.

Die load vs. back-pull at instant of drawing.

Frequency 60 Hz. Graph No. 14

Drawing speed 2 ft/min.

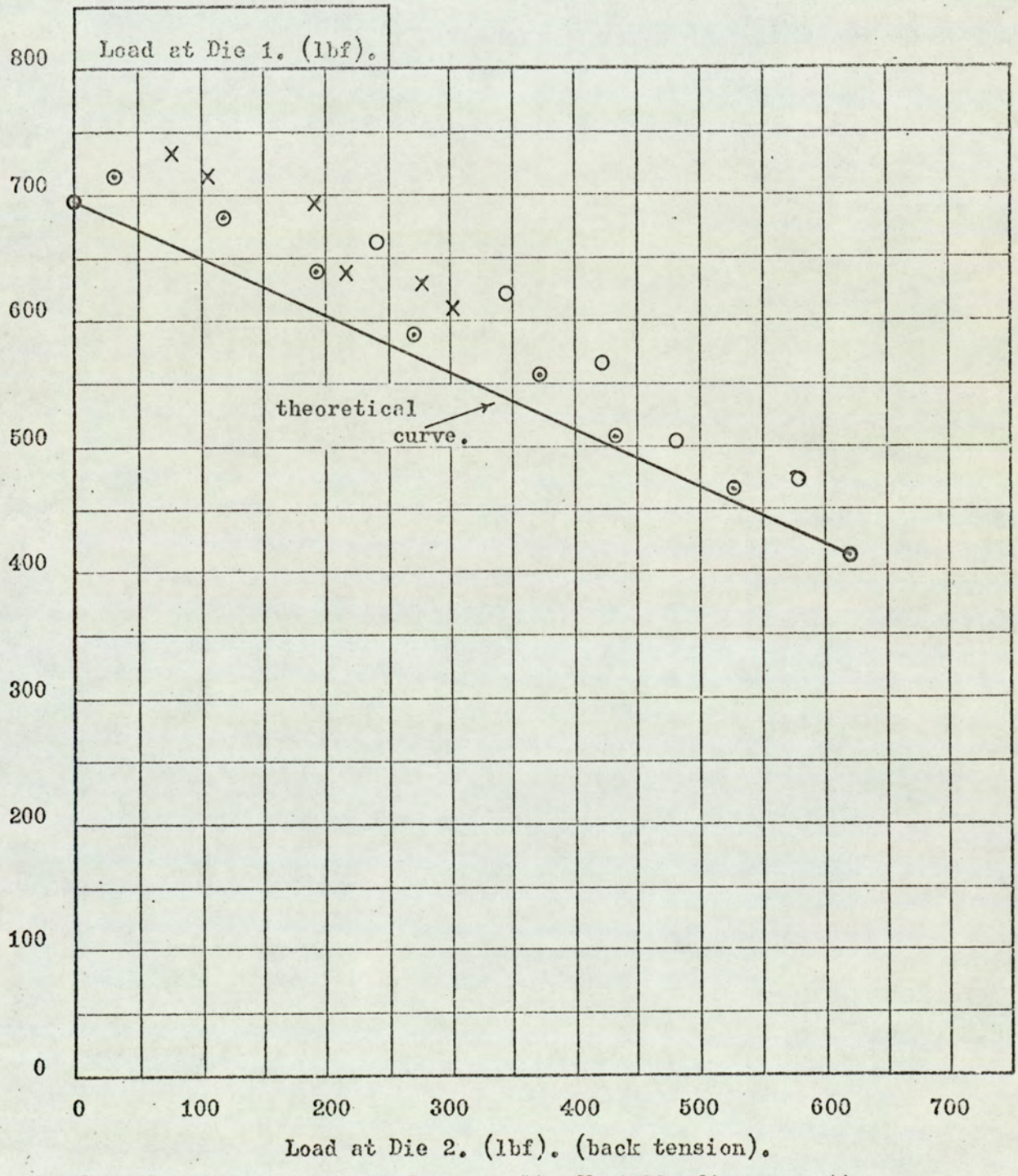

⊙ Die 2 oscillating only. × Variable die separation.

⊖ Die 1 oscillating only.

Cyclic stress magnitudes with 18 in. die separation.

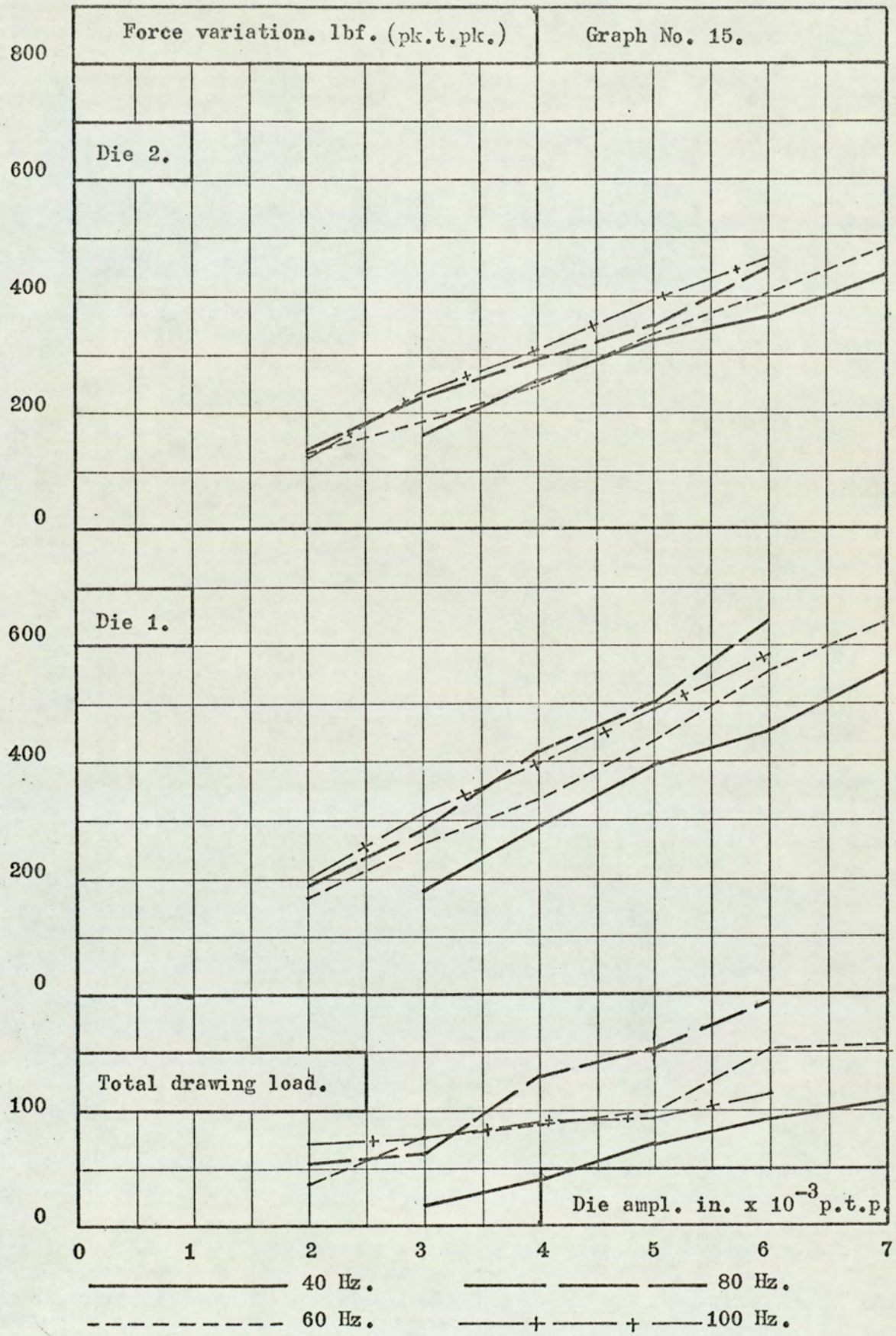

Cyclic stress magnitudes with 10 in. die separation.

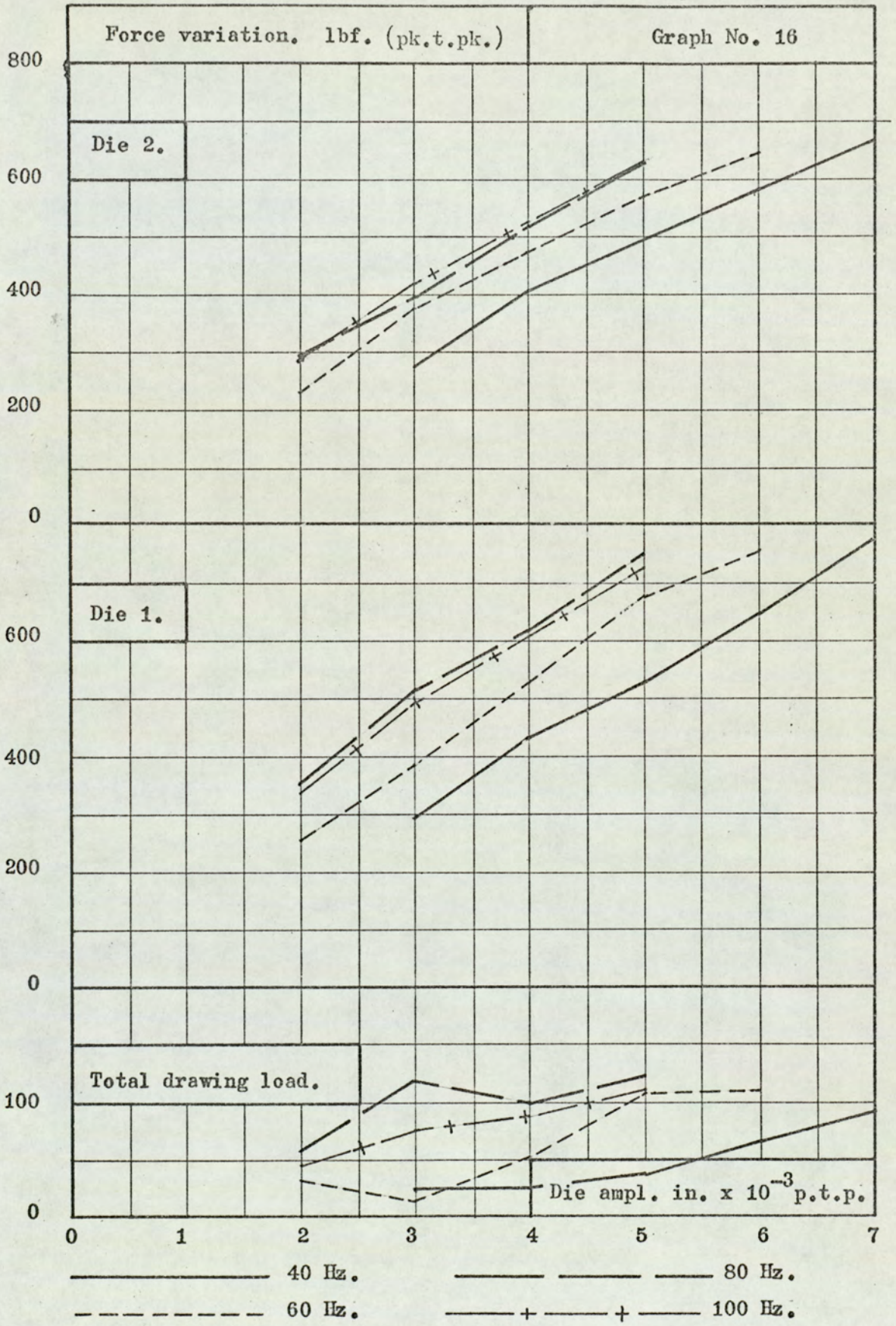

Drawing force magnitudes with 18 in. and 10 in. die separations.

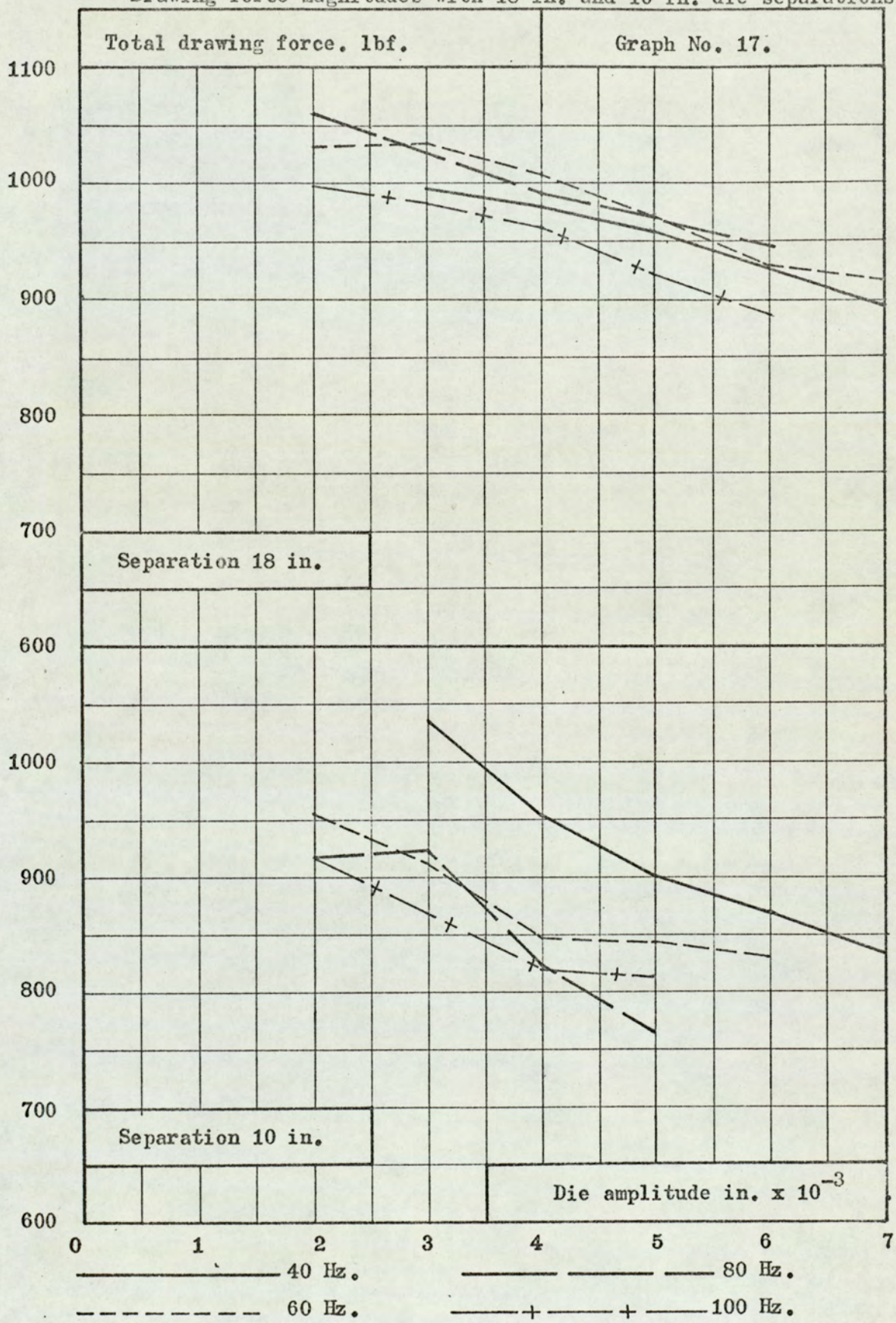

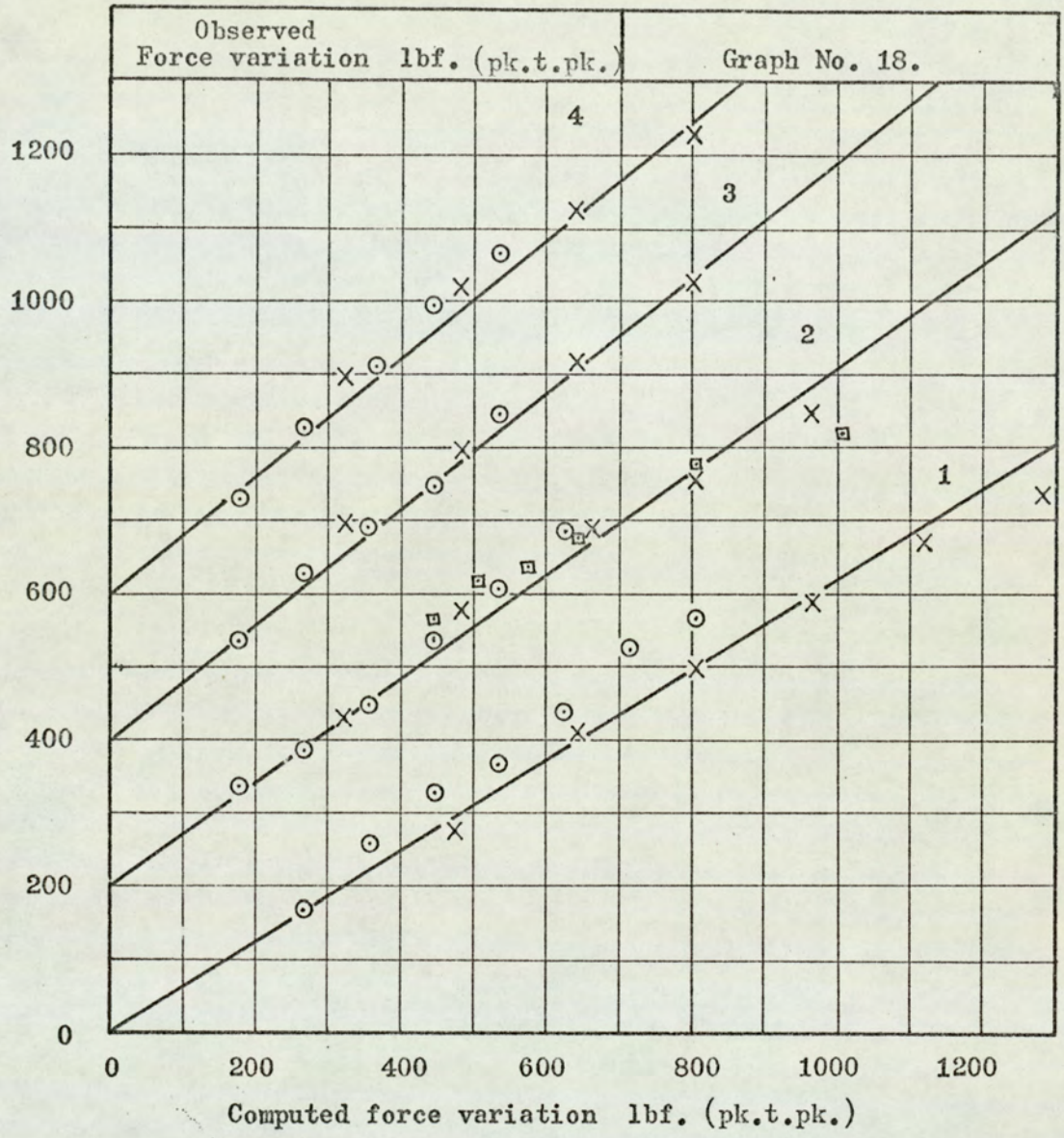

Force variation in die 2 vs. computed variation. Drawing speed 2 ft/min.

Curve 1 - 40 Hz.
Curve 2 - 60 Hz.
Curve 3 - 80 Hz.
Curve 4 - 100 Hz.

⊙ 18 in. separation.
× 10 in. separation.
⊡ Variable separation.

Computed variation = 2 x p.t.p. die amplitude x stiffness of wire between dies.

(Curves 2 - 4 have offset axes for clarity.)

Gradients:

1. 0.620
2. 0.710
3. 0.790
4. 0.800

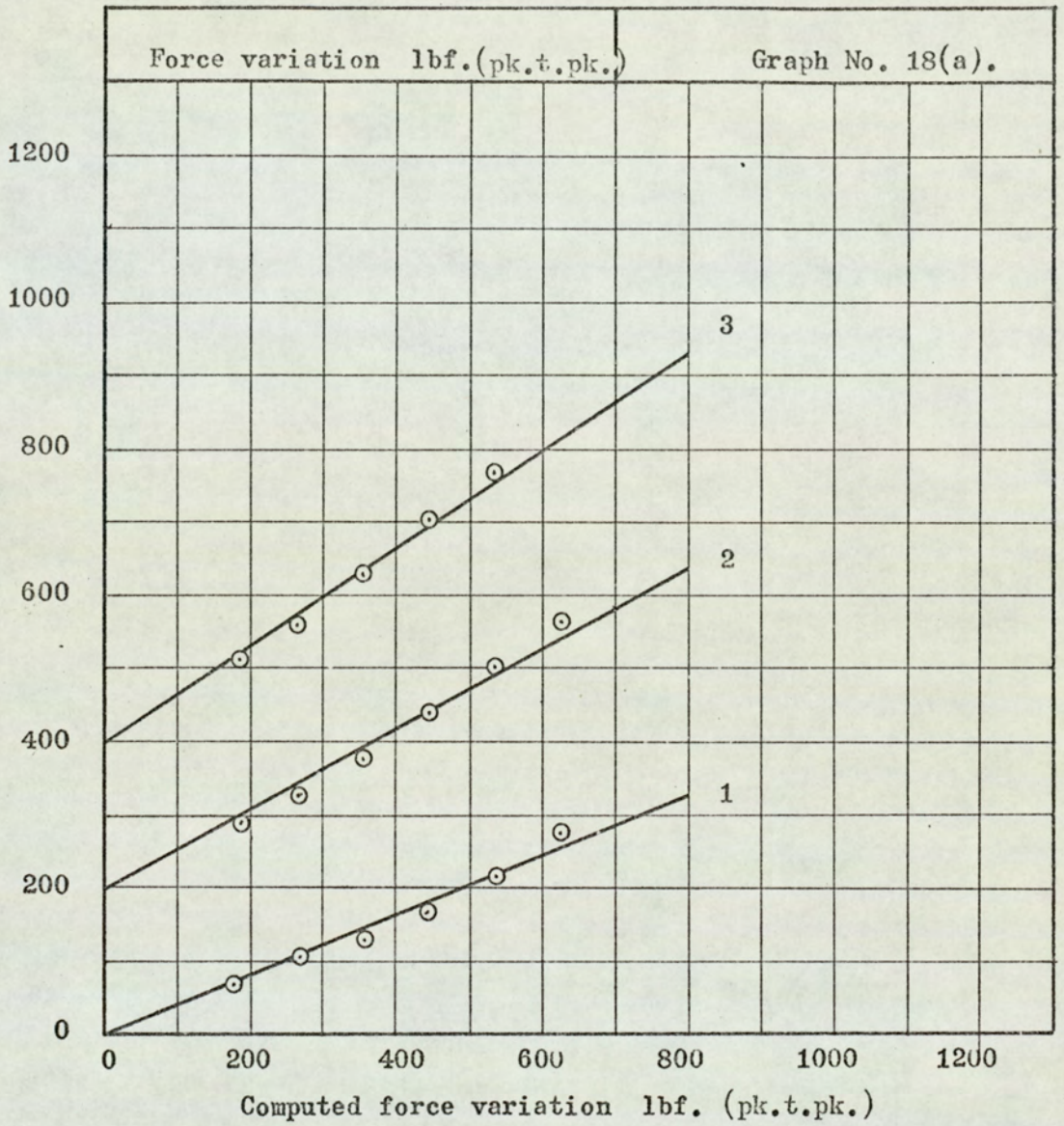

Force variation in die 2 vs. computed variation. Drawing speed 5ft/min.

Curve 1 - 60 Hz.

Curve 2 - 80 Hz.

Curve 3 - 100 Hz.

(Curves 2 and 3 have offset axes for clarity).

Gradients:

1. 0.403

2. 0.545

3. 0.788

Ampl. in.x10^{-3} p.t.p.	$\hat{L}1$ (lbf)	$\check{L}1$ (lbf)	$\hat{L}2$ (lbf)	$\check{L}2$ (lbf)	$\lessdot L_d$ (lbf)	$\lessdot L_{nd}$ (lbf)
Frequency 40 Hz. Speed 2 ft/min. 18 in. die separation. Both dies oscillating.						
3	503	323	657	493	996	980
4	563	271	659	407	970	930
5	620	227	660	333	958	887
6	621	170	672	307	928	842
7	659	99	685	246	898	784
8	694	69	699	173	867	768
9	725	40	688	123	848	728
Frequency 60 Hz.						
2	480	312	683	551	1031	995
3	547	286	673	488	1035	959
4	557	220	699	450	1007	919
5	610	175	697	362	972	872
6	643	87	691	287	930	778
7	695	55	708	224	919	763
Frequency 80 Hz.						
2	494	306	699	566	1060	1005
3	556	271	692	470	1026	963
4	598	194	683	393	991	863
5	619	118	701	352	971	819
6	682	41	711	263	945	752
Frequency 100Hz.						
2	493	293	634	506	999	927
3	545	234	674	439	984	908
4	568	168	705	395	963	873
5	605	117	713	318	923	830
6	659	78	696	230	889	774

Ampl. in.x10^{-3} p.t.p.	$\hat{L1}$ (lbf)	$\check{L1}$ (lbf)	$\hat{L2}$ (lbf)	$\check{L2}$ (lbf)	$\lessgtr L_d$ (lbf)	$\lessgtr L_{nd}$ (lbf)
Frequency 40 Hz. Speed 2 ft/min. 10 in. die separation. Both dies oscillating.						
3	554	259	753	481	1035	1012
4	632	201	731	322	954	932
5	689	158	707	212	901	865
6	720	72	733	150	870	805
7	770	9	734	65	835	743
8	750	-28	736	2	752	708
Frequency 60 Hz.						
2	549	290	635	407	956	925
3	568	183	716	343	911	899
4	627	102	694	220	847	796
5	686	8	727	156	842	735
6	747	-10	729	82	829	719
Frequency 80 Hz.						
2	535	181	674	378	913	855
3	606	90	715	318	924	805
4	661	42	683	164	825	725
5	715	-35	677	50	765	642
Frequency 100 Hz.						
2	555	216	655	361	916	871
3	610	116	675	257	869	791
4	672	64	668	147	819	732
5	705	-22	736	110	815	714

Ampl. in.x10^{-3} p.t.p.	$\hat{L}1$ (lbf)	$\check{L}1$ (lbf)	$\hat{L}2$ (lbf)	$\check{L}2$ (lbf)	$\{L_d$ (lbf)	$\{L_{nd}$ (lbf)
Frequency 60 Hz. Speed 5 ft/min. 18 in. die separation. Both dies oscillating.						
2	423	328	625	557	970	955
3	429	310	625	522	951	935
4	426	269	651	522	948	920
5	455	248	649	485	934	896
6	459	190	685	470	929	882
7	504	162	672	397	901	834
Frequency 80 Hz.						
2	414	299	680	592	1005	979
3	449	290	655	533	982	945
4	468	227	659	483	950	887
5	480	168	664	425	905	833
6	516	118	671	371	887	789
7	555	62	676	313	868	738
Frequency 100 Hz.						
2	439	293	662	552	991	954
3	483	242	672	513	996	924
4	505	186	691	462	967	876
5	557	137	679	379	935	816
6	584	45	675	307	891	719

Ampl. in.x10^{-3} p.t.p.	$\hat{L1}$ (lbf)	$\check{L1}$ (lbf)	$\hat{L2}$ (lbf)	$\check{L2}$ (lbf)	$\{L_d$ (lbf)	$\{L_{nd}$ (lbf)
Frequency 60 Hz. Speed 2 ft/min. 10 in. die separation. Die 1 only oscillating.						
2	473	340	665	580	1053	1005
4	503	234	659	484	987	893
6	565	178	679	424	989	857
8	621	108	653	296	917	761
10	664	-11	665	242	906	654
Die 2 only oscillating.						
2	465	361	646	527	992	1001
4	507	306	651	438	945	951
6	556	278	674	372	928	952
8	590	208	685	270	860	893
10	640	195	678	193	833	873
12	680	132	683	115	795	815
14	714	94	701	31	745	795

Die sep^{n}. in.	L1 (lbf)	L1 (lbf)	L2 (lbf)	L2 (lbf)	$\{L_d$ (lbf)	$\{L_{nd}$ (lbf)
Frequency 60 Hz. Speed 2 ft/min. Amplitude 5x10^{-3}in. p.t.p. Both dies oscillating.						
18	610	133	667	301	911	800
16	631	112	690	277	908	802
14	639	77	654	217	856	731
12	695	63	678	193	888	741
10	715	36	659	108	823	695
8	735	-20	697	78	813	677

Ampl. in.x10^{-3} p.t.p.	$\hat{L1}$ (lbf)	$\check{L1}$ (lbf)	$\hat{L2}$ (lbf)	$\check{L2}$ (lbf)	$\{L_d$ (lbf)	$\{L_{nd}$ (lbf)
Frequency 40 Hz. Speed 2 ft/min. 18 in. die separation. Both dies oscillating.						
5	649	186	562	212	861	748
			from bridge		824	738
5	648	213	671	296	944	884
			from bridge		941	856
Frequency 100 Hz. Speed 2 ft/min. 18 in. die separation. Both dies oscillating.						
5	605	90	809	403	1008	899
			from bridge		1000	856
Frequency 40 Hz. Speed 2 ft/min. 10 in. die separation. Both dies oscillating.						
5	634	144	731	266	900	875
			from bridge		949	881
Frequency 60 Hz. Speed 2 ft/min. 10 in. die separation. Both dies oscillating.						
5	652	36	745	241	893	781
			from bridge		835	738
Frequency 80 Hz. Speed 2 ft/min. 10 in. die separation, Both dies oscillating.						
5	736	11	713	134	870	724
			from bridge		857	716
Frequency 100 Hz. Speed 2 ft/min. 10 in. die separation. Both dies oscillating.						
5	682	6	730	159	841	736
			from bridge		809	724

B7: Investigation into the Mechanics of Oscillatory Drawing

B7: Investigations into the Mechanics of Oscillatory Drawing

Introduction

Whilst the mechanism of load reduction described in section B1 was proved experimentally, the above theory did not predict the levels of stress variation induced in the wire, and therefore no prediction of overall drawing force reduction could be achieved. It was therefore decided to conduct a thorough investigation into the basic mechanics of oscillatory drawing, so that such predictions of behaviour could be made. Preliminary theoretical investigation of tandem drawing proved unsuccessful, and it was therefore decided to initiate this investigation with a study of the less complex process of single die drawing with axial die oscillations.

B71 Single die drawing with oscillations

The object of this investigation was to develop a theory relating to the mechanics of the process, which would correlate with experimentally obtained data. The simple theory used initially, (B71(a)), was that developed by Winsper and Sansome, and modified for application to low frequencies.

This proved inadequate, especially near the natural frequency of the bull block drum, where the force variation induced in the tag received a sudden rise in magnitude, when the applied frequency exceeded the natural frequency of the drum. This was considered to be due to the change of phase of the drum oscillations, as the natural frequency was exceeded. It was therefore concluded that the theory should take into account the drum response to cyclic forcing, and since this forcing contained discontinuities within each cycle, it was further concluded that the analogue computor was most suited to the problem.

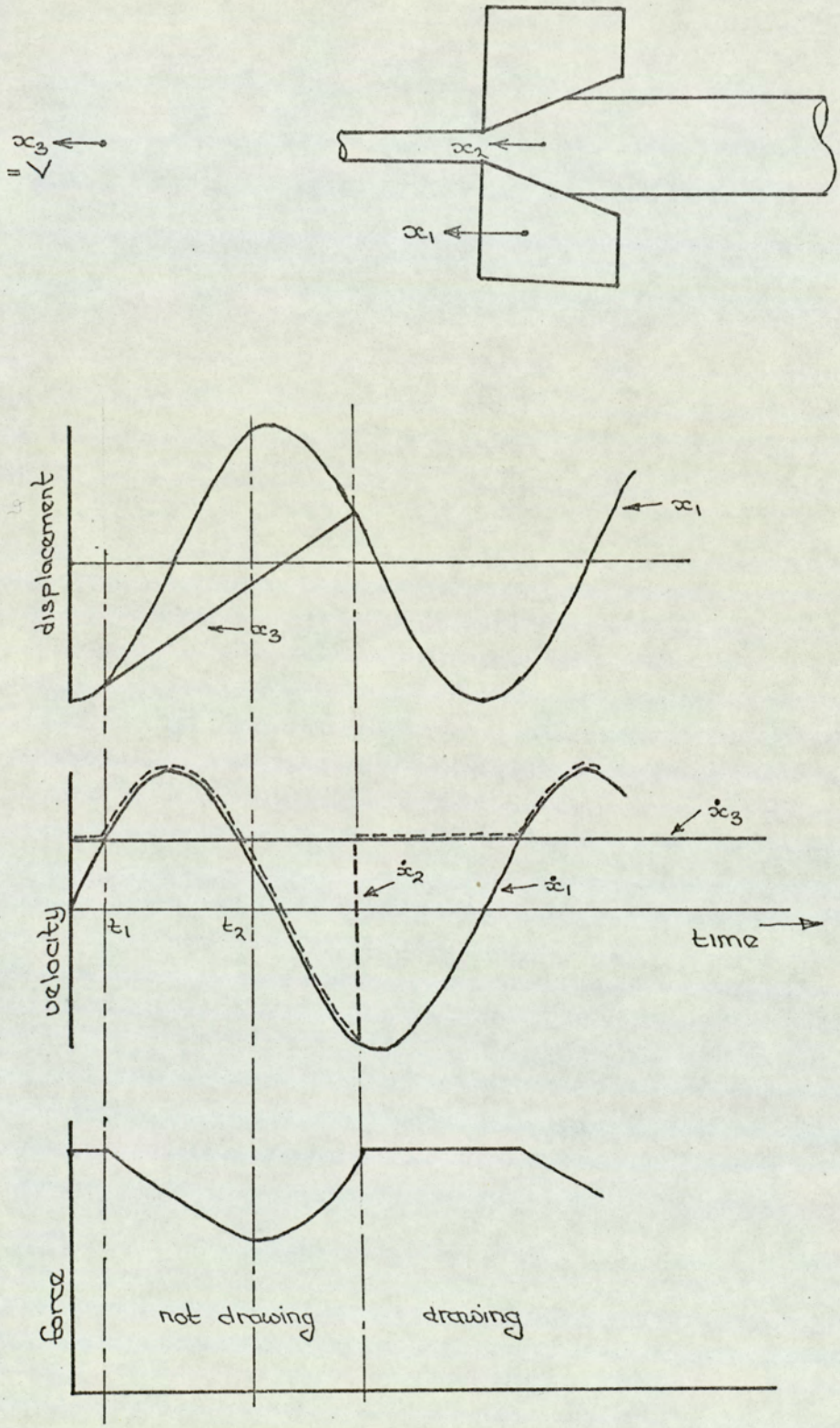

Graphical representation of simple oscillatory drawing theory.

Figure 25.

Having obtained experimentally the natural frequency and damping coefficient of the bull block drum (appendices 7 and 8), an analogue programme was written based on the simple theory in section B71(a) but incorporating drum oscillation. Whilst these results obtained from the analogue correlated more closely with experimental data, the predicted force variations were consistently higher than those observed.

Prior to this it had been assumed that the drawn wire, upon touching the drum surface, received no further cyclic straining, but moved with the drum. This assumption was considered justified because of the friction forces set up between the wire and the drum. However, because of the above results, a theoretical study was made of the effects of cyclic straining of the wire on the drum (section B71(b)). This theory was incorporated in the final form of the analogue programme. The measurement of the coefficient of friction between wire and drum, necessary to implement the theory in section B71(b), is described in Appendix 10.

B71(a) Simple theoretical considerations

Assumptions

1. During the period when wire is being drawn, the wire is under a constant load, equal to the drawing load under non-oscillatory conditions.
2. The velocity of the drum is constant; there are no periodic drum oscillations.
3. Once in contact with the drum, there is no cyclic straining of the drawn wire.
4. The wire is weightless.

Let $x_1 = -x \cos\omega t$ such that at $t = o$ the die is at its most backward position (see fig. 25). Assume that at $t = 0$ drawing is occurring and since it is doing so at a constant

load,

$$\dot{x}_2 = \dot{x}_3 = V$$

Drawing will stop when the velocity of the die reached that of the wire at $t = t_1$ say, where

$$\dot{x}_1 = \dot{x}_2 = \dot{x}_3$$

i.e. $X\omega\sin\omega t_1 = V$

$$\omega t_1 = \sin^{-1}(V/X\omega) = \phi, \text{ say}$$

where $0 \leqslant \phi \leqslant \pi/2$

Drawing is now stopped and the wire at the die will move with the die, whilst the wire at the drum will move with the drum.

i.e. $\dot{x}_2 = \dot{x}_1$

$$\dot{x}_3 = V$$

Since the die is now moving faster than the drum, this will cause the wire to partially off-load. If δ is the relative movement of the ends of the wire after $t = t_1$, then,

$$\delta = |x_{2-3}|_{t_1}^{t} = \int_{t_1}^{t} \dot{x}_{2-3}\, dt$$

$$= \int_{t_1}^{t} (X\omega\sin\omega t - V)dt$$

$$= X\cos\omega t_1 + Vt_1 - X\cos\omega t - Vt$$

$$\delta = X\cos\phi + \frac{V\phi}{\omega} - X\cos\omega t - Vt \qquad (2)$$

δ is a maximum when $\frac{d\delta}{dt} = 0$ at $t = t_2$, say.

Where $\frac{d\delta}{dt} = 0 = X\sin\omega t_2 - V$

i.e. $\omega t_2 = \sin^{-1}\frac{V}{X\omega} = \phi$ or $\pi - \phi$

Since drawing does not generally stop at the same instant as starting, $\omega t_2 \neq \theta$

$V/X\omega$	0.00	0.10	0.20	0.30	0.40	0.50
$\delta/2X$	1.0000	0.8475	0.7059	0.5742	0.4529	0.3424
	0.60	0.70	0.80	0.90	1.00	
	0.2436	0.1573	0.0852	0.0310	0.0000	

Calculation of the coupling coefficient between die and wire.

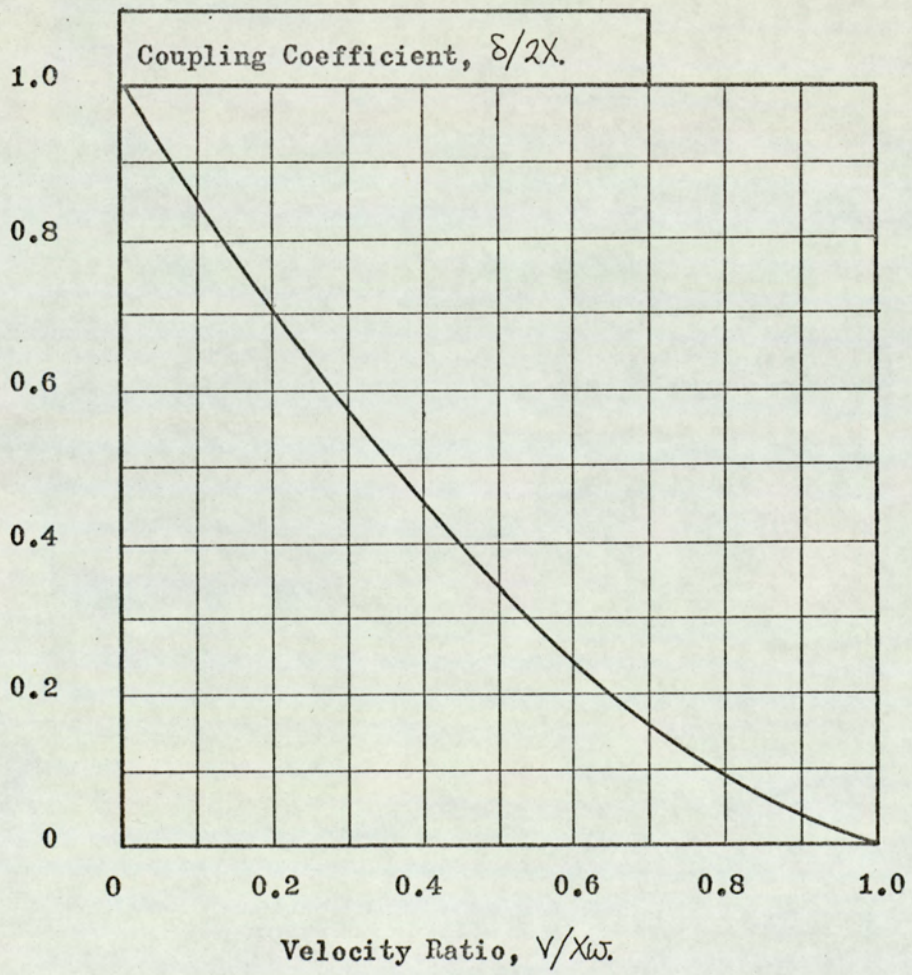

Figure 26.

$\hat{F}$ = 810 lbf. R = 9.0 in.

μ = 0.130. A = 0.01963 in^2.

l = 12.8 in. E = 30 x 10^6 lbf./in^2.

X = 10 x 10^{-3} in. z. t. p. V = 4.0 ft./min.

Frequency. Hz.	δ/X.	$\triangle$F.(lbf). (No slip).	$\triangle$F.(lbf). (With slip).
20	0.418	193	149
30	0.850	392	258
40	1.105	509	309
50	1.272	586	339
60	1.380	636	358
70	1.460	673	371
80	1.532	706	382
90	1.570	724	388
100	1.615	745	393

Computation of induced force variation in the drawn wire, based on simple theory, and simple theory with slipping of the wire on the drum.

Figure 27.

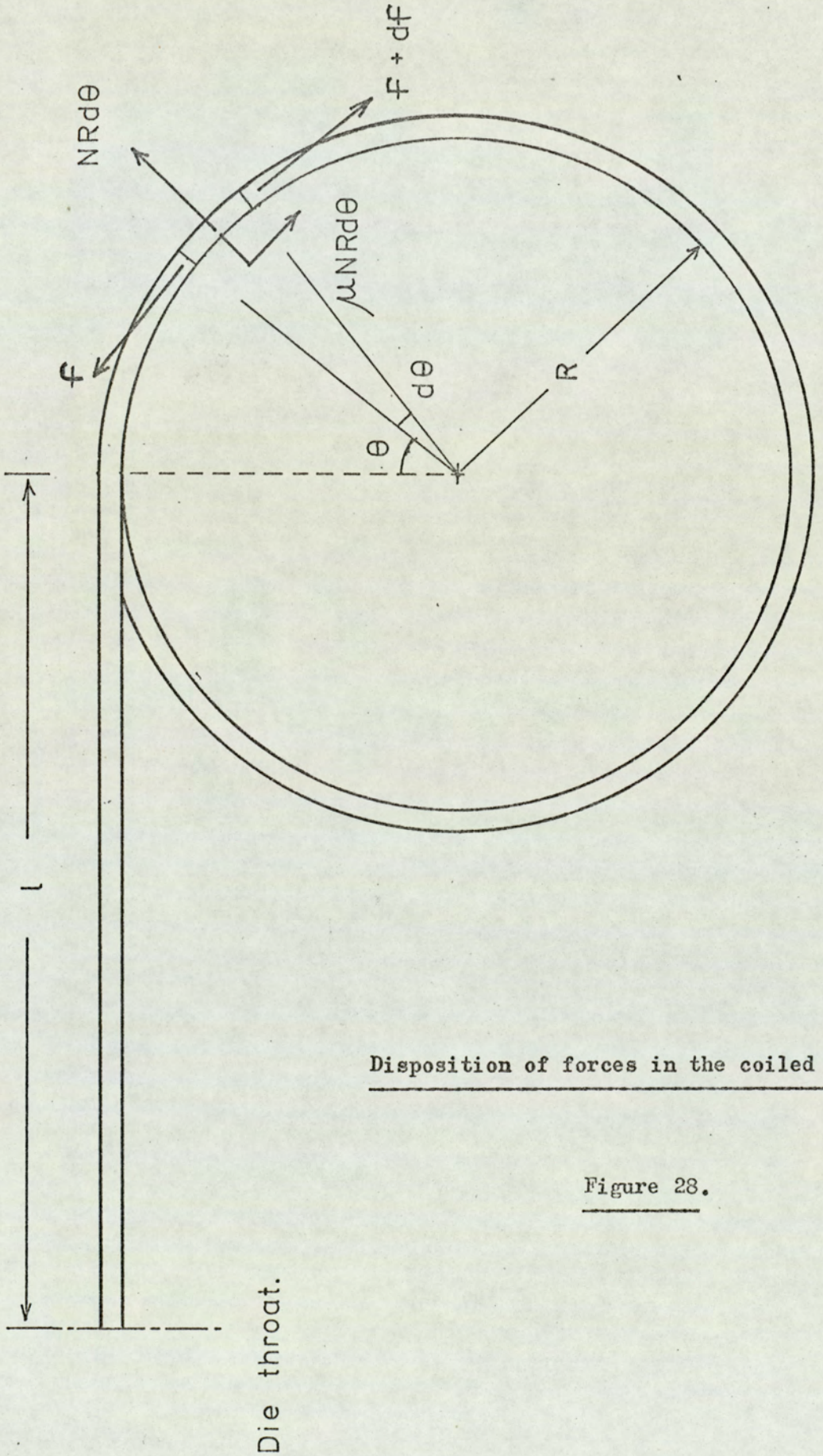

Disposition of forces in the coiled wire.

Figure 28.

i.e. $$\omega t_2 = \pi - \phi \qquad (3)$$

Thus $$\hat{\delta} = 2X\cos\phi - \frac{V}{\omega}(\pi - 2\phi)$$

$$\frac{\hat{\delta}}{2X} = \cos\phi - \sin\phi(\tfrac{\pi}{2} - \phi) \qquad (4a)$$

And thus $$\Delta F = 2\frac{AEX}{l}\left[\cos\phi - \sin\phi(\tfrac{\pi}{2} - \phi)\right]$$

or from (1) $$\Delta F = 2\frac{AEX}{l}\left[(1 - (\frac{V}{X\omega})^2)^{\frac{1}{2}} - \frac{V}{X\omega}(\frac{\pi}{2} - \sin^{-1}(\frac{V}{X\omega}))\right] \qquad (4b)$$

The variation of function 4a is shown in figure 26. This function represents the efficiency of coupling between the die and the wire. The cyclic force amplitude given in equation 4b is shown as a function of frequency in figure 27 and plotted graphically in figure 45.

B71(b) Calculation of the Effective Stiffness of the Drawn Wire

Assumptions

1. Consecutive coils on the drum do not touch.
2. There are no transverse oscillations induced in the drawn wire.
3. There is sufficient length of wire already coiled (see text).
4. The minimum force in the free length of wire is positive.
5. The weight of the wire on the drum is negligible.

Consider the equilibrium of the element shown in figure 28.

(a) Tangential

$$df\cos\frac{d\theta}{2} + \mu NRd\theta = 0 \qquad (1)$$

(b) Radial

$$NRd\theta - (2f + df)\sin\frac{d\theta}{2} = 0 \qquad (2)$$

Distribution of axial force in the drawn wire on the drum.

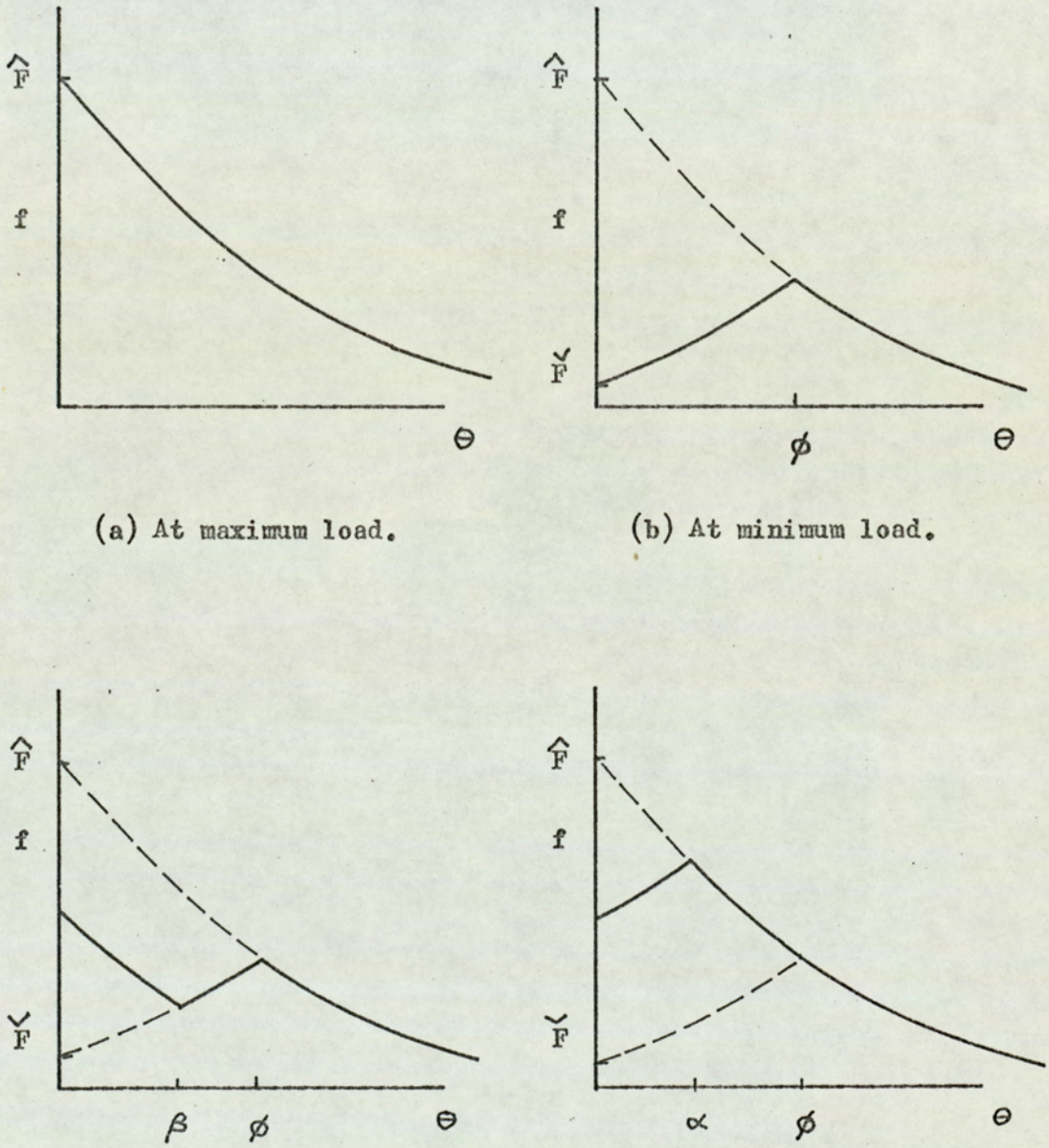

(a) At maximum load.

(b) At minimum load.

(c) With increasing load.

(d) With decreasing load.

Figure 29.

Yields, combining and neglecting second order terms:

$$\frac{df}{f} = -\mu d\theta \qquad (3)$$

Integrating:

$$\text{Ln } f = -\mu\theta + \ln C \text{ where C is a constant.}$$

Where $\theta = 0$ take f as F

$$\therefore \quad \frac{f}{F} = e^{-\mu\theta} \qquad (4)$$

Or for friction in the reverse direction

$$\frac{f}{F} = e^{\mu\theta} \qquad (4a)$$

Consider the wire as being initially loosely coiled around the drum. An external load is applied to the free wire of $\hat{F}$. The direction of the friction force will be positive, opposing the applied force. Therefore the axial force distribution in the wire round the drum is given by equation (4).

i.e. $$\frac{f}{\hat{F}} = e^{-\mu\theta} \qquad (5)$$

This distribution is shown in figure 29(a).

The externally applied load is now reduced to $\check{F}$. A section of wire will slip on the drum, and the equilibrium equation for this section is given by (4a).

i.e. $$\frac{f}{\check{F}} = e^{\mu\theta} \qquad (6)$$

Slipping occurs along the wire until such a position is reached where f, as defined by (6) is equal to f, as defined by (5). This angular position is designated as ϕ (see figure 29(b)). Hence for $\theta \leqslant \phi$ the force is given by (6).

and for $\theta > \phi$ the force is given by (5).

Also: $\check{F}e^{\mu\phi} = \hat{F}e^{-\mu\phi}$

or; $$\frac{\hat{F}}{\check{F}} = e^{2\mu\phi} \qquad (7)$$

If the externally applied load, F, is cycled between $\hat{F}$ and $\check{F}$, the force distribution during the cycles is as shown in figures 29(c) and 29(d).

Since during such cycling, the strain only changes in the range $0 < \theta < \phi$, it is only necessary to discover the strain in that range. The extension of the wire is considered relative to its position at maximum load.

(a) Decreasing load

The load in the wire is given by:-

$$f = Fe^{\mu\theta} \quad \text{for } 0 < \theta < \alpha$$

$$f = \hat{F}e^{-\mu\theta} \quad \text{for } \alpha < \theta < \phi$$

Therefore the strain in the wire relative to its maximum load condition, $\Delta\varepsilon$ is given by:-

$$\Delta\varepsilon = (Fe^{\mu\theta} - \hat{F}e^{-\mu\theta})/AE \quad \text{for } 0 \leqslant \theta \leqslant \alpha$$

and $$\Delta\varepsilon = 0 \quad \text{for } \alpha \leqslant \theta \leqslant \phi$$

The relative extension of the wire, U, is given by:-

$$U = \int \Delta\varepsilon \, ds$$

where ds is an elemental length.

$$\text{Thus } U = \frac{1}{AE} \int_0^{\alpha} (Fe^{\mu\theta} - \hat{F}e^{-\mu\theta}) R d\theta$$

$$= \frac{R}{\mu AE} \left[Fe^{\mu\theta} + \hat{F}e^{-\mu\theta} \right]_0^{\alpha}$$

$$\text{i.e. } U = \frac{R}{\mu AE} \left[F(e^{\mu\alpha} - 1) + \hat{F}\,(e^{-\mu\alpha} - 1) \right] \qquad (8)$$

Now α is given by:-

$$Fe^{\mu\alpha} = \hat{F}e^{-\mu\alpha}$$

$$\text{i.e. } \frac{\hat{F}}{F} = e^{2\mu\alpha} \qquad (9)$$

Therefore:-

$$U = \frac{R}{\mu AE}\left[2(F.\hat{F})^{\frac{1}{2}} - (F + \hat{F})\right]$$

i.e.

$$U = \frac{R}{\mu AE}\left|F^{\frac{1}{2}} - \hat{F}^{\frac{1}{2}}\right|^2 \qquad - I$$

(b) Increasing load.

The load in the wire is given by:-

$$f = Fe^{-\mu\theta} \qquad \text{for } 0 < \theta < \beta$$

and $$f = \check{F}e^{\mu\theta} \qquad \text{for } \beta < \theta < \phi$$

The strain in the wire relative to the maximum load condition is given by:

$$\Delta\varepsilon = (Fe^{-\mu\theta} - \hat{F}e^{-\mu\theta})/AE \quad \text{for} \quad 0 < \theta < \beta$$

and $$\Delta\varepsilon = (\check{F}e^{\mu\theta} - \hat{F}e^{-\mu\theta})/AE \text{ for } \beta < \theta < \phi$$

Therefore $$U_1 = \frac{R}{AE}\int_0^{\beta}(F - \hat{F})e^{-\mu\theta}\, d\theta$$

i.e. $$U_1 = \frac{R}{\mu AE}(\hat{F} - F)(e^{-\mu\beta} - 1) \qquad (10)$$

Now β is given by:-

$$Fe^{-\mu\beta} = \check{F}e^{\mu\beta}$$

or $$\frac{F}{\check{F}} = e^{2\mu\beta} \qquad (11)$$

Therefore

$$U_1 = \frac{R}{\mu AE}(\hat{F} - F)\left|\left(\frac{\check{F}}{F}\right)^{\frac{1}{2}} - 1\right| \qquad \text{II}$$

Similarly:-

$$U_2 = \frac{R}{AE}\int_{\beta}^{\phi}(\check{F}e^{\mu\theta} - \hat{F}e^{-\mu\theta})\, d\theta$$

i.e.

$$U_2 = \frac{R}{\mu AE}\left[\check{F}(e^{\mu\phi} - e^{\mu\beta}) + \hat{F}(e^{-\mu\phi} - e^{-\mu\beta})\right] \qquad (12)$$

Now ϕ is given by:-

$$\hat{F}e^{-\mu\phi} = \check{F}e^{\mu\phi}$$

or $$\frac{\hat{F}}{\check{F}} = e^{2\mu\phi} \qquad (13)$$

Therefore $$U_2 = \frac{R}{\mu AE}\left[\, 2(\hat{F}\check{F})^{\frac{1}{2}} - (F\check{F})^{\frac{1}{2}} - \hat{F}(\frac{\check{F}}{F})^{\frac{1}{2}} \,\right] \qquad III$$

Therefore the total relative extension of the wire is given by: $$U = U_1 + U_2 = \frac{R}{\mu AE}\left[2(\hat{F}\check{F})^{\frac{1}{2}} - 2(F\check{F})^{\frac{1}{2}} - (\hat{F}-F)\right] \qquad IV$$

As may be seen from equations I and IV, the relative extension of the wire for a given applied force is not the same for loading and unloading. To simplify the problem it is assumed that the relative extension is given by I for both unloading and loading. While this will give the correct value of extension at the minimum force, there will be an error in the extension computed for intermidiate increasing forces.

Therefore $$U = -\frac{R}{\mu AE}\left[F^{\frac{1}{2}} - \hat{F}^{\frac{1}{2}}\right]^2 \qquad (14)$$

The extension of the free length of wire will be:-

$$U = \frac{l}{AE}\left[\, F - \hat{F}\right] \qquad (15)$$

Therefore the total extension will be:-

$$U_{tot} = -\frac{R}{\mu AE}\left[F(1 - \frac{\mu l}{R}) - 2(\hat{F}F)^{\frac{1}{2}} + (1+\frac{\mu l}{R})\hat{F}\right] \qquad V$$

The variation of extension with force is shown in

$\hat{F}$ = 810 lbf. R = 9.0 in.

μ = 0.130. A = 0.01963 in^2.

l = 12.8 in. E = 30 x 10^6 $lbf./in^2$.

$$F^{\frac{1}{2}} = \frac{\hat{F}^{\frac{1}{2}}}{(1-\alpha)}\left[1 - \sqrt{\alpha^2 + \frac{\mu A E}{R\hat{F}}(1-\alpha).U_{tot.}}\right]$$

($\alpha = \mu l/R$).

$U_{tot.}$ in. x 10^{-3}.	F. lbf.
0	810.0
2	729.3
4	664.6
6	610.1
8	562.9
10	521.1
12	483.7
14	449.8
16	418.9
18	390.5
20	364.3

Variation of the extension in the drawn wire with applied force.

Figure30.

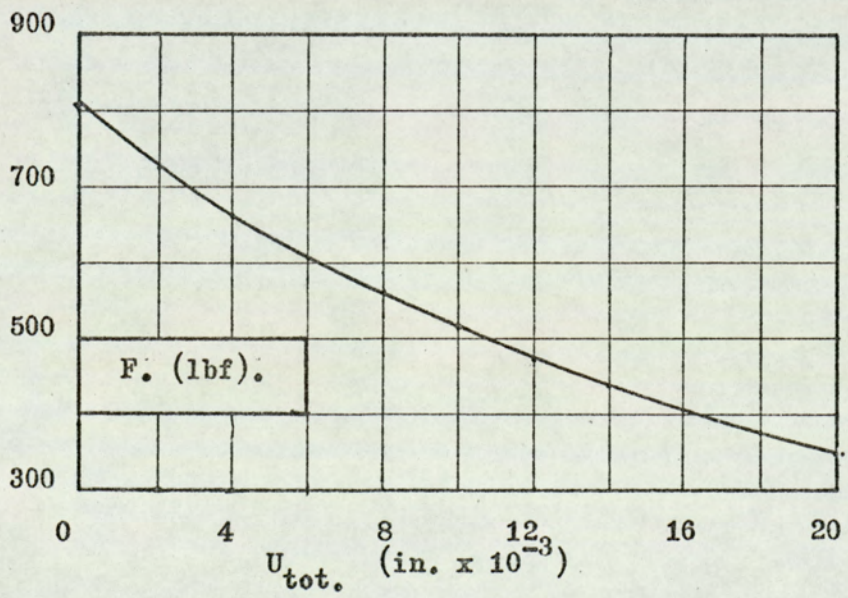

figure 30. The force variation induced in the drawn wire, based on the simple theory in section B71(a), is shown as a function of frequency in figure 27 and plotted graphically in figure 45.

B71(c): Development of the analogue programme

Assumptions:-

(1) During the period when wire is being drawn the wire is under a constant load, in excess of the non-oscillatory drawing load.

(2) The wire is weightless.

(3) Consecutive coils on the drum do not touch.

(4) There are no transverse oscillations induced in the drawn wire.

(5) There is sufficient wire already coiled on the drum to render the theory in section B71(b) valid.

(6) The minimum force in the free length of wire is positive.

The physical equations:-

$$\dot{x}_1 = X\omega\sin\omega t \qquad - (1)$$

$$\dot{x}_3 = V + R\dot{\theta} \qquad - (2)$$

Drawing is assumed to be occurring at $t = 0$, where $x_1 = -X$. While drawing is occurring, since the force in the wire is constant, the velocity of the wire at the die is equal to the velocity of the drum.

i.e. $$\dot{x}_2 = V + R\dot{\theta} \qquad - (3)$$

Drawing will stop when the velocity of the die reaches the velocity of the wire.

i.e. when $\dot{x}_2 = \dot{x}_1$

or $\dot{x}_{1-3} = 0$ - (4)

The rate of extension of the wire, $\dot{x}_{2-3}$ is:-

$\dot{x}_{2-3} = 0$ when drawing

$\dot{x}_{2-3} = \dot{x}_{1-3}$ when not drawing

Now, from equation V, section B72(b),

$$U_{tot} = -\frac{R}{\mu AE}\left[F(1 + \frac{\mu l}{R}) - 2\,(\hat{F}F)^{\frac{1}{2}} + (1 + \frac{\mu l}{R})\hat{F}\right]$$

In this equation, U_{tot} is the total extension of the wire relative to its maximum load condition. Thus, if when drawing is occurring, x_{2-3} is taken to be zero in the programme,

then $U_{tot} = x_{2-3}$

Now, from equation V above,

$$F - \frac{2\hat{F}^{\frac{1}{2}}F^{\frac{1}{2}}}{(1-\alpha)} + \frac{(1+\alpha)\hat{F}}{(1-\alpha)} - \frac{\mu AE}{R(1-\alpha)}\,x_{2-3} = 0$$

where $\alpha = \mu l/R$

This is a quadratic in $F^{\frac{1}{2}}$, the solution of which is:-

$$F^{\frac{1}{2}} = \frac{\hat{F}^{\frac{1}{2}}}{(1-\alpha)} \pm \frac{\hat{F}^{\frac{1}{2}}}{(1-\alpha)}\sqrt{\alpha^2 + (1-\alpha)\frac{\mu AE}{\hat{R}F}\cdot x_{2-3}}$$

The correct solution is obtained by considering the boundary condition when drawing is occurring: $F = \hat{F}$ and $x_{2-3} = 0$.

This yields the correct solution:-

$$F^{\frac{1}{2}} = \frac{\hat{F}^{\frac{1}{2}}}{(1-\alpha)}\left|1 - \sqrt{\alpha^2 + (1-\alpha)\frac{\mu AE}{\hat{R}F}\cdot x_{2-3}}\right| \qquad (5)$$

The equation of motion for the drum is:-

$$\ddot{\theta} = \frac{-FR}{I} - \frac{c\dot{\theta}}{I} - \frac{S\theta}{I}$$

i.e.

$$\ddot{\theta} = \frac{-FR}{I} - 2\xi\omega_n\dot{\theta} - \omega_n{}^2\theta \qquad - (6)$$

The intial conditions taken for the problem were that at t = 0 the die was at its most backward position relative to the drum and drawing was occurring.

i.e. $x_1 = -X \qquad - (7)$

$$\theta = -\frac{\hat{F}R}{S} = \frac{\hat{F}R}{I\omega_n{}^2} \qquad - (8)$$

$$x_{2-3} = 0 \qquad - (9)$$

The logic switching:-

Drawing stops when the velocity of the die exceeds the velocity of the drum, and starts when the force in the wire returns to the drawing force.

i.e. drawing stops when $\dot{x}_{1-3} \geqslant 0$

drawing starts when $\dot{x}_{2-3} = 0$

when drawing is stopped $\dot{x}_{2-3} = \dot{x}_{1-3}$

when drawing is started $\dot{x}_{2-3} = 0$

The machine equations:-

In order that the analogue computer may solve the problem, each mathematical operation must be expressed by a separate equation. This equation will define the function of a single amplifier in the circuit. Furthermore, the problem must be amplitude and time scaled, the former to ensure that no amplifier overloads, and the latter to ensure that the solution is not too rapid for the relay switches employed in the logic part of the problem. The

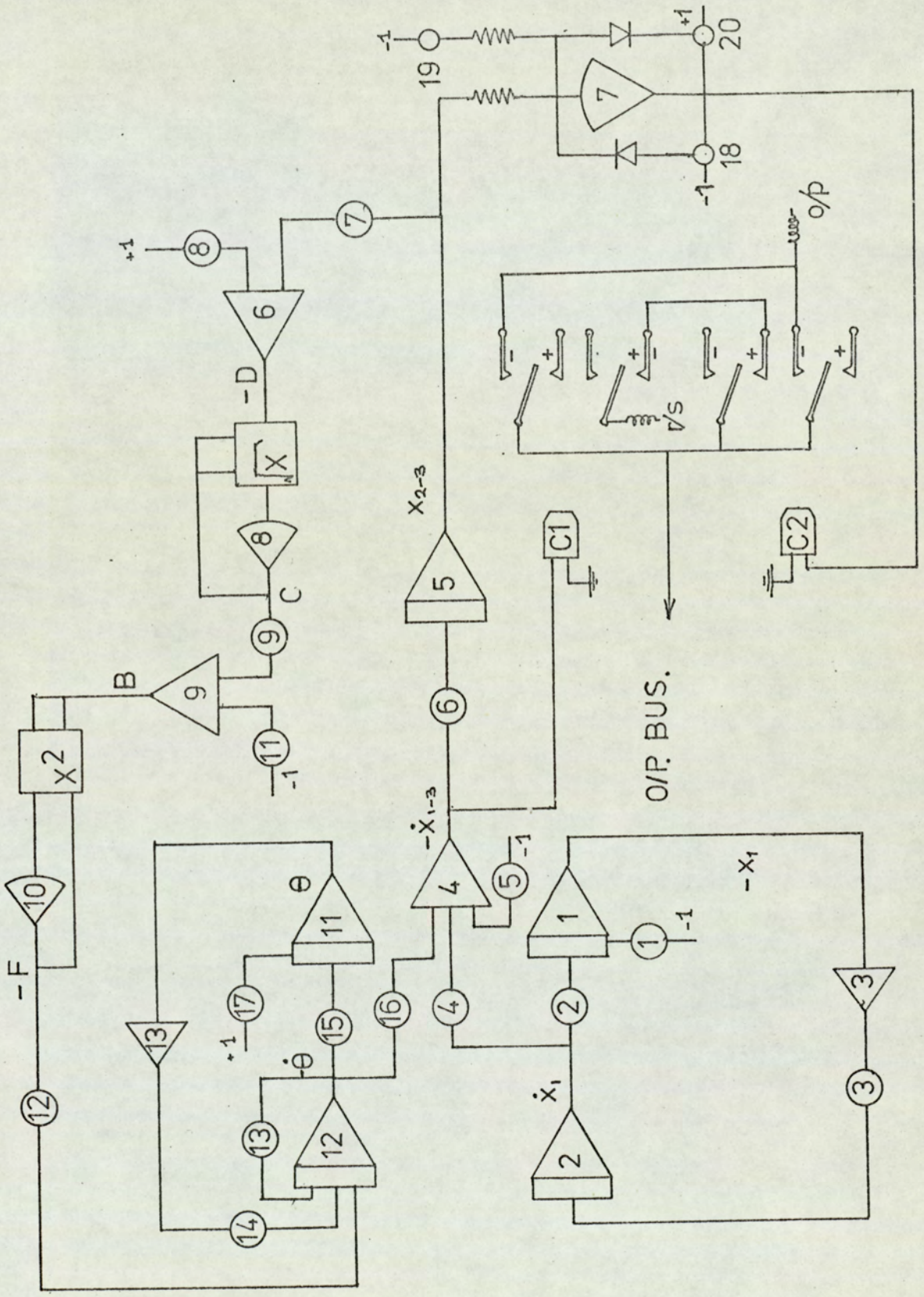

Electronic analogue circuit for single die oscillatory drawing.

Figure 31.

following equations have been so treated. In them, machine time, τ, is related to real time, t, by the identity $\tau = \beta t$.

$$\frac{d}{d\tau}\left[\frac{\dot{x}_1}{\hat{\dot{x}}_1}\right] = \frac{-\omega^2 \hat{x}_1}{\dot{x}_1 \beta}\left[\frac{x_1}{\hat{x}_1}\right] \quad - (1)$$

$$\frac{d}{d\tau}\left|\frac{x_1}{\hat{x}_1}\right| = \frac{\hat{\dot{x}}_1}{\hat{x}_1 \beta}\left[\frac{\dot{x}_1}{\hat{\dot{x}}_1}\right] \quad - (2)$$

$$\left[\frac{\dot{x}_{1-3}}{\hat{\dot{x}}_{1-3}}\right] = \frac{\hat{\dot{x}}_1}{\hat{x}_{1-3}}\left[\frac{\dot{x}_1}{\hat{\dot{x}}_1}\right] - \frac{\hat{V}}{\hat{\dot{x}}_{1-3}} - \frac{R\hat{\dot{\theta}}}{\hat{\dot{x}}_{1-3}}\left[\frac{\dot{\theta}}{\hat{\dot{\theta}}}\right] \quad - (3)$$

$$\frac{d}{d\tau}\left[\frac{x_{2-3}}{\hat{x}_{2-3}}\right] = \frac{\hat{\dot{x}}_{2-3}}{\hat{x}_{2-3}\beta}\left[\frac{\dot{x}_{2-3}}{\hat{\dot{x}}_{2-3}}\right] \text{ when not drawing} \quad -(4)$$

$$\left[\frac{B}{\hat{B}}\right] = \frac{\hat{F}^{\frac{1}{2}}}{(1-\alpha)\hat{B}} - \frac{\hat{F}^{\frac{1}{2}}\hat{C}}{(1-\alpha)\hat{B}}\left[\frac{C}{\hat{C}}\right] \quad - (5)$$

$$\left[\frac{F}{\hat{F}}\right] = \frac{\hat{B}^2}{\hat{F}}\left[\frac{B}{\hat{B}}\right]^2 \quad - (6)$$

$$\left[\frac{C}{\hat{C}}\right] = \frac{\hat{D}^{\frac{1}{2}}}{\hat{C}}\left[\frac{D}{\hat{D}}\right]^{\frac{1}{2}} \quad - (7)$$

$$\left[\frac{D}{\hat{D}}\right] = \frac{\alpha^2}{\hat{D}} + \frac{\mu AE(1-\alpha)\hat{x}_{2-3}}{R\hat{D}\hat{F}}\left[\frac{x_{2-3}}{\hat{x}_{2-3}}\right] \quad - (8)$$

$$\frac{d}{d\tau}\left[\frac{\dot{\theta}}{\hat{\dot{\theta}}}\right]_{\theta} = -\frac{R\hat{F}}{I\hat{\dot{\theta}}\beta}\left[\frac{F}{\hat{F}}\right] - 2\xi\omega_n\left[\frac{\dot{\theta}}{\hat{\dot{\theta}}}\right] - \frac{\omega^2 \hat{n}\hat{\theta}}{\beta\,\hat{\dot{\theta}}}\left[\frac{\theta}{\hat{\theta}}\right]_{\theta} \quad - (9)$$

$$\frac{d}{d\tau}\left[\frac{\theta}{\hat{\theta}}\right] = \frac{\hat{\dot{\theta}}}{\hat{\theta}\beta}\left[\frac{\dot{\theta}}{\hat{\dot{\theta}}}\right] \quad - (10)$$

The circuit:-

The analogue circuit adopted is shown in figure 31.

Values of constants.	Maximum values.
l : 12.8 in.	$\hat{x}_1$: 20×10^{-3} in.
E : 30×10^6 lbf./in.	$\hat{\dot{x}}_1$: 12 in./s.
A : 0.01963 in^2.	$\hat{\dot{x}}_{1-3}$: 24 in./s.
I : 53.77 lbf. in. s^2.	$\hat{x}_{2-3}$: 40×10^{-3} in.
w_n : 238.8 rad./s.	$\hat{F}$: 810 lbf.
ξ : 0.10; 0.30.	$\hat{\theta}$: 5×10^{-3} rad.
μ : 0.130.	$\hat{\dot{\theta}}$: 0.5 rad./s.
R : 9.0 in.	$\hat{B}$: 28.42 $(lbf)^{\frac{1}{2}}$.
α : 0.1846.	$\hat{C}$: 0.6000.
β : 250.	$\hat{D}$: 0.3333.

Amplifier.	Function.	Output.
1	Integrate.	$-\left[x_1/\hat{x}_1\right]$
2	Integrate.	$\left[\dot{x}_1/\hat{\dot{x}}_1\right]$
3	Invert.	$\left[x_1/\hat{x}_1\right]$
4	Sum.	$-\left[\dot{x}_{1-3}/\hat{\dot{x}}_{1-3}\right]$
5	Integrate.	$\left[x_{2-3}/\hat{x}_{2-3}\right]$
6	Sum.	$-\left[D/\hat{D}\right]$
7	Bi-stable.	
8	Square root.	$\left[C/\hat{C}\right]$
9	Sum.	$\left[B/\hat{B}\right]$
10	Square.	$-\left[F/\hat{F}\right]$
11	Integrate.	$\left[\theta/\hat{\theta}\right]$
12	Integrate.	$-\left[\dot{\theta}/\hat{\dot{\theta}}\right]$
13	Invert.	$-\left[\theta/\hat{\theta}\right]$

Figure 32.

Pot.	Function.	Setting.
1	$X/\hat{x}_1$	Variable.
2	$\hat{x}_1/\hat{x}_1\beta$	2.4000
3	$w^2\hat{x}_1/\hat{x}_1\beta$	Variable.
4	$\hat{x}_1/\hat{x}_{1-3}$	0.5000
5	$V/\hat{x}_{1-3}$	Variable.
6	$\hat{x}_{2-3}/\hat{x}_{2-3}\beta$	2.4000
7	$\mu AE(1-\alpha)\hat{x}_{2-3}/\hat{R}\hat{D}\hat{F}$	1.0290
8	$\alpha^2/\hat{D}$	0.1023
9	$\hat{F}^{\frac{1}{2}}\hat{C}/(1-\alpha)\hat{B}$	0.7350
11	$\hat{F}^{\frac{1}{2}}/(1-\alpha)\hat{B}$	1.2250
12	$R\hat{F}/I\hat{\theta}\beta$	1.0850
13	$2\zeta w_n/\beta$	0.1910; 0.5731
14	$w_n^2\hat{\theta}/\hat{\theta}$	2.2810
15	$\hat{\theta}/\beta\hat{\theta}$	0.4000
16	$R\hat{\theta}/\hat{x}_{1-3}$	0.1875
17	$\hat{F}R/Iw_n\hat{\theta}$	0.4757

Figure 32 (cont.)

The relative extension in the drawn wire, x_{2-3}, is generated by integrating $\dot{x}_{1-3}$, the relative velocity of the die to the drum. When drawing is occurring, the integrator is in 'reset', and in 'operate' when drawing is not occurring. This is achieved using two relay comparators, the inputs of which are $\dot{x}_{1-3}$ and x_{2-3} respectively. These comparators energise the 'operate' and 'reset' relays on the integrator. The connections are such that the integrator is in 'operate' if $\dot{x}_{1-3}>0$ or if $x_{2-3}>0$, whilst it is in 'reset' if $\dot{x}_{1-3}<0$ and if $x_{2-3}<0$. Thus drawing stops when the velocity of the die exceeds that of the drum, and starts when the force in the wire returns to the drawing force. To sharpen the switching and to eliminate relay instability a biased 'flip-flop' was inserted before the input to the relevant relay comparator.

The estimated maximum values of the variables, the values of the constants, and the potentiometer and amplifier functions are given in figure 32.

B71(d): The experimental investigation

The wire for the tests was previously drawn with a reduction of 25% to a diameter of 0.1847 in. to minimise surface and yield strength variations. During the tests the wire was given a further reduction of 26.3%. The tests were designed to investigate the effects of die amplitude, frequency, and drawing speed on the magnitude of cyclic force induced in the drawn wire. Before each test the drum was cleaned to ensure that the frictional conditions on the drum were representative of those in the friction measuring tests.

Several coils were also drawn to ensure that sufficient length of wire lay on the drum for the theory relating to the effective stiffness of the wire to be valid. To this end the coils were carefully separated before each test, so that no force was exerted by one coil on the next.

Amplitude tests:

To investigate the effect of die amplitude, wire was drawn under oscillatory conditions for a range of amplitudes up to 20×10^{-3} in. peak to peak, at 20 Hz., 60Hz. and 90Hz., and a drawing speed of 4 ft/min. Initially it was hoped to conduct these tests at 2 ft/min., but difficulty was found in maintaining this speed constant. Recordings were made of die amplitude and the peak to peak magnitude of the cyclic force in the die.

Frequency tests:

In these tests wire was drawn at 4 ft/min. with a die amplitude of 10×10^{-3} in. peak to peak, and for a range of frequencies, 20 Hz. up to 100 Hz.

Speed tests:

The effect of drawing speed was investigated by drawing wire with a die amplitude of 10×10^{-3} in. peak to peak and a frequency of 60 Hz. Drawing speeds ranged from 4 ft/min. to 20 ft/min.

During these tests it was observed that there was a phase shift between the die displacement and the die load, especially near the natural frequency of the drum. This was expected since in this frequency range the drum oscillates 90° out of phase with the die, and has its maximum amplitude. Thus it was not possible to merely add on the computed die

Analysis of load cell signals.

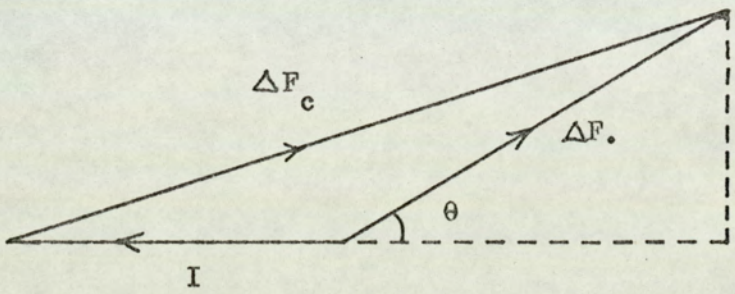

$\Delta F.$ = Observed force variation.

$\Delta F_c.$ = Corrected force variation.

I. = Inertia force.

$\theta.$ = Phase angle between die oscillations and observed force variation.

$$\Delta F_c^2 = (I + \Delta F. \cos\theta)^2 + \Delta F^2. \sin^2\theta.$$

$$= \Delta F^2 + I^2 + 2\Delta F. I \cos\theta.$$

Figure 33.

Amplitude in. x 10^{-3} z.t.pk.	$\triangle$F. lbf. pk.t.pk.	θ/360.	Inertia Force. lbf. pk.t.pk.	$\triangle$F. corr. lbf. pk.t.pk.
Frequency 20 Hz.				
5.0	67	-	6	73
7.5	121	-	8	129
10.0	148	-	11	159
12.5	191	-	14	205
15.0	224	-	17	241
17.5	290	-	20	310
20.0	345	-	22	367
Frequency 60 Hz.				
2	91	0.2424	20	94
4	163	0.2424	41	170
6	236	0.2239	61	253
8	303	0.1935	81	340
10	387	0.2154	102	421
12	472	0.2187	122	510
14	545	0.1720	142	625
16	557	0.1212	163	684
18	629	0.1875	183	719
20	629	0.1774	203	741

Amplitude tests. V = 4.0 ft./min.

Figure 34(a).

Amplitude in. x 10^{-3} z.t.pk.	$\triangle$F. lbf. pk.t.pk.	θ/360	Inertia Force. lbf. pk.t.pk.	$\triangle$F. corr. lbf. pk.t.pk.
Frequency 90 Hz.				
2	97	0.0769	23	118
4	169	0.0769	46	211
6	266	0.0952	69	325
8	296	0.0899	92	377
10	351	0.0714	114	456
12	423	0.0909	137	543
14	454	0.0788	160	600
16	484	0.0941	183	644
18	502	0.1022	206	678
20	502	0.1951	229	718

Amplitude tests. (cont.). V = 4.0 ft./min.

Figure 34(b).

Frequency. Hz.	△F. lbf. pk.t.pk.	θ/360.	Inertia Force. lbf. pk.t.pk.	△F. corr. lbf. pk.t.pk.
20	131	0.0980	11	140
25	175	0.1250	18	188
30	125	0.1045	27	156
35	139	0.1300	34	164
40	146	0.2527	45	152
45	242	0.2805	57	238
50	251	0.2331	71	268
55	342	0.2286	85	363
60	345	0.1494	102	414
65	315	0.2149	119	360
70	319	0.1579	138	411
75	393	0.1923	159	473
80	350	0.1428	181	486
85	351	0.1360	204	509
90	303	0.1364	229	485
95	315	0.1429	255	514
100	276	0.1200	281	514

Frequency tests.

$X = 10 \times 10^{-3}$ in. z. t. pk.

V = 4.0 ft./min.

Figure 35.

Speed. ft./min.	ΔF. lbf. pk.t.pk.	θ/360.	Inertia Force. lbf. pk.t.pk.	ΔF. corr. lbf. pk.t.pk.
1.67	411	0.1194	102	550
4.00	345	0.1494	102	414
4.90	342	0.2031	102	384
5.00	345	0.2083	102	384
5.70	296	0.2089	102	337
6.70	321	0.2615	102	330
8.35	266	0.2295	102	279
9.35	266	0.2576	102	280
10.00	266	0.2295	102	297
12.35	206	0.2576	102	226
12.66	194	0.3047	102	186
15.90	139	0.3534	102	112
17.25	127	0.3538	102	104

Speed tests.

Frequency = 60 Hz.

$X = 10 \times 10^{-3}$ in.
z.t.pk.

Figure 36.

inertia force to the observed die force to obtain the force in the wire. However, by measuring the phase shift it was possible to compute the force in the wire by means of vector addition (see figure 33).

Periodic measurements were made during the investigation of the peak force in the drawn wire. These values were averaged for use on the analogue programme as the drawing force under oscillatory conditions. The mean value was found to be 810 lbf.

Under all test conditions, considerable distortion of the loadcell signals was observed. These curves were smoothed by eye to an equivalent sine wave, and the force amplitude measured. The accuracy of this technique was checked using a planimeter for a selection of curves, and in all cases the two values of amplitude obtained were in close agreement.

The results of these tests are shown in figures 34 to 36.

B71(e): The analogue investigation

The range of the problem investigated on the analogue computer was designed to complement the experimental study described above. The problem was split therefore into three parts, comprising the effects of die amplitude, frequency, and drawing speed, on the magnitude of induced cyclic force. The same system constants and range of variables were employed.

To take into account the variation of the drum damping coefficient noted in Appendix 8 the upper and lower limits were used.

Taking results off the computer consisted of setting the desired values of amplitude, frequency, drawing speed, and damping coefficient on their respective potentiometers,

V = 4 ft./min.	Force variation. lbf. pk.t.pk.	
Amplitude. in. x 10^{-3} pk.t.pk.	ζ = 0.1	ζ = 0.3
Frequency 20 Hz.		
10	63	84
12	146	136
14	204	183
16	261	230
18	310	282
20	355	324
Frequency 60 Hz.		
4	125	94
6	282	225
8	376	334
10	449	405
12	502	460
14	549	507
16	585	554
18	627	585
20	658	622
Frequency 90 Hz.		
2	26	37
4	167	172
6	277	266
8	361	350
10	423	415
12	475	465
14	517	512
16	564	543
18	585	585
20	632	616

Analogue results: Amplitude tests.

Figure 37.

	Force variation lbf. pk.t.pk.	
Frequency. Hz.	ζ = 0.1	ζ = 0.3
20	73	84
21	115	—
22.5	185	—
25	172	—
27.5	143	—
30	125	141
35	99	162
40	131	199
45	334	277
50	478	340
55	470	387
60	455	397
70	428	408
80	418	413
90	418	413
100	418	418

Analogue results: Frequency tests.

V = 4 ft./min. ; X = 10×10^{-3} in. pk.t.pk.

Figure 38.

	Force variation. lbf. pk.t.pk.	
Speed. ft./min.	ζ = 0.1	ζ = 0.3
4	444	397
6	397	345
8	334	282
10	256	214
12	178	157
14	104	94
15	73	63
17	31	21

Analogue Results: Drawing speed tests.

Frequency 60 Hz. $X = 10 \times 10^{-3}$ in. pk.t.pk.

Figure 39.

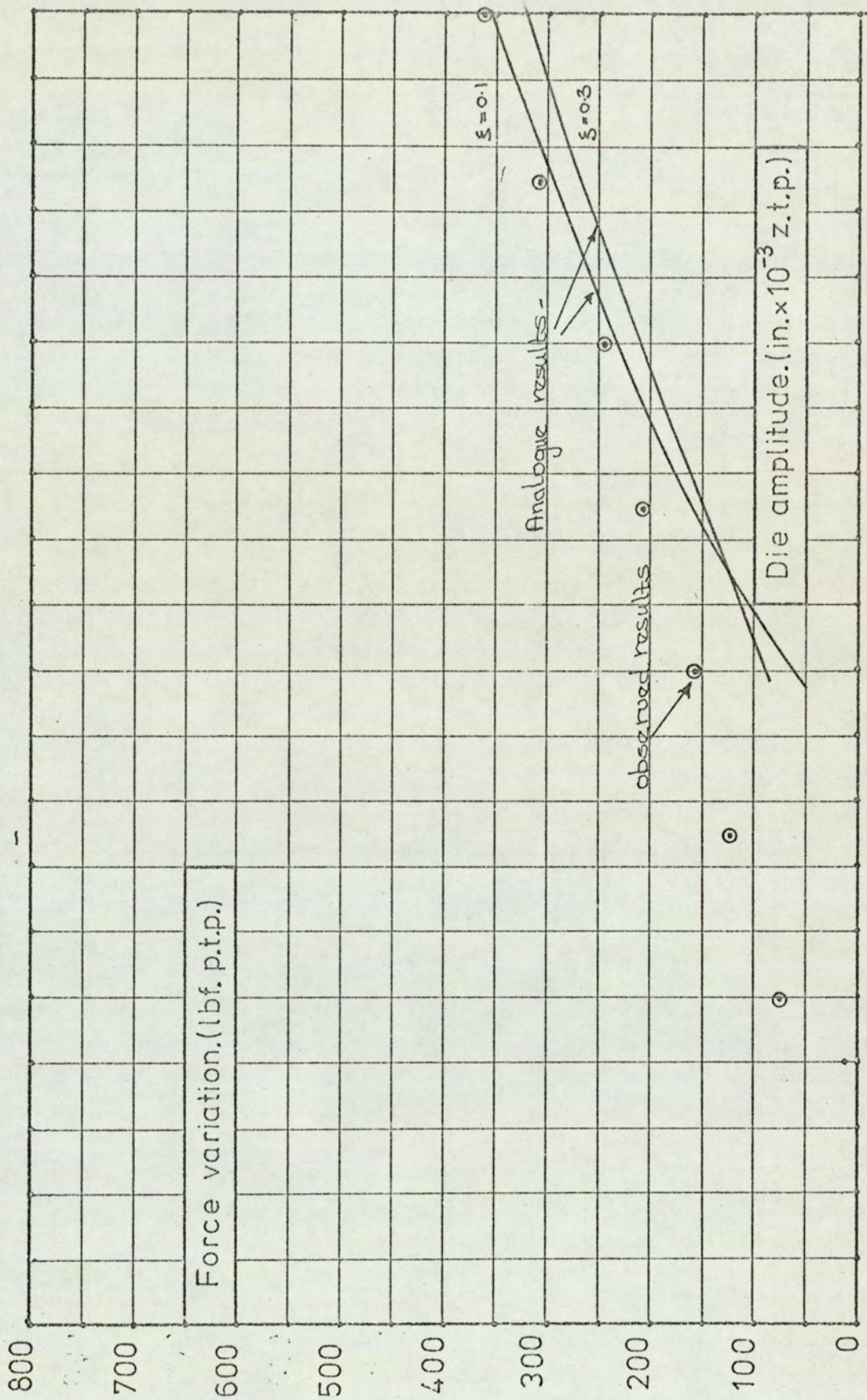

Amplitude tests: Comparison between theoretical and observed data.

20 Hz.

Figure 40a.

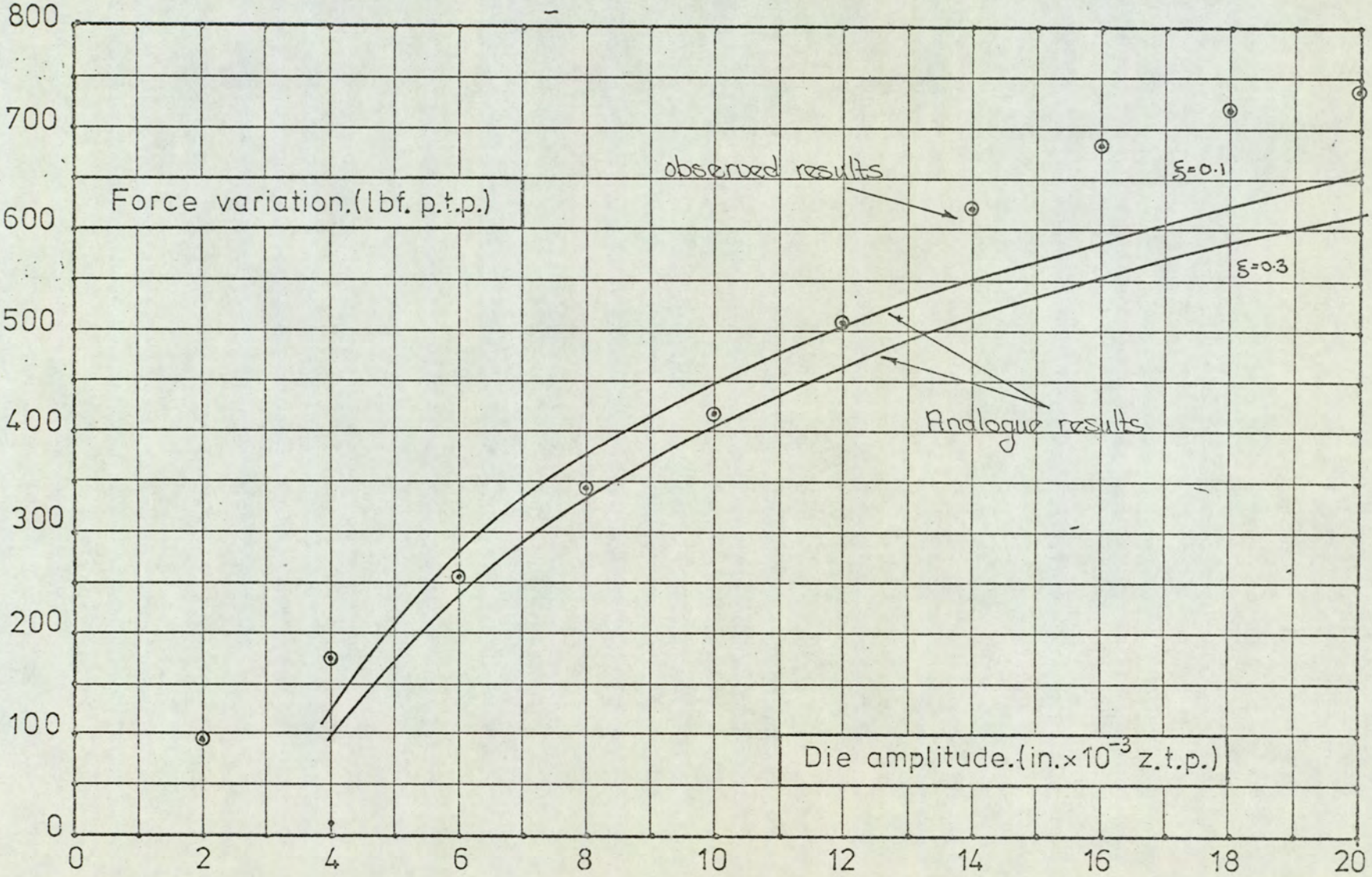

Amplitude tests: Comparison between theoretical and observed data.

60 Hz.

Figure 40b.

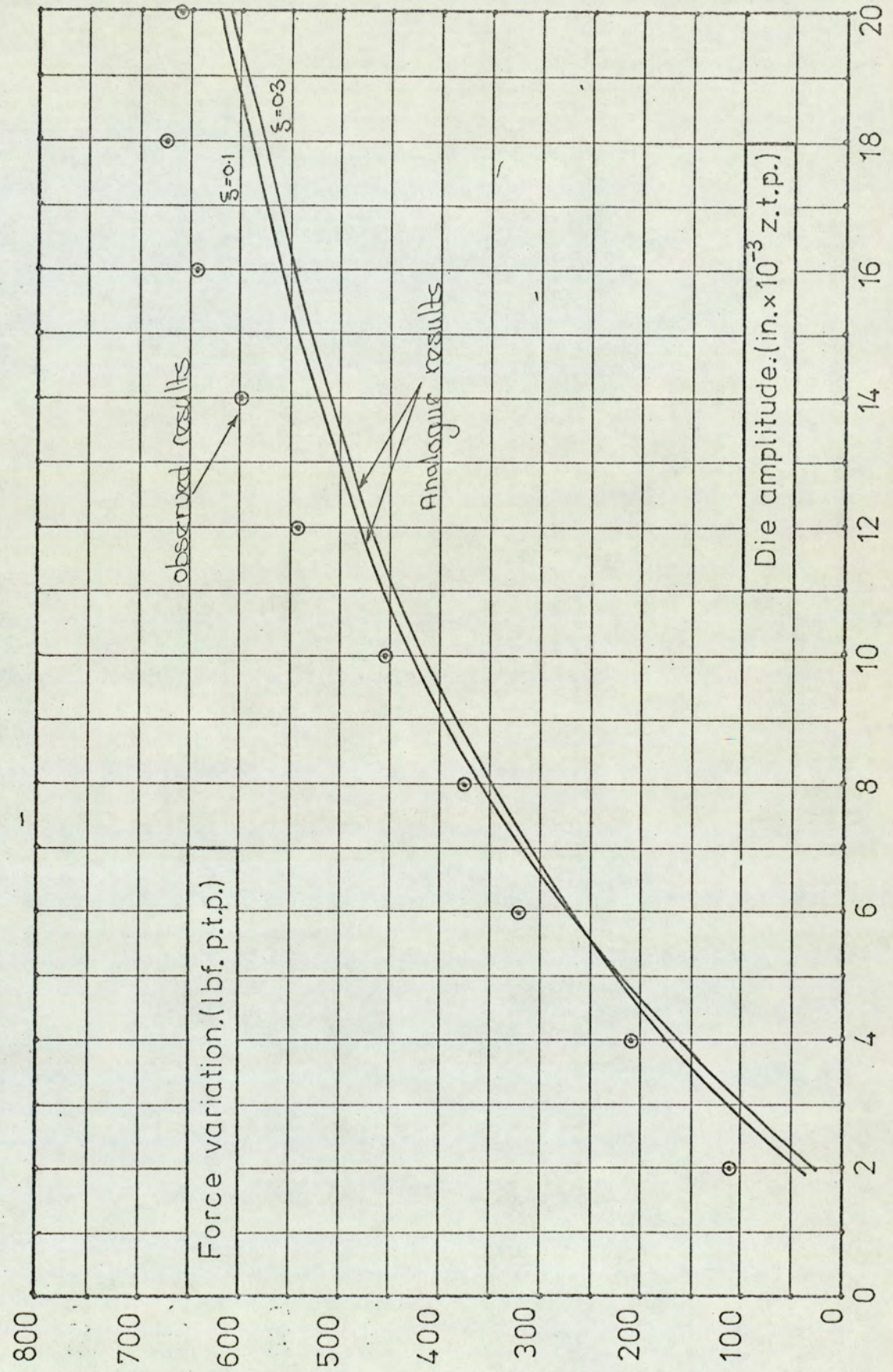

Amplitude tests: Comparison between theoretical and observed data.

90 Hz.

Figure 40c.

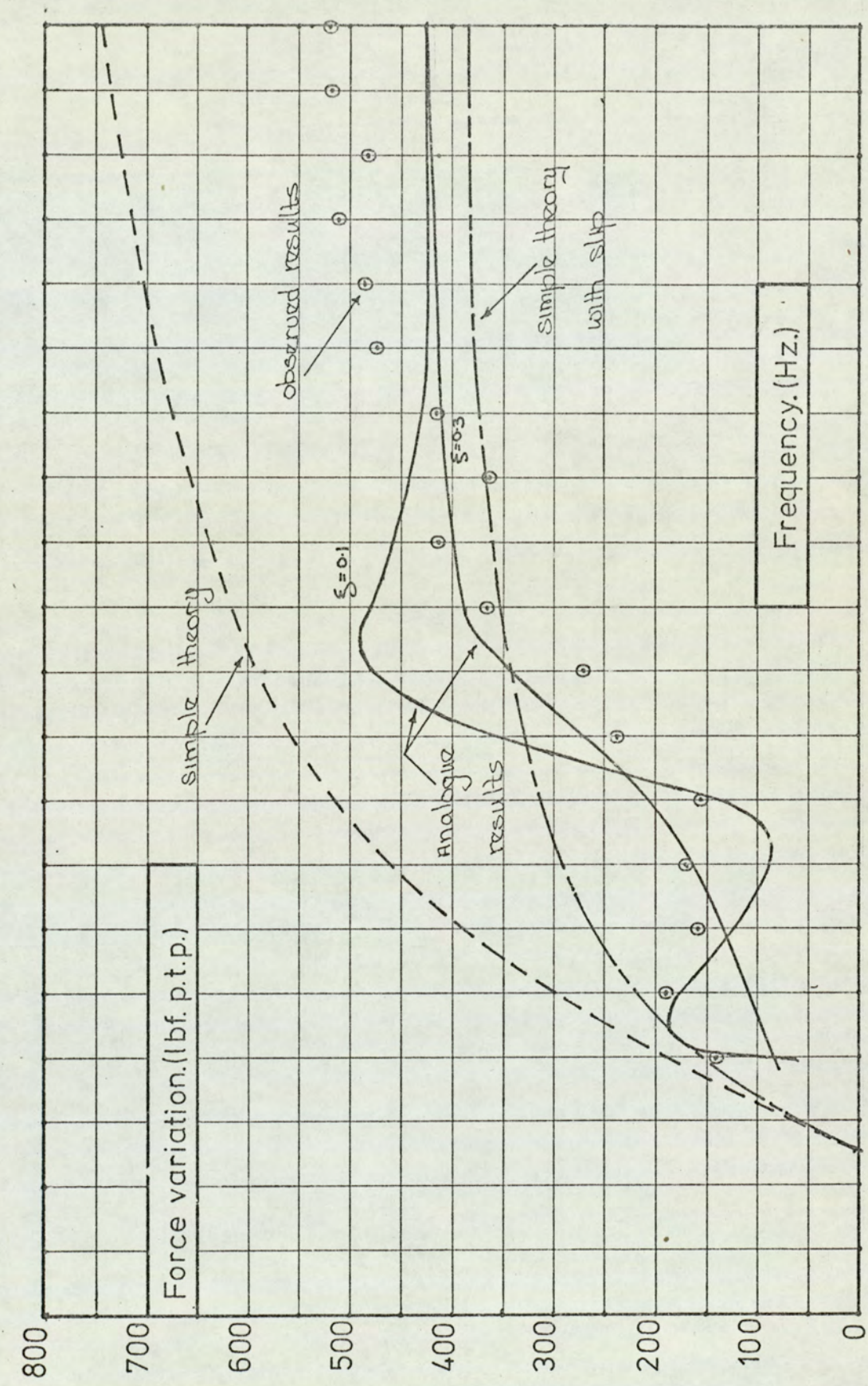

Frequency tests: Comparison between theoretical and observed data.

Figure 41.

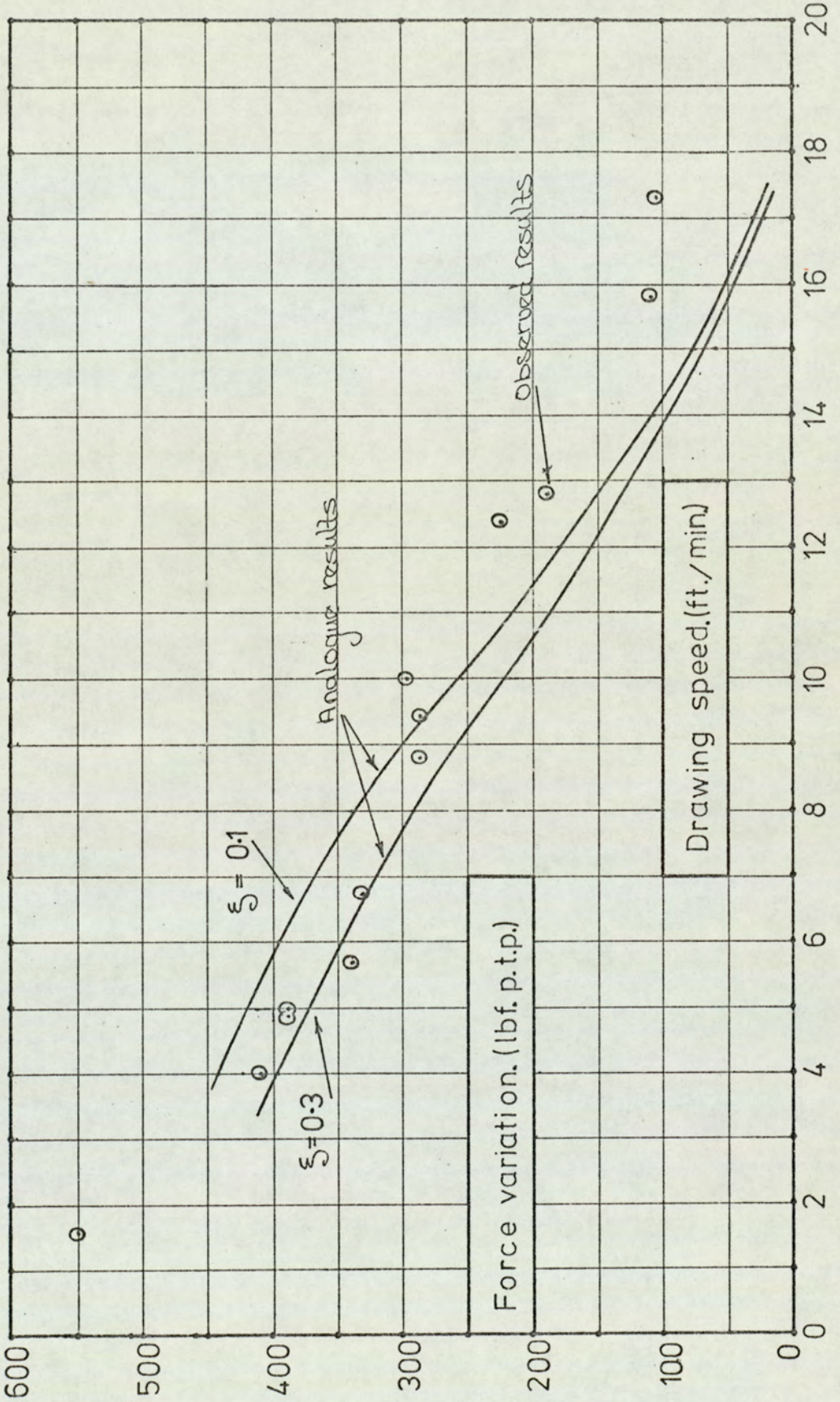

Drawing speed tests: Comparison between theoretical and observed data.

Figure 42.

switching the machine into operate, waiting for the transient response of the drum to pass, and recording the computed variation in wire force. These results are presented in figures 37 to 39. Figures 40 to 42 show a comparison between computed and actual values of cyclic force induced.

B72: Tandem drawing

Having established the mechanics of drawing wire through a single die with oscillations, the same approach was adopted in the study of wire drawing through two dies axially oscillated in antiphase. Initially an analogue programme was developed to simulate the process. However, initial results from this investigation revealed that the predicted force variations were much lower than those observed experimentally. This analysis did not take into account the increase in maximum load in the drawn wire when oscillations are applied to the die. It was therefore decided to develop a theoretical analysis including this effect. The results of the above analogue investigation showed that for frequencies of oscillation above and removed from the natural frequency of the drum, the effects of drum oscillations were minimal. The analysis was therefore considerably simplified by assuming no drum oscillations.

This section described the development of this analysis, and theoretical predictions are compared with experimental data.

B72(a): A discussion on the increase of maximum load in the drawn wire

In order to take this effect into account it was first necessary to hypothesise its true nature. In the previous investigation Winsper observed that when drawing wire through a single axially oscillated die, the maximum load in the wire was always in excess of the non-oscillatory drawing load. This effect was also observed in die 2 in this investigation. Winsper concluded that this increase in drawing load was a result result of sticking friction, and a transient non-equilibrium

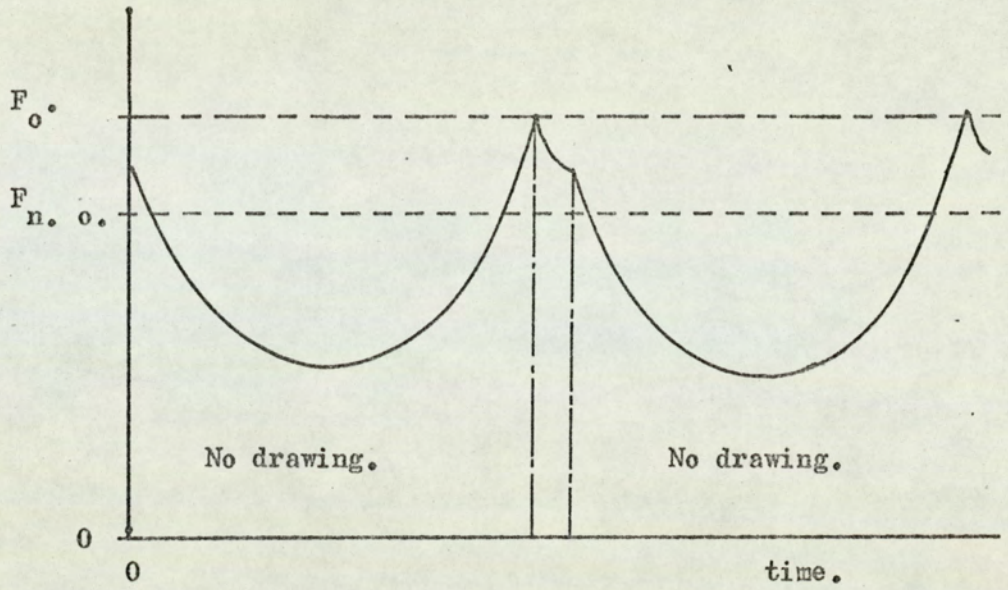

(a) Short drawing period.

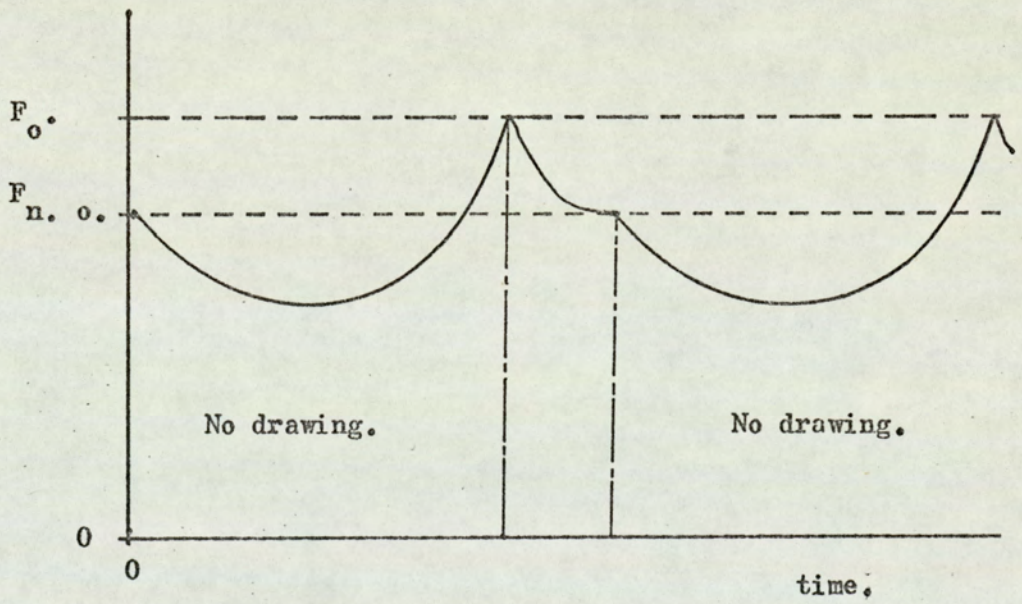

(b) Long drawing period.

F_o. = Peak oscillatory drawing load.

$F_{n.\ o.}$ = Non-oscillatory drawing load.

The effect of the transient drawing load on the induced cyclic stress.

Figure 43.

deformation pattern, both resulting from the intermittent nature of drawing. Experimental verification of this explanation was presented by Winsper, and is therefore considered acceptable here.

This transient increase in the drawing force will result in the following possibilities. If the period during which drawing occurs is in excess of the period of the transient force, then steady state drawing conditions are reached before the cessation of drawing. In this case the elastic off-loading of the drawn wire starts at a relatively low non-oscillatory drawing force. If however the drawing period is shorter than the transient period, then the elastic offloading is started at a higher load, whose value lies between the peak oscillatory load and the non-oscillatory drawing load. Furthermore, the shorter the drawing period, the closer the load (at cessation of drawing) approaches the peak oscillatory load. Thus, there are generally two components of force variation, namely that occurring during drawing, and that due to elastic off-loading. The magnitude of the former is greatest for the longer drawing periods, and in the limit is the difference between the peak oscillatory force and the non-oscillatory drawing force. The magnitude of the latter is a function of the drum to die velocity ratio and the die amplitude. These effects are shown diagramatically in figure 43.

In order to simplify the analysis, it was first assumed that steady state conditions were achieved during the drawing period. This assumption is correct if the drawing period is in excess of the transient period. The drawing period is longest for low amplitudes and frequencies, and high drawing speeds, and since the drawing speed was of the same order as

the peak die velocity, this assumption was thought justified.

The effect of this assumed behaviour is threefold:-

(1) It increases the maximum load in the wire.

(2) It increases the force variation in the drawn wire.

(3) It delays the start of drawing in each cycle.

B73(b): Modification to the stiffness of the drawn wire

Theoretical analysis has shown that the load - extension characteristic of the drawn wire is given by:-

$$U_{tot} = -\frac{R}{\mu AE}\left[F(1-\frac{\mu l}{R}) - 2\,(\hat{F}F)^{\frac{1}{2}} + (1+\frac{\mu l}{R})\hat{F}\right]$$

Experimental data has shown that the force variation in the drawn wire is small compared with its mean value. Thus it may be assumed that:-

$$(\hat{F}F)^{\frac{1}{2}} \doteq F$$

and therefore the above expression simplified to:-

$$U_{tot} = -\frac{R}{\mu AE}\left[(1+\frac{\mu l}{R})(\hat{F}-F)\right]$$

Therefore the effective stiffness of the drawn wire is:-

$$\frac{(F-\hat{F})}{U_{tot}} = \frac{AE}{(1+\frac{R}{\mu})}$$

The above simplified expression was used to determine the stiffness of the drawn wire in the following analysis.

B72(c): Theoretical analysis of oscillatory tandem drawing

The following subscripts are used:

1. initial die (die 2 on apparatus).
2. wire at die 1.
3. second die (die 1 on apparatus).
4. wire at die 3.
5. drum.

(a) wire between dies.

(b) wire between second die and drum

The dies are oscillated in anti-phase such that:-

$$x_1 = X\cos\omega t \qquad - (1)$$

$$x_3 = -X\cos\omega t \qquad - (2)$$

It is assumed that at t = 0 wire is being drawn in die (3), with exit velocity $\dot{x}_4$, and front tension F_b. It is also assumed that the transient phase in drawing is passed before drawing stops in die (1). In the period when steady state drawing occurs, the forces on the deformation in die (3) will be given by the conventional back pull equation:-

$$F_b = KF_a + F_{bo} \qquad - (3)$$

where K = back pull factor.

F_{bo} = drawing load for die (3) with no back pull.

From which is obtained:-

$$\frac{dF_b}{dt} = K\frac{dF_a}{dt} \qquad - (4)$$

but,

$$\frac{dF_b}{dt} = S_b(V - \dot{x}_4) \qquad - (5)$$

and,

$$\frac{dF_a}{dt} = S_a(r\dot{x}_4 - \dot{x}_2) \qquad - (6)$$

where r = Ab/Aa

S = stiffness.

If drawing is not occurring in die (1) whilst in die (3):

$$\dot{x}_2 = \dot{x}_1 \qquad - (7)$$

Combining equations (4) to (7),

$$\dot{x}_4 = \frac{S_b V - kS_a X\omega \sin\omega t}{rkS_a + S_b} \qquad - (8)$$

Since drawing is assumed to occur under steady state conditions before ceasing in die (3), drawing will stop in die (3) when the velocity of the die equals that of the wire at the die, at $t = t_1$, say,

i.e. when

$$\dot{x}_3 = \dot{x}_4$$

or $$X\omega \sin\omega t_1 = \frac{S_b V - KS_a X\omega \sin\omega t_1}{rKS_a + S_b}$$

$$\sin\omega t_1 = \frac{S_b}{(1+r)KS_a + S_b} \cdot \frac{V}{X\omega} \qquad - (9)$$

Now drawing has stopped in die (3), there follows a period of release of elastic strain in wire (b). The subsequent relative compression in wire (b) after $t = t_1$ is given by:-

$$\delta_b = x_{4-5} = \int_{t_1}^{t} \dot{x}_{4-5}.dt$$

Since drawing has stopped in die (3), the wire will follow the die, provided that the wire does not go into compression.

Thus: $\dot{x}_4 = \dot{x}_3$

Also it is assumed that the oscillations of the drum are negligible, and therefore the velocity of the other end of the wire will be the steady velocity of the drum.

i.e. $\dot{x}_5 = V$

$$\therefore \quad \delta_b = \int_{t_1}^{t} (X\omega \sin\omega t - V)\, dt$$

$$\delta_b = X[\cos\omega t_1 - \cos\omega t] - V(t - t_1) \qquad - (10)$$

The subsequent force in wire (b) is therefore given by:-

$$F_b = F_{b1} - S_b\left[X(\cos\omega t_1 - \cos\omega t) - V(t-t_1)\right] \qquad - (11)$$

where F_{b1} is the force in wire (b) when drawing stops.

During the period of elastic off-loading of wire (b), drawing will start in die (1). It is assumed that steady state conditions are established before drawing stops. Thus drawing will stop in die (1) when the velocity of the die exceeds that of the wire at the die, at $t = t_2$ say.

i.e. when $\dot{x}_1 = \dot{x}_2$

Since during this time drawing is not occurring in die (3), and the drawing force is constant for die (1):-

$$\dot{x}_2 = \dot{x}_4 = \dot{x}_3 = - X\cos\omega t$$

Thus drawing stops in die (1) when:-

$$\dot{x}_1 = \dot{x}_3$$

i.e. $X\cos\omega t_2 = - X\cos\omega t_2$

$$\omega t_2 = \pi \qquad - (12)$$

Since drawing has now stopped in die (1), there follows a period of release of elastic strain in wire (a). The subsequent relative compression in wire (a) after $t = t_2$ is given by:-

$$\delta_a = x_{2-4} = \int_{t_2}^{t} \dot{x}_{2-4}.dt$$

The wire at die (1) will follow the die, since drawing has stopped.

i.e. $\dot{x}_2 = \dot{x}_1$

The wire at die (3) will also follow the die since drawing has stopped.

i.e. $\dot{x}_4 = \dot{x}_3$

$$\therefore \delta_a = \int_{\pi/\omega}^{t} - 2X\sin\omega t \, dt$$

$$\delta_a = 2X\left[\cos\omega t + 1\right] \qquad - (13)$$

The subsequent force in wire (a) is therefore given by:-

$$F_a = F_{ao} - 2S_aX(\cos\omega t + 1) \qquad - (14)$$

where F_{ao} is the non-oscillatory drawing load for die (1)

The above equation will cease to be valid when drawing re-starts in die (3). This will occur when the applied front tension is sufficient to start drawing, at $t = t_3$, say. At this instant the forces are related by the equation:-

$$F_b = KF_a + F_{bo} + \Delta F_b \qquad - (15)$$

where ΔF_b is the magnitude of the drawing load increase during the transient phase.

(For the sake of simplicity it is assumed here that ΔF_b is constant for all conditions).

Substituting equations (11) and (14) in (15) yields:-

$$F_{b1} - S_b\left[X\cos\omega t_1 - \cos\omega t_3) - V\,(t_3 - t_1)\right]$$

$$= K\left[F_{ao} - 2SaX(\cos\omega t_3 + 1)\right] + F_{bo} + \Delta F_b \qquad - (16)$$

Drawing has now restarted in die (3). To render analysis from this point possible, it is assumed that the transient phase is infinitely short. Thus there follows in instantaneous adjustment of forces of magnitude δF_a and δF_b, brought about by the instantaneous drawing of a short length of wire, after which steady state conditions are achieved.

Now, at the initiation of drawing, the forces are related by:-

$$F_b = KF_a + F_{bo} + \Delta F_b \qquad - (15)$$

After the adjustment, the forces are related by the conventional drawing equation:-

$$F_b - \delta F_b = K(F_a + \delta F_a) + F_{bo} \qquad - (16)$$

Combining (15) and (17) gives:-

$$\Delta F_b - \delta F_b = K\delta F_a \qquad - (18)$$

If the short length of wire drawn during the adjustment is δx, then:

$$\delta F_b = S_b \delta x$$

and

$$\delta F_a = rS_a \delta x$$

i.e.

$$\frac{\delta F_b}{\delta F_a} = \frac{S_b}{rS_a}$$

Thus

$$\delta F_a = \Delta F_b \Big/ \left(K + \frac{S_b}{rS_a}\right) \qquad - (19)$$

where δF_a is the instantaneous rise of force in wire (a) due to the adjustment of forces, brought about by a change in the relationship between front and back tension.

And

$$\delta F_b = \frac{S_b}{(rKS_a + S_b)} \cdot \Delta F_b \qquad - (20)$$

where δF_b is the fall in front tension for the same reason. Drawing now continues in die (3) under steady state conditions with absolute velocity $\dot{x}_4$, given by equation (8).

Drawing is still not occurring in die (1), but the rate of off-loading of wire (a) has been modified by the initiation of drawing in die (3) at $t = t_3$. The subsequent compression in wire (a) after $t = t_3$ is given by:-

$$\delta_a = x_{2-4} = \int_{t_3}^{t} \dot{x}_{2-4}\, dt$$

$$= \int_{t_3}^{t} \left[- X\omega \sin\omega t - \frac{r(S_b V - KS_a X\omega \sin\omega t)}{rKS_a + S_b} \right] dt$$

i.e.

$$\delta_a = \frac{- S_b X}{(rKS_a + S_b)} \left[\cos\omega t - \cos\omega t_3 \right] - \frac{r\, SbV}{(rKS_a + S_b)} \left[t - t_3 \right] \quad -(21)$$

Drawing again stops in die (3) when $\omega t_4 = 2\pi + \omega t_1$.

At $t = t_4 = \frac{2\pi}{\omega} + t_1$, the force in wire (a) is given by combining equations (14), (19) and (21).

i.e.

$$F_a = F_{ao} - 2S_a X(\cos\omega t_3 + 1) + \frac{rS_a\, \Delta F_b}{(rkS_a + S_b)}$$

$$- S_a \left[\frac{S_b X}{(rKS_a + S_b)} (\cos\omega t_1 - \cos\omega t_3) - \frac{rS_b V}{(rKS_a + S_b)} \left(\frac{2\pi}{\omega} + t_i - t_3\right) \right] \quad - (22)$$

It has been assumed that drawing stops in die (3) under equilibrium conditions, and therefore the forces at this time are related by the equation:-

$$F_b = KF_a + F_{bo}$$

Substituting for F_a from (22) gives:-

$$F_b = K \left\{ F_{ao} - 2S_a X(\cos\omega t_3 + 1) + \frac{rS_a}{(rKS_a + S_b)} \cdot \Delta F_b \right.$$

$$\left. - S_a \left| \frac{S_b X}{(rKS_a + S_b)} (\cos\omega t_1 - \cos\omega t_3) - \frac{rS_b V}{(rKS_a + S_b)} \left(\frac{2\pi}{\omega} + t_1 - t_3\right) \right| \right\}$$

$$+ F_{bo} \quad - (23)$$

The value of F_b given by equation (23) is the magnitude of front tension in die (3) when drawing stops.

i.e. F_b(from (23)) $= F_{b1}$

Thus this expression for F_{b1} can be substituted in equation (16).

Manipulation of this equation yields:-

$$\cos\omega t_3 = \cos\omega t_1 - \frac{2\pi r K S_a}{(1+r)KS_a + S_b} \cdot \frac{\dot{V}}{X\omega}$$

$$+ \frac{\Delta F_b}{X\left|(1+r)KS_a+S_b\right|} + \frac{S_b}{(1+r)KS_a+S_b} \cdot \frac{Vt_1}{X} - \frac{S_b}{(1+r)KS_a+S_b} \cdot \frac{Vt_3}{X} \quad - (24)$$

The solution of equation (24) gives the time at which drawing starts in die (3), and hence the degree of elastic off-loading in wire (a) prior to this instant, given by equation (13).

Thus the cyclic force in wire (a) has five components:-

(1) A force drop during drawing in die (1), brought about by the change from transient to steady state drawing conditions, ΔF_a.

(2) A force drop after the cessation of drawing in die (1), and before the initiation of drawing in die (3), resulting from the release of elastic strain in the wire, $2S_aX(\cos\omega t_3+1)$ (equation (14)).

(3) An instantaneous rise in force due to the change in die (3) from transient to steady state drawing, $rS_a.\Delta F_b/(rKS_a+S_b)$ (equation (19)).

(4) A change in force due to the release and subsequent gathering of strain in wire (a) while wire is being drawn in die (3), $\frac{S_aS_bX(\cos\omega t_1 - \cos\omega t_3)}{(rKS_a + S_b)} - \frac{rS_aS_bV}{(rKS_a + S_b)}\left|\frac{2\pi}{\omega}+t_1-t_3\right|$ (equation (22)).

(5) An increase in force during the period between the cessation of drawing in die (3) and the initiation of drawing in die (1).

Similarly, the cyclic force in wire (b) has three components:-

(1) An instantaneous drop in force at the initiation of drawing in die (3), $Sb\Delta F_b/(rKS_a + S_b)$ (equation (20)).

(2) A change in force during drawing in die (3) under steady state conditions, due to the change in back tension applied by wire (a),

$$\frac{KS_aS_bX(\cos\omega t_1-\cos\omega t_3)}{rKS_a + S_b} - \frac{rKS_aS_bV}{rKS_a + S_b}\left(\frac{2\pi}{\omega} + t_1-t_3\right)$$

(equation (21)).

(3) A reduction and subsequent increase in force during the period when drawing does not occur in die (3), due to the release and subsequent gathering of strain in wire (b), $S_bX(\cos\omega t_1 - \cos\omega t_3) - S_bV(t_3-t_1)$ (equation (10)).

The above analysis assumes that the drawing period is sufficiently long for the transient phases in the drawing period to be passed before drawing ceases. The other extreme possibility is that the drawing period is so short that the forces during drawing are always higher by the fixed quantities ΔF_a and ΔF_b, and there is no time for the transient force to reduce, Thus the point in time when drawing stops in die (3) is still expressed by equation (9). The remainder of the analysis must be modified on two points.

(1) The back pull equation must be modified to include the increase in drawing force.

i.e. $F_b = KF_a + F_{bo}'$

where $F_{bo}' = F_{bo} + \Delta F_b$

(2) There will be no adjustment of forces at the initiation of drawing in die (3).

The result of this is the omission of one term in equation (24), which now becomes:-

Computed and observed values of drawing force reduction at 60 Hz.

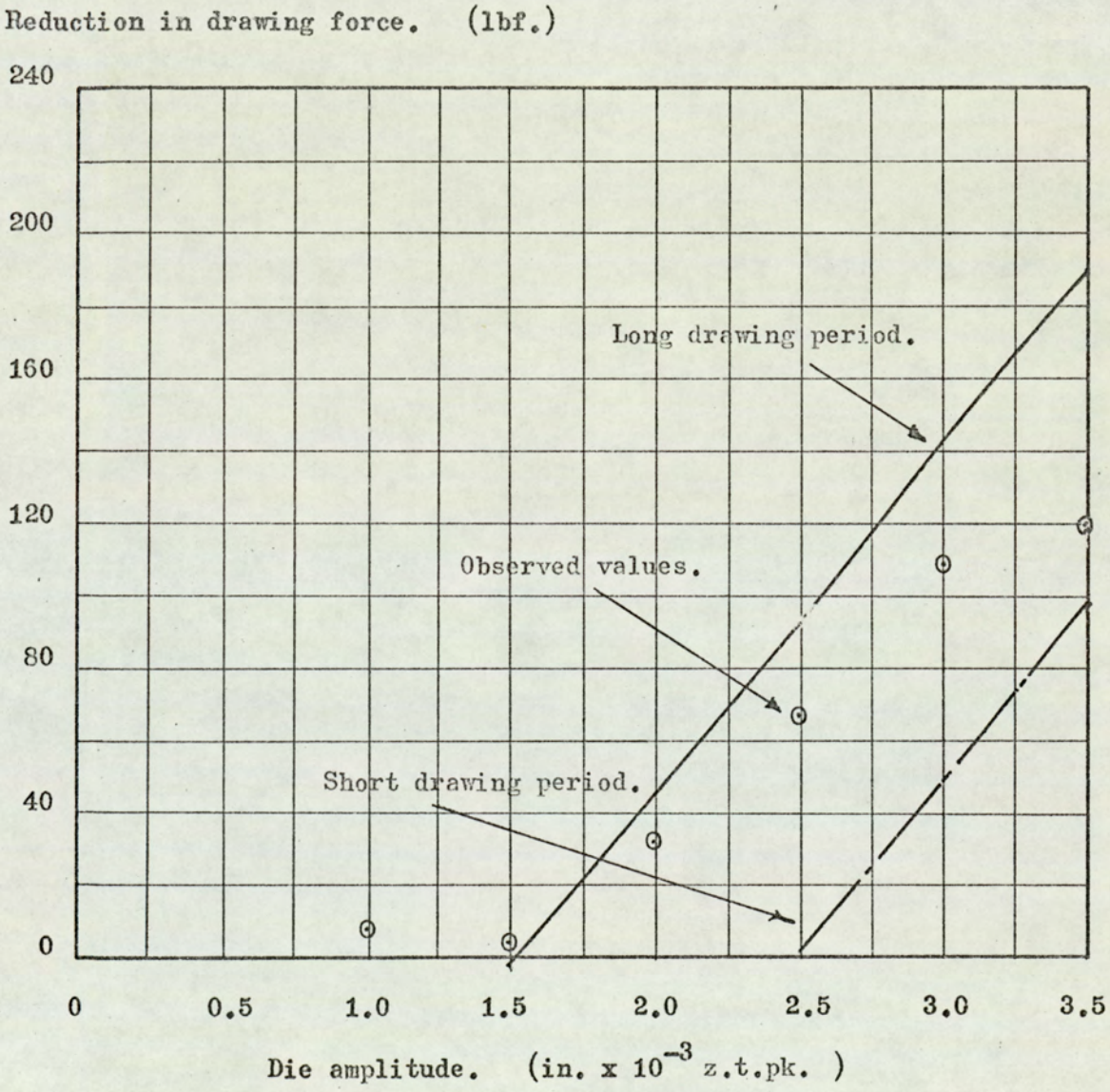

Figure 44.

Computed and observed values of drawing force reduction at 80 Hz.

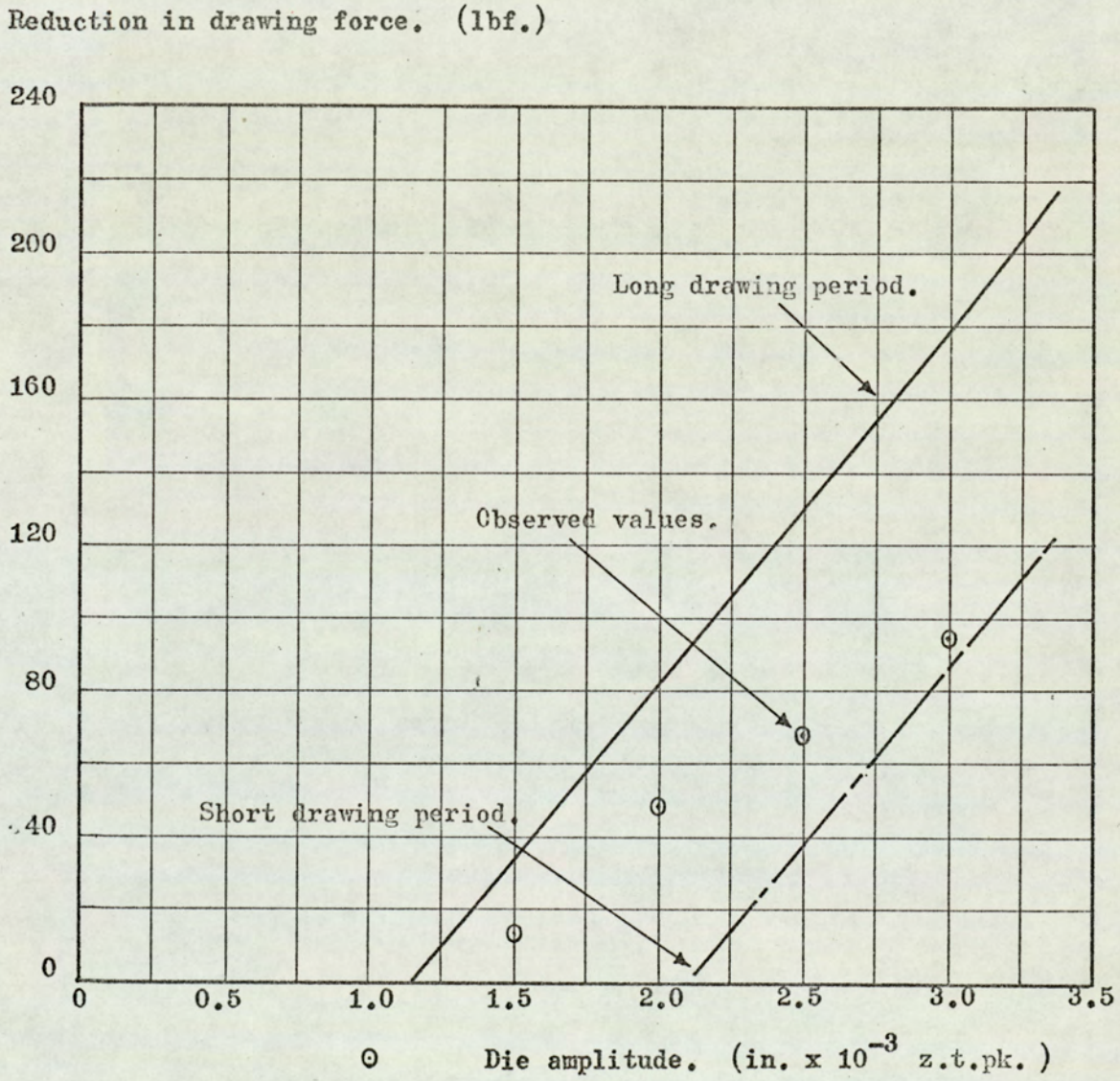

Figure 45.

Computed and observed values of drawing force reduction at 100 Hz.

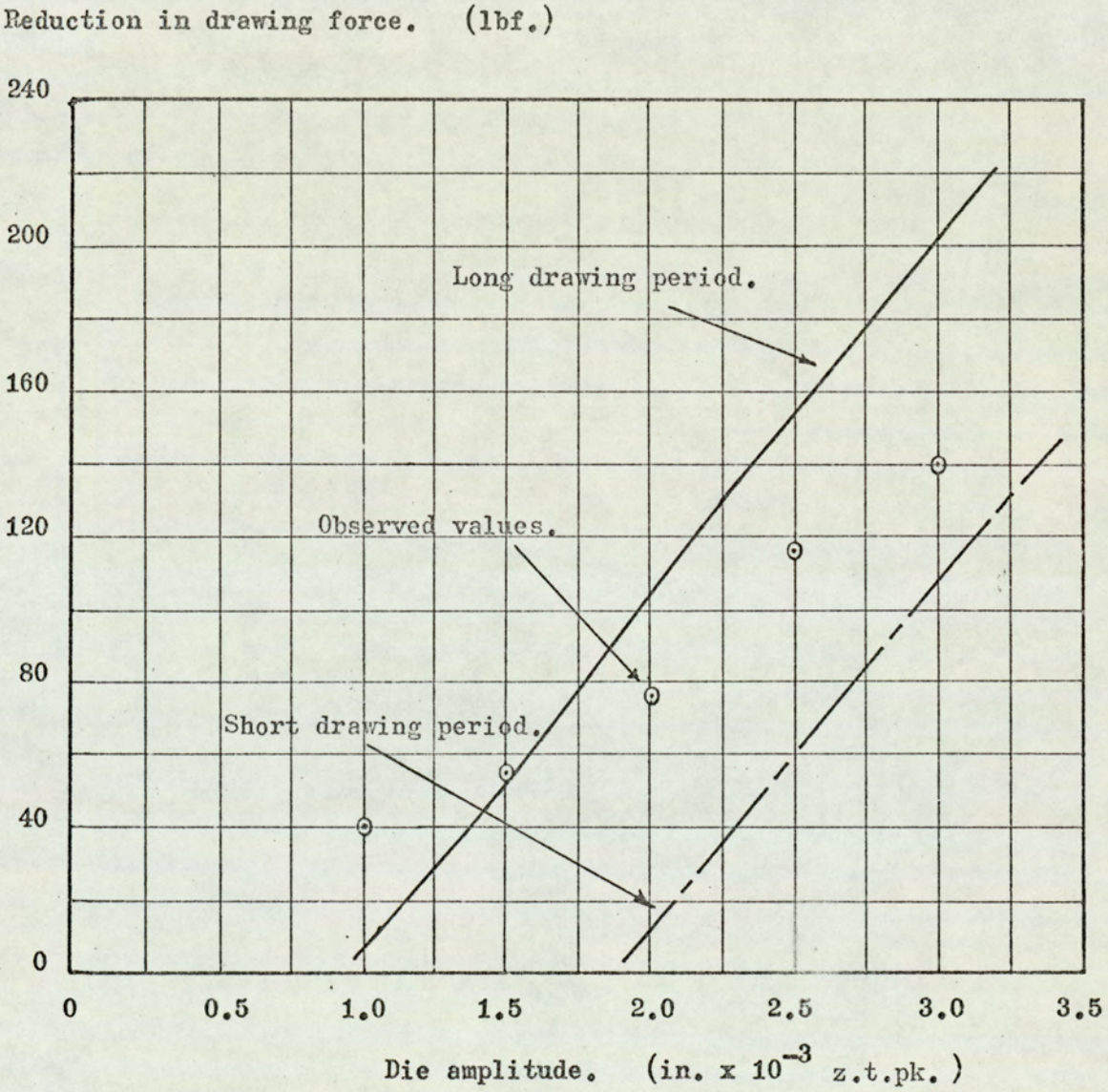

Figure 46.

$$\cos\omega t_3 = \cos\omega t_1 - \frac{2\pi rKS_a}{(1+r)KS_a + S_b} \cdot \frac{V}{X\omega} + \frac{S_b}{(1+r)KS_a+S_b} \cdot \frac{Vt_1}{X}$$

$$- \frac{S_b}{(1+r)KS_a+S_b} \cdot \frac{Vt_3}{X} \qquad - (24)$$

The reduction in peak drawing force was calculated using both theories, details of the calculations being given in appendix (11), and the results of which are plotted on figures (44) to (46).

B8: Discussion of Results

B8: Discussion of results

B81: Results of main tests

In order to evaluate the results obtained, it is first necessary to discuss the basic mechanics of wire drawing with back tension. The relationship between drawing load and back tension is of the form:-

$$F_b = KF_a + F_{bo} \qquad (1)$$

where F_b = drawing force

F_a = back tension

F_{bo} = drawing force without back tension

K = back pull factor

The load on the die in this cases is given by:-

$$F_d = F_b - F_a \qquad (2)$$

i.e. $$F_b = F_{bo} - CF_a \qquad (3)$$

where F_d = die load

$C = (1 - K)$

Thus it may be seen that the drawing load increases in proportion to the magnitude of back tension, whilst the die load decreases.

The basic mechanism proposed for the process was that wire is drawn alternately through each die, and for a short period during each cycle. The point at which drawing occurs in either die is when the die is at its most backward position in relation to the drum, since at this time the tension in the drawn wire for that die is greatest. During the remainder of the cycle, the wire which has been drawn through that die is elastically off-loaded and subsequently restressed by the forward and subsequent backward motion of the die. Now, since the dies are oscillated in antiphase, drawing will occur in die 1 when the back tension applied to it by die 2 is a

minimum. Thus the effect of oscillations is to reduce the magnitude of back tension at die 1 when drawing occurs in that die. Since this occurs when die 1 is at its most backward position, the subsequent forward motion of that die will cause the tension in the drawn wire to reduce. Hence the diminished drawing load for die 1 is the maximum load felt in the drawn wire. Thus the following features are to be expected in the experimental data obtained.

The maximum load in die 2 will be the load at which drawing occurs in that die, and will therefore be equal to the non-oscillatory drawing force for that die. Inspection of graphs 1 to 11 shows that in fact the effect of oscillations is to increase slightly the drawing load above its non-oscillatory value. Furthermore, the magnitude of this increase is greater for higher amplitudes of oscillation. This behavicur was expected, since it was observed in the previous investigation by Winsper. This was then attributed to a combination of sticking friction, retaining the wire in the die after the non-oscillatory drawing load was reached, and a transient, non-equilibrium deformation pattern, once drawing was initiated. Winsper provided independent experimental evidence for these mechanisms, which are therefore considered acceptable by the author.

The second feature to be expected in the data is that the minimum load in die 2, and hence that in the wire between the dies, will diminish with increasing amplitude of the dies. In the particular case when wire is not being drawn, and thus at no time does the wire move relative to the dies, the cyclic component of load will be proportional to amplitude. When wire is being drawn, provided that the length drawn per cycle, and

hence the relative movement of wire to die per cycle, is small compared with the total movement of both dies, then the proportionality will still hold. This is shown to be the case in practice, in particular in graphs 15 and 16, which show the magnitudes of cyclic loads induced.

During the period when wire is not being drawn, the wire behaves as a spring. Thus the cyclic component of force in the wire between the dies should increase with increased stiffness of this element. This effect is clearly demonstrated on graph 11, which relates to tests with varying die separation, and hence intermediate wire stiffness.

The magnitude of the cyclic force induced in the intermediate wire is of primary importance to the process, since it is that which dictates the diminished value of back tension applied to die 1, which results in a reduction in the total drawing load. The factors which affect this magnitude will be dealt with in a more quantitative manner when the effect of frequency is discussed.

Equation (2), at the beginning of this discussion, shows that a reduction in back tension during drawing will result in a proportional increase in the die load. Drawing will occur in die 1 when the back tension applied to it by die 2 is reduced, by an amount approximately equal to the peak to peak amplitude of cyclic force in die 2. Thus, according to equation (2), drawing will occur in die 1 with a die load which increases in proportion to the decrease in applied back tension. Graphs 1 to 11 clearly show that, as the minimum load in die 2 decreases, the maximum load in die 1 increases. Furthermore, if drawing occurs in die 1 under conditions which satisfy the steady-state drawing equation, the relationship between the min-

imum load in die 2 and the maximum load in die 1 should be expressed by equation (2). Graphs 12 to 14 compare the actual relationship of these forces with that given by equation (2). The constants in this equation were determined experimentally in the non-oscillatory drawing tests (see section B51). It may be seen from these comparisons that the actual die loads bear a distinct relationship with the applied back tensions, which is independent of amplitude, frequency, and die separation. Furthermore, the die loads are always in excess of those predicted by steady-state drawing theory, the difference being greatest at points corresponding to the highest amplitudes of oscillation. Thus again, in die 1, the drawing force under oscillatory conditions is always in excess of its corresponding non-oscillatory value, as is the case for die 2.

Drawing occurs in die 1 when the die is at its most backward position, and die 2 is at its most forward position. Subsequent to drawing die 1 moves forward, and the wire in die 1 moves with it, since drawing is not taking place. Thus the force in the final wire goes down. Concurrent with this, dies 1 and 2 are moving apart, and therefore the force in the wire between the dies goes up. This results in the net load in die 1 decreasing, by an amount equal to the change in loads in the two wires. Thus the degree of off-loading of die 1 will be proportional to the amplitude of the two dies. This is clearly demonstrated in graphs 15 and 16.

Under steady-state, non-oscillatory drawing conditions the back tension applied to die 1 is the drawing force for die 2. Since the effect of oscillations is to reduce the back tension applied to die 1 when drawing occurs there, this results in a

proportional reduction in the load in the drawn wire at this instant (see equation 1). Since the degree of reduction of back tension is proportional to die amplitude, then the degree of reduction of the drawing load on the drawn wire is similarly proportional. This is shown in graph 17.

As previously stated, after drawing occurs in die 1, its subsequent forward motion reduces the load in the drawn wire. Again, this off-loading will be proportional to die amplitude, as shown by graphs 15 and 16.

Throughout this investigation it was observed that the amplitude of cyclic loads, and consequently the reduction in peak drawing load, was greatest for the higher frequencies of oscillation. For example, graphs 1 to 8 show that a minimum die load of zero is reached at a lower amplitude of oscillation when the frequency is increased. However, these effects are more clearly demonstrated in graphs 15 to 17. These show that there is a general trend towards higher cyclic forces at all three stations, for a given die amplitude, as the frequency is increased (graphs 15, 16). As expected, this trend is reflected in the drawing loads, where it may be seen that the reduction in drawing load is greatest at the higher frequencies (graph 17).

These observations conflict with the findings of Winsper in the previous investigation. There it was observed that the level of cyclic stress was independent of frequency. The reasons for this apparent disagreement will be discussed later, when the results obtained from the analogue investigation are discussed.

A study of graphs 15 and 16 will reveal that this increase in effectiveness with frequency is most clearly observed in

the cyclic component of force in die 2. In this case, almost without exception, the level of cyclic force at a given amplitude increases for every increment of frequency. This is not the case for the cyclic force in the drawn wire, or in die 1. In these cases 80 Hz. is generally the frequency at which the greatest cyclic force is induced. It is thought that here there are two agencies effective in determining the level of cyclic stress for a given amplitude of die oscillation. The first is the general increase of effectivenss with frequency, which will be discussed later, and the second is the response of the drum to cyclic forcing. The amplitude of induced drum oscillations will have its maximum value near the natural frequency of the drum. For frequencies higher or lower than this, the drum amplitude will be diminished. Furthermore, below the natural frequency, the drum oscillations will be in phase with those of die 1, and in anti-phase for frequencies above. Thus, below the natural frequency, the effect of drum oscillations will be to diminish the effective cyclic stress induced in the drawn wire. Above the natural frequency, the cyclic stress will be increased, this effect diminishing with increasing frequency. The combination of the two agencies will result in a general increase in cyclic stress with frequency, with a resonant peak situated just above the natural frequency superimposed. Under these circumstances, the maximum effectiveness may be observed at frequencies below the maximum used. This effect is also reflected in the cyclic forces in die 1, since this is the algebraic sum of the cyclic forces in die 2 and the drawn wire.

In view of the above observations, it was decided to study the effects of frequency on the cyclic force in die 2, since in

this case, the oscillations of the drum have no effect. It was further decided to compare the above force with its theoretical maximum value. This maximum is achieved in the special case when wire is not being drawn, and thus there is no relative movement between the die and the wire. In this case the peak to peak cyclic force induced is simply given by:-

$$\Delta F = 4XS \qquad (4)$$

where X = zero to peak die amplitude

S = wire stiffness

Graph 18 shows this comparison for frequencies of 40, 60, 80 and 100 Hz., with die separations of 18 in. and 10 in. Also shown are the points corresponding to the test using various die separations at 60 Hz. From this graph it may be seen that for a given frequency the computed and actual force variations bear a linear relationship, and that observed values approximate more closely to the computed values at the higher frequencies. Thus, it may be concluded that the level of cyclic stress is proportional to amplitude and wire stiffness, the constant of proportionality approaching unity as the frequency increases.

The reason for this diminished effect at lower frequencies is considered to be the greater relative movement between dies and wire in these cases. The length of wire drawn per cycle in each die is greater at the lower frequencies, and thus in these cases the actual situation is furthest removed from the theoretical condition, where no relative movement is accounted for. Thus the gradients of the curves in graph 18 are an expression of the efficiency of coupling between the die and the wire, a coupling coefficient of unity meaning no relative movement.

The effect of increasing the drawing speed from 2 ft/min to 5 ft/min is shown in graphs 2 to 4, 12(a), and 18(a). Unfortunately, this increased drawing speed resulted in a diminution of the non-oscillatory die loads, and the back-pull factor, C. This is considered to be the result of an improvement in the frictional conditions afforded by a thicker lubricant film being generated. However, it may be seen that the qualitative behaviour is identical to that described above, but that the level of cyclic stresses induced is diminished. This effect is demonstrated quantitatively in graphs 18 and 18(a), which compare the computed and actual force variations in die 2, at drawing speeds of 2 ft/min. and 5 ft/min. respectively. Here it may be seen that, for a given frequency, the coupling coefficient between the dies and the intermediate wire is diminished for an increase in drawing speed. This effect is similarly considered to be the result of the increased relative movement of wire to die, as described above. This results in a diminution in the effective reduction in drawing force, as may be seen in graphs 2 to 4. However, the effect of the enhanced lubrication conditions is sufficiently great to produce a lower drawing force at 5 ft/min than at 2 ft/min. for the same oscillatory parameters.

Thus the effects of the variables are now defined. The degree of reduction of back tension applied to die 1 is proportional to amplitude and wire stiffness, the constant of proportionality approaching unity for high frequencies and/or low drawing speeds. There is a unique relationship between total drawing load and applied back tension, expressed in graphs 12 to 14, which is a coarse approximation to equation (1), the divergence from the equation being due to the previously discussed rise of the oscillatory force above its

non-oscillatory value. Therefore the reduction in total drawing force is likewise proportional to amplitude, wire stiffness, and coupling coefficient, and also the non-oscillatory back pull factor. The reduction in drawing force may be expressed in equation form as follows:-

Using the nomeclature in equation (3), and referring to graphs 12 to 14, the relationship between die load and back tension under oscillatory conditions may be expressed as:-

$$F_b = F_{bo} + \Delta F_{bo} + C'Fa \qquad - (5)$$

where ΔF_{bo} = the rise above the non-oscillatory die load for zero front tension.

C' = slope of line joining the oscillatory points.

Therefore, under oscillatory conditions, the drawing force is given by:-

$$F_b = K'F_a + F_{bo} + \Delta F_{bo} \qquad - (6)$$

where $K' = (1 - C')$

The magnitude of back tension applied to die 1 during drawing is:-

$$F_a = Fa_{n.o.} + \Delta F_a - 4XS\psi \qquad - (7)$$

where $Fa_{n.o.}$ = non-oscillatory drawing force in die 2.

ΔF_a = rise above the non-oscillatory force in die 2.

X = zero to peak amplitude of both dies.

S = stiffness of wire between dies.

ψ = coupling coefficient.

Combining equations (6) and (7):-

$$F_b = K'(Fa_{n.o.} + \Delta F_a - 4XS\psi) + F_{bo} + \Delta F_{bo} \qquad - (8)$$

Under non-oscillatory conditions, the front and back tensions are related thus:-

$$F_{bn.o.} = KF_{ano} + F_{bo} \qquad (9)$$

Thus the drop in drawing force due to oscillations is given by:

$$\delta F_b = F_{bno} - F_b = F_{ano}(K-K') - K'\Delta F_a - \Delta F_{bo} + 4K'XS\psi$$

i.e. $$\delta F_b = K'\left[4XS\psi - \Delta F_a\right] \qquad (10)$$

From the above equation it may be seen that the reduction in drawing force is a function of die amplitude, wire stiffness, the non-oscillatory back pull factor, the rise above the non-oscillatory drawing force, and the coupling coefficient. The following is a comparison between observed reductions in load, and those derived from equation (10).

Frequency = 100 Hz $S = 4.46 \times 10^4$ lbf/in

Die separation = 18 in $C' = 0.635$

ψ = 0.800 $K' = 0.365$

Die amplitude in $\times 10^{-3}$ t.p.	δF_b observed lbf	δF_b calculated lbf
1.0	40	47
1.5	55	59
2.0	76	74
2.5	116	97
3.0	150	129

Thus the values of drawing force reduction are in coarse agreement with those predicted by equation (10). A study of graph 12 will reveal that the oscillatory back pull factor, K', is not constant, thus accounting for the discrepancies observed. This variability of the back-pull

factor may be the result of either a variation in the friction conditions in die 1, resulting in a change in the value of the non-oscillatory back-pull factor, or the assumption that the rise above the non-oscillatory force in die 1 is proportional to the degree of reduction in effective back tension applied to that die. Examination of graph 12 reveals that this assumption is not strictly true, and furthermore, there is some random variability in the magnitude of this rise.

The above predictions of drawing load reductions can only be obtained with a prior knowledge of the coupling coefficient between the wire and the dies. Since this has been obtained experimentally, no prior predictions relating to the effectiveness of the process can be made. For this reason, the more complete analysis in section B73 was conducted. The results of this analysis will be discussed later.

The remaining tests to be discussed are those investigating the effects of oscillating one die only, the results of which are given in graphs 9, 10 and 14. Oscillating die 1 only has the same effect as oscillating both dies, but since it is only die 1 which is effective in inducing a cyclic force in the intermediate wire, to gain the same effectiveness as with two dies, the amplitude of oscillation must be approximately doubled. This therefore induces a greater cyclic force in the drawn wire. The relationship between front and back tension in die 1 at the drawing condition is of the same form as that when two dies are oscillated (see graph 14).

Oscillating die 2 only modifies the process, since there is no release of strain in the drawn wire resulting from the motion of die 1. In this case there is still an effective

reduction in back tension in die 1, and the relationship between front and back tension during drawing is unaltered. However, since there is no subsequent forward motion of die 1, there is no release of strain in the drawn wire, and the motion of the drum causes the force in the drawn wire to increase. The possibility of drawing continuing under these conditions will depend upon the relative magnitudes of the increase of load in the drawn wire and the increase of applied back tension in die 1. Examination of graph 10 shows that, generally, the increase in back tension is well in excess of the increase in load in the drawn wire, and hence it is unlikely that drawing will continue throughout the whole cycle. Again, to achieve the same effectivenss as with drawing with both dies oscillating, the die amplitude must be approximately doubled.

B82: Discussion of analogue investigation

This investigation attempted to discover the various factors which influence the magnitude of cyclic force induced in the drawn wire, when axial oscillations are applied to the die during drawing. Figure (41) shows the computed levels of cyclic force for a range of frequencies, with fixed die amplitudes and drawing speeds. Three computed curves are drawn, showing successively closer approximations to the experimental data. The basic mechanism underlying all three theoretical curves is described in section B71(a). This states that wire is drawn intermittently at a constant load, and between these drawing periods the drawn wire is elastically off-loaded and loaded.

If it assumed that during the elastic off-loading and loading, the wire is strained between the die and the drum only, and also that the drum is infinitely stiff, then the above mechanism gives predictions of cyclic force shown in the upper curve. In this case the cyclic force increases with frequency, thus agreeing with the experimental data, but grossly overestimates the magnitude at a particular frequency.

When the straining of the wire coiled on the drum is taken into account, the predicted cyclic stress magnitude is reduced considerably. However, below the natural frequency of the drum the computed magnitude is too high, and too low above the natural frequency.

When the oscillations of the drum are also taken into account, using the analogue computer, this rapid change of magnitude above the natural frequency is also predicted. This particular phenomenon is thought to be due to the change of phase relationship between the die and drum oscillations

about the natural frequency, Below this, the drum will move in phase with die, and thus tend to reduce the effective amplitude induced in the wire. Above the natural frequency the drum will oscillate out of phase with the die, thus increasing the effective amplitude. Thus it is concluded that the predictions of cyclic force amplitude obtained from the analogue investigation are in the closest agreement with experimental data.

The effect of die amplitude on the magnitude of cyclic force induced is shown in figures 40 a, b, c, with the analogue results shown for comparison. Here, it may be seen that the force amplitude increases with die amplitude for all frequencies considered, and that generally the predicted values are in close agreement with observed data.

Figure 42 indicates the experimental and theoretical variation of force amplitude with drawing speed, showing the force to be reduced at the higher drawing speeds. Again there is a close agreement between experimental and theoretical data.

The results of the analogue programme show that the experimentally observed variation of damping coefficient of the drum results in a large variation in the cyclic force magnitudes, especially near the natural frequency. This will account to some degree for the scatter observed in the experimental points. There are, however, two areas where the experimentally observed force amplitude is consistently higher than the predicted value, namely at the higher frequencies, and the higher values of mean drum to peak die velocity ratios.

During the drawing tests it was observed that at the higher frequencies the drawn wire was excited transversely,

particularly at high amplitudes. This is thought to account for the higher magnitudes of force variation in this region.

The second region of disparity is not so readily explained, but is thought to result from the rise of the peak drawing force above its non-oscillatory value. As discussed previously in section B73(a), this has the effect of producing a second component of force variation. If the drawing period is longer than the transient period for higher drawing loads, then drawing will stop at the steady state, non-oscillatory drawing force. In this case the force variation will have both the elastic off-loading component and an amount equal to the rise above the non-oscillatory drawing force. As the drawing period is diminished, this latter component is progressively reduced, since insufficient time elapses during drawing for the transient force to diminish.

The conditions for a long drawing period, and hence increased force variation by this mechanism, are a large drum to die velocity ratio, (see B71(a)), and a low frequency of oscillation. Since these are the conditions under which the observed force variations are excessive, the above mechanism is considered to be the probable explanation for this behaviour.

Thus it is concluded from the analogue investigation that axial oscillations of the die during wire drawing cause the drawing process to be intermittent. Between these drawing periods the drawn wire is elastically off-loaded and loaded, by an amount dependent on the drum to die velocity ratio, the die amplitude, the dynamic response of the drum, the degree of frictional constraint by the drum on the coiled wire, the transverse response of the drawn wire, the magnitude of

the rise of the drawing force above its non-oscillatory value, and the duration of the drawing period.

These findings are in conflict with those of Winsper in that during that investigation it was observed that there was no effect of frequency on the cyclic force amplitude. However, this is to be expected, since in that investigation the oscillation frequencies were always above the natural frequency of the drum, and under these conditions the force variation is almost constant with frequency. Some increase of force was observed in this investigation, and this was attributed in part to the induction of a transverse mode into the drawn wire. This effect was not reported by Winsper, since in that case the free length of drawn wire was less, and the diameter generally greater, both differences resulting in a stiffer system in the transverse mode, with a higher natural frequency.

B83: Tandem drawing analysis

The object of this analysis was to obtain predictions of drawing load reductions for a given set of system variables. The simple theory discussed at the beginning of this section did not achieve this, since an experimentally obtained coupling coefficient was necessary for solution. Also the analysis was designed to evaluate the effects of the increased oscillatory force.

Several major assumptions were made during the analysis, for the purposes of simplification, and these will now be discussed.

It was assumed that the velocity of the drum was constant at the mean value of drawing speed. This implies that no oscillations are induced in the drum due to cyclic forcing. This is considered justified since the level of cyclic stress induced in the drawn wire was small, and the frequencies considered were above and removed from the natural frequency of the drum.

A constant value for the magnitude of the oscillatory force rise was adopted. Inspection of the experimental data shows that while the magnitude is approximately constant at high oscillation amplitudes, it diminishes at low amplitudes.

In order to obtain a linear load-extension characteristic for the drawn wire, the theoretical relationship derived was simplified by assuming that the force variation induced in the drawn wire was small. The experimental data indicates that this is a justified approximation.

It was also assumed that no transverse oscillations were induced in the drawn wire, these having the effect of increasing the magnitude of cyclic stress induced. However, since transverse oscillations were not observed during the

investigation, this assumption was considered justified.

Two conditions were considered in the analysis, constituting the extremes of behaviour for the system. Firstly it was assumed that the drawing periods were sufficiently long for the transient period during drawing to pass. This condition will arise when the frequency and amplitudes are low. The other extreme considered was that the drawing period was short, such that the drawing forces were always at their maximum transient value. This corresponds to high frequencies and amplitudes.

The results of these analyses are shown in figures (44) to (46), together with the corresponding experimental points. From these it may be seen that the experimental points generally lie within the computed extreme values. Furthermore, for low amplitudes of die oscillation, corresponding to a long drawing period, the experimental points lie in closest proximity to the computed values corresponding to this condition. Similarly for high amplitudes, and thus a short drawing period, the experimental data approaches the computed values relating to this condition.

The reason for the marked difference between the two computed curves is primarily that in the case of a long drawing period the cyclic force in the wire between the two dies has two components, the former being the elastic component and the latter the change in force during drawing due to the transition from transient to steady state drawing. In the case of a short drawing period, only the former component is obtained. Thus the degree of off-loading of back tension applied to the second die is greater for a long drawing period, and thus the reduction in total drawing

load is similarly increased.

Thus, while the analysis does not give accurate predictions of drawing force reductions, it does provide upper and lower limits for the process.

B9: Appendices

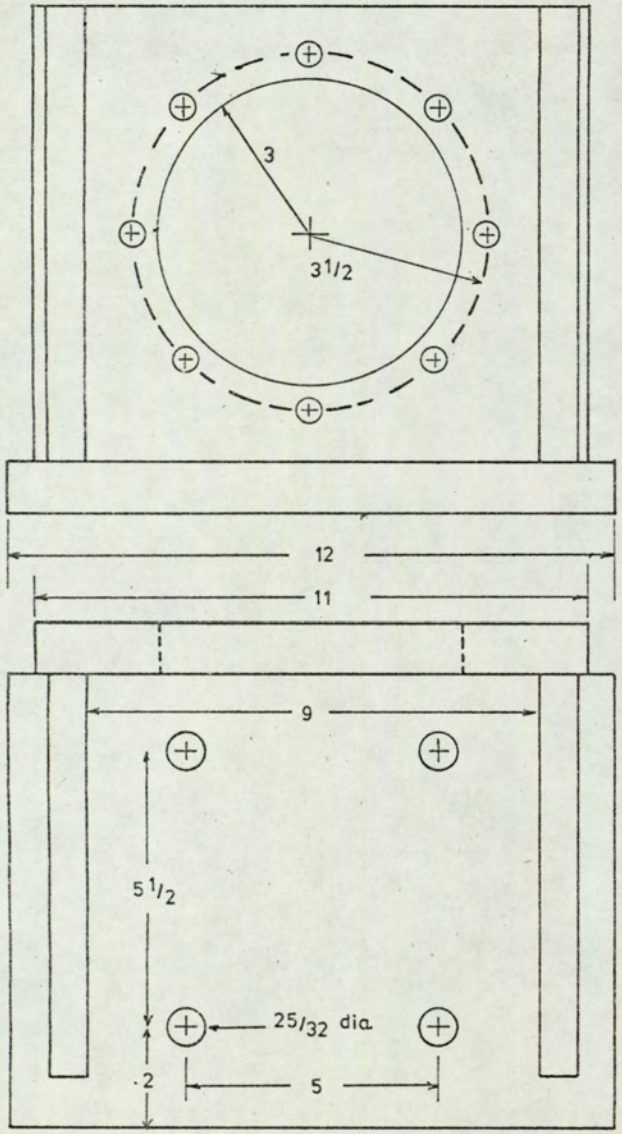

FIXED OSCILLATOR MOUNT

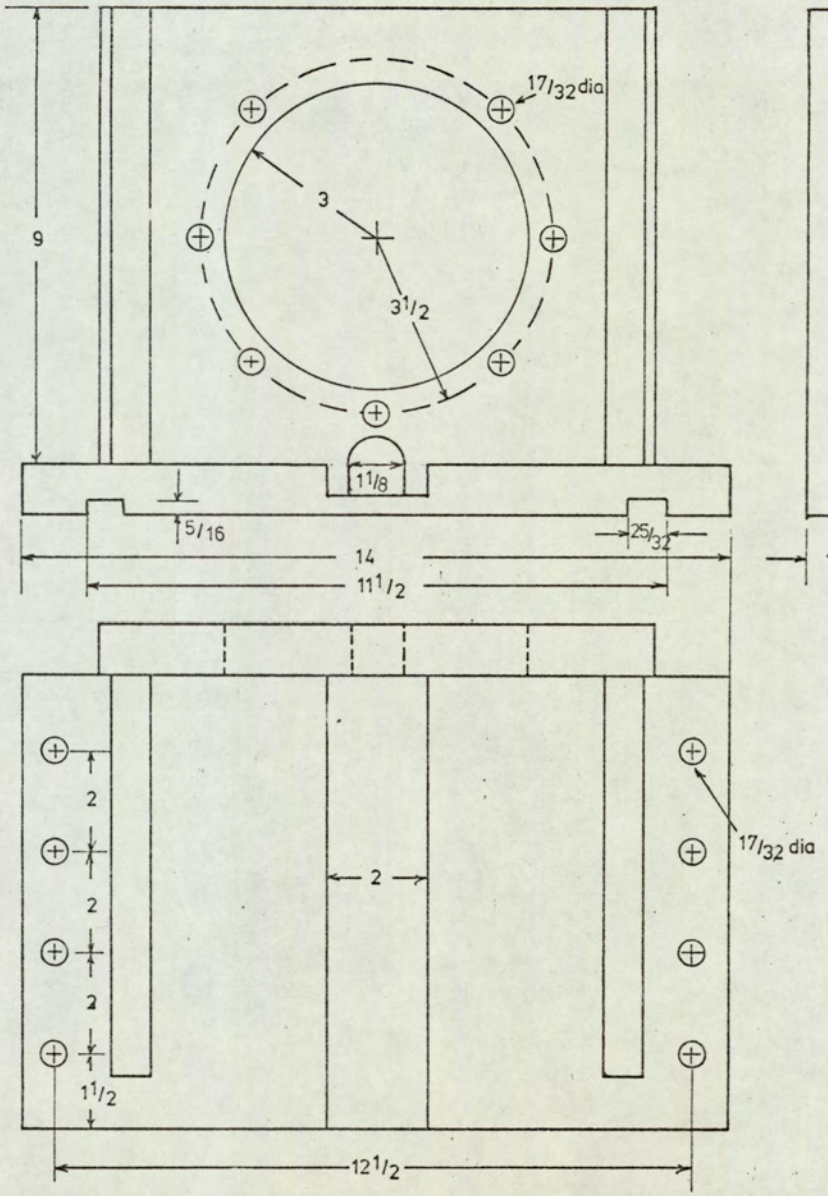

MOBILE OSCILLATOR MOUNT

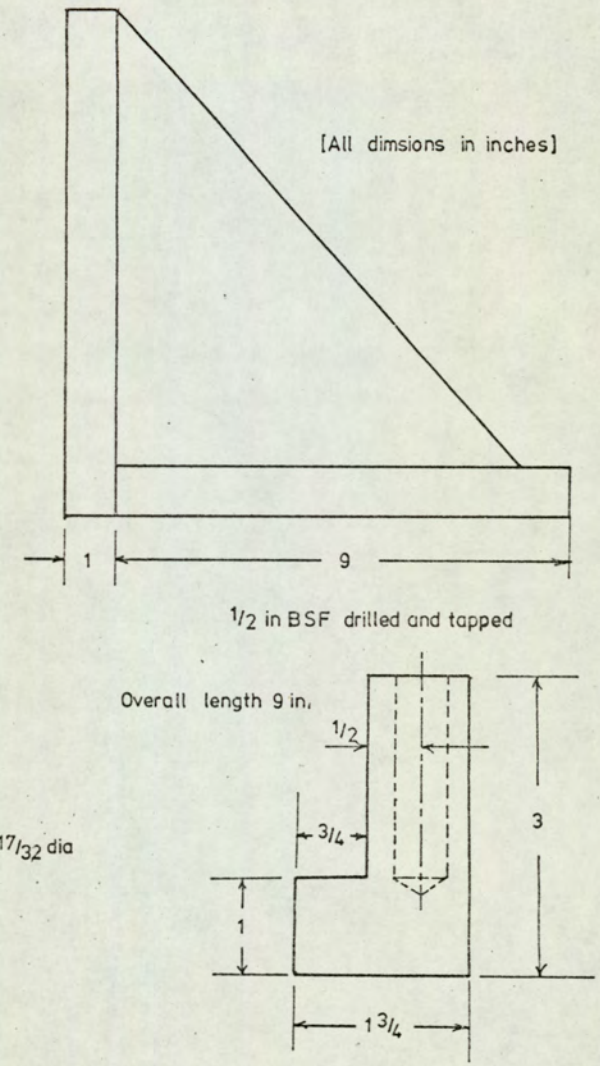

MOBILE OSCILLATOR CLAMPING RAIL

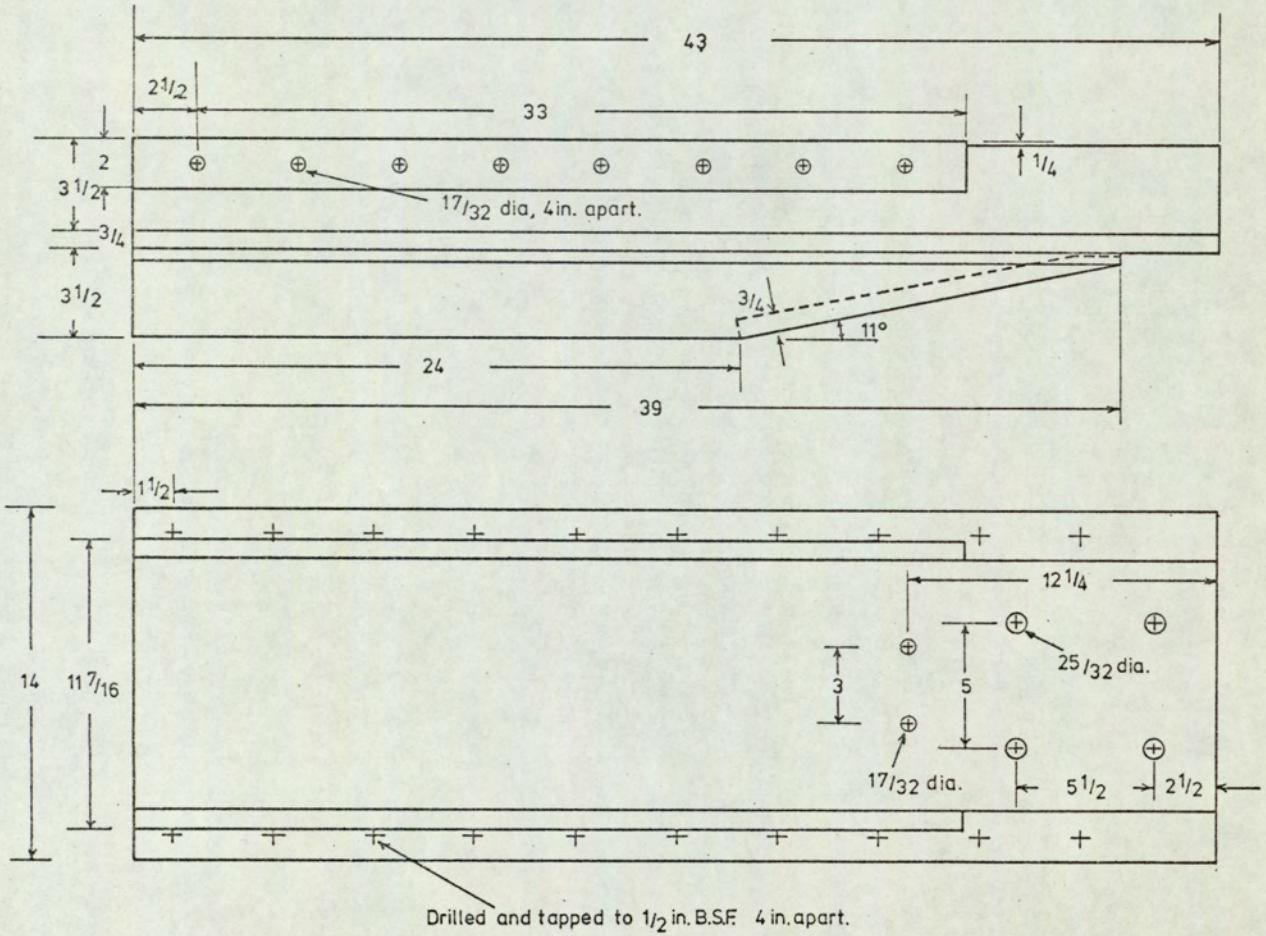

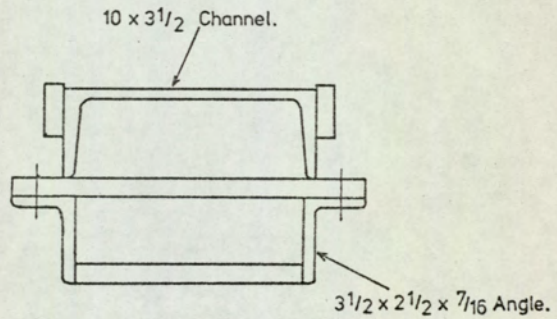

CANTILEVER BEAM SUPPORT

[All dimensions in inches]

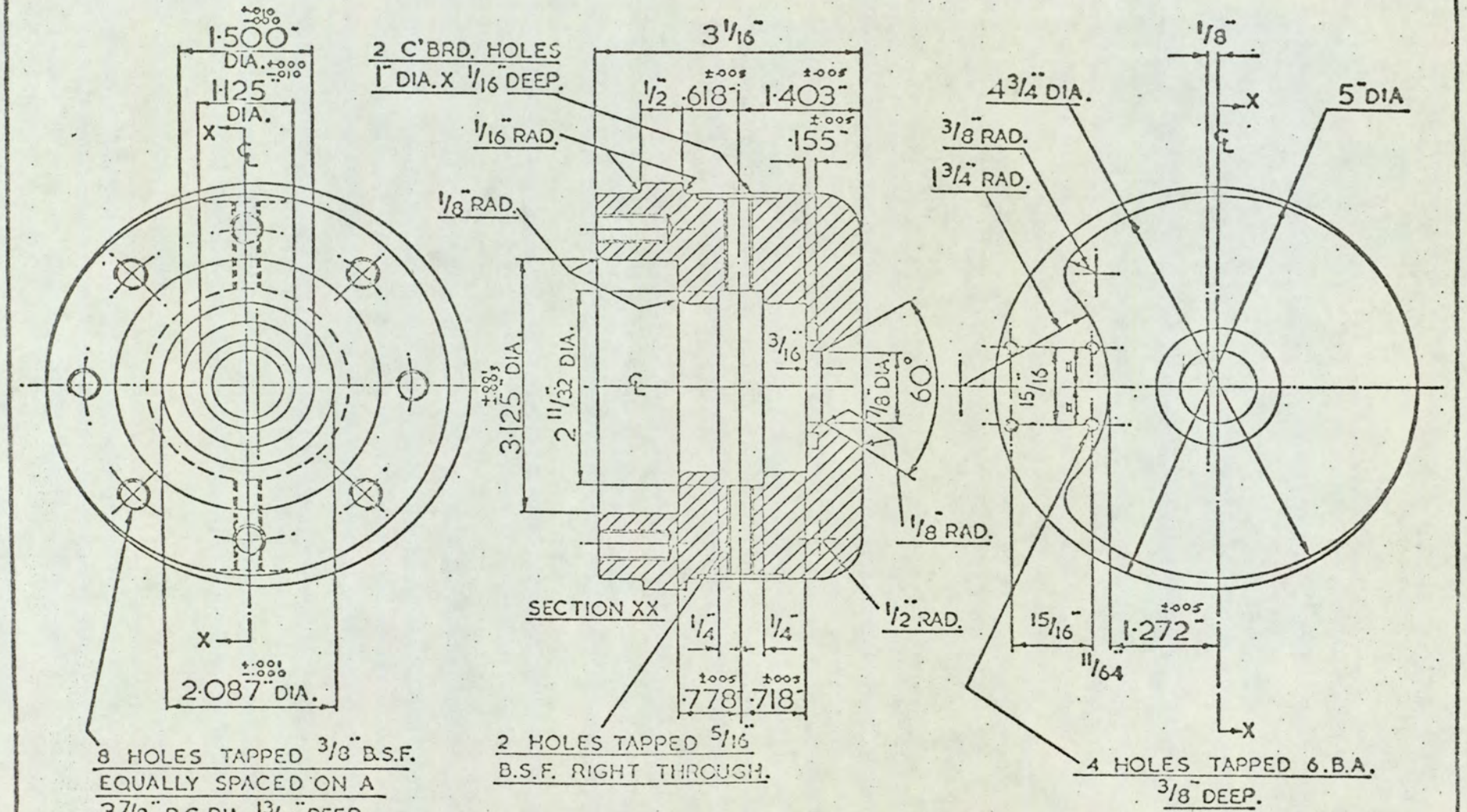

DIE HOLDER DESIGN DETAILS

FIGURE NO. 44

FRACTIONAL DIMENSIONS ±·010"

(From Winsper).

B9: Appendices

B91: The drawing machine

The machine used was a horizontal bull-block with an 18 in. diameter drum, having an 18 in long working surface. The drum was driven by a totally enclosed worm as through a carbon steel shaft, and supported by heavy duty roller bearings. The machine was provided with a traversing die box table, mounted on plane bearing guides, and driven by a leadscrew giving 0.75 in. traverse per revolution of the drum.

The designed drawing speeds for the machine were 120, 240, 360 and 480 ft/min., provided by a four speed gearbox. This speed was rendered infinitely variable by driving the gearbox by a 15 h.p. squirrel cage induction motor, through a variable speed oil gear. The maximum die pull of 2,300 lbf. was attainable up to 120 ft/min., this figure reducing to 575 lbf. at 480 ft/min.

The product was pulled by the drum by means of gripping jaws attached to the drum periphery by a chain linkage. The jaws could accept products up to 0.375 in. diameter.

B92: The vibrator systems

These were essentially double acting hydraulic jacks powered by hydraulic oil at 3,000 lbf/in^2. The oil flow was controlled by two flow valves, operated by an electrical signal from a servo amplifier.

The controlling signal to the summing junction of the servo amplifier was supplied by a low frequency electronic oscillator for vibrator 2, and by the phase shifting adapter for vibrator 1. A displacement transducer mounted on each ram fed back a signal to the corresponding servo amplifier

summing junction in such a way as to cancel the controlling signal, thus providing closed loop servo control. The displacement transducer for vibrator 1 was a linear differential transformer having d.c. input and output. The transducer for vibrator 2 was a rotary differential transformer, energised by a 2.4 kHz. supply, the signal from which was demodulated prior to insertion into the amplifier summing junction.

The output of the servo amplifier for vibrator 2 was passed through a constant current circuit, prior to the servo valves, this facility providing an enhanced frequency response for that unit.

B92(a): The vibrators

These were double acting hydraulic jacks with rod extensions at either end. Both jacks had a 1 in. diameter hole machine through them for the product to pass through them. A 1⅞ in. b.s.f. thread was provided at one end of each ram for load cell attachment, whilst the other end actuated the feedback transducer. Both units were provided with annular mounting flanges. The performance characteristics of each unit are given at the end of this appendix.

B92(b): Hydraulic power supply units

The vibrators were powered by identical hydraulic pumps. These were pressure compensated, variable delivery pumps driven by electric motors. Each pump was immersed in the hydraulic reservoir, and delivered fluid under pressure through an accumulator and micro-filter to the vibrator. The return flow passed through a cooling system back to the reservoir.

B92(c): Electronic control unit

The servo amplifiers were provided with rotary gain controls, being variable resistors, setting the magnitude

of the controlling signal, thus providing a variable amplitude at the vibrator. A second ponentiometer provided a variable d.c. bias at the summing junction of the servo amplifier, enabling the mean position of the ram to be adjusted.

The supply to the displacement feedback transducer was 6 v. d.c. for vibrator 1, and 24 v. r.m.s. at 2.4 kHz. for vibrator 2.

Both units incorporated a 12 v. - 0 - 12v. stabilised d.c. supply.

Specifications

Vibrator 1.

Bearing type	drained gland
Maximum static thrust	12,000 lbf
Maximum dynamic thrust	4,500 lbf
Stroke	0.500 in
Frequency range	0 to 200 Hz
Effective ram area	4 in^2
Ram	2 in diameter. At one end a 1⅛ in b.s.f. thread to attach load cell
Mounting	flange, 8 holes, 17/32 dia. on 7 in p.c.d.

Vibrator 2.

As above except the following:-

Maximum static thrust	4,500 lbf
Maximum dynamic thrust	3,000 lbf
Stroke	0.250 in
Frequency range	0 to 500 Hz
Effective ram area	1.5 in^2

Hydraulic supply units.

Fluid type	Shell Tellus 27
Fluid capacity	15 gall
Filter	5 micron
Pump delivery	6 gall/min
System pressure	3,000 lbf/in^2
Pump motor	15 h.p.
Cooler motor	0.5 h.p.
Accumulator	Charged at 1,500 lbf/in^2

Servo amplifier 1.

Input impedance	10 kΩ
Supply voltage	12v. - 0 - 12v.
Oscillator signal input	5 v. peak

Servo amplifier 2.

Input impedance	20 kΩ
Supply voltage	12v. - 0 - 12v.
Oscillator signal input	5 v. peak

B93: Instrumentation

Ultra violet recorder (S.E. Laboratories, type 2005)

The recorder will accept up to 12 galvanometers, and has 15 paper speeds from 1.25 mm/s. to 2,000 mm/s., in steps of 1, 25, 5, 10 and 20, with a speed change over switch giving x 1, x 10, and x 100. Accuracy of speed ± 2%.

Stabilised d.c. supply (Thorn Electronics type V P 21)

Output voltage	3 to 30 v. continuously varibale
Output current	Up to 1 amp.
Output impedance	d.c. less than 0.01Ω
	a.c. less than 0.3Ω at 10 kHz

Ripple	less than 2 millivolt p.t.p.
Mains variation	up to ± 10% from nominal
Overload protection	Electronic cut out incorporated

Digital counter (Research Electronics Model 5321)

Frequency measurement range	0 to 5 kHz
Revolution speed range	0 to 3×10^5 r.p.m.
Accuracy of time measured with 1 kHz reference signal	± 0.001 s.

Slip ring assembly

Current rating	2.5 amp. r.m.s. max.
Circuit resistance	40×10^{-3} Ω max.
(between slip ring and two brushes in parallel)	
Starting torque	0.25 lbf.in. max.
Noise level	less than 8 microvolt/milliamp

Vibration meter (Bell and Howell Ltd.)

Input impedance	10 kΩ
Linear deviation	less than ± 3% of full scale
Attenuation accuracy	less than ± 2% of set value

For velocity measurement:-

Frequency response	± 3% from 5Hz. to 5 kHz
Sensitivity (V x 1.0)	278.0 to 834.0 millivolt
(V x 0.1)	27.8 to 83.4 millivolt

For displacement measurement:-

Frequency response	± 4% from 5Hz. to 5 kHz.
Sensitivity (d x 1.0)	278.0 to 834.0 millivolt
(d x 0.1)	27.8 to 83.4 millivolt

Linear seismic transducers (Bell and Howell Ltd.)

Sensitivity (transducer 1)	131 millivolt/in/s at 100 Hz
(10kΩ load) (transducer 2)	133.5 millivolt/in/s at 100 Hz
Frequency range	15 Hz. to 2 kHz.
Natural frequency	6 Hz
Amplitude range	0.25 in p.t.p.

Torsiograph (Bell and Howell)

Sensitivity (10kΩ load)	8.8 millvolt/degree/s.
Frequency range	up to 10 kHz.
Maximum revolution speed	6,000 r.p.m.
Natural frequency	3 Hz

Oscillator (Dawe Instruments type 445)

Frequency range	0.01 to 1 kHz
Calibration accuracy	± 3% of scale reading
Distortion	less than 0.5% over range 20 Hz to 1 kHz.
Hum and noise level	less than 0.2%
Output level	15 volts max., continuously variable. Minimum load 10 kΩ.

Phase shifting adaptor (Dawe Instruments type 446)

Frequency range	0 to 10 kHz
Input	Accurate quadrature signals up to 5 v. r.m.s.
Variable phase output	Continuously variable 0 to 360° calibrated to ± 2% Output at unity gain constant to within ± 5%. Minimum load 20 kΩ.
Distortion	less than 2%.
Hum and noise	less than 1%

B94: Measurement of drawing speed

Radius of drum 9 in

Reduction ratio of drum drive shaft worm gear 14.66 : 1

Let V = drum surface speed (ft/min)

N = drum rotational speed (r.p.m.)

n = worm rotational speed (r.p.m.)

t = time for revolution of worm (min)

$\therefore$ $V = 9/12 \times 2\pi N$

But, $n = 14.66\ N$

$\therefore$ $V = 9/12 \times 2\pi \times \frac{n}{14.66}$

Now, $n = 1/4t$

$\therefore$ $V = 9/12 \times 2\pi \times \frac{1}{4 \times 14.66t} = \frac{1}{T}$

Where T = time in min. for 1 ft. drawn

The digital counter counts the number of cycles from the oscillator in a revolution of the worm shaft, i.e. in t min. The number of cycles displayed on the counter is set at 1000 x T, such that the display represents 1000 x the reciprocal of drawing speed in ft/min.

Thus $1000\ T = f \times 60t$

where f = oscillator frequency in Hz

i.e. $t = \frac{1000T}{60f}$

From above,

$$f = \frac{1000 \times 4 \times 14.66 \times 12}{60 \times 9 \times 2\pi}$$

i.e. $\underline{f = 207.2\ Hz}$.

B95: Loadcell and torquecell calibration curves.

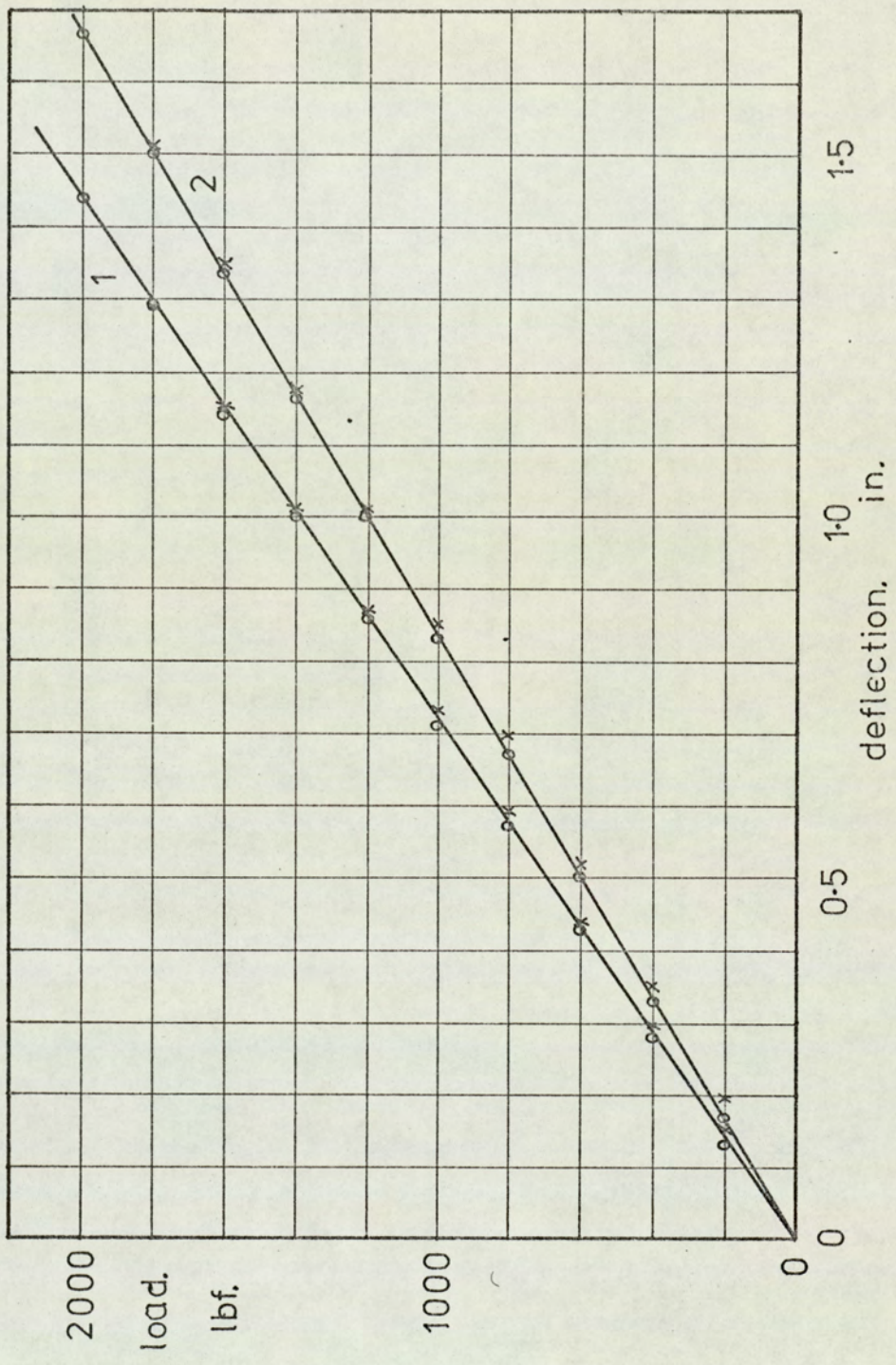

Calibration curves for load cells 1 and 2.

o Increasing load.

× Decreasing load.

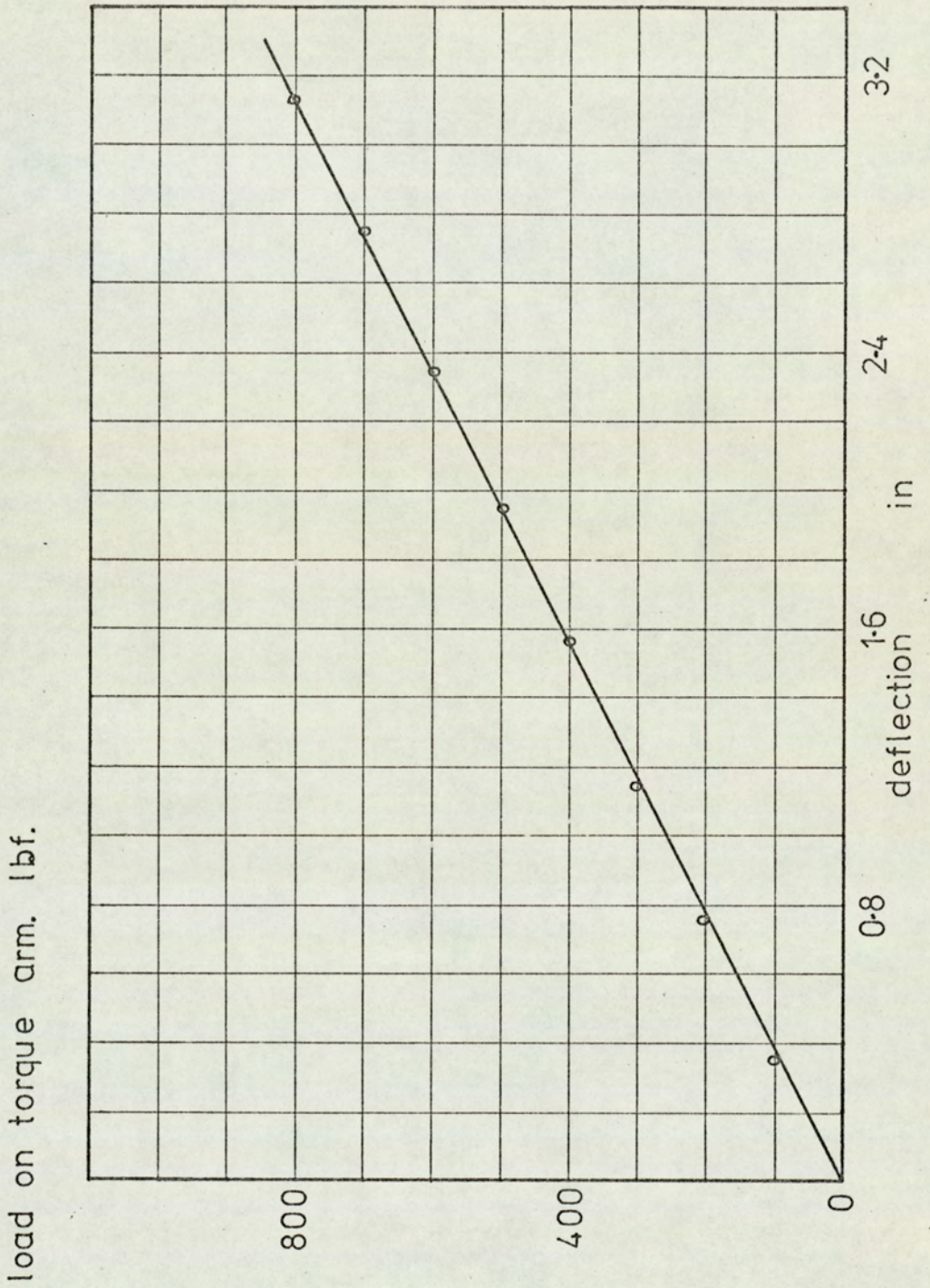

Torque cell calibration curve.

(Radius of torque arm 24 in.)

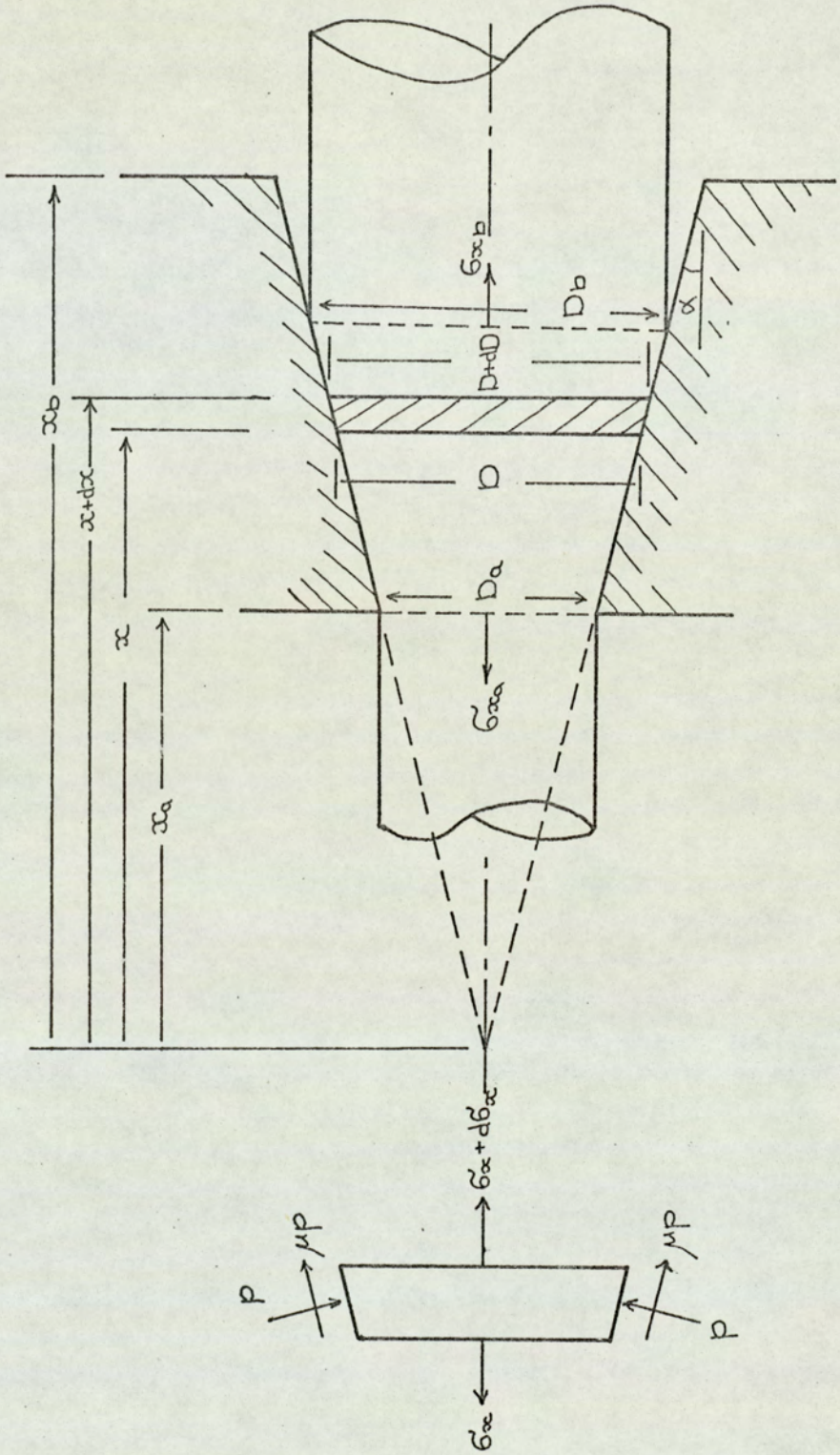

State of stress of wire element in a die. Figure 47.

B96 Derivation of the drawing force equation with back tension

(From Hoffman and Sachs (106))

Assumptions:-

1. Idealised metal, i.e. no elastic strains, no work hardening.
2. Coulomb friction, coefficient constant.
3. Uniform state of stress existing on all planes normal to the die axis.
4. Cylindrical state of stress exists throughout, with the die axis being a principal direction.

Considering the state of stress of the element bounded by the two transverse planes at a distance x and x + dx from the die cone apex, (see figure 47), yields the following equilibrium equation:-

$$\frac{\pi D}{4}\left[D d\sigma_x + 2\sigma_x dD\right] + \frac{\pi}{2} pDdD + \mu p \frac{\pi}{2\tan\alpha} DdD = 0$$

where second and higher order infinitesimals are neglected.

The yield criterion expresses the relationship between σ_x and p thus:-

$$\sigma_x + p = \sigma_y$$

where σ_y = the yield stress in uniaxial tension. (This relationship holds true for both the Tresca and Von Mises yield criteria.)

Combining the two equations and setting

$$B = \mu/\tan\alpha$$

yields:-

$$\frac{d\sigma_x}{B\sigma_x - \sigma_y(1+B)} = \frac{2dD}{D}$$

Integrating yields:-

$$\frac{1}{B}\ln\left[\sigma_x B - \sigma_y(1+B)\right] = 2\ln D + C$$

where C is the constant of integration.

Solving for σ_x:-

$$\sigma_x = C' \frac{D^{2B}}{B} + \sigma_y \frac{(1+B)}{B}$$

where $C' = e^{CB}$

The constant C' is determined by considering the conditions at entry to the die where $D = D_b$, $\sigma_x = \sigma_{xb}$ = the back pull stress.

$$C' = \left| \sigma_{xb} - \sigma_y \frac{(1+B)}{B} \right| \frac{B}{D_b^{2B}}$$

This gives:-

$$\frac{\sigma_x}{\sigma_y} = \frac{(1+B)}{B} \left| 1 - \left(\frac{D}{D_b}\right)^{2B} \right| + \frac{\sigma_{xb}}{\sigma_y} \left(\frac{D}{D_b}\right)^{2B}$$

and the drawing stress, σ_{xa}, is:-

$$\frac{\sigma_{xa}}{\sigma_y} = \frac{(1+B)}{B} \left| 1 - r^B \right| + \frac{\sigma_{xb}}{\sigma_y} r^B$$

where $r = \left(\frac{D_a}{D_b}\right)^2$ = area ratio

The drawing forces are therefore related thus:-

$$\frac{F_a}{A_a \sigma_y} = \frac{(1+B)}{B} \left[1 - r^B \right] + \frac{F_b}{A_b \sigma_y} r^B$$

$$F_a = \sigma_y A_a \frac{(1+B)}{B} \left| 1 - r^B \right| + F_b r^{(1+B)}$$

i.e. $F_a = F_{ao} + KF_b$

where F_{ao} is the drawing force without back tension, and K is the back-pull factor.

From the above, it may be seen that the back-pull factor K is a function of the reduction of area, the die angle and the coefficient of friction only, and is therefore constant for a given die and wire.

Frequency. (Hz).	Phase Angle. ($\theta/2\pi$).
33	0.163
34	0.181
35	0.193
36	0.224
37	0.236
38	0.255
39	0.270
40	0.282
41	0.308
42	0.318

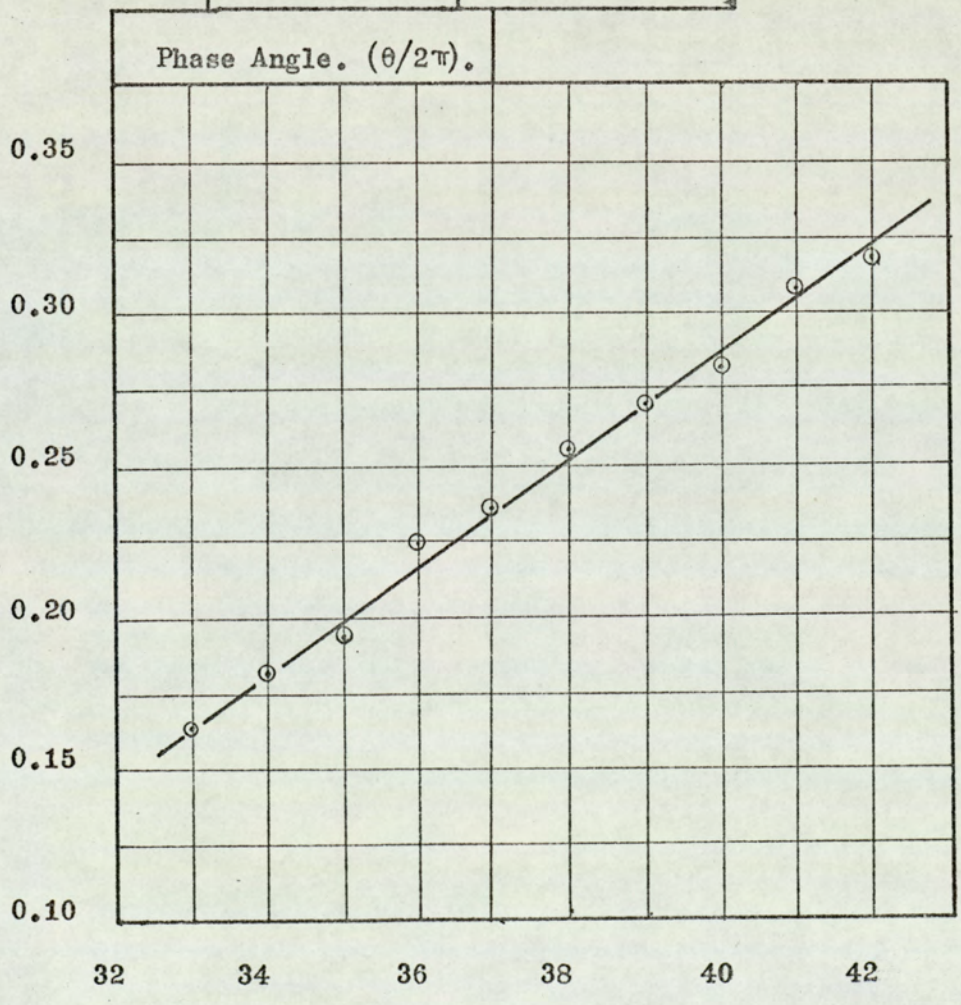

Determination of the natural frequency of the drum.

Figure 48.

B97: Measurement of the natural frequency of the drum

This was achieved by observing the frequency at which the phase angle between drum oscillation and the periodic torque applied by the wire was 90^{o}. To this end, mild steel wire of initial diameter 0.1847 in. was drawn with a reduction of 26.3% at a speed of 2 ft/min. The die was oscillated at a peak to peak amplitude of 20×10^{-3} in. for a range of frequencies, whilst recordings were made of die load and drum displacement. The results are shown in Figure 48.

B98: Measurement of the damping coefficient of the drum

The determination of this parameter was attempted in two ways. Initially the frequency response was obtained by drawing wire under the same conditions as described in section B97. Since for a fixed die amplitude, the cyclic force amplitude varied with frequency, the drum amplitude observed was converted to that corresponding to a fixed cyclic force amplitude. The drum amplitude was then plotted against frequency, and the damping coefficient obtained from the identity:-

$$\xi = \frac{(\omega_1 - \omega_2)}{2\omega_n}$$

where ω_1 and ω_2 are the frequencies at which the drum amplitude is $1/\sqrt{2}$ times the maximum drum amplitude. This method was discarded since it was found that the drum response near the natural frequency was erratic, and therefore the shape of the response curve could not be determined with sufficient accuracy.

This variability of response was investigated by drawing a length of wire as above, but with the frequency fixed at the previously determined natural frequency. From this test it was

Torque ampl. (lbf. in.)	Drum ampl. (rad. x 10^{-4})	Damping coefficient. ξ
1058	12.30	0.1405
1058	9.30	0.1860
1165	8.94	0.2135
1025	12.75	0.1320
1058	10.15	0.1700
1220	8.56	0.2325
1220	8.94	0.2230
1000	12.68	0.1290
1165	9.78	0.1950
1165	8.94	0.2130
1138	12.58	0.1480
Die amplitude 20 x 10^{-3} in. pk. to pk.		
481	4.85	0.1620
688	4.04	0.2780
688	3.92	0.2870
416	6.04	0.1130
635	4.60	0.2260
635	3.54	0.2930
635	3.54	0.2930
554	5.35	0.1690
580	4.48	0.2120
635	3.98	0.2610
635	5.35	0.1940
Die amplitude 10 x 10^{-3} in. pk. to pk.		

Average value of ξ = 0.198
Maximum value = 0.293
Minimum value = 0.113

Determination of the damping coefficient of the drum.

Figure 49.

observed that the drum exhibited marked periodic fluctuations in its amplitude. It was initially hypothesised that this behaviour could be the result of periodic fluctuations in the drawing speed, so a test was conducted to investigate this possibility. This is described in section B99. However, no periodic fluctuations in the drum speed were observed.

It was therefore concluded that this variability in response was attributable to real changes in the damping coefficient of the drum, and therefore could not be neglected. In view of this it was decided to estimate the range of variation of the damping coefficient, and to use both upper and lower limits in any calculation.

To achieve this, wire of an initial diameter of 0.1847 in. was drawn with a reduction of 26.3% at a speed of 2 ft/min. The die was oscillated at the natural frequency of the drum, with amplitudes of 10×10^{-3} and 20×10^{-3} in. peak to peak. Recordings were made of die loads and drum oscillation. The damping coefficient was calculated from the identity:-

$$\xi = T/2\theta I\omega_n^2$$

where T = applied cyclic torque amplitude

θ = amplitude of torsional oscillations of the drum.

Eleven randomly selected points were used to calculate for each amplitude. The results are given in figure 49.

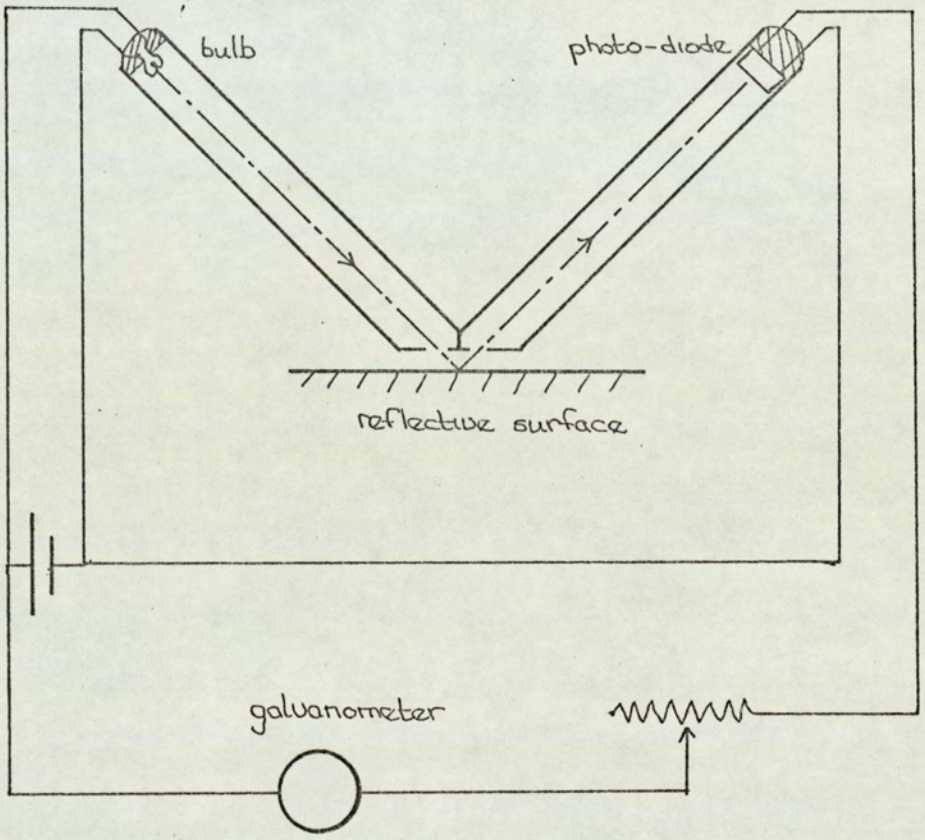

Drum speed measuring device. Figure 50.

B99: Measurement of the Constancy of the drum rotational speed

It was decided to measure the drum rotational speed by imposing equally spaced reflective surfaces about the circumference of the drum, and detecting the passage of these by means of a photo-diode. To this end the following equipment was constructed.

Two resinated cardboard tubes were cemented together in the form of a vee, as shown in figure 50. The base of the vee was cut horizontally across and a copper plate was cemented over the joint opening of the two tubes. A narrow slit was cut in the centre of this plate in the plane of the vee. A small light bulb was secured with leads attached in one free end of the vee, whilst a photo-diode, similarly with leads attached, was secured in the other free end. These ends were sealed-off with Plasticine, and the whole assembly made light-proof by a liberal coat of matt black paint. Both faces of the copper end plate were similarly painted.

A strip of light-reflective adhesive tape was secured round the circumference of the drum, on top of which was bonded a matt black paper strip with regularly pitched holes punched in it.

The vee assembly was fastened to a flexible clamp and positioned approximately ⅛ in. above the tape on the drum. The bulb was illuminated by a d.c. supply, which was also connected to the photo-diode, in series with which was an attenuating resistor and an ultra-violet recorder galvanometer.

A drawing test was again conducted as previously described, recordings being mace of die load, drum oscillation, and the pulsed switching of the photo-diode, corresponding to the passage of a light-reflecting circle under the detector. By

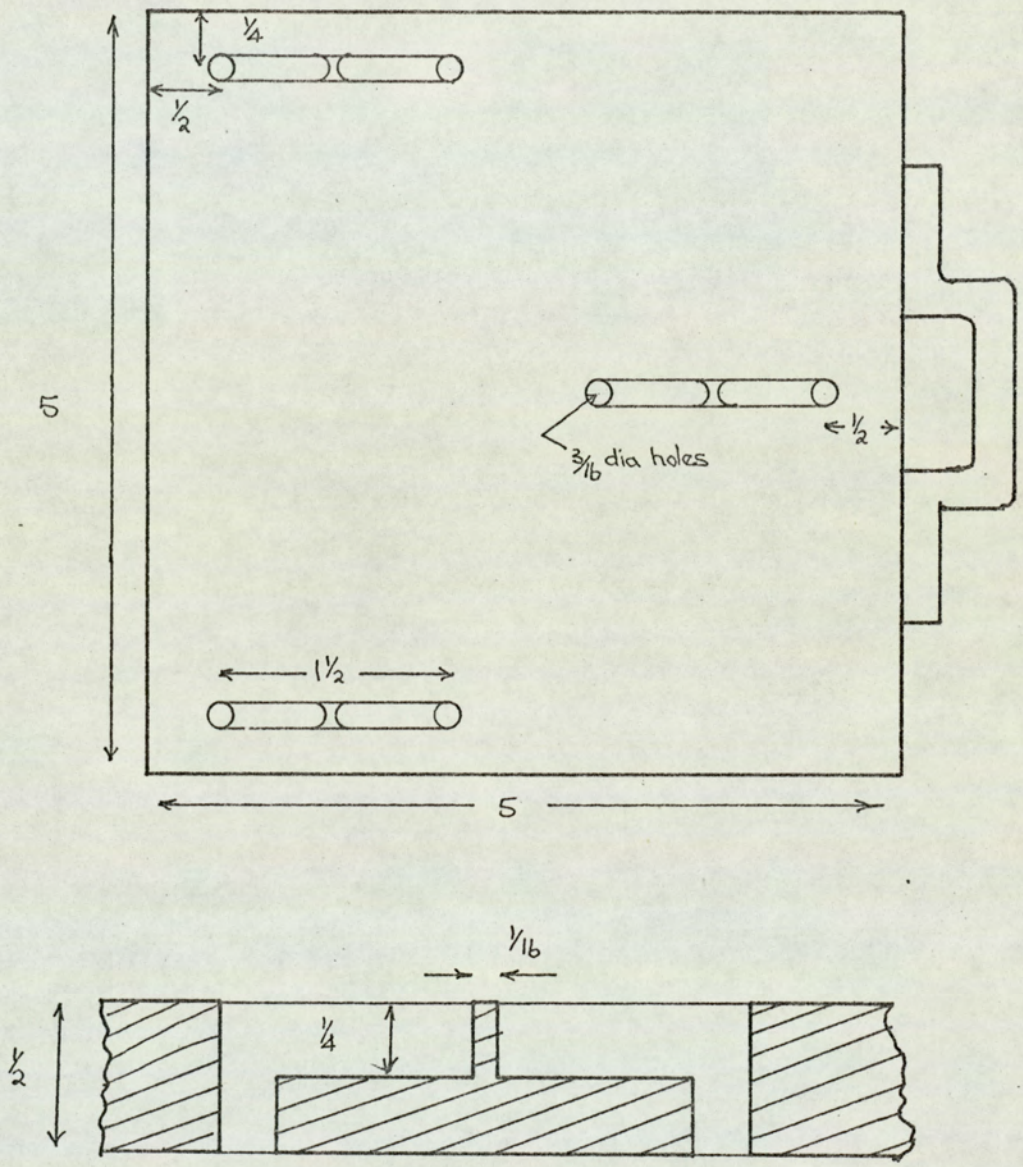

Dimensions in inches.

Slider for drum friction measurement. Figure 51.

Test No.	Normal Load (lbf). 4	8	12	16	20	24
1	0.84	1.42	1.88	2.63	3.27	4.20
	0.65	1.30	1.60	2.75	3.15	
2	1.00	1.50	1.95	2.70	3.25	4.30
	0.90	1.50	1.90	2.75	3.35	
3	0.75	1.30	1.70	2.25	2.75	3.55
	0.85	1.40	1.90	2.65	3.30	
4	1.00	1.55	2.10	2.80	3.50	4.60
	0.70	1.40	2.00	2.50	3.60	
	Frictional force (lbf).					

Weight of slider: 3.5 lbf.

Normal load	4	8	12	16	20	24
Average frictional force	0.836	1.421	1.880	2.630	3.271	3.662

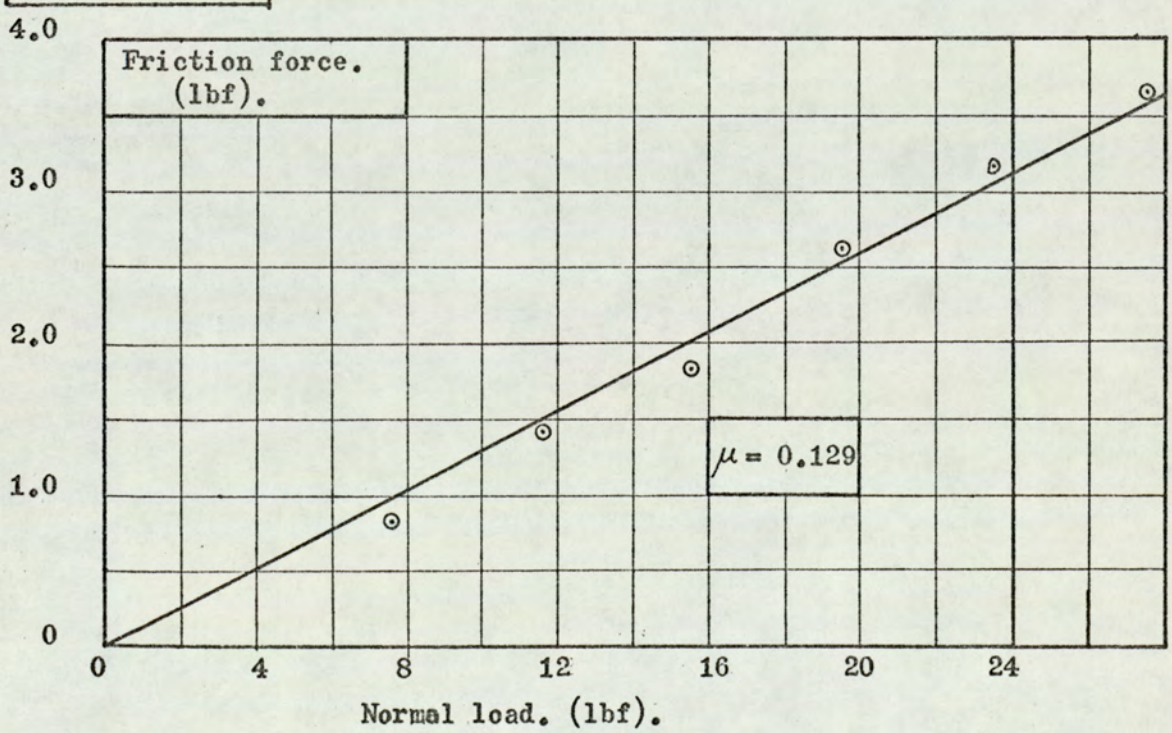

Determination of the Coefficient of Friction between wire and drum.

Figure 52.

counting the frequency of these pulses, it was concluded that there were no periodic fluctuations of speed corresponding to those of drum response.

B910: Measurement of the coefficient of friction between wire and drum

This was achieved using the slider shown in figure 51, into which were inserted three lengths of freshly drawn wire, care being taken not to disturb the lubricant film upon them. By bending the wire into this slider, high normal pressures could be achieved at the interface, with small weights applied to the slider. The slider was pulled by a cord attached to it which was coiled round a pulley mcunted on the machine frame. A light spring balance was interposed in this cord to measure the tension in the cord.

The slider was positioned before each test with the cord at right angles to the drum axis, and with the slider surface horizontal. The latter was achieved using a spirit level. The slider was symmetrically loaded with weights, and the pulley wound slowly. The force required to just sustain motion was noted. The wire samples were renewed after each loading and unloading.

Initially, the results obtained by this technique were not repeatable, which was thought to be due to the varying surface condition of the drum. The drum was thus scoured with pumice and degreased, and the tests repeated, the position of the drum being changed for each set of wire specimens. Considerable scatter was still observed in these results, an average line being taken on the graph to give a mean value for the coefficient of friction (see figure 52).

V/X_w.	Cos wt_1.	wt_1.
0.0	1.0000	0.0000
0.1	0.9999	0.0125
0.2	0.9997	0.0247
0.3	0.9993	0.0372
0.4	0.9988	0.0497
0.5	0.9981	0.0620
0.6	0.9972	0.0745
0.7	0.9962	0.0870
0.8	0.9951	0.0995
0.9	0.9938	0.1120
1.0	0.9923	0.1245
1.1	0.9907	0.1370

Determination of the point of cessation of drawing in Die 3.

$$\text{Sin } wt_1. = \frac{S_b}{(1 + r)kS_a + S_b} \cdot \frac{V}{X_w} .$$

S_a = 4.4655 lbf./in. (18 in. die separation)

S_b = 0.6026 lbf./in. (Simplified theory)

r = 0.7327

k = 0.55

Figure 53.

B911: Calculations for the tandem drawing theory

The numerical values of the constants used in the calculations are:-

$A_a = 0.02680 \text{ in}^2$

$A_b = 0.01962 \text{ in}^2$

$E = 30 \times 10^6 \text{ lbf/in}^2$

$\ell_a = 18.0 \text{ in}$

$\ell_b = 28.5 \text{ in}$

$R = 9.0 \text{ in}$

$\mu = 0.0130$

$K = 0.550$

From which are derived:-

$r = A_b/A_a = 0.7327$

$S_a = A_a E/\ell_a = 4.4655 \times 10^4 \text{ lbf/in}$

$S_b = A_b E/\ell_b = 0.6026 \times 10^4 \text{ lbf/in}$

The magnitude of the drop in drawing force in die (1) when changing from non-equilibrium to equilibrium is taken as the difference between the average of the observed peak oscillatory load in wire (a) and the average of the observed non-oscillatory drawing load.

i.e. $\Delta F_a = 60 \text{lbf}$

In the absence of any data for the corresponding drop in die (3), the same value is taken for this die also.

i.e. $\Delta F_b = 60 \text{ lbf}$

The time at which drawing stops in die (3), t_1, is calculated from equation (9), and shown in figure 53.

The time at which drawing restarts in die (3), t_3, assuming a long drawing period, is calculated from equation (24) by a graphical method. The equation is of the form:-

$$\cos \omega t_3 = P_1 - P_2 \, \omega t_3 \qquad - (25)$$

	X. (in. x 10^{-3} z.t.pk.)						
V/Xw.	1.0	1.5	2.0	2.5	3.0	3.5	4.0
0.1	2.0024	1.5907	1.3849	1.2616	1.1790	1.1202	1.0761
0.2	1.7699	1.3582	1.1523	1.0288	0.9465	0.8877	0.8436
0.3	1.5375	1.1258	0.9200	0.7965	0.7142	0.6553	0.6112
0.4	1.3053	0.8936	0.6878	0.5643	0.4820	0.4232	0.3790
0.5	1.0733	0.6616	0.4557	0.3322	0.2499	0.1911	0.1470
0.6	0.8414	0.4297	0.2239	0.1004	0.0180	-0.0408	-0.0849
0.7	0.6096	0.1930	-0.0079	-0.1314	-0.2137	-0.2725	-0.3166
0.8	0.3781	-0.0336	-0.2395	-0.3630	-0.4453	-0.5041	-0.5482
0.9	0.1467	-0.2650	-0.4709	-0.5944	-0.6767	-0.7355	-0.7796
1.0	-0.0846	-0.4963	-0.7021	-0.8256	-0.9080	-0.9968	
1.1	-0.3157	-0.7274	-0.9333				
	P_1						

V/Xw.	0.1	0.2	0.3	0.4	0.5	0.6	0.7
P_2.	0.0124	0.0248	0.0372	0.0496	0.0620	0.0744	0.0868

0.8	0.9	1.0	1.1
0.0992	0.1116	0.1240	0.1364

Values of constants in equation 24.

Figure 54.

	X. (in. x 10^{-3} z.t.pk.)						
V/Xw.	1.0	1.5	2.0	2.5	3.0	3.5	4.0
0.1							358
0.2			358	332	324	319	315
0.3		335	316	307	301	298	295
0.4	358	309	296	288	284	280	278
0.5	317	290	279	272	268	265	262
0.6	297	274	264	257	252	249	246
0.7	281	259	248	240	235	232	229
0.8	265	243	230	220	215	210	205
0.9	250	226	209	194			
1.0	234	201					
1.1	216						
	wt_3. (degrees.)						

Determination of the point of initiation of drawing in Die 3.

(Long drawing period assumed).

Figure 55.

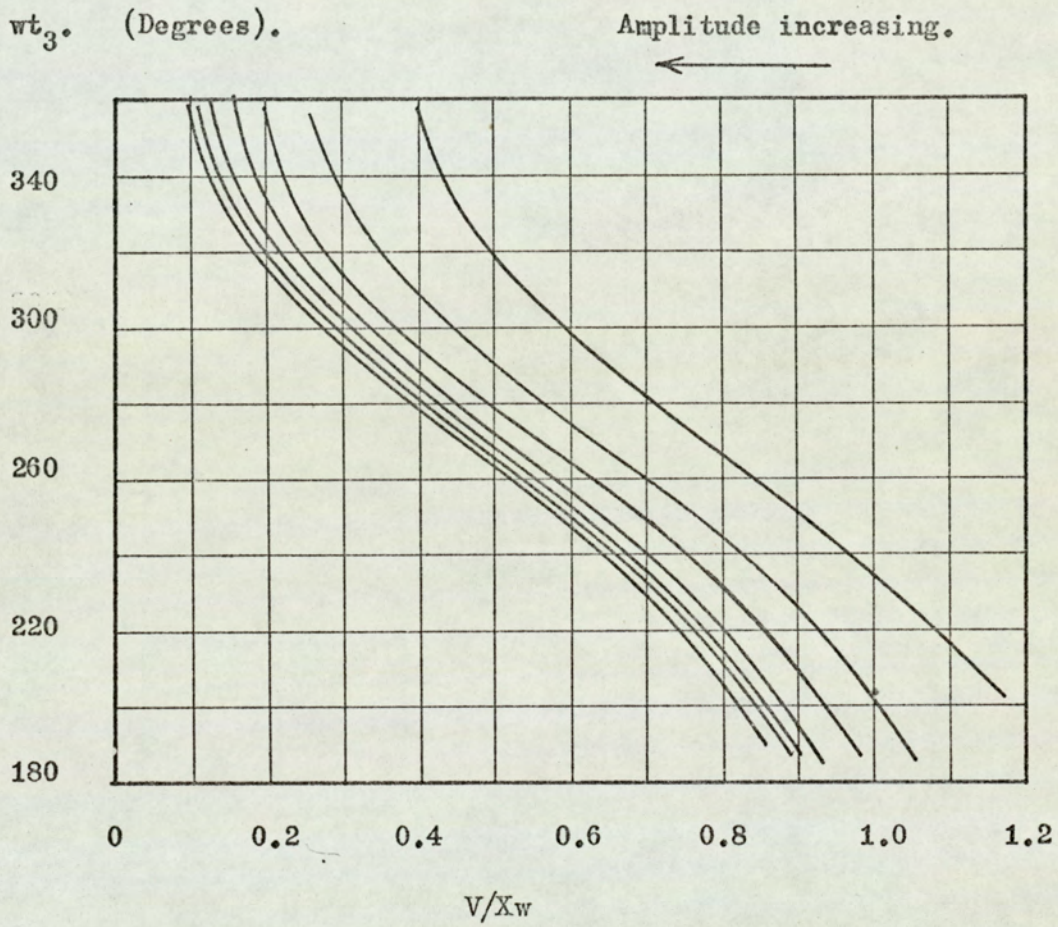

Effect of velocity ratio and amplitude on the point of initiation of drawing in Die 3.

Figure 56.

(Long drawing period assumed).

V/Xw.	P_1.	P_2.
0.0	1.0000	0.0000
0.1	0.7673	0.0124
0.2	0.5348	0.0248
0.3	0.3025	0.0372
0.4	0.0703	0.0496
0.5	-0.1618	0.0620
0.6	-0.3937	0.0744
0.7	-0.6254	0.0868
0.8	-0.8570	0.0992

Values of the constants in equation 24'.

Figure 57.

V/Xw.	wt_3. (Degrees).
0.0	360
0.1	315
0.2	294
0.3	277
0.4	261
0.5	245
0.6	227
0.7	201

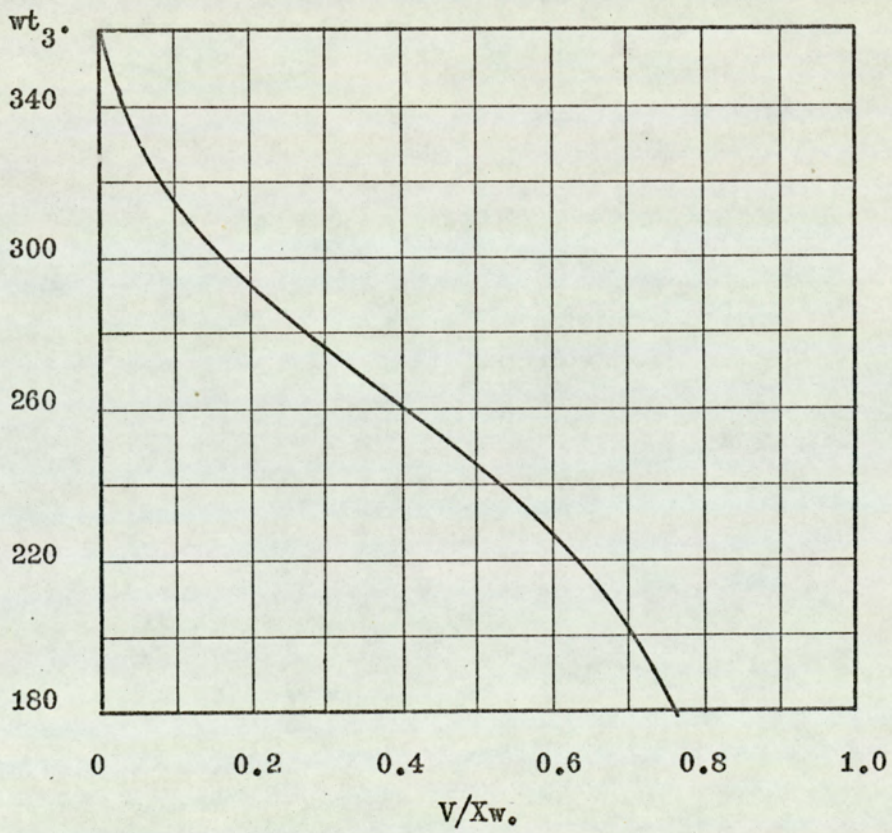

Effect of velocity ratio on the point of initiation of drawing in Die 3.

Figure 58.

(Short drawing period assumed).

where $P_1 = \cos\omega t_1 \quad \frac{-2\pi r K S_a}{(1+r)KS_a+S_b} \cdot \frac{V}{X\omega}$

$$+ \frac{S_b}{(1+r)KS_a+S_b} \cdot \frac{V}{X\omega} \cdot \omega t_1 + \frac{\Delta F_b}{X\left|(1+r)KS_a+S_b\right|}$$

and

$$P_2 = \frac{S_b}{(1+r)KS_a+S_b} \cdot \frac{V}{X\omega}$$

The values of P_1 and P_2 were calculated for a range of velocity ratios, $V/X\omega$, and amplitudes, X. The results are shown in figure 54. Equation (24) was solved by plotting the both sides of equation (25), and noting the intercepts. The values of ωt_3 obtained are shown in figure 55, and plotted on figure 56.

The time at which drawing restarts in die (3), t_3, assuming a short drawing period, is calculated from equation (24) by a similar graphical method. The corresponding values of P_1 and P_2 are shown in figure 57. The derived values of ωt_3 are shown and plotted on figure 58.

In order to compare with experimental data, the reductions of drawing force were calculated using amplitudes and frequencies corresponding to the experimental data. Since it was assumed that there were no drum oscillations, the frequencies considered were those removed from the natural frequency of the drum, i.e. 60, 80 and 100 Hz.

Preliminary calculations showed that the force variation in wire (b) whilst drawing was occurring in die (3), was small, and it was therefore neglected. The calculated values of the reduction in total drawing force are therefore based on the force in wire (b) at the instant of initiation of drawing (i.e. at

X in. x 10^{-3} z.t.pk.	V/Xw.	Cos wt_3.	δF_a. lbf.	δF_b. lbf.
Frequency 60 Hz.				
1.0	1.0610	-0.7431	22.9	-43.5
1.5	0.7074	-0.2079	106.0	- 2.6
2.0	0.5305	0.0698	191.0	45.0
2.5	0.4244	0.2419	277.5	92.5
3.0	0.3537	0.3665	366.0	142.0
3.5	0.3032	0.4540	454.0	190.0
Frequency 80 Hz.				
1.0	0.7958	-0.0698	83.0	-14.6
1.5	0.5305	0.2588	168.6	32.6
2.0	0.3979	0.4384	256.9	81.0
2.5	0.3183	0.5446	344.9	130.0
3.0	0.2653	0.6157	432.9	178.0
Frequency 100 Hz.				
1.0	0.6366	0.3584	121.2	6.7
1.5	0.4244	0.5592	208.9	51.5
2.0	0.3183	0.6691	298.1	104.0
2.5	0.2546	0.7254	385.2	152.0
3.0	0.2122	0.7771	476.1	202.0

Computation of the reduction in peak drawing force, assuming a long drawing period.

Figure 59.

X in. x 10^{-3} z.t.pk.	V/Xw.	Cos wt_3.	δF_a. lbf.	δF_b. lbf.
Frequency 60 Hz.				
1.0	1.0610	-	0.0	-93.0
1.5	0.7047	-0.9409	6.0	-89.7
2.0	0.5305	-0.5075	89.5	-44.2
2.5	0.4244	-0.2250	171.5	1.4
3.0	0.3537	-0.0349	258.0	49.0
3.5	0.3032	0.1045	344.8	97.0
Frequency 80 Hz.				
1.0	0.7958	-	0.0	-93.0
1.5	0.5305	-0.5075	66.0	-56.7
2.0	0.3979	-0.1564	150.0	-10.5
2.5	0.3183	0.0612	237.5	37.6
3.0	0.2653	0.2217	325.5	86.0
Frequency 100Hz.				
1.0	0.6366	-0.7880	19.5	-82.2
1.5	0.4244	-0.2250	102.8	-36.4
2.0	0.3183	0.0698	190.0	11.5
2.5	0.2546	0.2504	277.5	59.8
3.0	0.2122	0.3746	366.0	108.0

Computation of the reduction in peak drawing force, assuming a short drawing period.

Figure 60.

$t = t_3$). The magnitude of the force reduction was obtained by first calculating the degree of off-loading, δF_a, in wire (a) at $t = t_3$. This is given by equation (14).

i.e. $$\delta F_a = 2S_a X(\cos\omega t_3 + 1)$$

In the case where a long drawing period is assumed, this drop in force is relative to the non-oscillatory drawing force in wire (a), since drawing stopped and the off-loading started under equilibrium conditions. In the case where a short drawing period is assumed, it is relative to the peak oscillatory force, since it is assumed that the transient force has insufficient time to decay.

Under non-oscillatory conditions, the front and back tensions during drawing are related by the equation:-

$$F_b = KF_a + F_{bo}$$

and under oscillatory conditions with a long drawing period:-

$$F_b = K(F_a - \delta F_a) + F_{bo} + \Delta F_b$$

Thus in this case the reduction in drawing load is:-

$$\delta F_b = K\delta F_a - \Delta F_b$$

However, under oscillatory conditions with a short drawing period:-

$$F_b = K(F_a + \Delta F_a - \delta F_a) + F_{bo} + \Delta F_b$$

and therefore the reduction in drawing load is:-

$$\delta F_b = K(\delta F_a - \Delta F_a) - \Delta F_b$$

Figures 59, 60 show the calculated values of drawing force reduction, which are plotted on figures 44 to 46, together with experimentally observed values.

B912: Tensile test results for wire.

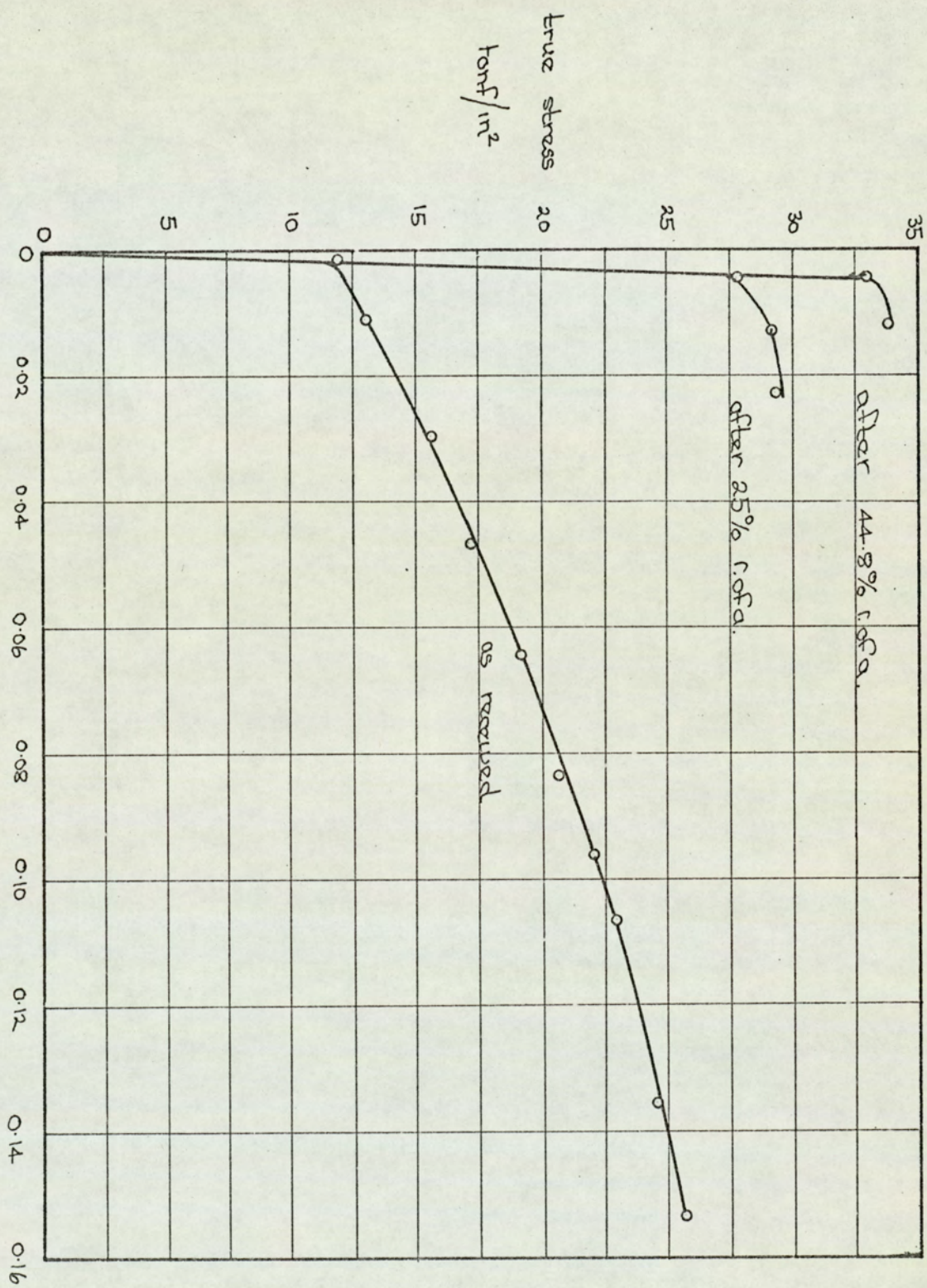

Stress - strain curves for wire before and after drawing.

B913: Material compositions

(a) EN2B

Carbon	0.50% max
Manganese	0.50% max
Phosphorus	0.50% max
Sulphur	0.50% max

(b) Vibrac 45

Carbon	0.38% - 0.45%
Silicon	0.30% max
Manganese	0.50% - 0.70%
Nickel	2.30% - 2.80%
Chromium	0.50% - 0.70%
Motybdenum	0.55% - 0.65%

(c) EN24

Carbon	0.35% - 0.45%
Manganese	0.45% - 0.70%
Nickel	1.30% - 1.80%
Chromium	0.90% - 1.40%
Molybdenum	0.20% - 0.35%

PART C: OSCILLATORY TUBE DRAWING

General view - tube drawing.

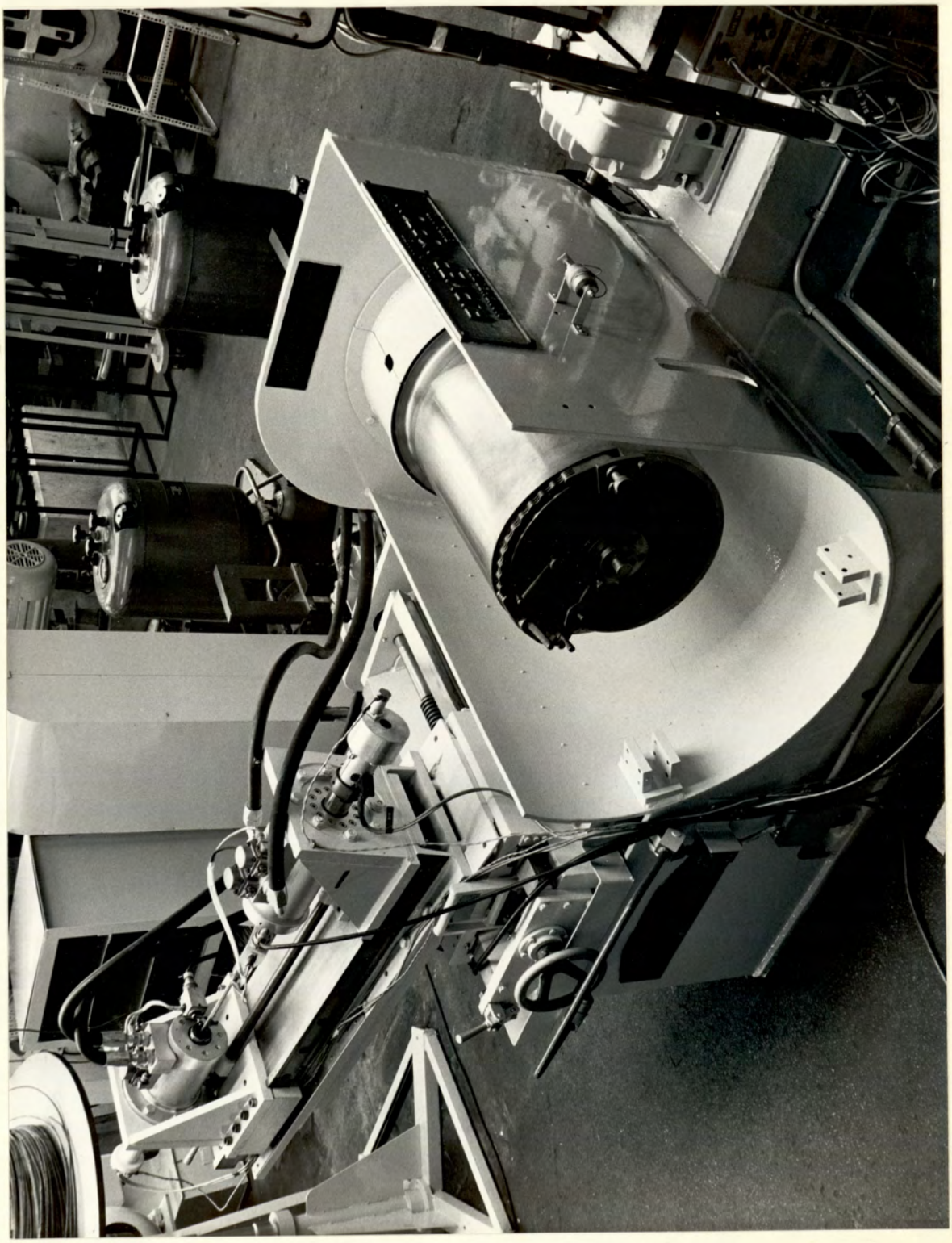

C1. Introduction to Oscillatory Tube Drawing

C1. Introduction to Oscillatory Tube Drawing

C11: Basic Considerations

The object of this investigation was to try to achieve substantial reductions in drawing load by applying low frequency axial oscillations to fixed plug tube drawing, and to investigate the mechanics of such a process.

Previous work in this field of metalworking had been exclusively concerned with the application of ultrasonic axial oscillations to one or both tools in fixed plug tube drawing, and to the die in tube sinking. All investigators reported a reduction in drawing force and some observed a reduction in chatter and improved surface finish. From the published results generally it is not possible to determine the extent to which the load reductions observed could be attributable to superposition. However, Winsper and Sansome[81] succeeded in recording the level of cyclic stress induced in the drawn tube when axial ultrasonic oscillations were applied to the plug. They observed a genuine reduction in drawing load, which was attributed to a reduction in plug/tube friction forces, with possibly friction reduction at the die/tube interface also.

The only quantitative mechanism proposed to account for a reduction in plug friction is that presented by Verderevskii et al[100], where he suggests that the relative velocity of plug to tube periodically reverses, thus producing a periodic reversal of the friction vector. This effectively reduces the mean value of friction force on the tube bore. The investigation by Young[104] has verified this mechanism in the case of a plane strain deep drawing analogue. Thus it is apparent that at ultrasonic frequencies the deformation only responds to the mean

component of cyclic plug force. If this mechanism is the only one in reducing drawing forces, then the greatest benefit which may be achieved is the elimination of plug friction when the ratio of drawing speed to plug speed is very low.

It was believed that at low frequencies of oscillation the deformation would respond to the cyclic component of plug force. It was therefore decided to investigate the process where both die and plug were oscillated out-of-phase. It was considered that the oscillation of the die would cause the tube to be drawn intermittently and for a short period when the die was at its most backward position. If the correct choice of phase was made, then the plug force could be reduced, or even reversed during the drawing period, thus aiding the motion of the tube through the die. Thus in such a process, not only are the detrimental effects of plug friction eliminated, but also the friction force on the plug may be used to aid the deformation. This process has therefore a greater potential in reducing loads than has the application of ultrasonic oscillations to the plug alone.

The purpose of this research programme was to investigate the possibility of such a mechanism, and to determine the underlying mechanics of the process. It was therefore decided to investigate the effects of the following variables upon the plug force, die force and total drawing force:

(1) frequency of oscillation

(2) amplitude of oscillation

(3) phase relationship

The same modified bull block unit was used for this investigation, with vibrator 1 driving the drawing die and vibrator 2 the plug bar. A loadcell inserted between the ram

of vibrator 1 and the dieholder measure the die loads, and a loadcell was also incorporated in the plug bar to measure the plug bar loads. The load in the drawn tube was derived from the aljebraic sum of these two loads, and checked using a strain gauge bridge mounted directly on the drawn tube. The same velocity transducers were mounted on the die-holder and the plug bar mounting flange to measure the plug bar and die displacement amplitudes.

C2. Equipment

Die holder - loadcell assembly.

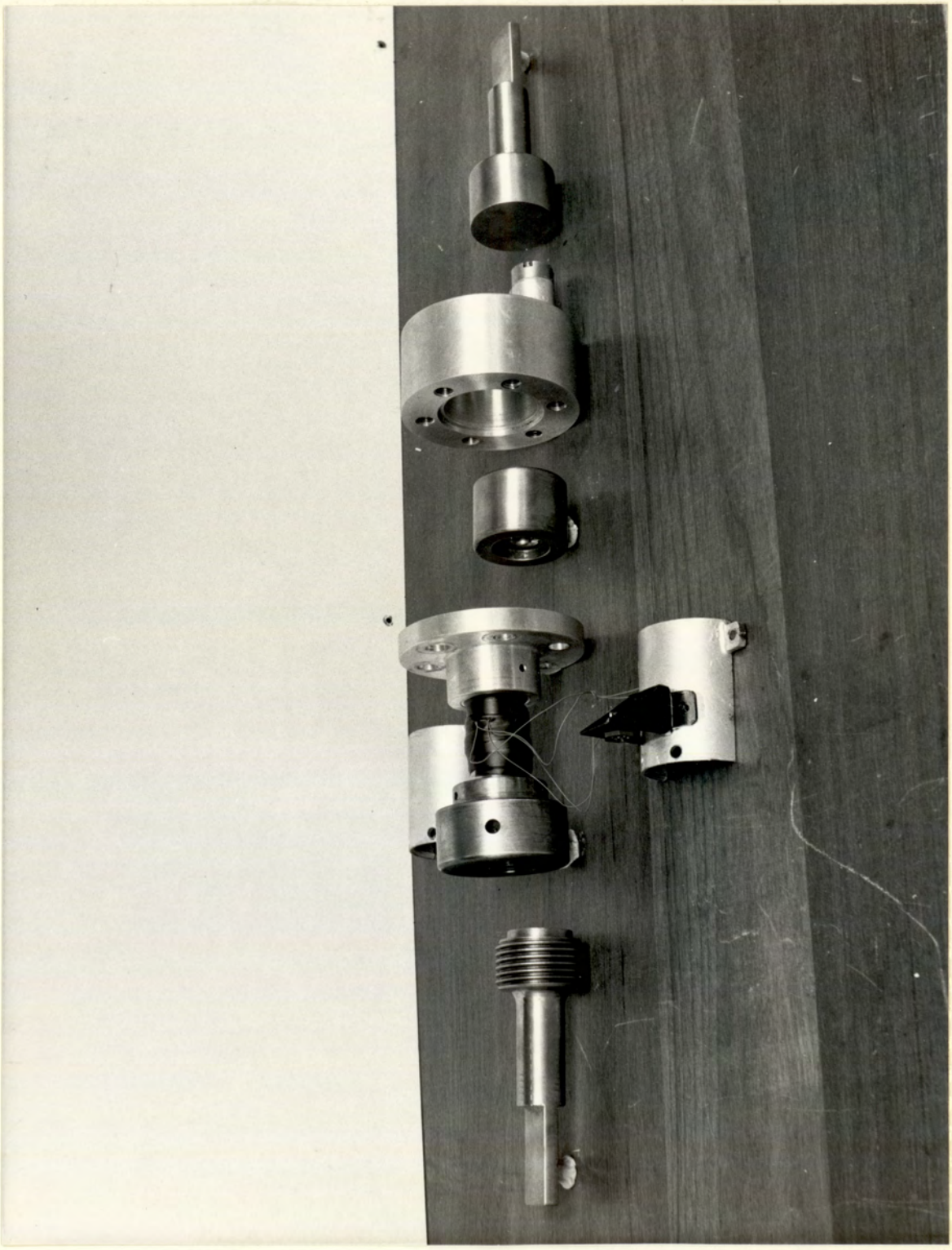

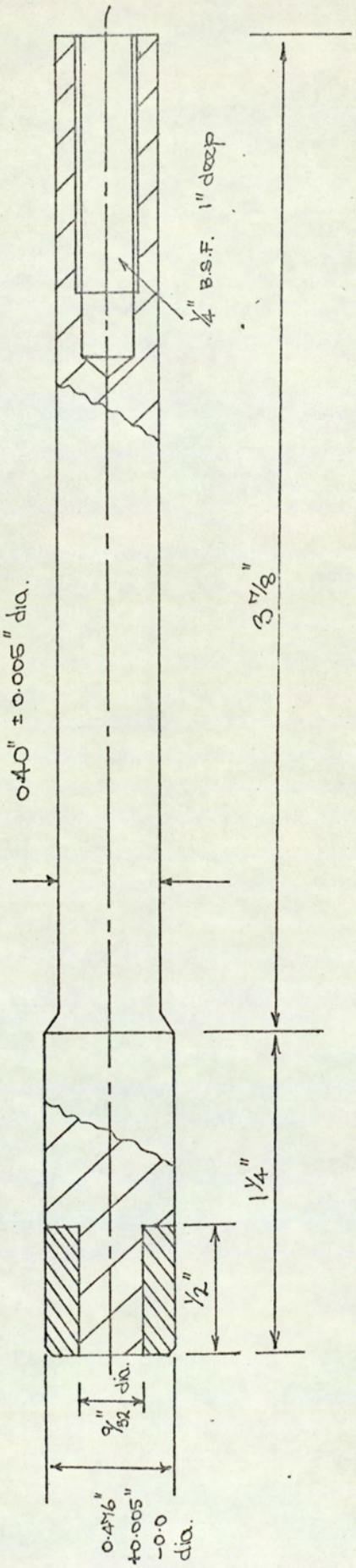

Details of plug dimensions.

Figure 61.

C2. Equipment

This investigation was conducted on the same bull block drawing machine as used in the wire drawing study, the only difference being that both vibrator units were turned round on their mounting flanges to accommodate the plug bar between the die, attached to vibrator 1, and the plug bar mounting flange, attached to vibrator 2.

C21: Drawing die

The drawing die used throughout the investigation consisted of a tungsten carbide insert brazed into a mild steel case. The orifice had a straight taper of 12° and a throat diameter of 0·5 in with a minimum parallel section. The mild steel case had a diameter of 2·083 in and length 1·575 in. This die unit was manufactured smaller than the standard size in order to minimise the inertia forces induced by the oscillations.

C22. Drawing plug

This was originally designed for use on a draw-bench using ultrasonic oscillations applied to the plug. It consisted of a tungsten carbide cylinder 0·5 in long and 0·476 in outer diameter brazed over a K.Monel shank, 5⅛ in long, the latter material being chosen for its good acoustic properties. Attachment of this shank to the plug bar was enabled by a drilled and tapped hole in the end of the shank. A drawing of this unit is shown in figure 61.

C23. Plug bar

This was manufactured from IMI Titanium 318 alloy rod, having additives of 6% Al., and 4% V alloy. The properties of this alloy are given in appendix 5.

This material was chosen because of its combined lightness

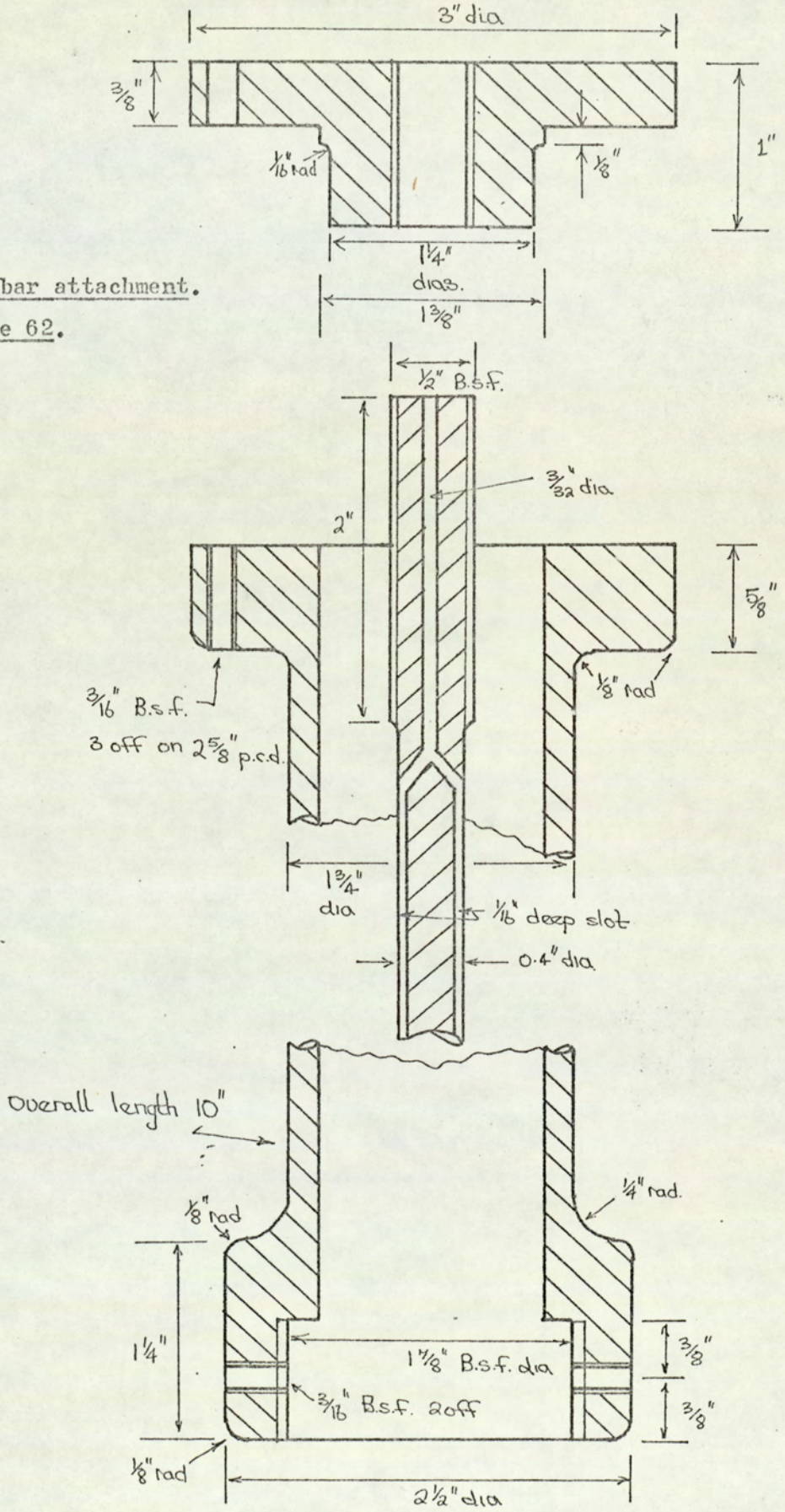

Plug bar attachment.

Figure 62.

and strength, together with good fatigue properties. Lightness was desirable to reduce the inertia of the attached mass on the vibrator and to minimise the severity of any transverse oscillation which might be induced in the plug bar.

The plug bar had a diameter of 0·4 in and a length of 47⅜ in. A loadcell was interposed between the plug bar and the plug shank, and attachment to this loadcell was enabled by a drilled and tapped hole in the end of the bar (see section C3). The other end of the bar was screwed into the mounting flange. In order to protect the leads of the loadcell which were passed up the plug bar to the mounting flange, two diametrically opposed slots were milled along the length of the bar to carry them. Araldite resin was used to bond the leads in the slots. These leads passed the screwed end of the bar via a centrally drilled hole. In order to minimise the weakening effect in the proximity of the drilled hole at the other end of the plug bar, the slot was discontinued in this region, and the wire passed over two diametrically opposed flats, 1/16 in wide, machined on the bar. A drawing of this unit is shown on figure 62.

C24. Plug bar mount

To secure the plug bar on the end of the vibrator ram, a mild steel cylinder was screwed on to the end of the vibrator ram, on to which the mild steel plug bar flange was attached by means of three 3/16 in b.s.f. screws. Drawing of these units are shown in figure 62.

C25. Die holder and flange

In order to minimise the inertial loads induced in the die loadcell (see section C3) by the mass of the die holder, this was manufactured from HE15 aluminium alloy in the fully heat

Die holder and mounting flange.

Figure 63.

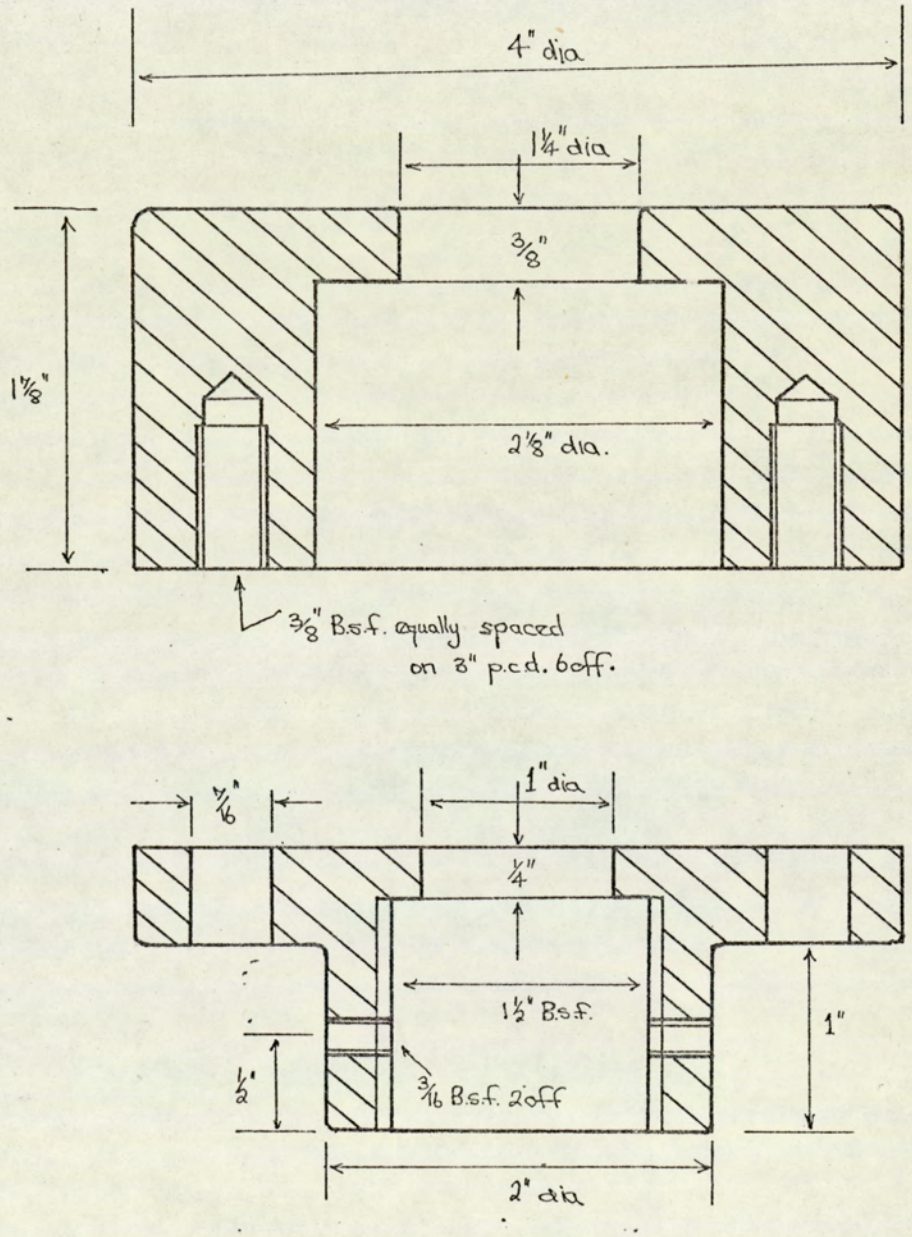

treated condition with a tensile strength of 44·1 tonf/in^2 and a proof stress of 39·4 tonf/in^2. The composition of this alloy is given in appendix 5.

The holder and flange were machined from bar, the latter unit being screwed to the loadcell. The holder was mounted on the flange by means of 6 x ⅜ in bolts. Details of these units are given in figure 63.

C26. Material

In view of the mechanical nature of low frequency oscillatory drawing evidenced by previous investigations, it was decided that only one material would be drawn in this investigation. The tube selected was a medium carbon steel because of its availability and ease of drawing. The composition and properties of this steel is given in appendix 5.

The tube was supplied in 4 ft lengths in the fully annealed condition, and in three sizes, all with an internal diameter of approximately 0·5 in. in order to obtain a minimum sink component in the reductions. The sizes were as follows:-

	Outer diameter (in)	Wall thickness (in x 10^{-3})
Light reduction	0·527	13
Medium reduction	0·532	15
Heavy reduction	0·532	16

These sizes gave a nominal sink component of 5% and overall reductions in area of 12·3%, 24·5% and 29% respectively.

Unfortunately there was insufficient time available to study the effects of reduction of area on the process, and all the tests were conducted with the medium reduction of 24·5%, save for one test conducted for the low reduction of

12·3%.

Stress-strain curves for this material are presented in appendix 1.

C27. Lubricant

Prior to the initiation of drawing trials, it was hoped to use a straight mineral oil, SAE 90, as the lubricant. This was chosen for its relatively poor lubrication properties. Since the proposed oscillatory process was considered to be most effective for large plug forces, i.e. poor lubricant conditions in the tube bore, use of this lubricant would accentuate the reductions in drawing force achieved. However, initial trials revealed a large scale variation in total drawing force, and also a tendency for chatter to be induced, and therefore use of this lubricant was discontinued. The lubricant adopted for the investigations was a commercial product, "Bondalube", consisting essentially of a baked or soap film (sodium stearate). Prior to the application of this lubricant the tube was pickled and phosphated. Whilst this lubricant eliminated chatter and produced a reduced variability in drawing force, this latter phenomenon was not eliminated, and was considered to be due to observed variations in the thickness and texture of the film. An attempt to further minimise these effects by painting a thick soap solution on the outer surface of the tube and allowing to dry before drawing was only partially successful, and therefore this variability was reluctantly accepted.

C3. Instrumentation

Die loadcell.

Figure 64.

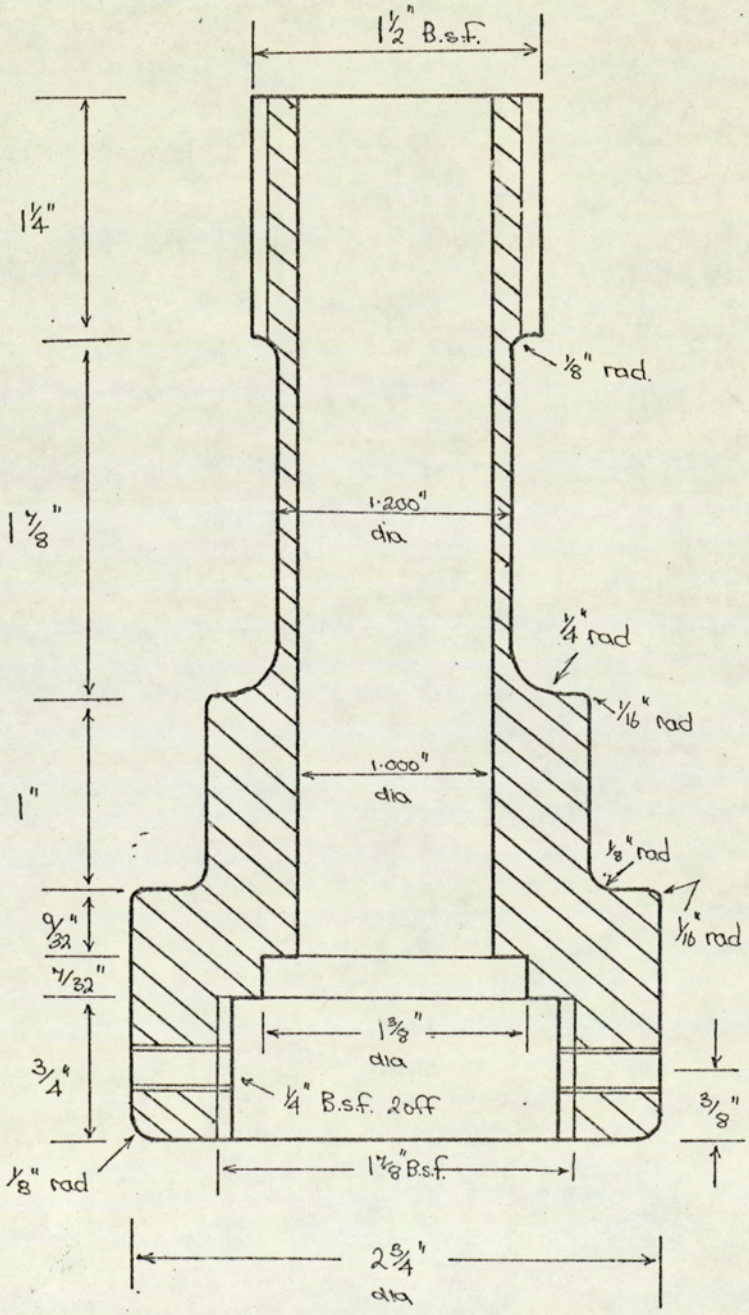

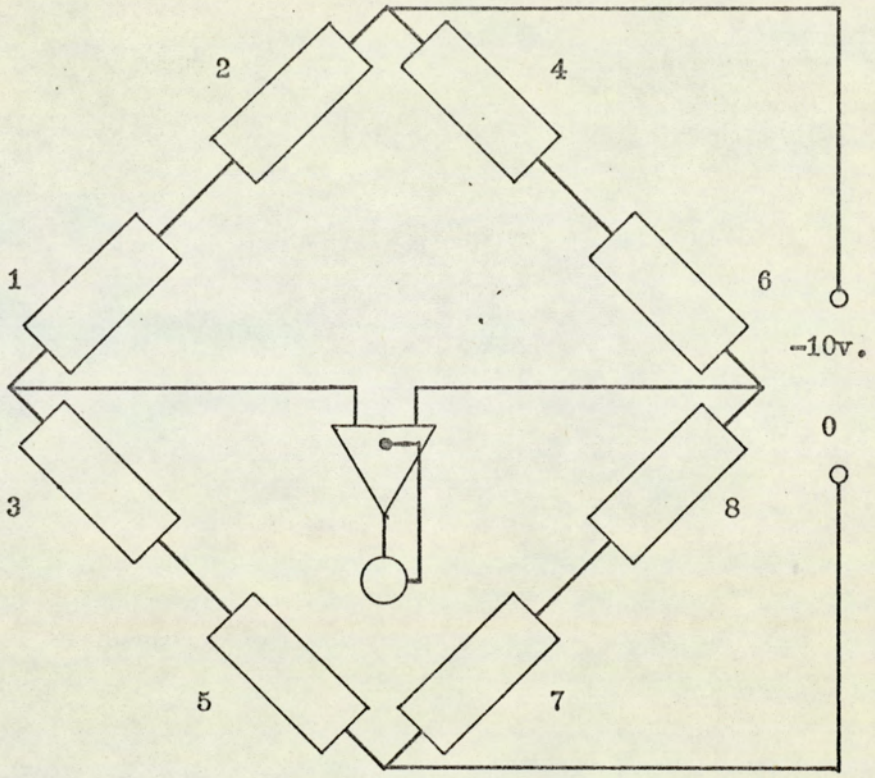

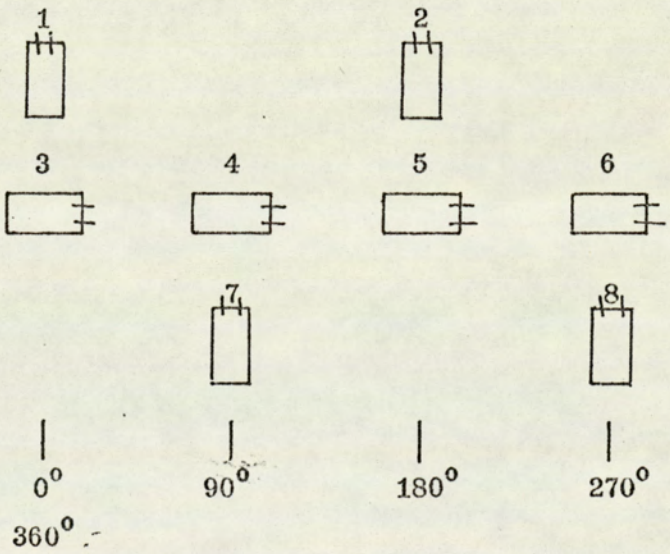

Strain gauge bridge on die .

Figure 65.

C3. Instrumentation

C31. Die loadcell design and construction

The load experienced by the die during drawing was measured by a loadcell interposed between the die vibrator ram and the die holder. Connections were provided by means of an internal screw thread, 1⅞ in B.S.F., for attachment to the ram, and an external thread, 1½ in B.S.F., for the die holder.

The loadcell was manufactured from carbon steel, EN24, heat treated to a tensile strength of 80 tonf/in^2. The composition of this material is given in section B31.

The loadcell was essentially a cylinder of 1 in internal diameter, 0.1 in wall thickness, designed to experience a strain of 0·02% at the maximum load of 2,000 lbf. The full design details are given in figure 64. The cylindrical section was ground to size and eight foil strain gauges, resistance 100 ohms, were bonded to the outer surface in the manner described in section B31. Four gauges were equally spaced around the circumference in the axial direction, each of which had an adjacent gauge place in the transverse direction. These gauges were interconnected in the form of a Wheatstone Bridge, as shown in figure 65, thus compensating for both bending stresses and temperature rises. The voltage supplied to all bridges was 10v. d.c.

C32. Plug bar loadcell design and construction

The force experienced by the plug during drawing was measured by a loadcell interposed between the titanium plug bar and the plug shank. Interconnection was via integral studs, ¼ in B.S.F. machined on the loadcell extremities. The loadcell

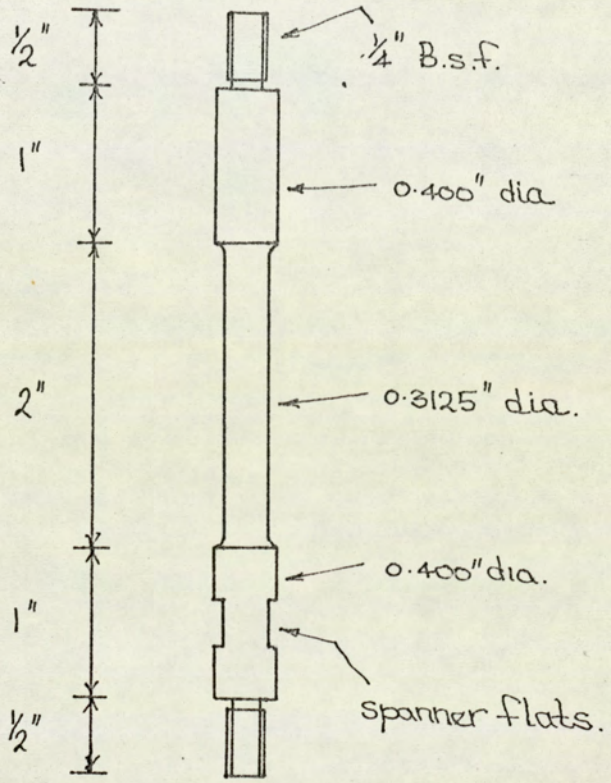

Plug bar loadcell details.

Figure 66.

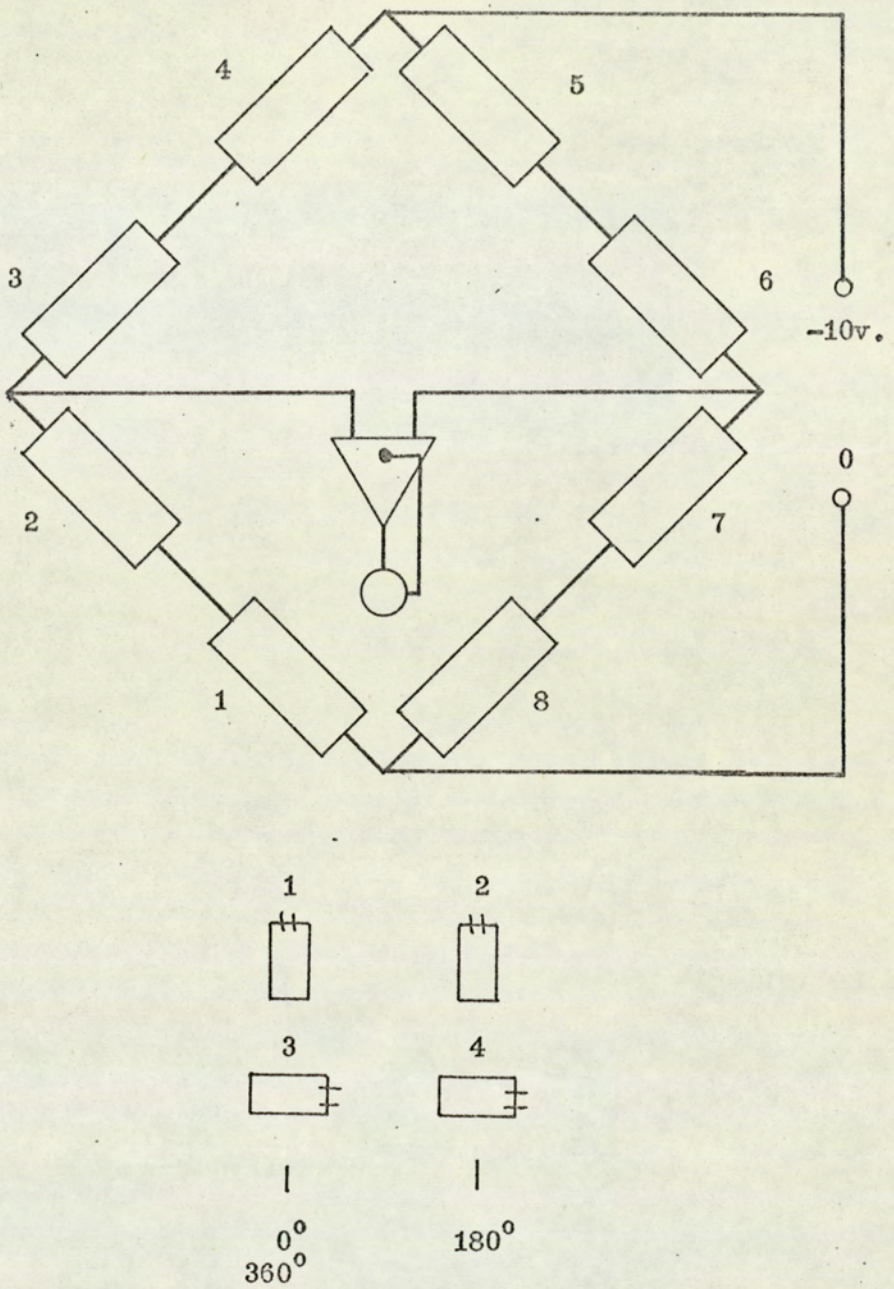

Elements 5 to 8 are 130 ohm, high stability resistors.

Strain gauge bridge on plug bar.

Figure 67.

was manufactured from EN24 carbon steel (see section B913) heat treated to a tensile strength of 80 tonf/in^2.

The loadcell working section was a cylindrical rod, 5/16 in, diameter, designed to experience a strain of 0.02% at the maximum load of 500 lbf. A detailed drawing of this component is given in figure 66. The working section was ground to size, and four foil gauges of 120 ohms resistance were bonded in the usual manner to this surface. Two gauges were positioned axially, and two transversely, each pair being diametrically opposed. These gauges were interconnected in the form of a half-bridge, as shown in figure 67, the other side of the bridge being two high stability resistors, resistance 260 ohms.

In order to reduce the vulnerability of the leads passing from the working section to the plug bar, two diametrically opposed flats, 1/16 in wide were machined from the working section to the edge of the loadcell. To facilitate assembly spanner flats were machined on the other end of the loadcell. In order that the flats for the loads on the plug bar and loadcell were aligned a soft copper washer was inserted in the joint, after being ground to the correct thickness. A similar connecting washer was used at the junction between plug shank and loadcell. In order that vibrations did not cause the units to unscrew during operation, a screw thread locking compound was used at both junctions.

C33. Loadcell on drawn tube

In order to check the accuracy of the derivation of the drawing load from the die and plug loads, strain gauges were bonded directly to the drawn tube for a selection of amplitudes and frequencies. Two axial gauges of 100 ohms resistance

Bridge on drawn tube.

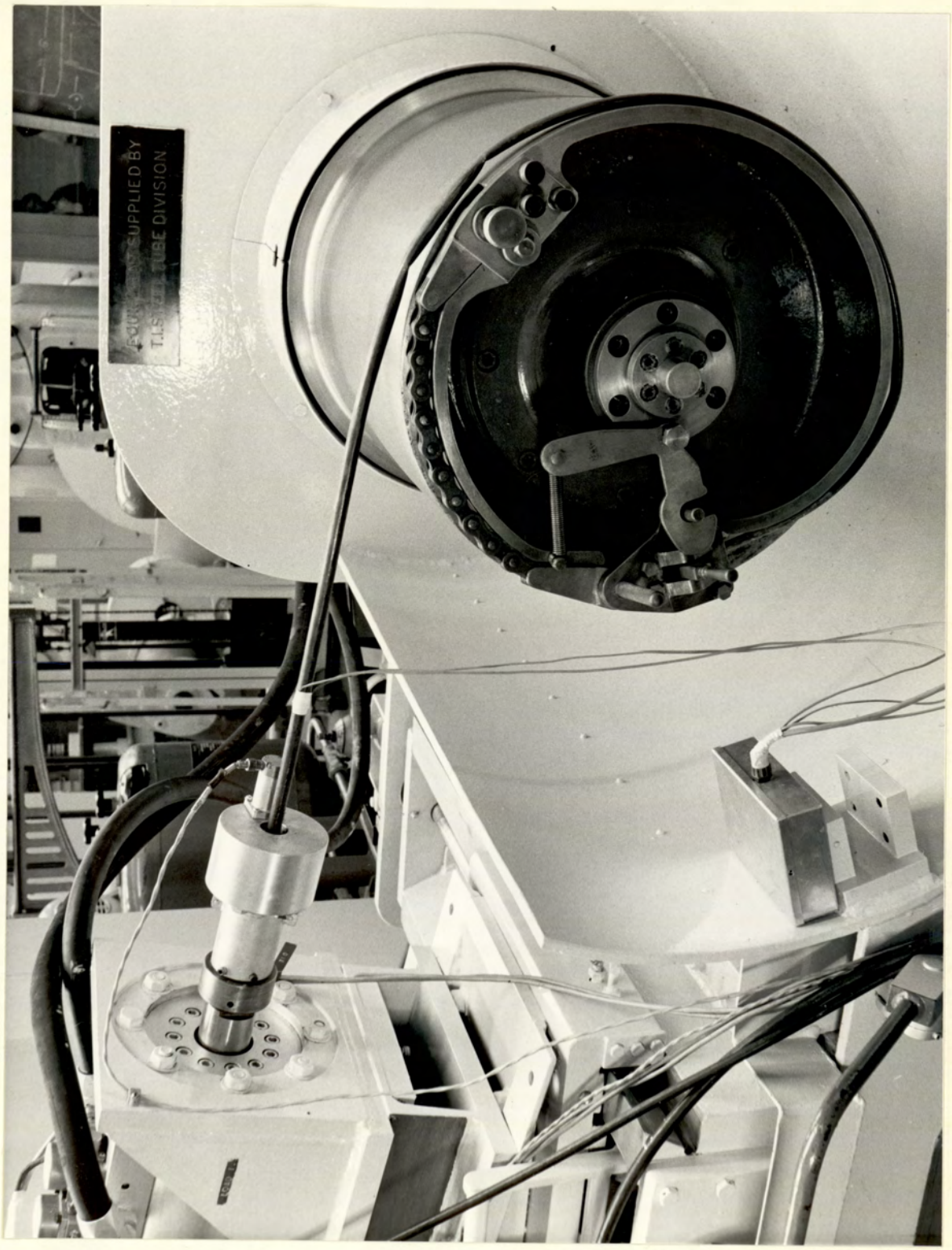

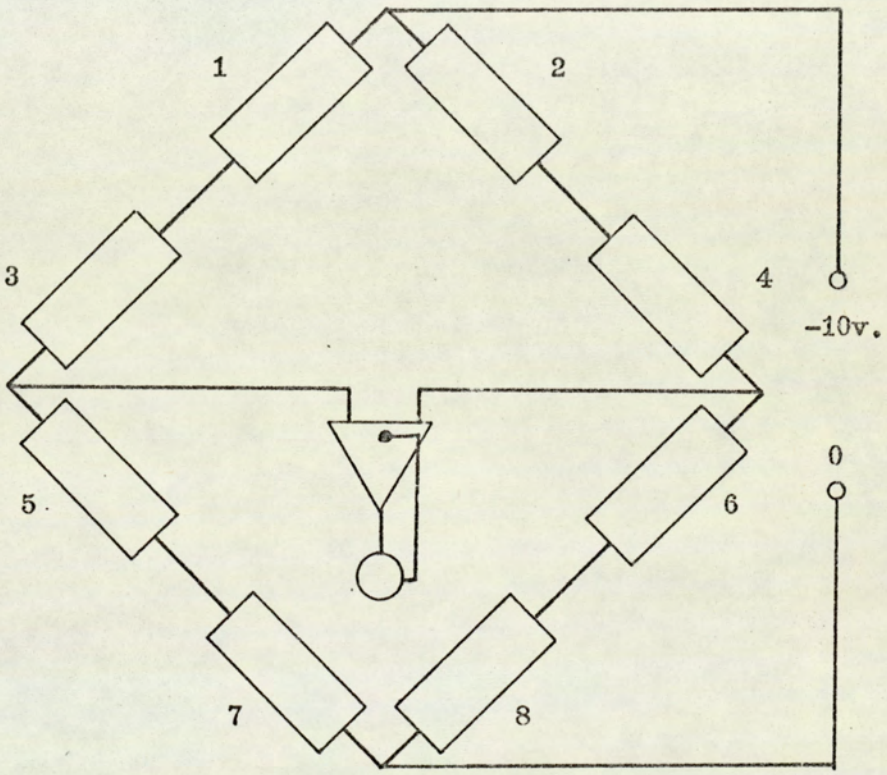

Gauges 3 and 6 are active, gauges 4 and 5 are dummy.
Elements 1,2,7,and 8 are 100 ohm, high stability resistors.

Strain gauge bridge on drawn tube.

Figure 68.

were bonded in the usual manner to the drawn tube in diametrically opposed positions to compensate for bending. Two gauges were similarly bonded to a section of unstrained drawn tube, these forming the dummy gauges for temperature compensation. In order that this bridge could be powered by the same 10v d.c. supply, each arm of the bridge consisted of a gauge and a high stability resistor of 100Ω as shown in figure 68. These resistors served to reduce the sensitivity of the bridge to a level acceptable to the d.c. amplifiers, and to ensure that power dissipation by each gauge was at an acceptable level.

In order to minimise electrical noise, all leads associated with these bridges were screened.

C34. Other instrumentation

For the reasons given in section B34, the outputs of these loadcells were amplified using the d.c. amplifiers described in that section. Again, a frequency compensating input network was employed for each amplifier. The gain of each amplifier was adjusted to give an adequate deflection of the galvanometer under test conditions.

The oscillatory displacement of the die was measured by the velocity transducer and meter described in section B35. The transducer was mounted on the die holder. Similarly the other velocity transducer was mounted on the plug bar mounting flange to measure the amplitude of oscillation imparted to the plug bar. The signals from both vibration meters were recorded on the ultraviolet recorder, and also displayed on the oscilloscope in order that the phase relationship between die and plug bar could be observed during testing, and recorded permanently.

During initial investigations it was observed that the position of the plug in the die throat affected the drawing load. In order to maintain the relative positions of die and plug during testing, the outputs from the displacement transducers in the control systems were connected to a d.c. voltmeter, and also recorded on the ultraviolet recorder. The signals to the recorder were smoothed by resistive - capacitive networks, which also served to adjust the galvanometer sensitivities.

C4. Calibration of load recording equipment

C4. Calibration of load recording equipment

C41. Static calibration of die loadcell

The loadcell was calibrated in tension using a Denison dead-weight testing machine. The load was applied using two mild steel adaptors, which terminated in tongues, suitable for gripping in the jaws of the testing machine. One adaptor was screwed into the internal thread of the loadcell. The other had an enlarged cylindrical end, of the same diameter as the die, and was placed in the die holder, with the tongue protruding, before assembly.

The loadcell was calibrated for loads up to 2000 lbf by the same technique as described in section B41, a typical calibration curve being presented in appendix 2.

C42. Static calibration of plug loadcell

The loadcell was originally calibrated before assembly of the plug bar in the Denison dead-weight testing machine. However, circuit modifications after assembly necessitated the recalibration of the plug load cell after incorporation in the plug bar. This was achieved by moving the plug vibrator flange towards the die by means of the leadscrew until the head of the plug protruded through the die holder. A mild steel clamp was then attached to the head of the plug. The load was applied by moving the plug vibrator backwards by the leadscrew, and recorded by the calibrated die loadcell.

After allowing sufficient time for the amplifiers to stabilise, the loads were applied in approximately equal increments up to 500 lbf, and released with similar decrements, to zero, records being taken of the galvanometer deflections at each stage. A typical calibration curve is shown in appendix 2.

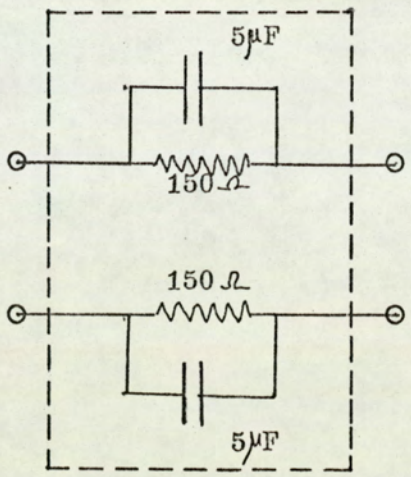

Die and Plug loadcells.

→ To amplifiers.

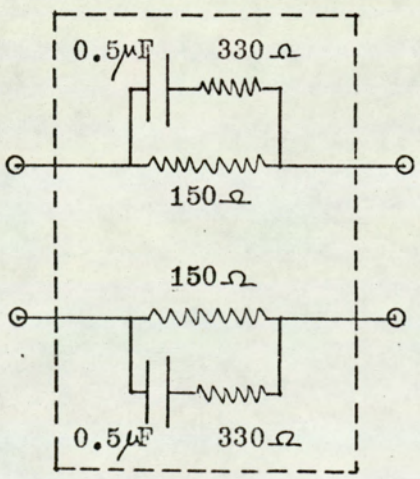

Loadcell on tube.

Amplifier input networks.

Figure 69.

Calibration by this technique necessitated the load in the die loadcell to be compressive, but since the strains experienced were small (<0·02%), this was considered to be satisfactory.

C43. Dynamic calibration of loadcells

The frequency response of the amplifiers was matched to that of their respective galvanometers to give a flat response, ± 3%, in the range 0 - 150 Hz, by the technique described in section B44. The input networks necessary for each amplifier/galvanometer unit are shown in figure 69.

C44. Measurement of referred inertia of die/loadcell assembly

This was achieved by the technique described in section B45. The effective mass of the assembly was found to be 6·24 lb.

The inertia forces induced in the plug bar loadcell when the plug bar was oscillated freely were found to be negligible. The plug was therefore considered massless in the analysis of the plug forces signals.

C5. Experimental procedure

C5. Experimental Procedure

Before the commencement of each test series, the electronic equipment was switched on for one hour to allow time for the units to stabilise. The outputs of the d.c. amplifiers were balanced to give zero galvanometer deflections under zero load.

A length of tube was swaged down at one end to pass through the die, and placed on the plug bar, which was bolted in position on the plug bar mount. The hydraulic compressors were switched on, the die positioned so that the output from the servo system displacement transducer was zero, and the plug moved back to be well clear of the die. The outputs of the amplifiers were balanced and a record taken of their zero positions. Drawing was commenced and the plug moved into the die throat until the output from the servo system displacement transducer was zero. Under these conditions of zero output from both position transducers, the position of the plug vibrator mounting flange was such that the contact length on the plug was approximately 0·08 in. The drawing speed was adjusted to the required value if necessary and a record taken of the drawing loads. The machine was stopped, the plug moved back to clear the deformation zone, and the stress in the drawn tube released by reversing the drum a short distance. Under this unloaded condition, a record was again taken of the galvanometer deflections.

For the subsequent oscillatory test, the frequency of oscillation was set for the vibrators on the low frequency oscillator, the vibrators switched on, and the requisite amplitude adjusted approximately. Because the d.c. amplifiers in the oscillator drifted slightly, the die position was

again adjusted to give zero output from the position transducer. The phase angle between the die and plug bar oscillations was set on the phase shifting adaptor using the oscilloscope. Drawing was commenced and the plug moved into the die orifice until its position transducer again gave no signal. The amplitudes of oscillation and drawing speed were adjusted when necessary, and a record taken of the oscillatory drawing loads. Drawing was terminated, the vibrators switched off, and the loads in the system released as described above. A record was taken of the unloaded galvanometer deflections.

Tests using a strain gauge bridge mounted on the drawn tube were conducted as above, the non-oscillatory drawing test serving to calibrate the bridge, using the recorded plug and die forces. A simple check on the linearity of response of the tube load recording equipment was provided by recording both the sinking and subsequent drawing load under non-oscillatory conditions. In all cases the calibration was found to be linear.

In order that the stiffness of the drawn tube was held as constant as possible during the oscillatory tests, recordings were not made until the drawn tube contacted the surface of the bull-block drum, i.e. when the gripping jaws and associated chain were coiled on the drum. The wire drawing investigation showed that even under these conditions the stiffness of the drawn product was variable due to the partial loads experienced by the coiled product on the drum. However, since only short lengths of tube could be drawn, this variability could not be avoided.

During these tests where high amplitudes were used, and hence compressive forces were induced in the plug bar, this

element was frequently forced into transverse oscillation, especially when the majority of tube had been drawn, and its constraining influence on the plug bar was not effective. Under these conditions it was therefore necessary to damp out the oscillations manually.

Initial tests showed that after several tests there was a lubricant build-up at the entry to the die. It was considered that such a build-up could affect the lubricant conditions at the die tube interface, and therefore the die was periodically cleaned. Similarly, a build-up of lubricant was observed on the plug; this also was removed after each test.

It was observed during early investigations that the bore of the tube, and to a lesser extent the outer surface exhibited ring markings, especially at the lower frequencies and high amplitudes. This was considered to be the result of the edge of the plug indenting the tube as it was pushed into the tube bore by the vibrators. To overcome this, the sharp edge of the plug was ground away. This had the effect of reducing the severity of the marking, but did not remove it completely under all conditions. To quantise this effect, several tubes were drawn under various oscillatory conditions and their surface topography measured axially on a Talysurf machine.

C6. Results

C6. Results

The experimental data obtained from this investigation are presented in graphical and tabular form at the end of this section. All tests were conducted at a nominal speed of 2 ft/min, with a reduction of area of 24·5%, except in one case where the reduction is 12·3%.

Graphs 1 to 8 show the observed values of plug and die maximum and minimum forces, and the derived values of maximum and minimum drawing force.

Graph 1 shows the results of the test designed to determine the optimum phase angle between plug-bar and die oscillations. In this case the frequency of oscillation was 60 Hz and both plug and die amplitude was 10×10^{-3} in peak to peak.

The results of tests conducted to investigate the effects of frequency and amplitude are shown in graphs 2 to 6 corresponding to frequencies of 40, 60, 80 and 100 Hz respectively. The phase angle for these and subsequent tests was 180^{o}. The amplitudes of oscillation in each test were the same for both plug and die, and were increased in steps of 2×10^{-3} in peak to peak until the transverse oscillations of the plug bar became excessive.

Finally, two tests were conducted with only one tool oscillating at 60Hz. Graph (7) shows the effects of oscillating the die only, and graph (8) the plug bar only.

The remaining graphs were constructed from data obtained from the above mentioned tests.

The relationship between the reduced plug bar load and the die load at the instant of drawing is shown in graph (9).

Graph (10) shows a comparison between calculated and observed values of plug bar force variation.

Finally, graph (11) shows the magnitude of the reduced drawing force as a function of amplitude for the whole range of frequencies.

The data presented in graphs (9) to (11) correspond to the results presented in graphs (2) to (5). Due to the degree of scatter observed in the experimental data, the values of force used in the former graphs are taken from the averaged curves on the latter graphs.

The results of the tests using a strain gauge bridge on the drawn tube are presented in tabular form at the end of this section, together with the surface finish records of the drawn tube.

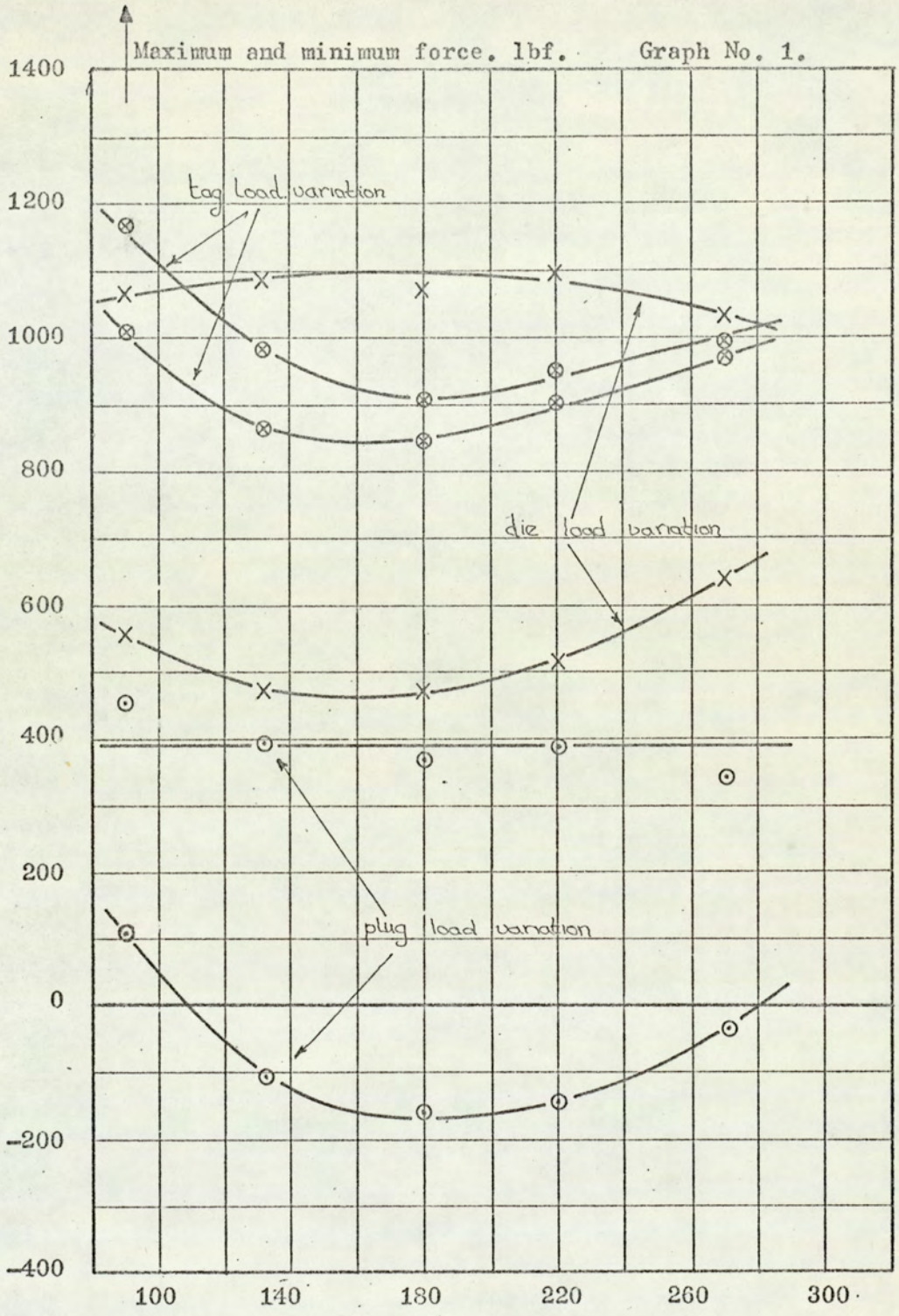

Phase lead of plug over die. degrees.

⊙ Plug.
× Die.
⊗ Drawn tube.

Frequency 60 Hz.

24.5% reduction of area.

Oscillation amplitude of plug and die 10×10^{-3} in. pk. t. pk.

Drawing speed 2 ft./ min.

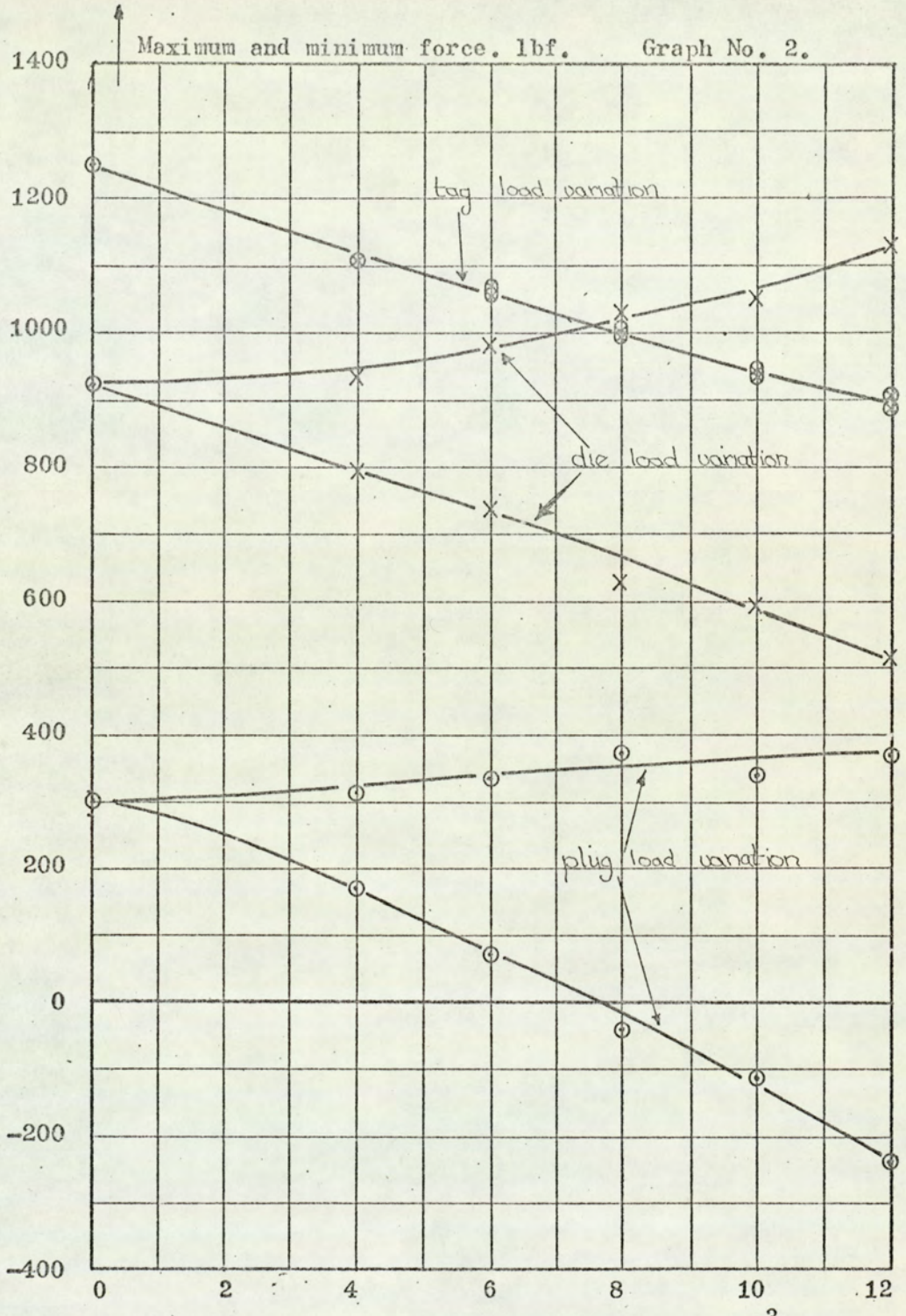

⊙ Plug.
× Die.
⊗ Drawn tube.

Frequency 40 Hz.

24.5% reduction of area.

Phase angle 180 degrees.

Drawing speed 2 ft./ min.

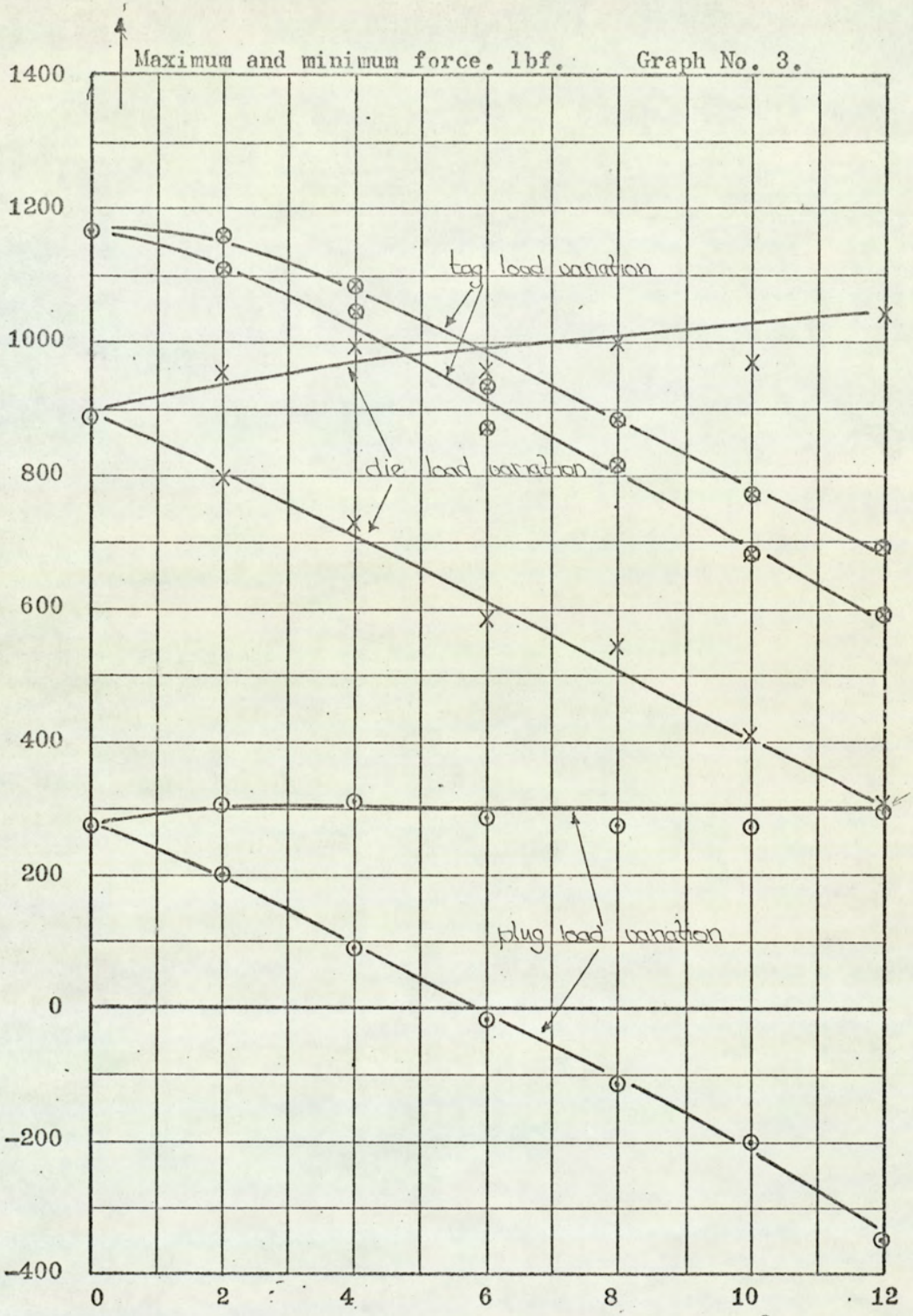

Oscillation amplitude of plug and die. in. x 10^{-3} p. t. p.

⊙ Plug.
× Die.
⊗ Drawn tube.

Frequency 60 Hz.

24.5% reduction of area.

Phase angle 180 degrees.

Drawing speed 2 ft./ min.

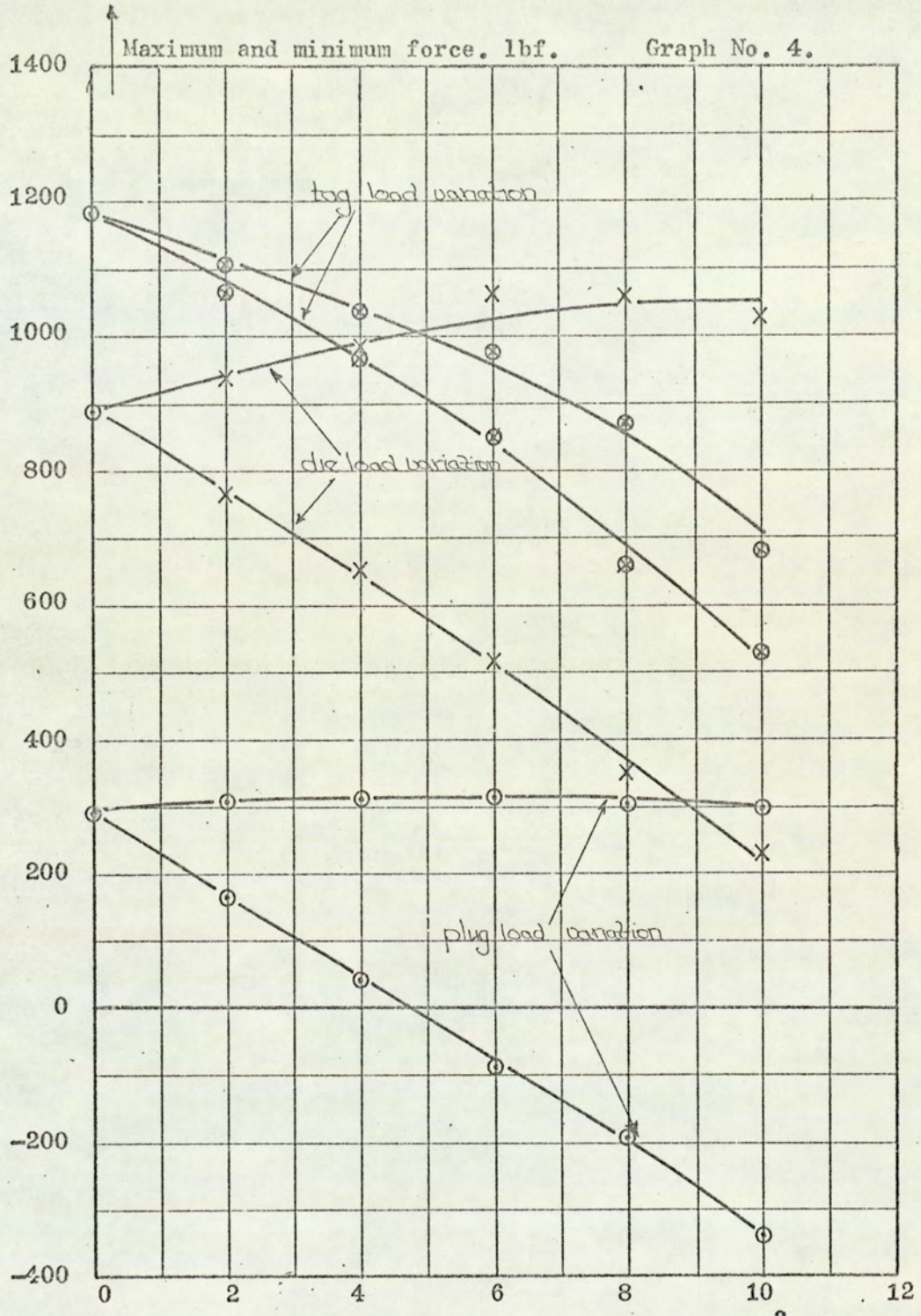

→ Oscillation amplitude of plug and die. in. x 10^{-3} p. t. p.

⊙ Plug.
× Die.
⊗ Drawn tube.

Frequency 80 Hz.

24.5% reduction of area.

Phase angle 180 degrees.

Drawing speed 2 ft./ min.

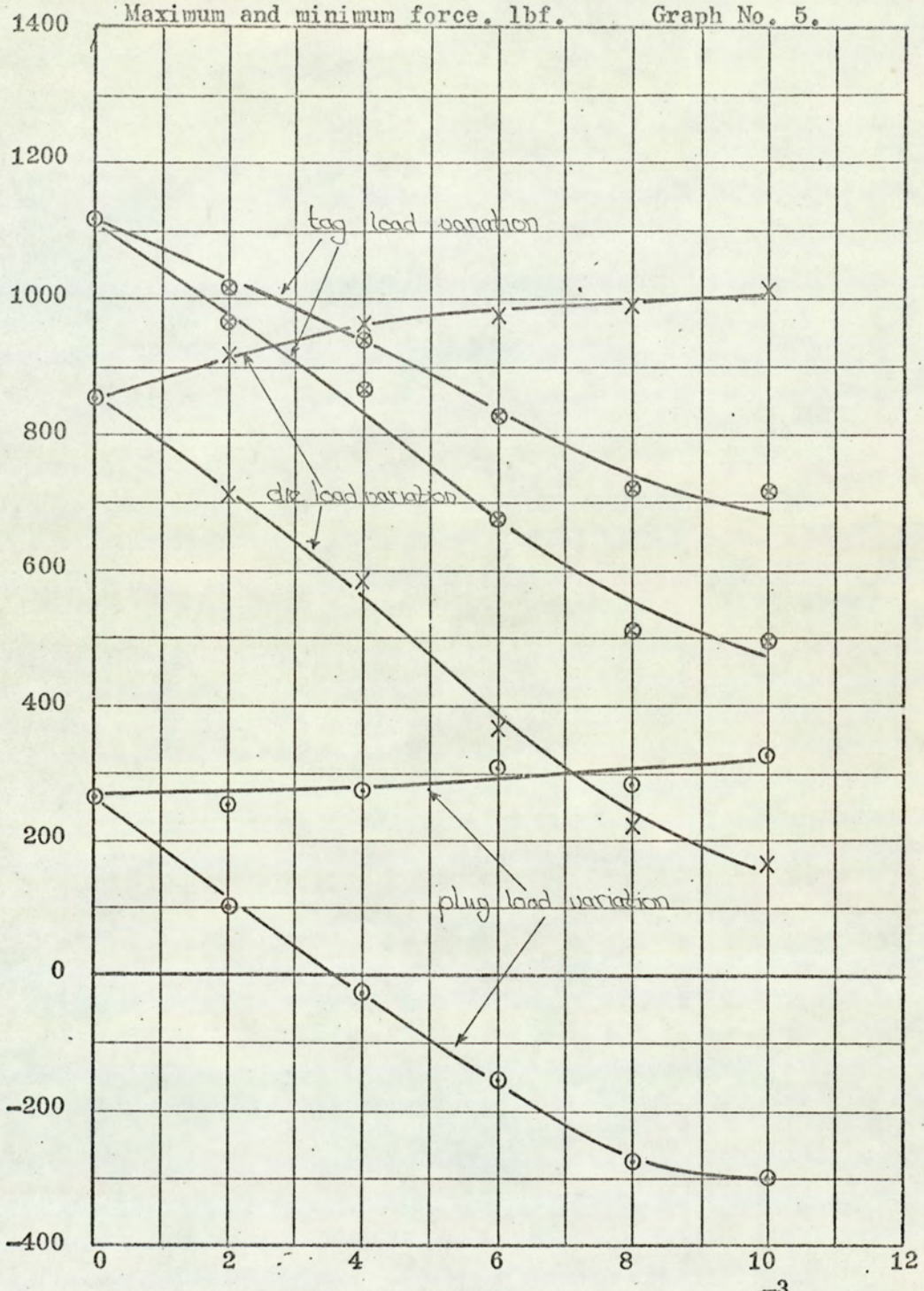

Oscillation amplitude of plug and die. in. x 10^{-3} p. t. p.

⊙ Plug.
× Die.
⊗ Drawn tube.

Frequency 100 Hz.

24.5% reduction of area.

Phase angle 180 degrees.

Drawing speed 2 ft./ min.

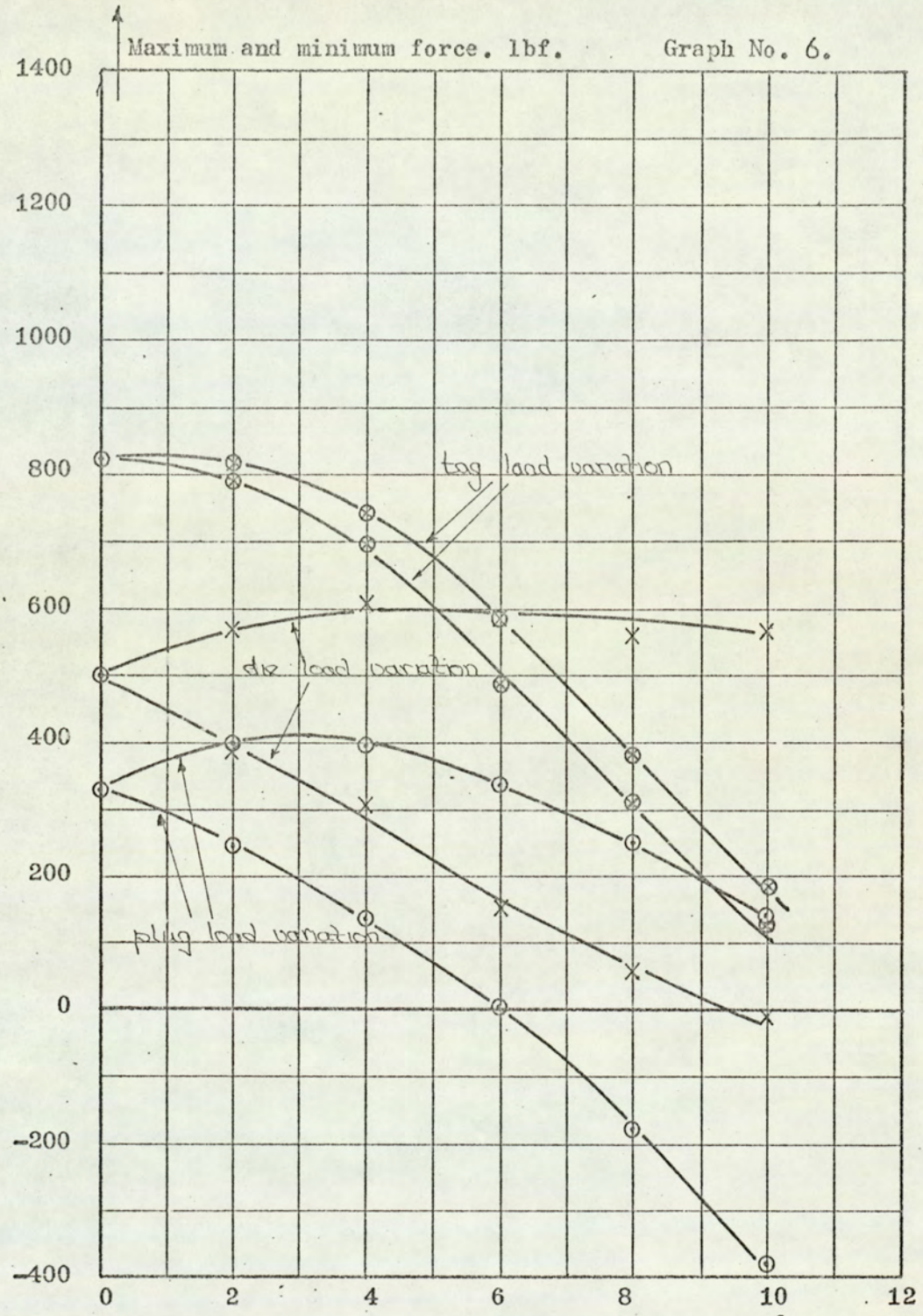

→ Oscillation amplitude of die and plug. in. x 10^{-3} p. t. p.

⊙ Plug.
× Die.
⊗ Drawn tube.

Frequency 60 Hz.

12.3% reduction of area.

Phase angle 180 degrees.

Drawing speed 2 ft./ min.

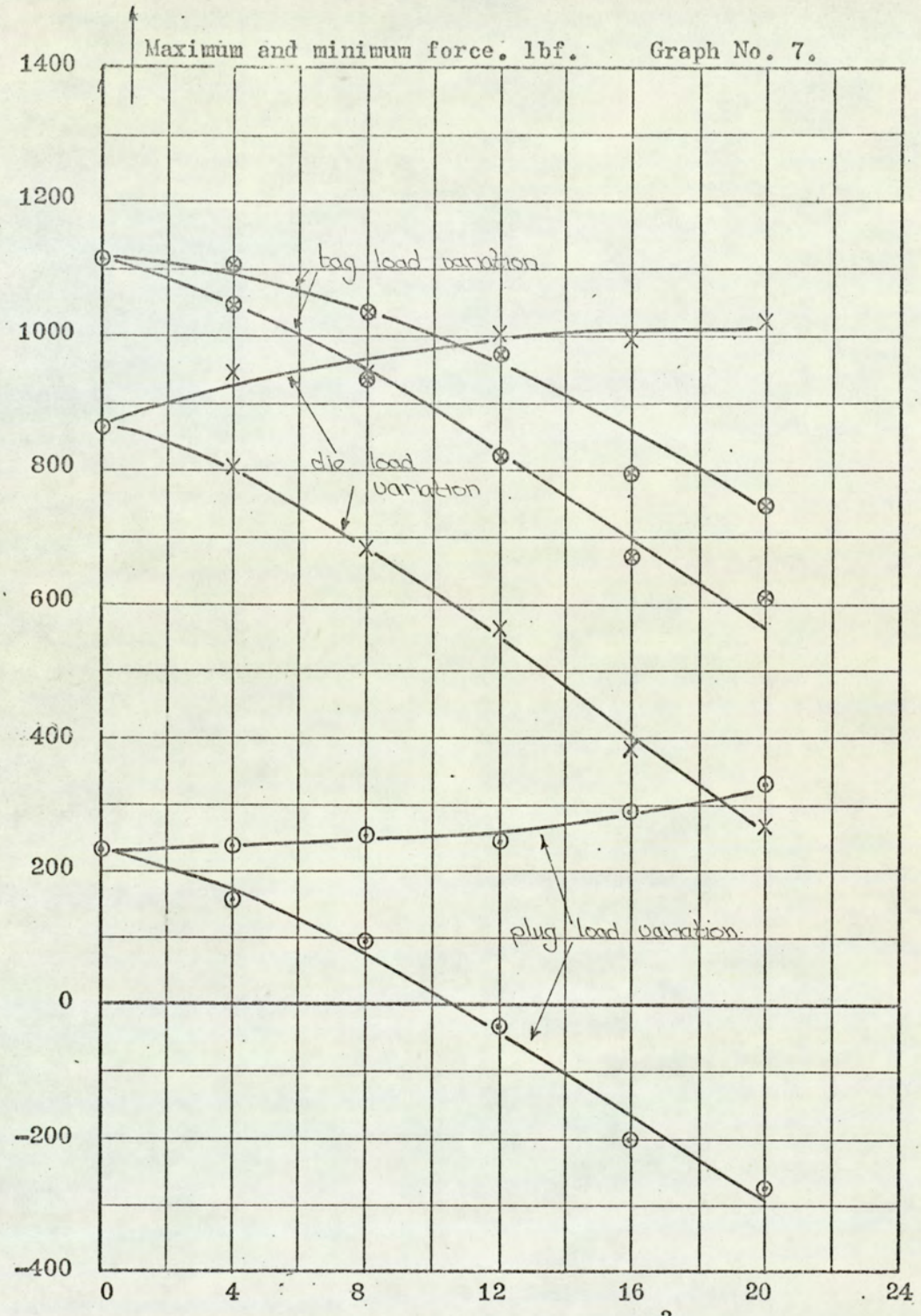

Oscillation amplitude of die, in. x 10^{-3} p. t. p.

⊙ Plug.
× Die.
⊗ Drawn tube.

Frequency 60 Hz.

24.5% reduction of area.

Die only oscillated.

Drawing speed 2 ft./ min.

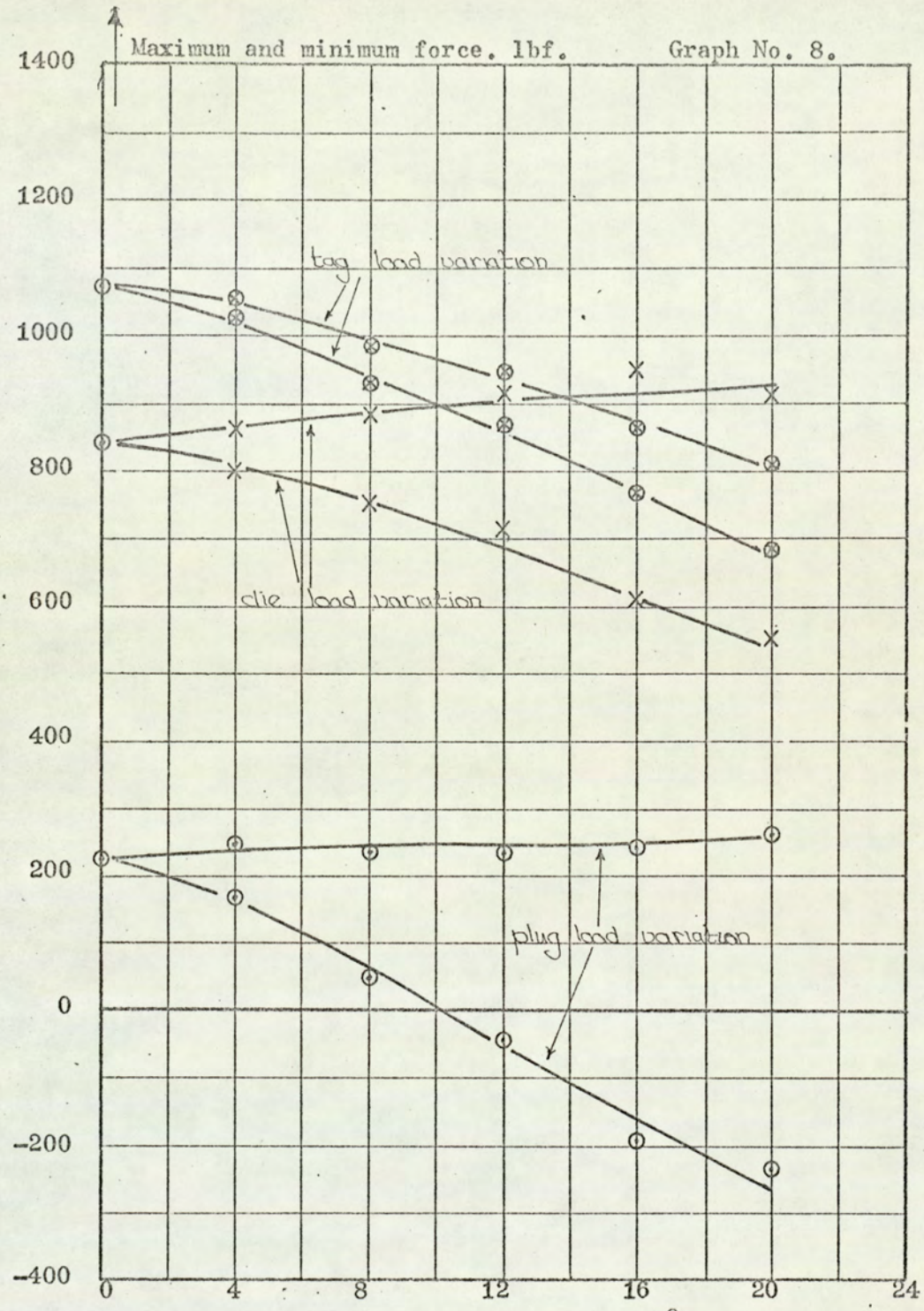

⊙ Plug.
× Die.
⊗ Drawn tube.

Frequency 60 Hz.

24.5% reduction of area.

Plug only oscillated.

Drawing speed 2 ft./ min.

Relationship between plug and die loads at instant of drawing.

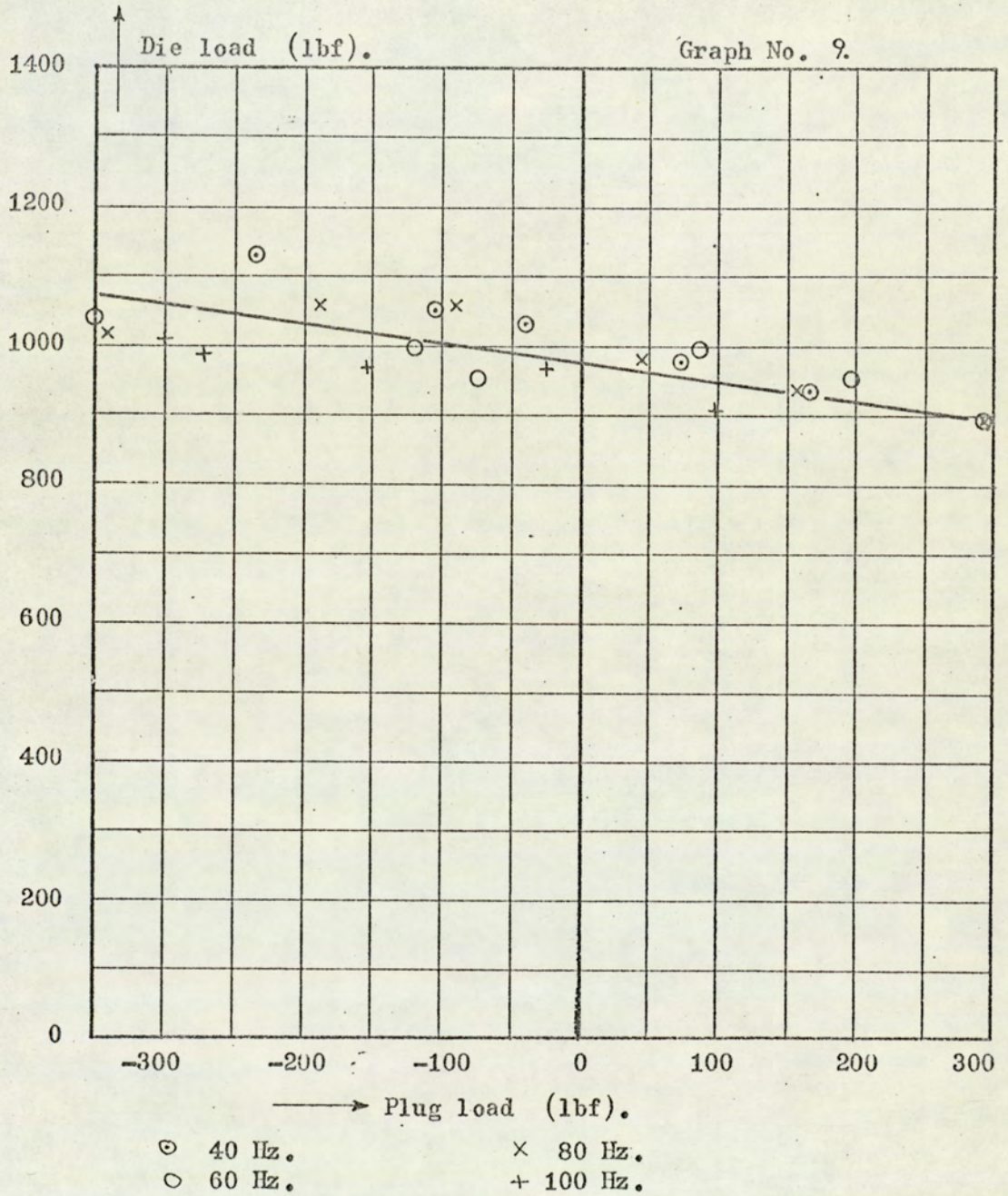

Drawing speed 2 ft/min. Plug and die oscillating in anti-phase.
Reduction of area 24.5%.

Comparison between computed and actual force variations in the plug bar.

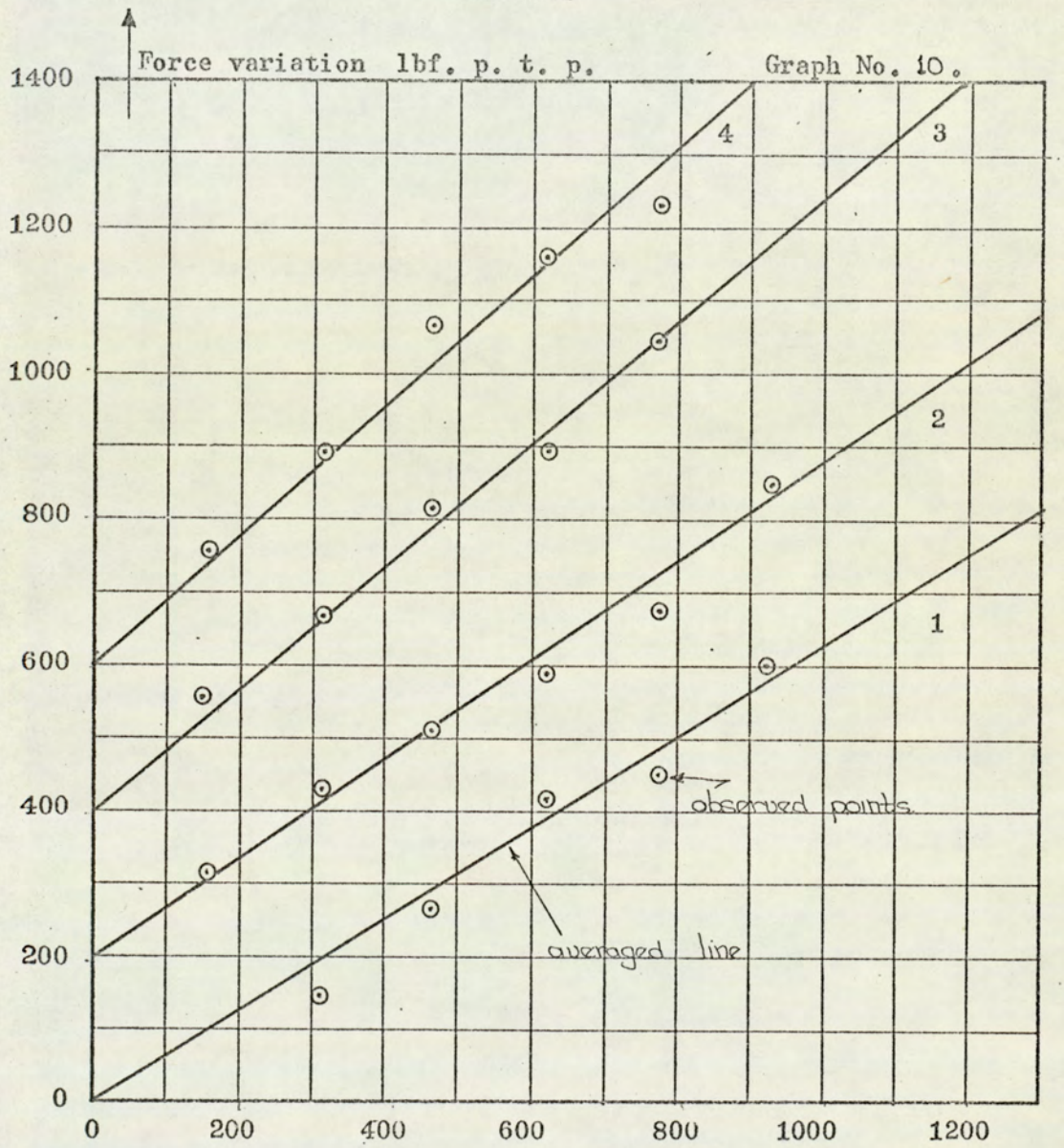

Curve 1 - 40 Hz. Curve 3 - 80 Hz.

Curve 2 - 60 Hz. Curve 4 - 100 Hz.

Computed variation = 2 x p. t. p. die amplitude x stiffness of plug bar.

Drawing speed 2 ft/min. Plug and die oscillating in anti-phase.

Reduction of area 24.5%. (Curves 2 to 4 have offset axes).

Gradients:

1. 0.626
2. 0.683
3. 0.845
4. 0.890

Reduction in drawing force as a function of amplitude.

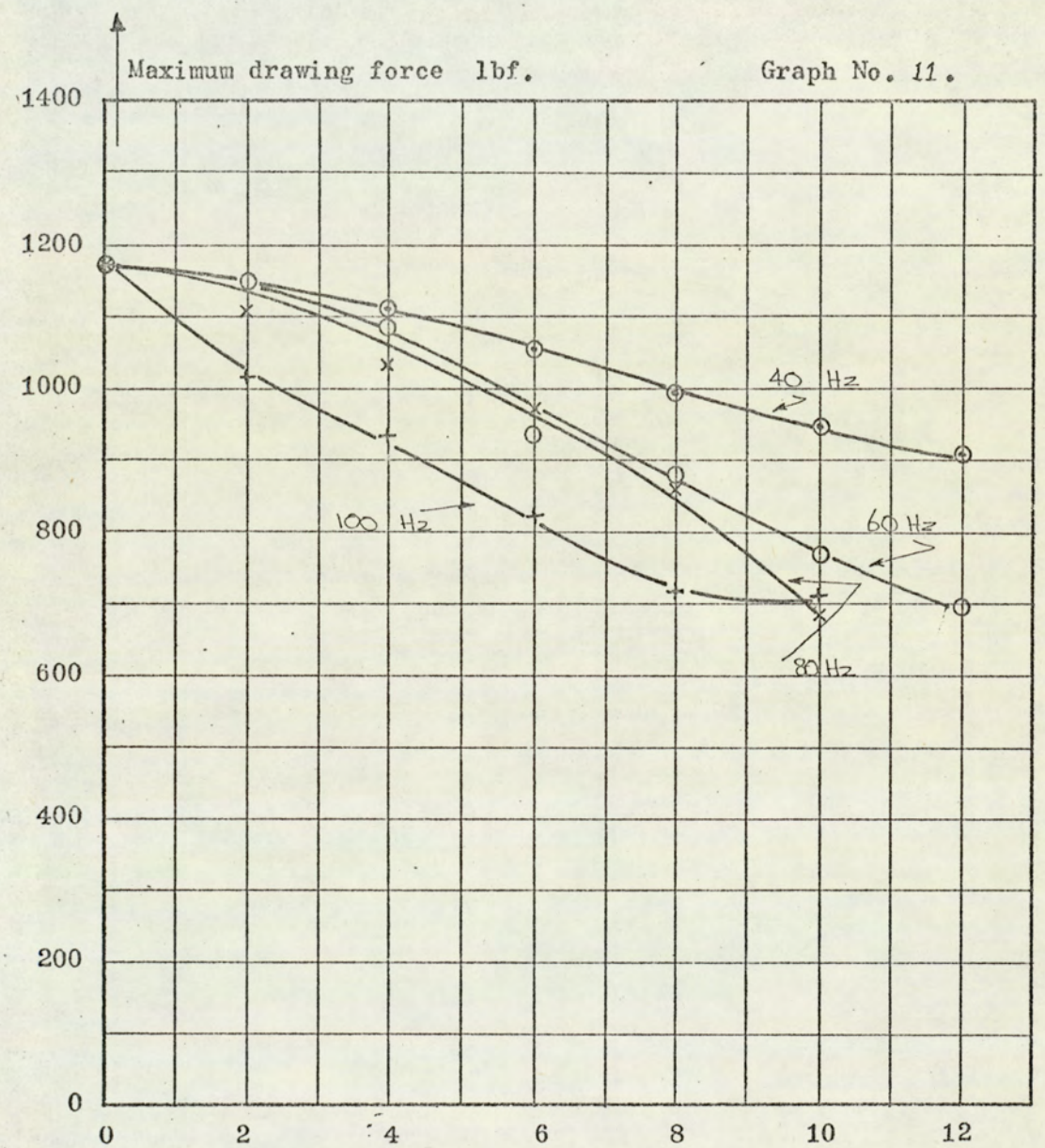

→ Die and plug amplitude. in. x 10^{-3} p. t. p.

⊙ 40 Hz. × 80 Hz.

○ 60 Hz. + 100 Hz.

Drawing speed 2 ft/min. Plug and die oscillating in anti-phase.

Reduction of area 24.5%.

Ampl. in.x10^{-3} p.t.p.	L1 (lbf)	L1 (lbf)	L2 (lbf)	L2 (lbf)	L_d (lbf)	L_{nd} (lbf)
Frequency 40 Hz. Die and plug oscillating. 180° phase.						
0	956		299		1255	
4	938	793	314	169	1107	1107
6	982	738	337	76	1058	1075
8	1033	629	376	- 39	994	1005
10	1055	595	342	-103	947	937
12	1136	514	368	-232	904	882
Frequency 60 Hz.						
0	888		273		1161	
2	951	798	310	200	1151	1108
4	996	728	316	89	1085	1044
6	957	587	287	- 21	934	970
8	1000	545	271	-118	882	816
10	970	409	271	-200	770	680
12	1045	302	295	-350	695	597
Frequency 80 Hz.						
0	892		294		1186	
2	940	762	306	163	1103	1068
4	986	651	314	47	1033	956
6	1062	515	321	- 89	973	846
8	1056	350	306	-187	869	656
10	1028	230	300	-342	686	530
Frequency 100 Hz.						
0	857		264		1121	
2	916	710	252	100	1014	962
4	963	587	276	- 26	937	863
6	977	364	310	-153	824	674
8	991	224	284	-272	719	508
10	1016	164	329	-300	716	493

Drawing speed 2 ft/min. 24.5% reduction in area.

plug phase lead.	L1 (lbf)	L1 (lbf)	L2 (lbf)	L2 (lbf)	L_d (lbf)	L_{nd} (lbf)
Frequency 60 Hz. Die and plug amplitude 10 x 10^{-3} in. p.t.p.						
90°	1061	554	450	103	1164	1004
132°	1085	472	395	-105	980	867
180°	1071	477	368	-163	908	845
221°	1098	512	390	-147	951	902
270°	1028	637	342	- 31	1028	997
Non - oscillatory forces:-						
	927		350		1277	
Plug only oscillating. Frequency 60 Hz.						
Ampl. in.x10^{-3} p.t.p.						
0	848		223		1071	
4	866	800	252	163	1029	1052
8	883	750	234	47	930	984
12	916	716	231	- 47	869	947
16	958	616	247	-195	763	863
20	912	554	258	-231	681	812
Die only oscillating. Frequency 60 Hz.						
0	877		236		1113	
4	945	809	240	158	1104	1049
8	942	681	253	95	1037	934
12	1004	561	258	- 32	972	819
16	998	382	290	-200	798	672
20	1023	268	336	-274	747	604

Drawing speed 2 ft/min. 24.4% reduction in area.

Ampl. in.x10^{-3} p.t.p.	L1 (lbf)	L1 (lbf)	L2 (lbf)	L2 (lbf)	L_d (lbf)	L_{nd} (lbf)
Frequency 60 Hz. 180° phase angle.						
5	1006	594	302	- 63	943	896
			from bridge		966	879
10	1090	430	342	-174	916	772
			from bridge		923	766
Frequency 100 Hz. 180° phase angle.						
5	1119	609	369	- 32	1087	978
			from bridge		1104	970
10	1040	284	316	-263	777	600
			from bridge		778	595

Drawing speed 2 ft/min. 24.5% reduction in area.

Frequency 60 Hz. Die and plug oscillating. 180° phase.						
0	492		348		840	
2	568	390	400	248	816	790
4	605	303	395	137	742	698
6	586	151	337	0	586	488
8	559	54	253	-179	380	307
10	565	- 11	145	-384	181	134

Drawing speed 2 ft/min. 12.3% reduction in area.

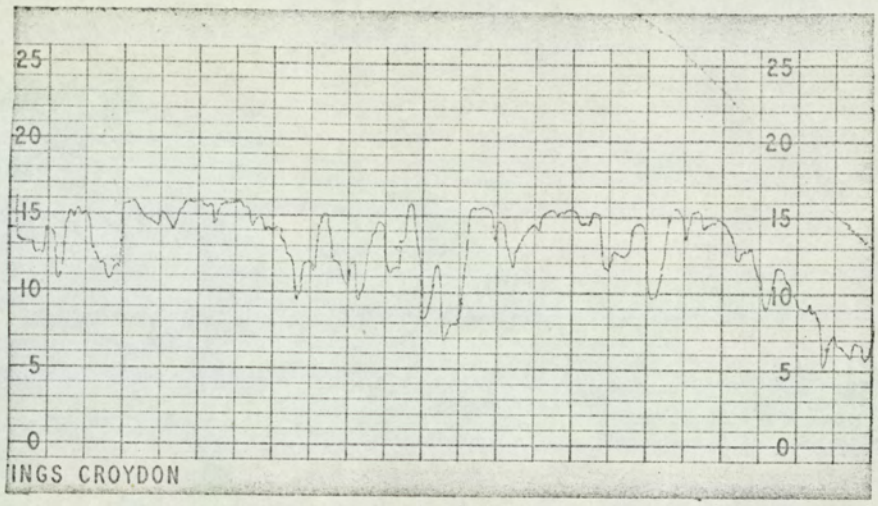

Inside surface. C. L. A. value = 0.580

Outside surface. C. L. A. value = 0.780

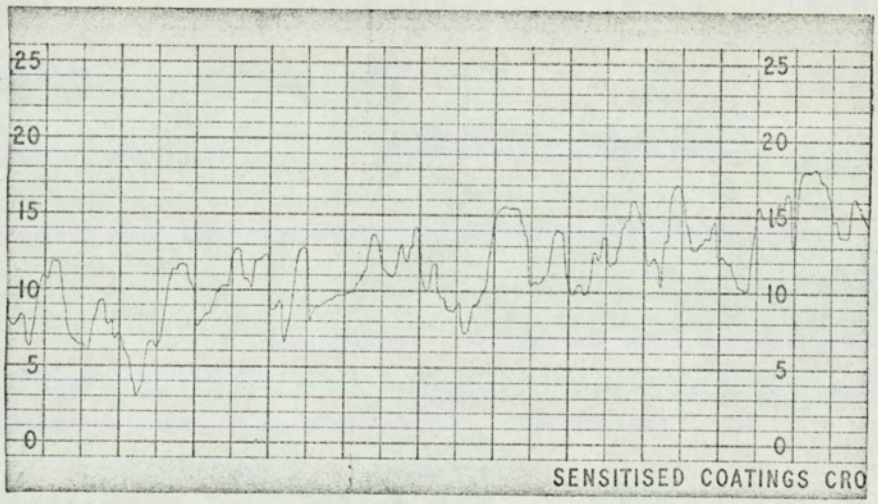

Non - oscillatory. 2 ft/min., 24.5% reduction.

Vertical x 5000, horizontal x 100.

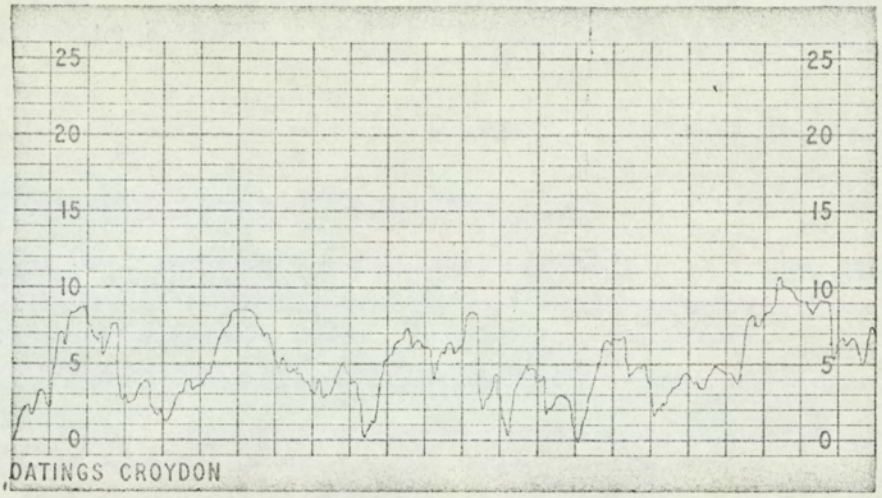

Inside surface. C. L. A. value = 0.920

Outside surface. C. L. A. value = 0.700

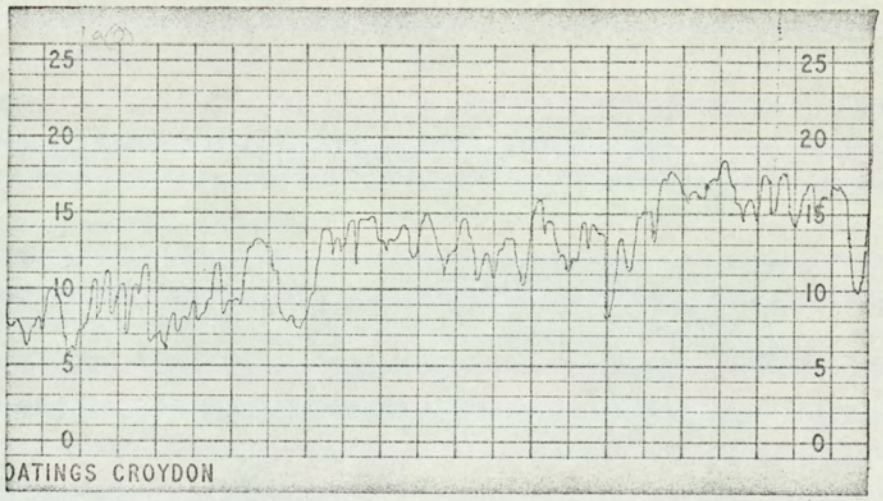

40 Hz., 5 x 10^{-3} in.p. t. p., 2 ft/min., 24.5% reduction.

Vertical x 5000, horizontal x 100.

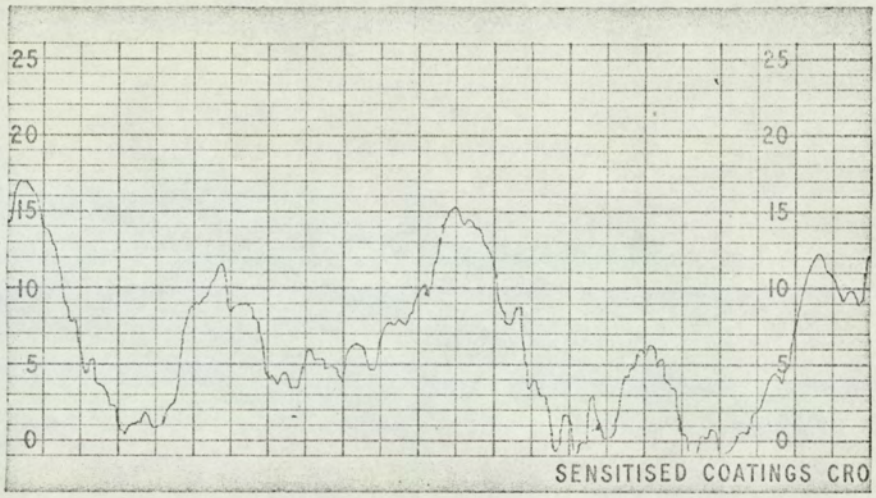

Inside surface. C. L. A. value = 1.100

Outside surface. C. L. A. value = 0.930

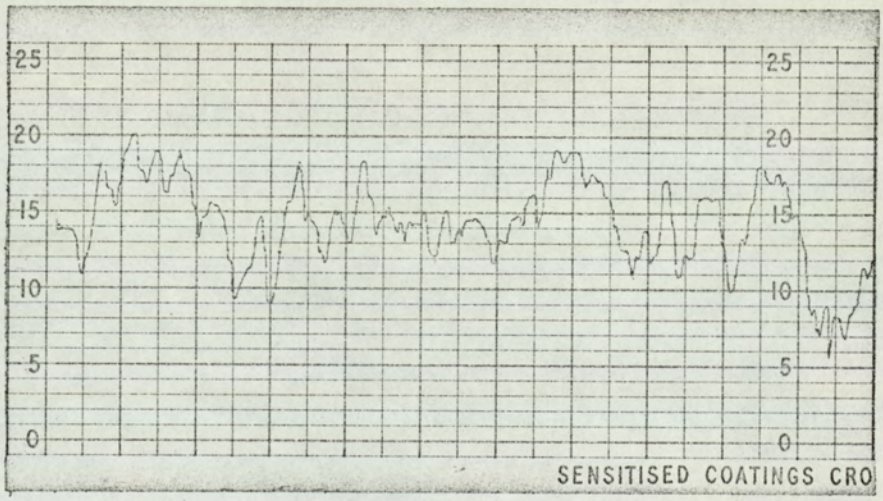

40 Hz., 10 x 10^{-3} in. p. t. p., 2 ft/min., 24.5% reduction.

Vertical x 5000, horizontal x 100.

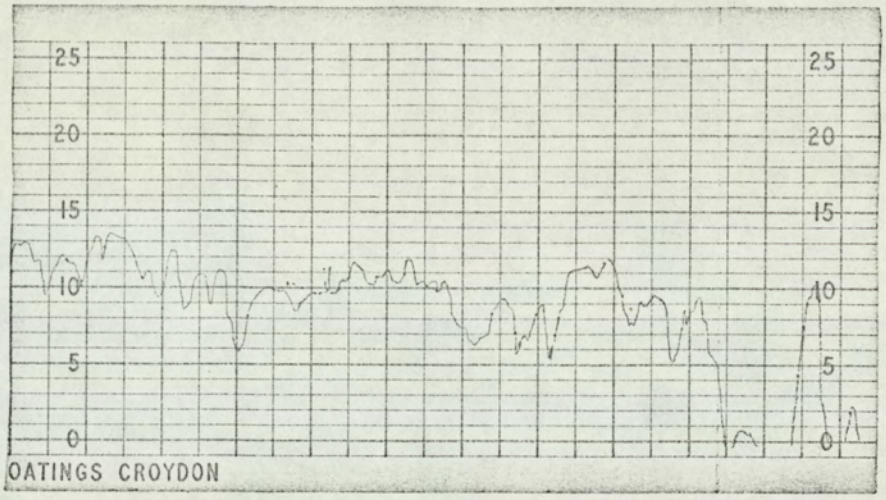

Inside surface. C. L. A. value = 1.000

Outside surface. C. L. A. value = 0.700

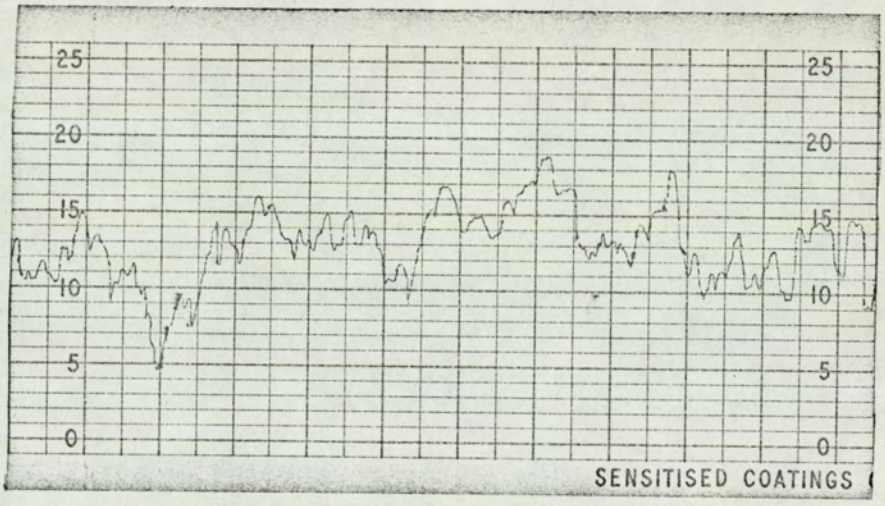

100 Hz., 5 x 10^{-3} in. p. t. p., 2 ft/min., 24.5% reduction.

Vertical x 5000, horizontal x 100.

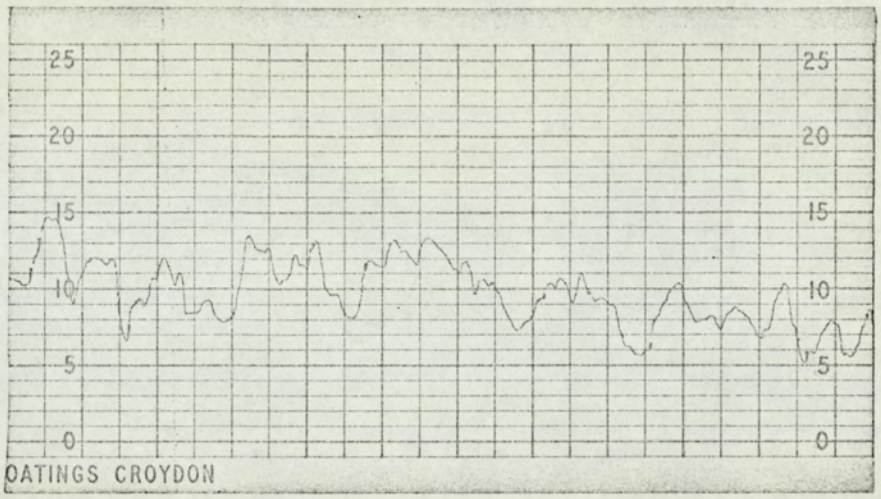

Inside surface. C. L. A. value = 0.600

Outside surface. C. L. A. value = 0.300

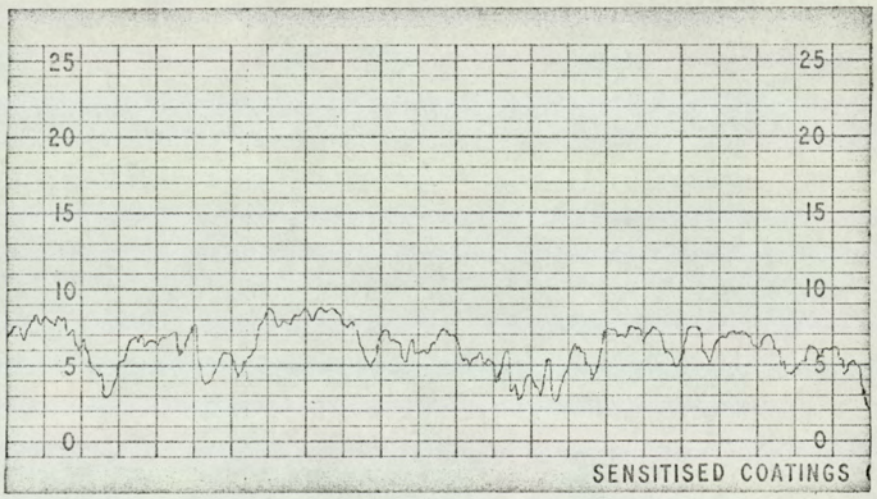

100 Hz., 10 x 10^{-3} in. p. t. p., 2 ft/min., 24.5% reduction.

Vertical x 5000, horizontal x 100.

C7. Discussion of Results

C7. Discussion of Results

In order to evaluate the results obtained from this investigation it is first necessary to restate the proposed mechanism for drawing force reduction by this technique.

The basic principle was to oscillate both the plug and the die in such a manner that, when drawing was taking place through the die, the motion of the plug bar relative to the die was such that the force applied by the plug to the deformation zone was diminished, thus reducing the force necessary for drawing.

The relationship between drawing force and plug force under these conditions was investigated theoretically, the results of which are shown in appendix 3. This shows that there is a linear relationship between the back tension applied by the plug and the corresponding drawing load. Thus the process is similar to wire-drawing with applied back tension. This relationship may be expressed thus:-

$$F_t = KF_p + F_{to} \qquad \text{---------- (1)}$$

where F_t = force in drawn tube.

F_p = plug force.

F_{to} = force in drawn tube for zero plug force. (frictionless over plug).

K = back pull factor.

The die load may be easily shown to have a similar relationship with plug load,

i.e. $F_d = F_{do} - CF_p$ ---------- (2)

where F_d = die load.

F_{do} = die load for zero plug force.

$C = I - K$

Thus it may be seen that the drawing force increases

and the die load decreases in proportion to an increase in plug force.

In view of the above observations the following features are to be expected in the experimental data corresponding to plug and die oscillations in anti-phase.

The maximum tensile force in the plug bar will occur when the tube slips over the plug in the direction of drawing. This will occur when the plug bar mount and die are at their furthest distance apart. Provided that the die pressure and the frictional conditions at this instant are identical to that experienced during non-oscillatory drawing, the force in the plug bar at this instant should be equal to the non-oscillatory plug bar force. Graphs 2 to 5, relating to 24·5% reduction of area, show that the maximum force in the plug bar is in fact slightly increased by oscillations. This is thought to be caused by sticking friction between the plug and the tube resulting from the intermittent nature of movement between these two members. This feature is also shown for the lower amplitudes in graph 6, (12·3% reduction in area). However, for the higher amplitudes the maximum plug bar force is progressively reduced, This is thought to be due to the lower values of minimum die load observed, constituting a reduction in the normal pressure on the plug and hence a reduced frictional constraint on relative movement.

The plug bar mount and die now move towards one another, releasing the tensile strain on the plug bar, and reducing the plug bar force. For a given plug bar stiffness and neglecting the movement of the tube relative to the tools, this reduction in plug bar force will be proportional to die and plug amplitude. This effect is clearly demonstrated.

When the die reaches its most backward position relative to the drum, the force in the drawn tube reaches a maximum and drawing occurs. However, from the above observations, the back tension applied by the plug at this instant is at a minimum, and less than its corresponding non-oscillatory value. Equation (2) shows that a reduction in plug bar load causes an increase in die load when drawing occurs. This increase is again clearly demonstrated in graphs (2) to (6). Graph (9) shows the relationship between plug and die load at this instant, and while considerable scatter is evident in the results there is a general trend towards higher die loads for reduced plug loads. In the case of wire drawing described in section B, it was possible to obtain experimentally the back-pull factor, and thus compare the relationship between die load and back tension during drawing under oscillatory and non-oscillatory drawing. Unfortunately in this instance this was not possible since drawing could not be conducted without back tension applied by the plug. Therefore it is not possible to assess the magnitude of any rise above the non-oscillatory drawing force which may occur.

Equation (1) predicts a reduction in drawing force proportional to the reduction in plug bar force described above. Again, the graphs clearly show this.

The reduction in drawing force and the increase in die load has been shown theoretically to be proportional to the reduction in plug bar load. Since generally the maximum plug bar load is constant, and the variation of plug bar load is proportional to die and plug amplitude, then the reduction in drawing force and increase in die load associated with this will be similarly proportional to amplitude. Again this is indicated in the experimental data.

Subsequent to this drawing period, the die moves towards the drum and drawing stops. Further motion of the die causes a release of the tensile stress in the drawn tube, the magnitude of which is again proportional to amplitude. Thus the reduced drawing force is the maximum load the tube sustains. This release of strain in the drawn tube is not clearly observed at 40 Hz. This is considered to be the result of the drum oscillating in phase with the die and with comparable amplitude, since this frequency is just below the natural frequency of the drum. Under these circumstances the drum motion tends to minimise the effects of die oscillation on the forces in the drawn tube.

During this period the die and the plug bar mount will move apart, increasing the tensile load in the plug bar up to its maximum value. This increase in plug bar force and decrease in force in the drawn tube, both proportional to amplitude, will result in a net decrease in the force on the die, again proportional to amplitude.

As in the case of wire-drawing, the above description of behaviour does not account for all the effects observed. It may be easily seen that for a given amplitude, the magnitude of cyclic stress, and hence the reduction of drawing force is greater at the higher frequencies. Again, this is considered to be due to the reduced relative movement between the tube and the tools per cycle under these circumstances. Since the response of the drum to the cyclic forces tends to confuse the effect of frequency on the process, it was again decided to consider the force variation in the plug bar, where the effects of drum oscillations are minimal. Graph (10) shows the relationship between computed and actual force variations in this member, the former value being obtained by assuming a fixed contact

between the plug, die and tube. As in the case of wire drawing, the slopes of these curves express the efficiency of coupling between the members. From these curves it may be seen that the coupling efficiency increases with increasing frequency, i.e. decreasing relative movement per cycle. Since this level of cyclic force variation in the plug bar dictates the minimum value of plug force, the effect of frequency will be similarly shown in reduction in drawing force, as shown in graph (11). Here it may be seen that the reduction in drawing force increases with increasing amplitude and frequency.

In order to obtain a quantitative understanding of the effects of frequency, an analysis of a similar nature to that conducted for wire drawing was attempted. However, no accurate predictions were possible since no data was available on the magnitude of the rise above the non-oscillatory drawing force, if indeed it existed in this case. The wire drawing analysis showed that this parameter was important in the analysis if accurate results were to be obtained. Similarly, the non-oscillatory back pull factor was unknown in this case. However, in view of the close similarity between the two processes and the results obtained from them, it may be concluded that the effect of frequency is qualitatively identical.

Graph (7) shows the results obtained when the die only is oscillated. Here the behaviour is similar to that relating to both tools oscillating, but twice the amplitude is required to achieve the same reduction in drawing load. Since all the oscillatory energy is put into the process at the die, this results in a greater cyclic force in the drawn tube.

The behaviour is modified, however, when only the plug bar is oscillated. In this case, the maximum force in the drawn tube does not occur when the plug bar force is a minimum. At this instant drawing occurs, but since there is no subsequent forward motion of the die to release the strain in the drawn tube, the force in that member is not released. Indeed, the motion of the drum increases the load in the drawn tube. The motion of the plug bar at this time causes a rise in the plug force, however, so drawing will not occur during this period, since the increase in plug bar force is well in excess of the increase in front tension in the drawn tube.

Thus the behaviour when one tool only is oscillated is similar to that observed in wire drawing, and in both cases the deformation does respond to the cyclic component of back tension.

Graph (1) shows the effects of phase angle between plug and die oscillations on the process, and it may be seen that the maximum reduction in minimum plug load is obtained for oscillation in antiphase, since in this case there is the greatest relative movement between the die and the plug bar mount. This is reflected in the reduction in drawing load in the drawn tube.

Before the start of this experimental programme, a theoretical investigation was conducted into the effects of plug and die oscillation on the tube drawing process (appendix 4). In this case it was assumed that the motion of both tools at the deformation zone was sinusoidal. The object of the analysis was to derive the optimum phase angle between die and plug oscillations, and the maximum drawing speed possible to achieve beneficial results. If the motion of the plug is purely sinusoidal then the force

on the plug bar is fixed in magnitude but alternating in sign, depending upon the direction of motion of the plug relative to the tube. The analysis showed those conditions under which the plug motion was such as to push the tube through the die throughout the whole of the period when the tube was drawn through the die. This drawing period was arrived at using the simple theory described in section B71(a).

However, it became clear during the initial stages of this investigation that this theoretical analysis was not strictly relevant to the process considered. Whilst the motion of the plug bar mount was sinusoidal, the elasticity of the plug bar allowed relative movement of the ends of the plug bar, resulting in a non-sinusoidal motion of the plug, thus making the analysis invalid.

If ultrasonic oscillations are employed, however, then sinusoidal motion of the plug may be achieved without difficulty, since the static stiffness of the plug bar is not important in this case. It is thought that under these circumstances the theory will be valid.

C8: Appendices

C81: Tensile test results for tube.

Stress - strain curves; light reduction tubes.

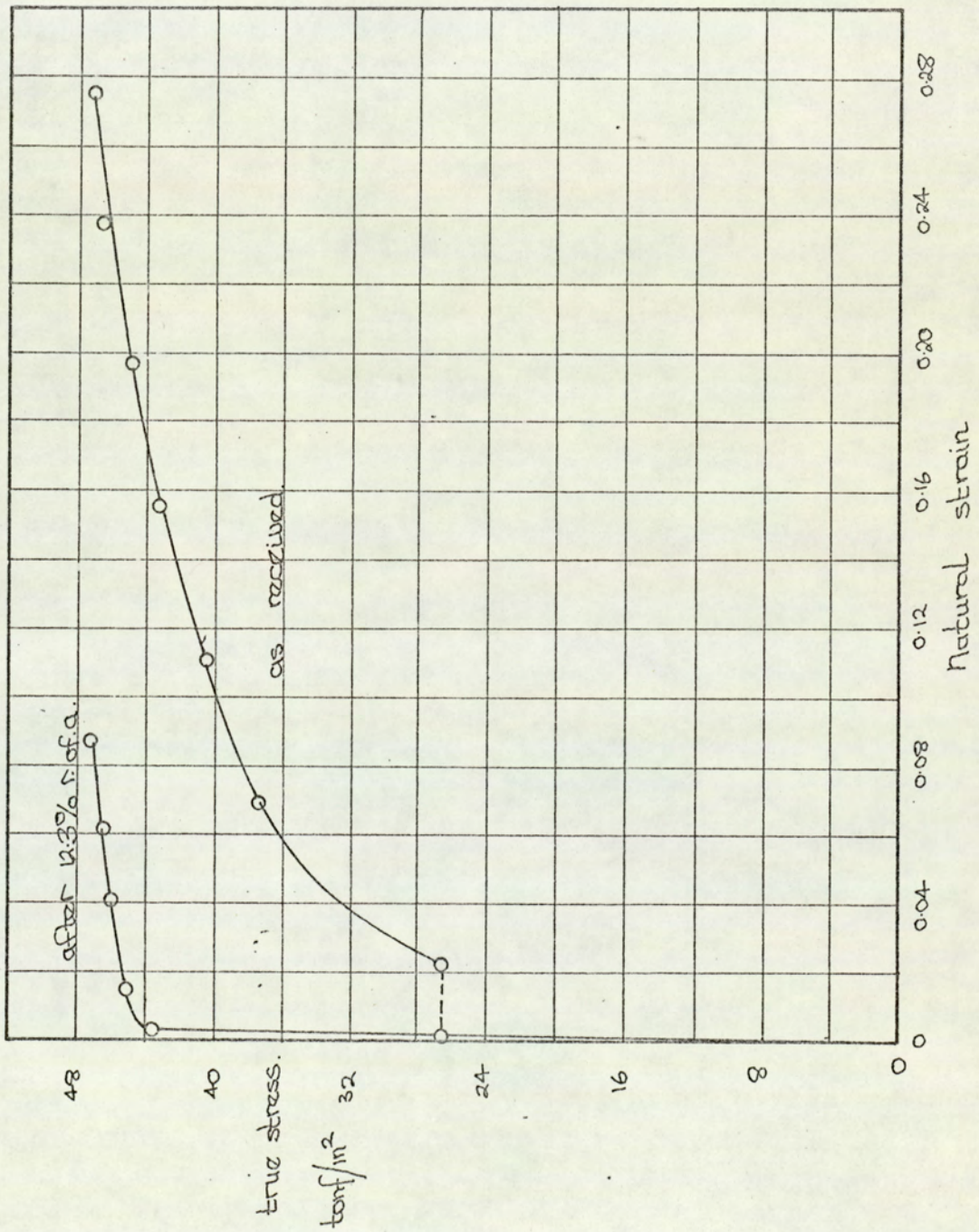

Stress - strain curves; medium reduction tubes.

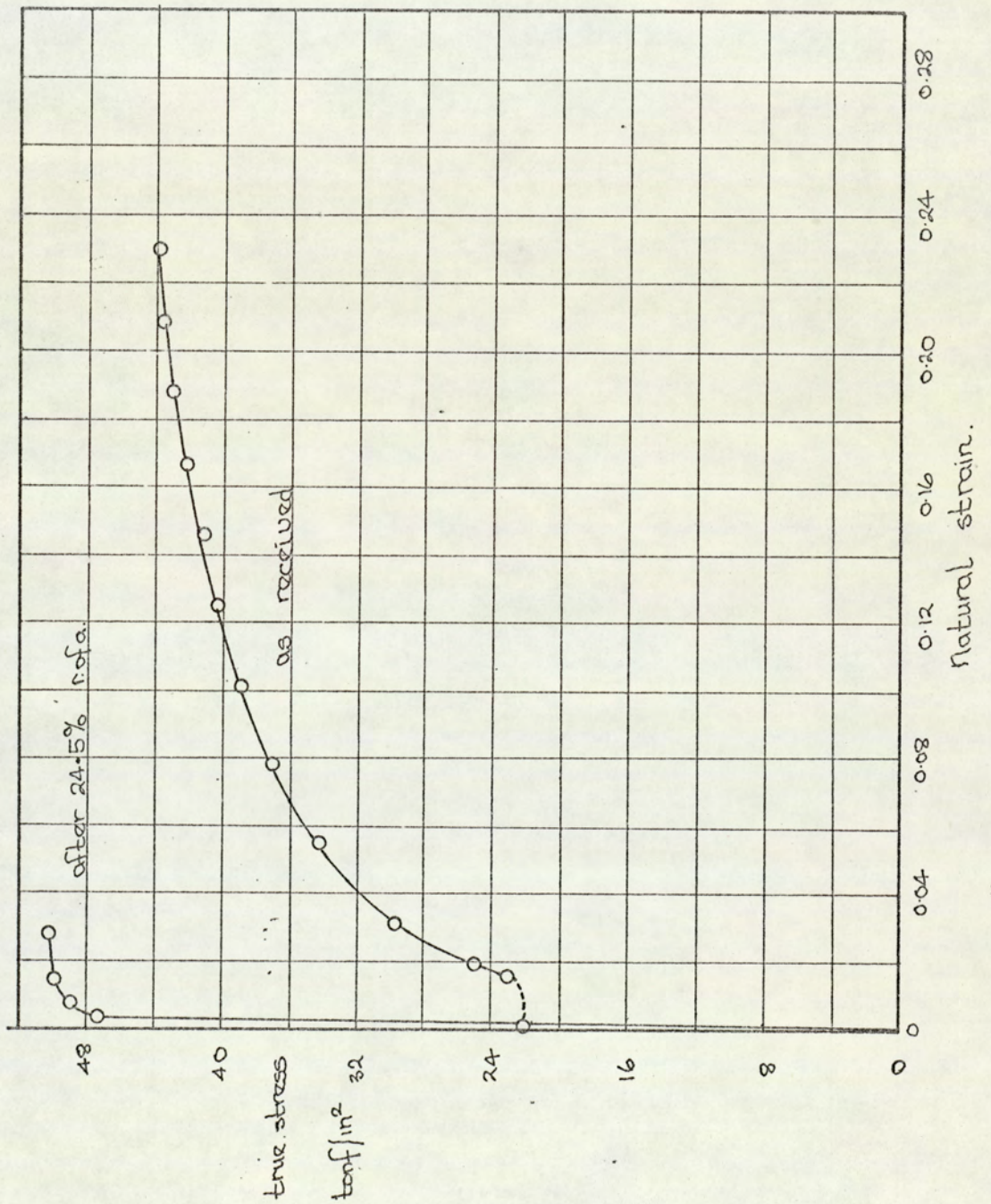

C82: Loadcell calibration curves.

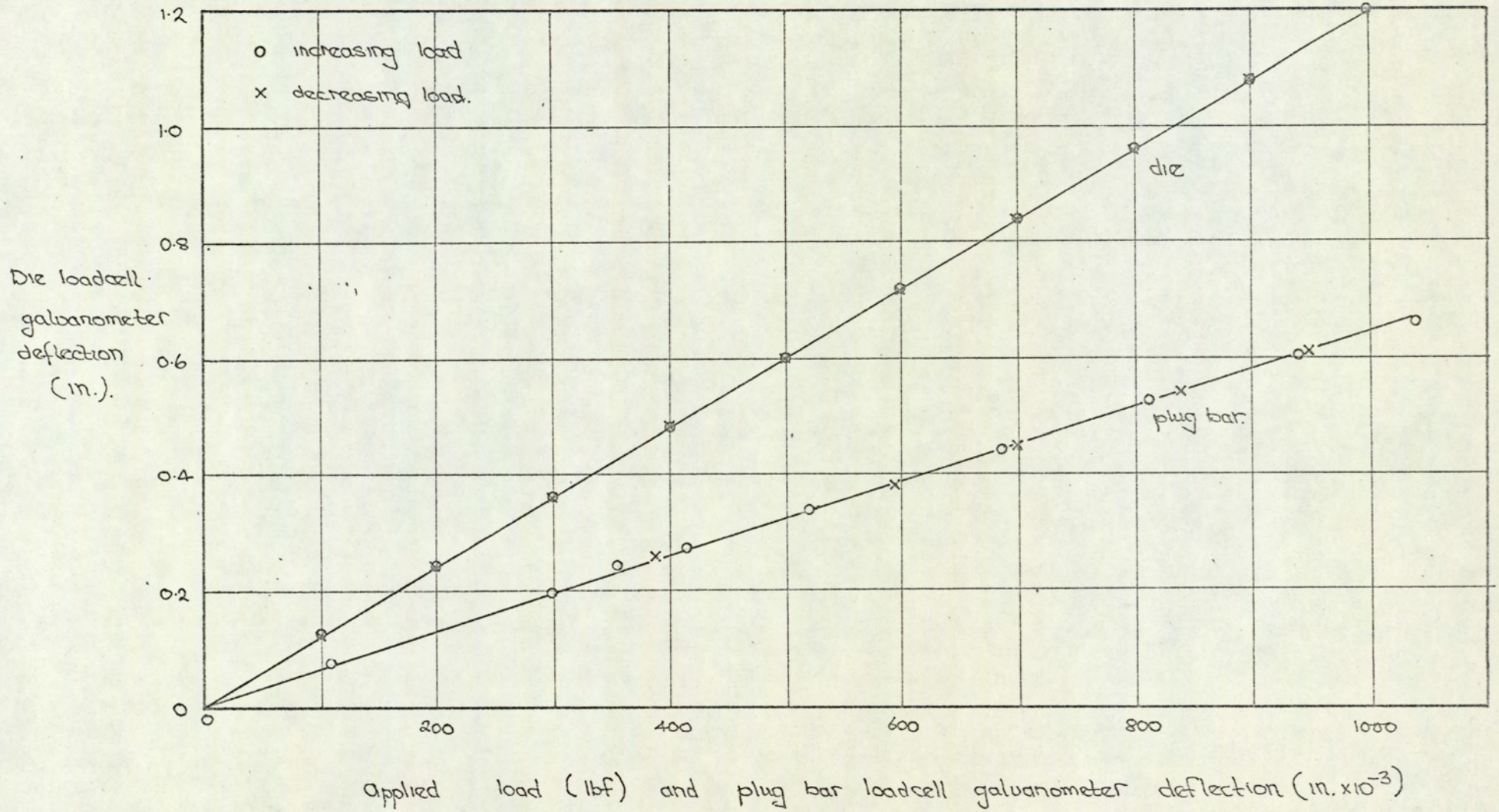
o increasing load
x decreasing load.
die
plug bar
Die loadcell galvanometer deflection (in.).
1·2
1·0
0·8
0·6
0·4
0·2
0
0
200
400
600
800
1000
Applied load (lbf) and plug bar loadcell galvanometer deflection (in. x10⁻³)

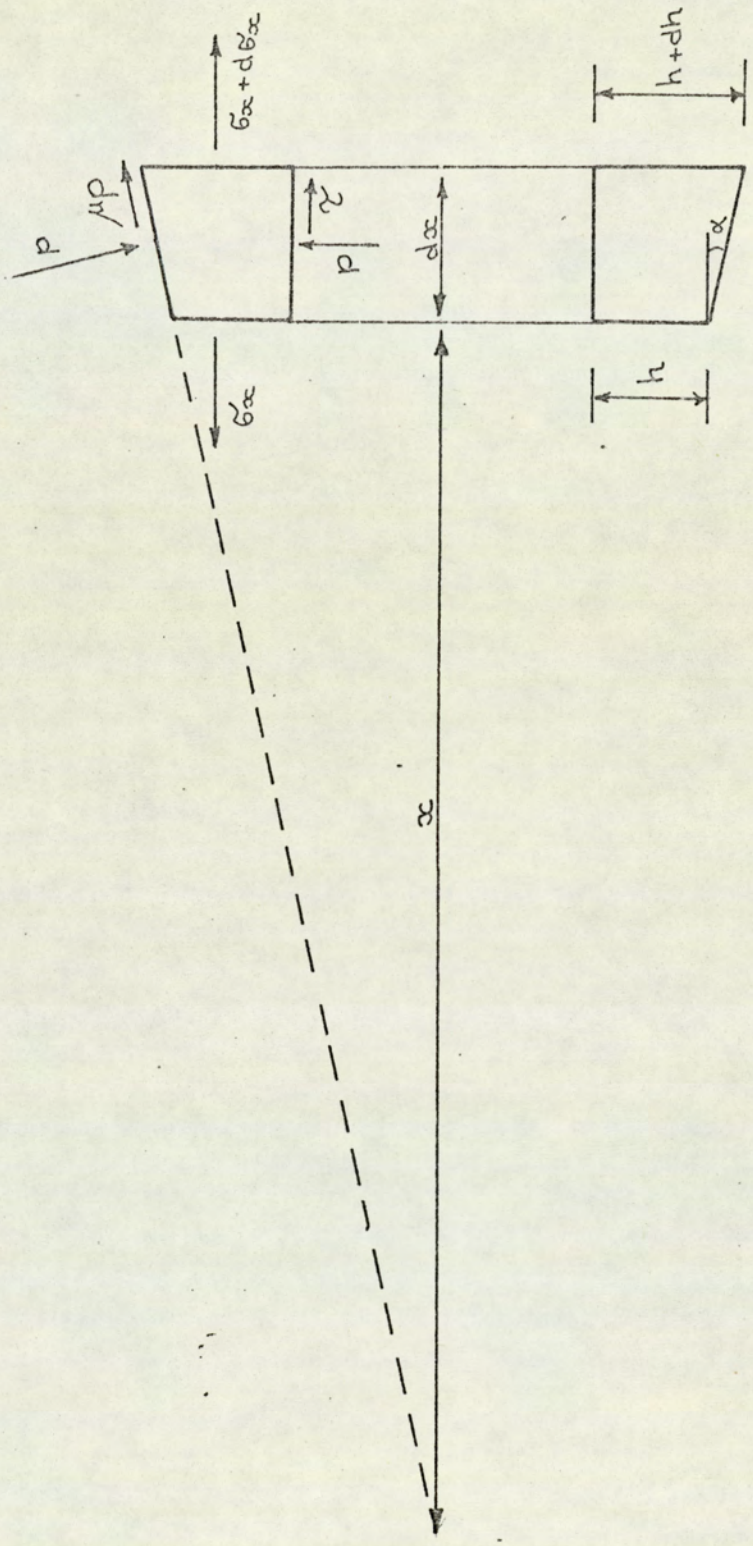

Forces acting on tube element in die. Figure 70.

C83: Determination of the back pull factor for tube drawing

(Based on the tube drawing theory of Hoffman and Sachs (107))

Assumptions

(1) There is no sink component in the reduction, i.e. close pass.

(2) The shear stress on the plug during drawing is constant over the whole contact surface.

(3) The deformation is plane-strain.

(4) The stresses normal to the tool surfaces and in the axial direction are principal stresses.

(5) The normal pressure on the tube in the deformation zone. is constant throughout its thickness at any normal plane.

(6) The axial stress in the tube is uniform across any cross-section.

(7) The thickness of the tube is small by comparison with its diameter.

Consider the equilibrium of the element shown in figure 70.

Resolving horizontally,

$$(\sigma_x + d\sigma_x)\pi D(h + dh) - \sigma_x \pi Dh + \pi Dp\tan\alpha dx + \pi D\mu p dx + \pi D\tau dx = 0$$

i.e. $$hd\sigma_x + \sigma_x dh + pdh + \mu p\frac{dh}{\tan\alpha} + \frac{\tau dh}{\tan\alpha} = 0 \qquad (1)$$

(neglecting second order terms and substituting $\frac{dh}{dx} = \tan\alpha$)

Now, from the Von Mises yield criterion,

$$p = \sigma_y - \sigma_x \quad \text{where } \sigma_y = 2y/\sqrt{3}$$

y = yield stress in uniaxial tension.

Substituting for p in (1) yields:-

$$hd\sigma_x + \left|\sigma_y(1+B) - B\sigma_x + \frac{\tau}{\tan\alpha}\right| dh = 0$$

i.e.

$$\frac{dh}{h} = \frac{d\sigma_x}{\left| B\sigma_x - (1+B)\sigma_y - \frac{\tau}{\tan\alpha} \right|}$$

Integrating yields.

$$\ln h = \frac{1}{B} \ln \left| B\sigma_x - (1+B)\sigma_y - \frac{\tau}{\tan\alpha} \right| + C$$

where C is the constant of integration.

Now, when $h = h_b$, $\sigma_x = \sigma_y$

Thus $\ln h_b = \frac{1}{B} \ln \left| -\sigma_y(1+B) - \frac{\tau}{\tan\alpha} \right| + C$

i.e. $C = \ln h_b - \frac{1}{B} \ln \left| -\sigma_y(1+B) - \frac{\tau}{\tan\alpha} \right|$

Thus $\ln \frac{h}{h_b} = \frac{1}{B} \ln \left| \frac{B\sigma_x - (1+B)\sigma_y - \tau/\tan\alpha}{-\sigma_y(1+B) - \tau/\tan\alpha} \right|$

$$\left(\frac{h}{h_b}\right)^B = \left| \frac{(1+B)\sigma_y + \tau/\tan\alpha - B\sigma_x}{(1+B)\sigma_y + \tau/\tan\alpha} \right|$$

$$\sigma_x = \frac{1}{B} \left| (1+B)\sigma_y + \frac{\tau}{\tan\alpha} \right| \left| 1 - \left(\frac{h}{h_b}\right)^B \right| \qquad - I$$

Thus the drawing stress may be obtained by substituting $h = h_a$ in equation I.

The relationship between the shear stress on the plug and the plug bar load, F_p, is as follows:

$$\frac{\tau(h_b - h_a)\pi D_p}{\tan\alpha} = F_p$$

where D_p is the plug diameter.

Furthermore the drawing force is related to the drawing stress thus:-

$$\sigma_x \pi b_a h_a = F_t$$

F_t = the force in the drawn tube

Substituting in equation I:-

$$\frac{F_t}{\pi D_a h_a} = \frac{1}{B} \left| (1+B)\sigma_y + \frac{F_p}{(h_b - h_a)\pi Dp} \right| \left| 1 - \left(\frac{h_a}{h_a}\right)^B \right|$$

$$\text{i.e. } F_t = \pi D_a h_a \frac{(1+B)}{B} \sigma_y \left|1-\left(\frac{h_a}{h_b}\right)^B\right| + \frac{\pi D_a h_a}{B(h_b-h_a)\pi D_p} \left|1-\left(\frac{h_a}{h_b}\right)^B\right| F_p \quad \text{- II}$$

which is of the form $F_t = F_{to} + kF_p$

F_{to} is the drawing force for zero shear stress on the tube bore (i.e. frictionless in bore)

k is the back pull factor for the plug

$$k \doteq \frac{1}{B\left|\left(\frac{h_b}{h_a}\right) - 1\right|} \left|1-\left(\frac{h_a}{h_b}\right)^B\right| \quad \text{- III}$$

C84: Theoretical study

Prior to the initation of the experimental programme, a theoretical study was conducted to determine the effect of the parameters on the forces during drawing.

Symbols

X_1 die amplitude

X_2 plug amplitude

ω angular frequency

V drum velocity

η X_2/X_1

t time

x instantaneous displacement

Suffices

1 die

2 tube at die

3 drum

4 plug

Assumptions

(1) Infinitely stiff drawing machine (V constant with time).

(2) No slipping of the drawn tube on the drum.

(3) The drawing force is constant during the drawing period.

(4) Inertia forces in the tube are negligible.

(5) A parallel plug is used, therefore only friction forces are experienced by the plug bar.

It is taken that the die has a $\frac{\pi}{2}$ phase lag relative to the plug, and at t = 0 is at its maximum distance from the drum, and drawing is taking place

i.e. $x_1 = - X_1 \cos \omega t$ (1)

$x_4 = x_2 \sin \omega t$ (2)

These conditions are adopted since when the die is at its most backward position, and hence the tube is being drawn, the plug has its maximum forward velocity, and is therefore in the most favourable situation to push the tube through the die.

Drawing will stop when the velocity of the tube relative to the die is zero. Now since drawing occurs under constant load there will be no relative movement of the ends of the tube during this period.

i.e. $\dot{x}_2 = \dot{x}_3 = V$ (3)

Now, drawing stops when $\dot{x}_2 = \dot{x}_1$, at $t = t_1$, say.

$\therefore$ from above,

$$X_1\omega \sin \omega t_1 = V$$

$$\omega t_1 = \sin^{-1} \frac{V}{X_1\omega} = \phi \text{ say} \qquad (4)$$

$$0 \leqslant \phi \leqslant \pi/2$$

For drawing to have stopped at the reduced load, the plug must be moving forward relative to the tube at this time, i.e. $\dot{x}_4 > \dot{x}_2$. The limiting condition for the cessation of drawing under reduced load is therefore expressed by

$$\dot{x}_4 = \dot{x}_2$$

i.e. $X_2\omega\cos \omega t_1 = V$ (from (2), (3))

$$\cos\phi = \frac{V}{nX_1\omega} \qquad \text{(from (4))}$$

$$= \frac{1}{n} \sin\phi$$

$$\underline{\text{i.e. } n = \tan \phi} \qquad \text{I}$$

Thus the minimum value of the ratio of plug to die amplitudes necessary to ensure that the drawing force is at its reduced value when drawing stops, is tan ϕ when $\phi = \sin^{-1}V/X_1\omega$

For $t > t_1$ drawing has stopped, and the drawn tube is elastically off-loaded by the forward motion of the die relative to the drum. If δ is the relative compression of the drawn tube,

$$\delta = \left[x_2 - x_3\right]_{t_1}^{t} = \int_{t_1}^{t} \dot{x}_{2-3}\, dt$$

Now, since drawing has stopped, the tube at the die will follow the die

i.e. $\dot{x}_2 = \dot{x}_1$

Also $\dot{x}_3 = V$

$\therefore$ $\delta = \int_{t_1}^{t} (X_1\omega \sin \omega t - V)\, dt$

i.e. $\delta = X_1(\cos \omega t_1 - \cos \omega t) + V(t_1 - t)$ (5)

The relative compression of the drawn tube, δ, is a maximum when $d\delta/dt = 0$ at $t = t_2$, say.

i.e. when $X_1\omega \sin \omega t_2 = V$

$$\omega t_2 = \sin^{-1} \frac{V}{X_1\omega} = \Psi, \text{ say.}$$

Now, from equation (4), $\omega t_1 = \sin^{-1} \frac{V}{X_1\omega} = \phi$, and since $\omega t_1 \neq \omega t_2$, $\phi \neq \Psi$, then:-

$$\Psi = \pi - \phi \quad \text{--------} \quad (7)$$

Thus, substituting equation (7) in (5) will give the magnitude of the maximum relative compression of the drawn tube.

$$\hat{\delta} = X_1(\cos \omega t_1 - \cos \omega t_2) + V(t_1 - t_2)$$

$$= 2X_1 \cos\phi - \frac{V}{\omega}(\pi - 2\phi)$$

i.e. $\frac{\hat{\delta}}{2X_1} = \left[\cos\phi - \sin\phi \left(\frac{\pi}{2} - \phi\right)\right]$ II

The function expressed in equation II is identical to that derived for the relative compression of the drawn wire in single die wire-drawing, and is calculated and plotted on figure 26.

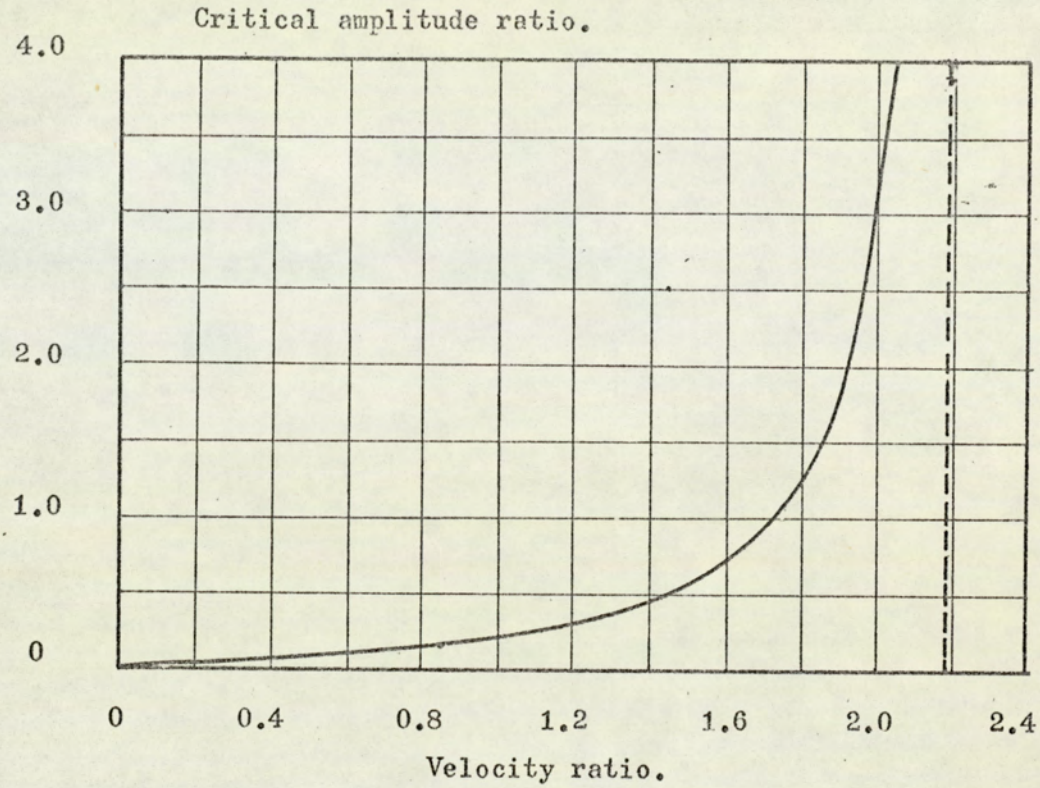

$V/X_1\omega$	n
0.000	0.000
0.025	0.029
0.050	0.069
0.075	0.125
0.100	0.207
0.125	0.337
0.150	0.569
0.175	1.081
0.200	3.090

Critical amplitude ratio versus velocity ratio; fixed phase.

Figure 71.

Drawing is taken to start again at $t = t_3$.

This will occur when the force in the drawn tube reaches the current value of drawing force. If this force is again the reduced value, then drawing will start when the relative compression in the tube is again zero. Thus t_3 is given by substituion in equation (5).

$$X_1 (\cos\omega t_1 - \cos\omega t_3) + V(t_1 - t_3) = 0 \qquad (8)$$

If drawing is to start at the reduced load, then the velocity of the plug must again exceed the velocity of the tube, or in the limit they must by equal.

i.e. $\dot{x}_4 = \dot{x}_2$

or $X_2\omega \cos \omega t_3 = V$

$$\cos \omega t_3 = \frac{V}{nX_1\omega} = \frac{1}{n} \sin\phi \qquad \text{(from (4))}$$

Since $t_3 \neq t_1$,

$$\omega t_3 = 2\pi - \cos^{-1} \frac{\sin\phi}{n} \qquad \text{---------} \qquad (9)$$

$$(0 \leqslant \cos^{-1} \frac{\sin\phi}{n} \leqslant \frac{\pi}{2})$$

Substituting in (8) for t_1 and t_3 from (4) and (9) gives:-

$$X_1\cos\phi - \frac{X_1}{n} \sin\phi + \frac{V\phi}{\omega} - \frac{V}{\omega} (2\pi - \cos^{-1} \frac{\sin\phi}{n}) = 0$$

Dividing through by X_1, substituting $\sin\phi$ for $V/X_1\omega$, equation (4), yields,

$$\frac{1}{n} = \cos\phi - 2\pi + \phi + \cos^{-1} \frac{\sin\phi}{n} \qquad \text{III}$$

Equation III shows the minimum value of the ratio of plug to die amplitude for drawing to start at the reduced load, for a given value of ϕ and hence drum to die velocity ratio. The solution for n was obtained by iteration, the results of which are shown on figure (71).

There are two equations expressing the minimum value of amplitude ratio, one for drawing to stop at the reduced load, equation I, and one for drawing to start at the reduced load, equation III. If both of these conditions are satisfied then drawing will be conducted throughout at the reduced load. Since the minimum values of n expressed by equation III are higher than those for equation I, it is only necessary to satisfy the former for the process to be effective.

There will be a maximum value of drum to die velocity ratio, above which no reduction in load can be achieved. This corresponds to the condition where drawing starts when the plug velocity passes through zero, thus requiring an infinite plug amplitude for drawing to start at the reduced load. Thus drawing starts when:-

$$\omega t_3 = \frac{3\pi}{2}$$

Now drawing starts when:-

$$X_1 \cos\phi + \frac{V\phi}{\omega} = X_1 \cos \omega t_3 + V t_3 \quad \text{(from (8))}$$

$$\text{i.e. } X_1 \cos\hat{\phi} + \frac{V\hat{\phi}}{\omega} = X_1 \cos \frac{3\pi}{2} + \frac{V}{\omega}\cdot\frac{3\pi}{2}$$

$$\text{Thus} \quad \text{Cot } \hat{\phi} = \frac{3\pi}{2} - \hat{\phi} \qquad \text{IV}$$

The solution of this equation was obtained graphically and is:-

$$\sin\hat{\phi} = \left|\frac{V}{X_1\omega}\right|_{max} = 0{\cdot}2196$$

Thus, for a velocity ratio of drum to die of 0·2196 it is necessary to have a plug amplitude of infinity to ensure that drawing occurs at the reduced load throughout. Therefore, for velocity ratios in excess of this figure, drawing cannot by conducted at the reduced load throughout the whole drawing period.

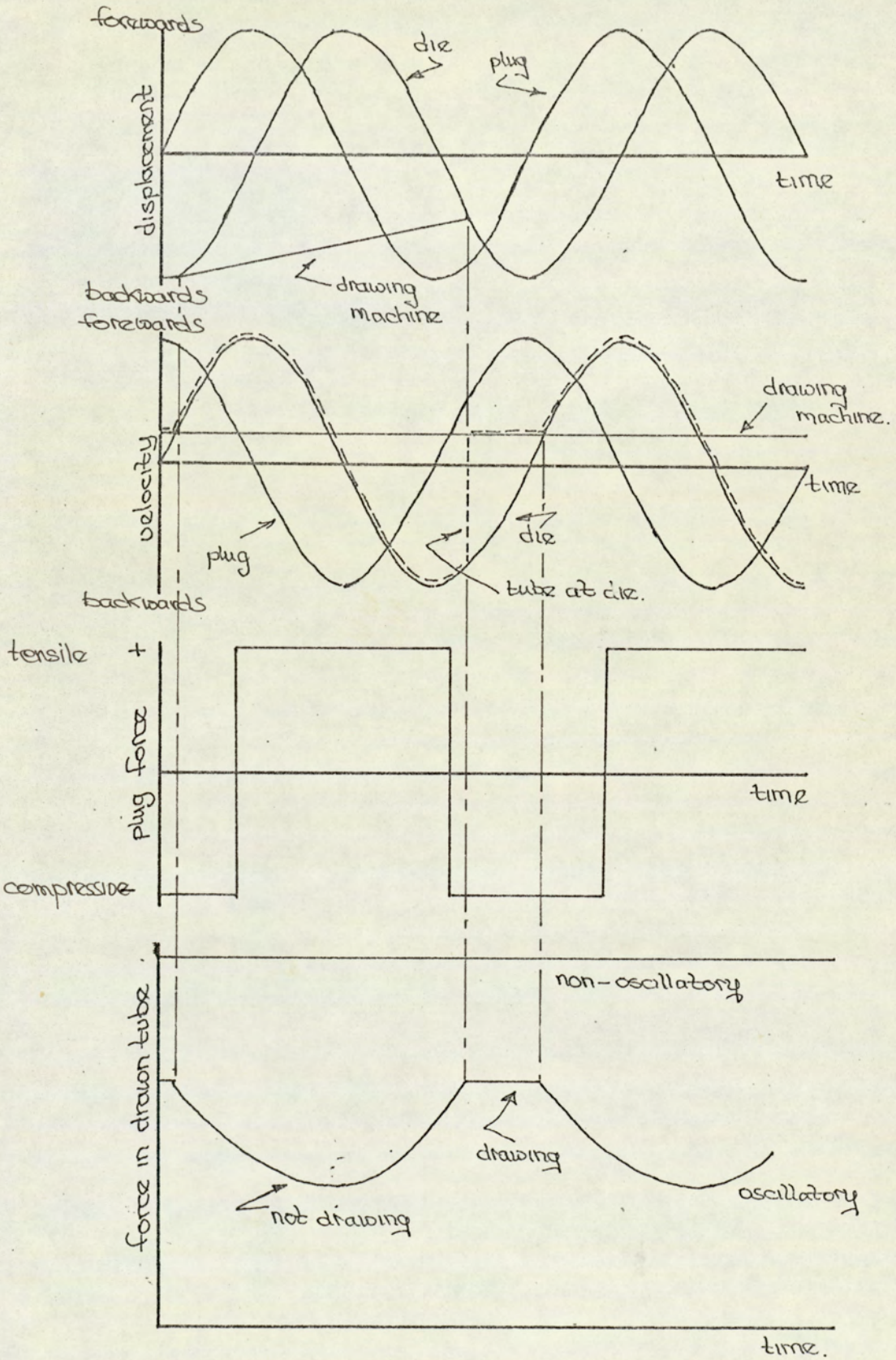

Graphical representation of oscillatory tube drawing: fixed phase.

Figure 72.

This analysis has derived the necessary requirements for drawing to occur when the velocity of the plug exceeds the velocity of the tube at the die. Under these conditions, the plug will push the tube through the die, rather than restrain its motion as in conventional drawing. The relationship between drawing load and plug force is not readily obtainable, but this process will reduce the drawing force by an amount depending upon this relationship, and the magnitudes of the conventional and reversed motion plug forces.

The analysis shows that for a ratio of drawing speed to peak die velocity less than 0·2196, this reduction in drawing force can be achieved, provided that the plug has an amplitude in excess of a critical value, expressed by equation III. If these conditions are satisfied, then the variations of displacements, velocities, and forces with time are of the form shown in figure 72.

One modification to the process which offers a greater potential is to have a variable phase relationship between die and plug oscillations. The purpose of this is to place the period of reversed plug motion symmetrically about the drawing period. If this is achieved, the critical value of amplitude ratio, and hence plug amplitude may be reduced, or the drawing velocity may be increased. Under these conditions the critical value of n is the same for starting and stopping drawing, and the phase relationship adopted is the optimum. This phase relationship is now derived.

Using the same nomenclature and procedure as before:-

$$x_1 = -X_1 \cos\omega t \qquad (10) \text{ (see (1) \& (2))}$$

$$x_4 = X_2 \sin(\omega t + \theta) \qquad (11)$$

Drawing stops at $t = t_1$, where,

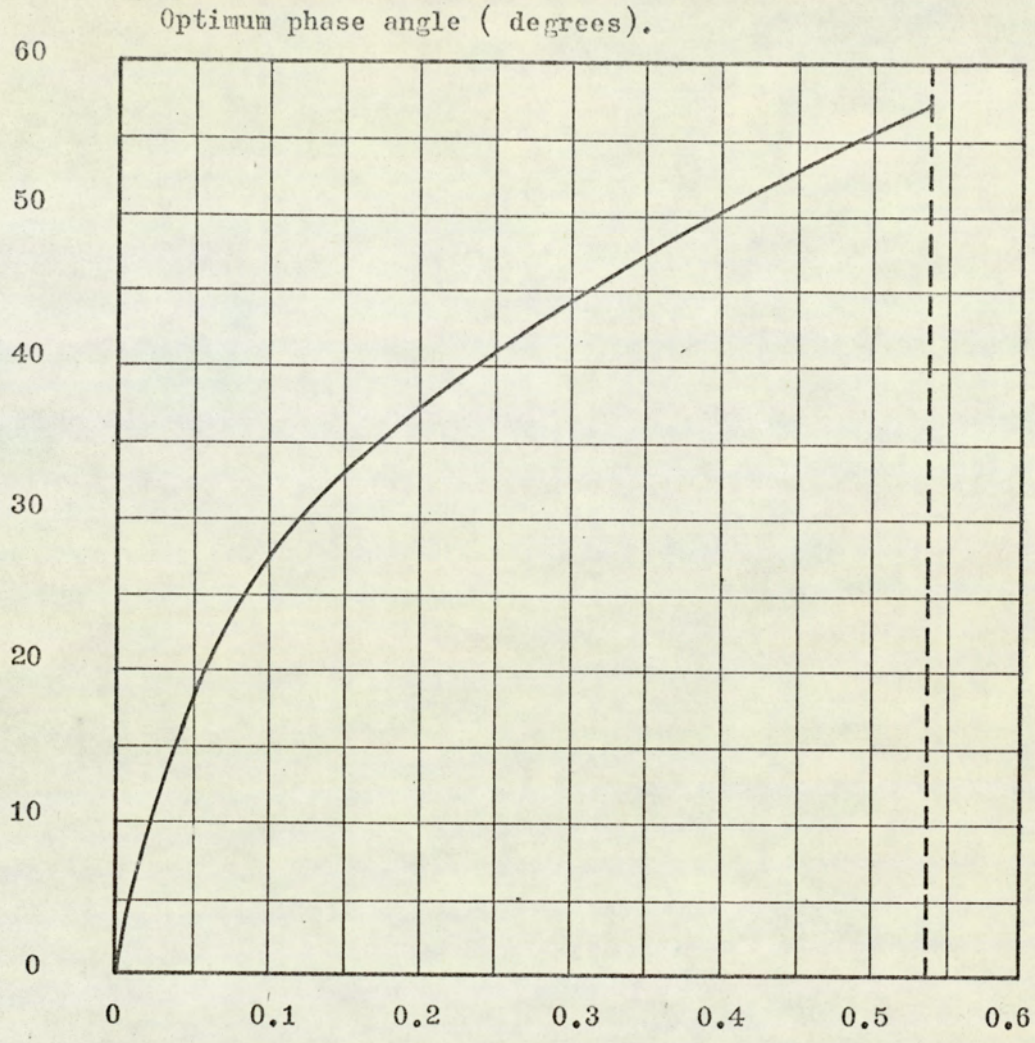

$V/X_1\omega$	θ
0.000	0° 0'
0.100	27° 40
0.200	37° 22
0.300	44° 28
0.400	50° 22
0.500	55° 40
0.537	57° 30

Optimum phase angle versus velocity ratio.

Figure 73.

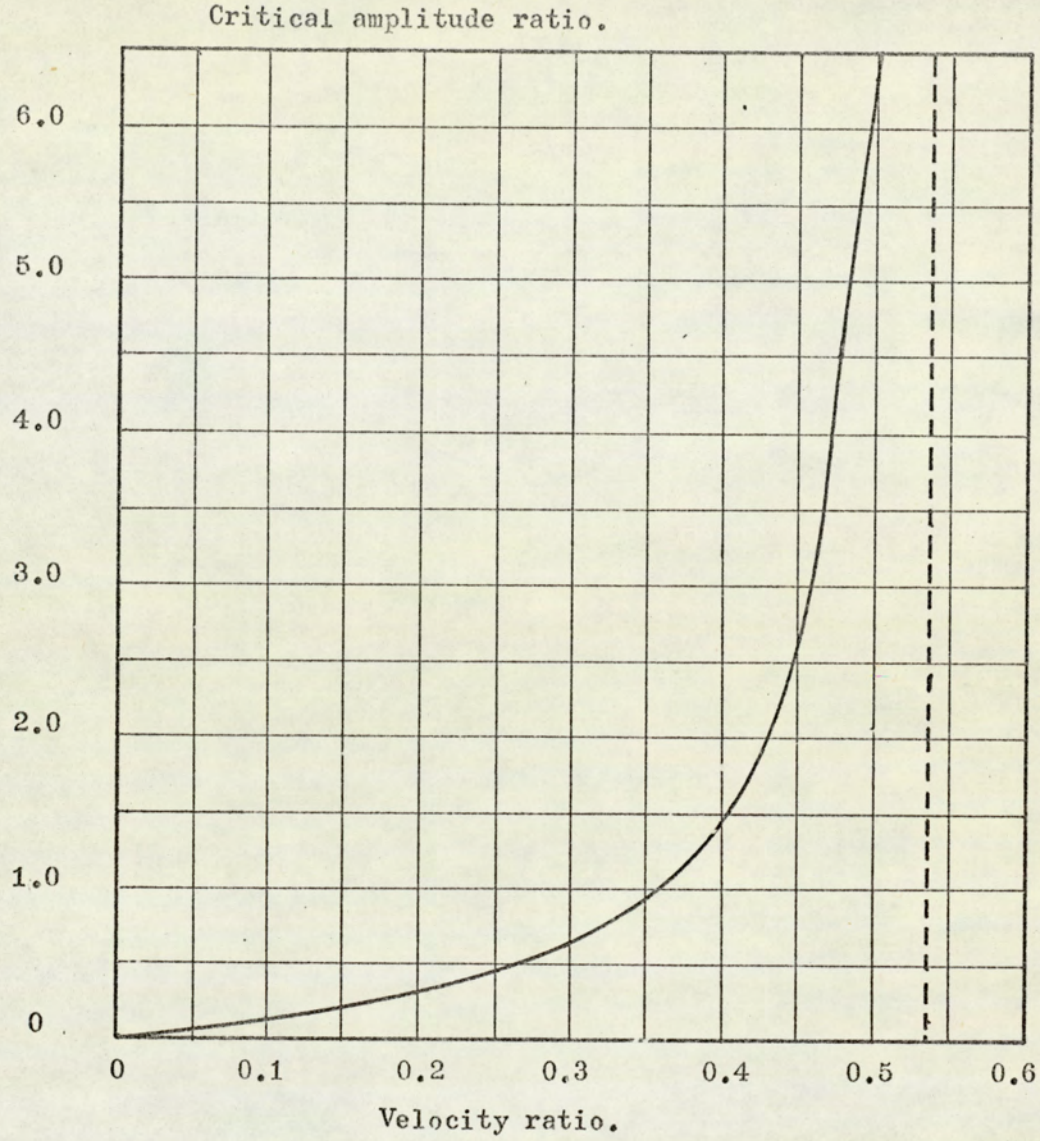

$V/X_1\omega$	n
0.000	0.000
0.100	0.119
0.200	0.303
0.300	0.636
0.400	1.438
0.500	6.320
0.537	∞

Critical amplitude ratio versus velocity ratio for optimum phase.

Figure 74.

$$X_1 \omega \sin \omega t_1 = V \qquad \text{(see (4))}$$

$$\omega t_1 = \sin^{-1} \frac{V}{X_1 \omega} = \phi, \text{ say} \qquad (12)$$

The critical value of n for drawing to stop at the reduced load is given by:

$$X_2 \omega \cos (\omega t_1 + \theta) = V \qquad \text{(see I)}$$

$$\cos(\omega t_1 + \theta) = \frac{\sin\phi}{n}$$

$$\text{i.e. } n = \frac{\sin\phi}{\cos(\phi + \theta)} \qquad (13)$$

Drawing starts at $t = t_3$ where,

$$X_1 \cos\phi + \frac{V\phi}{\omega} = X_1 \cos \omega t_3 + V t_3 \qquad \text{(see (8))} \quad (14)$$

The critical condition for drawing to start at reduced load is given by:-

$$(\omega t_3 + \theta) = 2\pi - \cos^{-1} \frac{\sin\phi}{n} \qquad \text{(see (9))}$$

Thus $\omega t_3 = 2\pi - \theta - \cos^{-1} \frac{\sin\phi}{n}$

Substituting for n from (13) gives:

$$\left.\begin{aligned} \omega t_3 &= 2\pi - 2\theta - \phi \\ \text{and } \cos\omega t_3 &= \cos(2\theta + \phi) \end{aligned}\right\} \qquad (15)$$

Substituting (15) in (14),

$$X_1 \cos\phi + \frac{V\phi}{\omega} = X_1 \cos(2\theta + \phi) + \frac{V}{\omega}(2\pi - 2\theta - \phi)$$

which simplified to:

$$\sin\theta \cot\phi + \cos\theta = \frac{\pi - \theta - \phi}{\sin\theta} \qquad (V)$$

The above equation expresses the relationship between the optimum phase angle θ, and the drum to die velocity ratio, $\sin\phi$. The solution of this equation was obtained graphically, the results of which are shown on figure (73). The corresponding values of the critical amplitude ratio were determined graphically from equation (13) and are shown on

figure (74).

In the case of a variable phase relationship there is similarly a maximum value of velocity ratio above which drawing cannot be achieved at the reduced load throughout the whole of the drawing period. This situation arises when the drawing period extends over one half-cycle, since this is the maximum length of time for which the plug velocity can be in excess of the drawing velocity, and corresponds to a necessary infinite plug amplitude.

Now drawing stops when $t = t_1$ where,

$$\omega t_1 = \phi = \sin^{-1} \frac{V}{X_1 \omega} \qquad (12)$$

and drawing starts when $t = t_3$ where,

$$X_1 \cos\phi + \frac{V\phi}{\omega} = X_1 \cos\ \omega t_3 + V t_3 \qquad (14)$$

In the critical condition, $\omega t_3 = \pi + \omega t_1 = \pi + \hat{\phi}$

Thus $$X_1 \cos\hat{\phi} + \frac{V\hat{\phi}}{\omega} = X_1 \cos\ (\pi = \hat{\phi}) + \frac{V}{\omega}\ (\pi + \hat{\phi})$$

$$2X_1\ \cos\hat{\phi} = \frac{V\pi}{\omega}$$

$$\cos\hat{\phi} = \frac{\pi}{2} \sin\hat{\phi}$$

$$\tan\hat{\phi} = \frac{2}{\pi}$$

giving $$\sin\hat{\phi} = \left|\frac{V}{X_1 \omega}\right|_{max} = 0{\cdot}5370 \qquad (VI)$$

The optimum phase angle at this critical condition can now be derived.

Drawing starts when $\omega t_3 = \hat{\phi} + \pi$

Drawing subsequently stops when $\omega t_1 = 2\pi + \hat{\phi}$

If drawing is occurring with the optimum phase relationship, then the velocity curve of the plug is symmetrically placed about the drawing period, and therefore the plug velocity has

its maximum value in the middle of the drawing period.

i.e. when $\omega t = \hat{\phi} + \frac{3\pi}{2}$

If the phase relationship was $\frac{\pi}{2}$, ($\theta = 0$), then $\omega t_1 = 2\pi$. Therefore, the phase angle under these conditions is given thus:-

$$\theta = 2\pi - \frac{3\pi}{2} - \hat{\phi}$$
$$= \frac{\pi}{2} - \tan^{-1} \frac{2}{\pi}$$

i.e. $\theta = 57^{\circ}\ 30'$ (VII)

This figure serves as a check on the validity of the derivation of the optimum phase angle given in equation V.

The above analysis shows that by setting the phase angle at its optimum level, the process becomes effective for higher values of drum to die velocity ratio. Thus, for a given frequency and die amplitude, the process will be effective for higher drawing speeds.

If a variable phase angle is employed, the physical system would be simplified if the phase angle and amplitude ratio could be set at the value corresponding to the operating drawing speed. However, if this is done there remains the question: is the process effective for lower values of velocity ratio, and hence ϕ, corresponding to the lower speeds encountered when drawing is initiated? Now, for lower values of ϕ, the optimum phase angle, θ, is reduced, and thus the drawing period occurs later. Thus, at lower values of ϕ, if n is reduced, the instant of friction reversal will coincide first with the instant of drawing stopping. This condition is said to be critical, since any further reduction of n will result in drawing at a higher load for some period.

It has been shown that drawing stops at $t = t_1$, where:

$$X_1 \omega \sin \omega t_1 = V$$

$$\omega t_1 = \sin^{-1}\frac{V}{X_1\omega} = \phi \qquad \text{(see equation (12))}$$

and the corresponding critical value of n is given by the condition that the plug velocity equals the drawing speed at that instant.

i.e. $X_2\omega\cos(\omega t_1+\theta) = V$

giving $$n = \frac{\sin\phi}{\cos(\phi+\theta)} \qquad \text{(see equation (13))}$$

If the phase angle, θ, and amplitude ratio n, are set at their requisite values for the operating value of ϕ, then for lower values of ϕ, the tube will still be drawn under reduced load, provided that the amplitude ratio, n, defined by the above equation, is always exceeded. This is so if the value of n defined above always decreased with decreasing ϕ, i.e. if $\frac{dn}{d\phi} > 0$ for the whole range of ϕ.

Now:

$$\frac{dn}{d\phi} = \frac{\cos(\phi+\theta)\cos\phi + \sin\phi\sin(\phi+\theta)}{\cos^2(\phi+\theta)}$$

$$= \frac{\cos\theta}{\cos^2(\phi+\theta)} \qquad \left[\begin{array}{l}\theta \text{ here is constant}\\ \text{at its set value.}\end{array}\right]$$

since $0 < \theta < 57^{\circ}30'$, $dn/d\phi > 0$,

and therefore the process is effective in the intermediate speed range. Thus it is only necessary to decide upon the magnitude of the operating value of velocity ratio, determine the optimum phase angle and minimum amplitude ratio and set them on the machine. During the period when the tube accelerates from rest up to the operating drawing speed, the tube will still be drawn at the reduced drawing force.

From the above analysis, if the plug and die in the tube

drawing process are oscillated sinusoidally, the following conclusions may be drawn.

(1) If the plug velocity exceeds the tube velocity throughout the whole of the drawing period, then the tube will be drawn under a reduced load, the magnitude of the reduction being dependent upon the conventional plug force, the reversal motion friction force on the plug, and the relationship between plug force and drawing force, all other variables being equal. Thus this reduction will be fixed in magnitude for given tube, lubricant, reduction and tooling.

(2) If the plug velocity exceeds the tube velocity for part of the drawing period only, then there will be no reduction in the peak tag load, since for the remainder of the drawing period, the plug force is in the conventional sense. Thus under these conditions no greater reductions of area are possible.

(3) When the plug displacement has a fixed phase lead of $\frac{\pi}{2}$ on the die, there is a maximum value of drawing speed to peak die velocity ratio of 0·2192, above which the plug velocity cannot exceed the tube velocity for the whole of the drawing period, and thus there will be no reduction in the peak tag load.

(4) For a fixed phase relationship, and for velocity ratios within the limit expressed above, for each velocity ratio there is a minimum value of the plug to die amplitude ratio, below which drawing will

not occur throughout the whole drawing period under the reduced load.

(5) If the phase angle may be varied to optimise the process, there is a maximum velocity ratio of 0·5370, above which tube may not be drawn under reduced load for the whole of the drawing period. The phase lead of the plug oscillations over the die corresponding to this maximum velocity ratio is $147^{\circ}30'$.

(6) For intermediate values of velocity ratio, there is an optimum phase relationship which minimises the minimum value of plug to die amplitude ratio necessary for drawing to be conducted at the reduced load throughout.

(7) If the phase angle is set at its optimum value corresponding to the operating value of velocity ratio, and the amplitude ratio is set above the corresponding minimum value for those conditions, the drawing will occur at the reduced load, both during the period of acceleration of the tube from rest, and during the period when the tube has settled down to its steady drawing speed.

In order to give some estimation of the degree of reduction of drawing force by this technique, the following assumptions may be made:-

(1) The 'back pull factor' for tube drawing is unity, i.e. there is a direct relationship between drawing force and plug load.

(2) The reversal motion friction force on the plug is equal in magnitude but opposite in sense to the non-oscillatory plug force.

(3) The plug load constitutes 30% of the total drawing load.

Under these assumptions, the process offers a 60% reduction in drawing load.

C85: Material compositions and properties

(a) Titanium 318 alloy

0·2% proof stress (min)	54 tonf/in^2
Tensile strength	58-75 tonf/in^2
Elongation (min)	8%
Young's modulus	15-17 x 10^6 lbf/in^2
Fatigue limit	55-60% of tensile strength

(b) HE15 aluminium alloy

Cu	3·8%
Mg	0·2%
Si	0·5%
Fe	0·7%
Mn	0·3%
Ni	0·2%
Zn	0·2%

(c) Tube composition and properties

C	0·45%
Mn	1·3%
Cr	0·25%
Bo	trace

Yield stress	27 tonf/in^2
Ultimate strength	38 tonf/in^2
Elongation	30%

PART D

D1. Conclusions

D1: Conclusions

The application of low frequency axial oscillations to the tools in wire and tube drawing causes the product to be drawn intermittently once every cycle. At these instances drawing occurs under a slightly higher load than that observed for steady state drawing under the same conditions. This increase in load is thought to be the result of sticking friction and a transient, non-equilibrium deformation pattern, due to the intermittency of drawing.

During the remainder of the cycle, the drawn product is elastically off-loaded and loaded by the forward and subsequent backward motion of the die relative to the drawing machine. The degree of off-loading is greater for higher die amplitudes and frequencies, and reduced for higher drawing speeds. When the frequency of oscillation is close to the natural frequency of the drawing machine, the response of this to the cyclic forcing must be taken into account when considering the degree of off-loading. This has the effect of reducing the degree of off-loading for frequencies close to and below the natural frequency of the machine, and increasing the off-loading for frequencies close to and above the natural frequency. Also the off-loading is increased if the amplitudes and frequencies adopted are such as to induce transverse oscillations in the drawn produce. Finally, the off-loading is increased if the drawing period is sufficiently long for the transient deformation to pass before the cessation of drawing. This condition corresponds to low frequencies and amplitudes and high drawing speeds. In the absence of the three modifying

influences outlined above, it is thought that intermittency of drawing will only be achieved when the peak velocity of the die exceeds the speed of drawing, since drawing may cease only when the die moves faster than the product.

In processes where a second tool serves to apply a back tension to the die, e.g. a second die in tandem drawing of wire or bar, or a fixed plug in tube drawing, then the intermittency of drawing produced by the oscillation of the die described above enables real reductions in drawing force to be realised. This is achieved since the backward motion of the die causes the tension in the drawn product to rise, and thus the product to be drawn further, and also the back tension applied by the second tool to fall due to the elastic member connecting the two tools. This elastic member is the intermediate wire in tandem wire drawing, and the plug bar in tube drawing. Thus drawing proceeds in the die with a reduced value of back tension and hence the drawing force is reduced. Half a cycle later on, the distribution of forces is reversed, and the product moves relative to the second tool. Thus the effect of oscillations is to alternate the relative movement from one tool to the other, such that the drawn product never experiences the force necessary to move the workpiece relative to both tools simultaneously.

The degree of reduction of force in the elastic member when drawing proceeds in the vibrated die, and hence the reduction in force in the drawn product, is increased for greater amplitudes and frequencies and stiffness of the member, and reduced for higher drawing speeds. This reduction in force may be enhanced by vibrating the other end of the elastic member in anti-phase with the vibrated die. This

has the effect of doubling the amplitude induced in that member. The greatest benefit is achieved when the amplitudes are sufficiently great to put the elastic member in compression, producing a negative back tension, and thus pushing the product through the die. This however is not universally possible to achieve since, if the member is slender, it may buckle and oscillate transversely and thus not sustain the compressive load.

If only the second tool is vibrated, this provides a cyclic back tension as before, but since the die is not oscillated the intermittent nature of drawing is not dictated independently, and thus the behaviour is modified. Drawing occurs in the die when the back tension is minimum, and thus at a reduced load. However, since there is no subsequent release of elastic strain in the drawn product by the forward motion of the die, the force in the product increases due to the coiling of the product on the drum. Drawing does not occur at this increased load, however, since there is a simultaneous increase of back tension. Thus oscillating the second die only is not so effective in reducing the peak load in the drawn product. Furthermore, at these low frequencies, the deformation of the product in the die does respond to the instantaneous value of back tension, and not the mean value as observed at ultrasonic frequencies. However, this difference in behaviour with frequency does not apply for a cyclic front tension, since for all frequencies investigated, the deformation responds to the instantaneous and not the mean force.

Finally, no change in the tensile strength of the product was observed when oscillations were applied, and generally the surface of the product was not changed. In the case of

wire drawing, oscillations produced a variation in the lubricant film thickness on the drawn product, but no marking of the wire surface was detected optically. In some cases tube drawn under oscillatory conditions exhibited ring markings in the bore. This effect was most marked at low frequencies and with sufficently large amplitudes to put the plug bar into compression during the cycle. However, no marking was detected at high frequencies or low amplitudes.

Industrial Implications

(a) Wire drawing:

Whilst the process of tandem drawing with oscillations does produce a reduction in the drawing force, and hence provides the opportunity for an increased reduction of area per pass, it is limited in the speed at which the wire may be drawn, since this must be less than the peak velocity of the dies for an effect to be achieved. Since wire is drawn commercially at very high speeds in relation to that achieved by currently available vibrator units, the process is thought inapplicable in this case.

However, in the case of bar drawing, the speeds are much lower, and may fall within the capacity of vibrator units. Furthermore, the stiffness of bar is high, and therefore only low amplitudes induced in the bar would be required to achieve the necessary cyclic variation in back tension, and therefore a reduction in drawing load. Thus, by applying oscillations, bar stock may be reduced with fewer passes.

(b) Tube Drawing:

Generally tube is drawn over a fixed plug at speeds

compatible with available vibrator units, and thus, in principle, oscillations may be applied with benefit to the process. However, for the process to be effective, a stiff plug bar is required to produce the necessary cyclic back tension, and with a high buckling load to minimise transverse oscillations of that member. These conditions are satisfied when drawing large diameter stock in short lengths.

Therefore, in conclusion, the process of low frequency oscillatory drawing may find application in the breaking down of large diameter stock in short lengths at low speed, where it offers the possibility of a reduction in the number of passes to achieve a given size.

D2: Suggestions for Further Work

D2: Suggestions for further work

Whilst the investigations conducted have indicated the basic mechanisms of the processes investigated, there remains several questions to be answered.

Insufficient time was available in this programme to conduct a rigorous investigation into the limiting effect of drawing speed. Whilst simple theoretical considerations indicate that no beneficial effect is achieved at drawing speeds in excess of the peak die velocity, experiment data shows that the behaviour departs from that predicted by simple theory due to such effects as drum oscillations, transverse oscillations of the wire, and the transient, non-equilibrium deformation produced by the intermittency of drawing. Thus there remains the question; what effect do these modifying influences have on the speed limitation to the process, do they increase or decrease the maximum speed at which drawing may be conducted with benefit?

No attempt was made to investigate the effect of reduction of area upon the process. Thus, in the case of wire drawing, what is the optimum distribution of work for each die, and what is the greatest overall reduction in area for the process? Also, theory indicates that the back-pull factor is a function of reduction of area, coefficient of friction, and die angle. Therefore, can the process be further optimised by the correct choice of lubricant and die geometry? In the case of tube drawing, investigations have shown that the process is most effective when the non-oscillatory plug bar load is high in proportion to the total drawing load. Therefore what is the effect of reduction of

area, coefficient of friction, and die angle upon the plug bar force and the back pull factor for the plug? How may these parameters be optimised, and what is the maximum reduction of area which may be achieved using oscillations?

These investigations have shown an essential difference between the effects of ultrasonic and low frequency vibrations. At ultrasonic frequencies the deformation only responds to the mean value of a cyclic back tension, but responds to its instantaneous value at low frequencies. Why does the deformation not respond to the instantaneous value of back tension at ultrasonic frequencies, and at what frequency does the transition occur?

Finally, it is suggested that a rigorous investigation be conducted into the fixed plug tube drawing process with oscillations applied to both plug and die at ultrasonic frequencies, and with a variable phase angle between the oscilllations. The purpose of this investigation should be to answer the following questions:-

(1) Is it possible to have two ultrasonic waveguides connected by a plastically deforming metal, that will resonate with a phase angle between the two oscillations applied to the deforming metal, or will they interact such that the phase relationship cannot be maintained?

(2) If both the die and the plug are oscillated, will the deformation respond to the instantaneous or mean value of back tension applied by the plug?

(3) Is it possible by the correct choice of phase angle to have the shear stress on the tube applied by the plug to act in the direction of drawing when drawing occurs, and thus push the tube through the die?

(4) What effects do the variables of amplitude, frequency, drawing speed and phase relationship have upon the peak and mean values of drawing load, and to what extent is the theoretical study described in section C84 valid?

Acknowledgements

The author wishes to express his gratitude to Dr. D.H. Sansome for his invaluable guidance and encouragement during the course of this investigation.

Thanks are also due to the following:-

Professor A.J. Ede, for his permission to carry out the investigation in the Department of Mechanical Engineering at the University of Aston in Birmingham.

Dr. C.E. Winsper, for his excellent investigation into single die wire drawing with low frequency oscillations, a direct result of which was this present investigation. Much of the equipment and techniques used in the investigation were evolved by him. Thanks are also due to Dr. Winsper for many helpful discussions during the course of this investigation.

Mr. E.W. Denchfield, Mr. H.F. Pratt, Mr. G.M. Jones and members of the departmental workshop for their help in the manufacture of the apparatus.

Mr. C. Bayliss, of Accles and Pollock, for the supply and treatment of tubing.

Dr. D. Rothman and Mr. M.J. Young, for many helpful discussions and finally,

Mrs. E.A. Csertan, for the typing of this thesis.

REFERENCES

REFERENCES

(1) Rosenfield, A.R. (Ed.) "The application of ultrasonic energy in the deformation of metals", Defence Metals Information Centre, Battelle Memorial Institute Colombus, Ohio, Rep. 187, Aug. 1963

(2) Winsper, C.E. & Sansome, D.H. "A review of the application of oscillatory energy to metals deforming plastically", Proc. 8th International machine tool design and research conference, p. 1349, Manchester 1967.

(3) Gentzsch, G. "Ultrasonic vibrations in deformation processes", Bänder Blech Rohre June 1968, p.354.

(4) Hansen, N. & Tries, H. "Metal forming using vibrations", Bänder Blech Rohre, Oct. 1968, p. 573.

(5) Blaha, F., & Langenecker, B. "Elongation of zinc mono-crystals under ultrasonic action", Die Naturwissenschaften, 1955, 42(20), 556.

(6) Blaha, F., & Langenecker, B. "Plasticity test on metal crystals in an ultrasonic field," Acta Metallurgica, 1959, 7, 93.

(7) Blaha, F., Langenecker, B., Oelschlagel, D. "Plastic behaviour of metals under ultrasonics", Zeitschrift für Metallkunde, 1960, 51, 636.

(8) Oelschlagel, D. "The deformation of zinc single crystals under the action of

ultrasonics", Zeitschrift für Metallkunde, 1962, 53, 361.

(9) Nevill, G.E. & Brotzen, F.R. "The effect of vibrations on the static yield strength of low-carbon steel", Proc. Am. Soc. for testing materials, 1957, 57, 751.

(10) Langenecker, B. "Effect of ultrasonic radiation on safety factors of rockets and missiles", A.I.A.A. Jnl., 1963, 1(1), 80.

(11) Langenecker, B. et al., "Effect of ultrasound on deformation characteristics of structural metals", NAVWEPS rep. 8482. NOTS TP3447. Naval Ordnance Test Station, China Lake, California.

(12) Langenecker, B. "Effect of ultrasound on deformation characteristics of metals", I.E.E.E. Trans., Sonics and Ultrasonics, 1966, SU-13, 1.

(13) Severdenko, V.P., & Klubovich, V.V., "Effect of ultrasonic oscillations on the process of extension of copper", Ul'trazvuka v Mashinostr, Nauka i Tekhnika, Minsk, 1964, p.3.

(14) Konovalov, Ye, G. "Osnovy Nouykh Spostov Metallabrab-rabotki", "Foundations of new metalworking techniques" (book), Akad, Nauk. B.S.S.R. Fiziko-Tekhnich. Institut. Minsk. 1961, pp 92, 150, 246. Abstract ref No. 1.

(15) Konovalov, Ye. G., et al. "Effect of ultrasonic vibrations on the mechanical properties of some metals and alloys", Ul' trazvuka v Mashinostr, Nauka i Tekhnika, Minsk, 1964, p.61.

(16) Konovalov, Ye. G., et al. "The influence of ultrasonic vibrations on the mechanical properties of metals under strain" Russian Engng. Jnl., 1965, 45(8), 31.

(17) Severdenko, V.P. Klubovich, V.V. & Elin, V.I. "Research into the elongation of copper at high temperatures in an ultrasonic field", Plastichn i Orbrabotka Metallov Davleniem, Nauka i Tekhnika, Minsk, 1966, p. 242.

(18) Skripnichenko, A.L. "Using ultrasound to test metals under tension", Industrial Labs., 1966, 32(8), 1188.

(19) Baker, G.S. & Carpenter, S.H., "Deformation under combined static and vibratory stresses", Trans. Met. Soc. of A.I.M.E., May, 1966, 236, 700.

(20) Pohlman, R. & Lehfeldt, E. "Influence of ultrasonic vibration on metallic friction," Ultrasonics, Oct. 1966, p 178.

(21) Friedrich, R., Kaiser, G. & Pechhold, W. "Effect of mechanical oscillations of the plastic behaviour of metals" Zeitschrift für Metallkunde, 1969, 60(5), 390.

(22) Langenecker, B. "Metal deformation in macrosonic fields", S.A.E. Trans., 1966, 74, 499.

(23) Langenecker, B. et al. "A critical look at ultrasonic metalworking processes", Tech. Rept. No. C6-26, 1, 1966.

(24) Fridman, H.D. and Levesque, P. "Reduction of static friction by sonic vibration", Jnl. Appl. Phys. Oct. 30, 1959, p 1572.

(25) Godfrey, D. "Vibration reduces metal to metal contact and an apparent reduction in friction" A.S.L.E. Trans., 1967, 10(2), 183.

(26) Balamuth, L. "Sonic press for forging, forming" American Machinist, 1965, 109(1), 116.

(27) Tolstoi, D.M. "Normal vibrations in contact friction" Wear, 1967, 10, 199.

(28) Lenkiewicz, W. "The sliding friction process - effect of external vibrations", 1969, 13, 99.

(29) Mitskevich, A.M. "Motion of a body over a vibrating surface", Soviet Physics - Acoustics, 1968, 13(3), 348.

(30) Nosel, V.V. and Rymsha, O.M. "Reducing the drawing forces by ultrasonic oscillations of the drawplate, and determination of the technological parameters of tube drawing", Stal (in English),

Feb. 1966, 2, 135.

(31) Schneider, G. "Theoretical and practical investigations of the influence of vibrations on friction", Schmierstoffe U. Schmierungskechnik 1969 (32), p. 43.

(32) Golubev, T.M., and Dyadechko, G.P., "On the problems of contact friction in the deformation zone during vibration drawing", Izv. V.U.Z., Chernaya Metall., 1965 (2), 99.

(33) Winsper, C.E., Dawson, G.R. and Sansome, D.H. "An introduction to the mechanics of oscillatory metalworking", Metals and Materials, April 1970, pp 158 - 162.

(34) Stankovic, P. "Principles of static-dynamic forging and some of its characteristics", Metal Treatment and Drop Forging, 1958, 25 (159), 489.

(35) Shestakov, S.N., Karnov, M. Ya., "Structure and properties of alloys and steels after vibrational working", Metallov. i Termich Obrabotka Metallov, 1958 (7), 35.

(36) Karnov, M. Ya., and Shestakov, S.N., "Vibroforging of aluminium alloys", Metallov. i Termich Obrabotka Metallov, 1959, (1), 57.

(37) Sogrishin, Yu. P., "Vibrational working of metal", Metallov. i Termich Obrabotka Metallov, 1959, (1), 55.

(38) Lysak, L.I., and Sogrishin, Yu. P. "Effect of method of plastic deformation on internal stresses in metal", Sborn. Nauch. rab. Inst. Metallofiz. Akad. Nauk. Ukr. (Kiev) SSR, 1959 (9), 22.

(39) Karnov, M. Ya., and Voronin, A.A., "Metal forming by vibration", Kuzneckno-Shtamp. Proizv. 1960, 2(3), 3.

(40) Karnov, M. Ya., "On the determination of the work of deformation under conditions of vibrational loading", Kuznechno-Shtamp. Proizv, 1961, (6), 21.

(41) Karnov, M. Ya., "Problems connected with the vibrational working of metals with restriction of width", Kuznechno-Shtamp. Proizv, 1961 (5), 16.

(42) Karnov, M. Ya., and Shchennikova, A.E. "Effect of vibrational working on the structure of metals", Metallov. i Termich Obrabotka Metallov, 1966, (4), 22.

(43) Polyakov, N.V., Mikhailov, N.V., and Rehbinder, P.A., "On the influence of vibration on the plastic deformation of metal", Doklady Akad. Nauk. S.S.S.R., 1966, 167(4), 873.

(44) Polyakov, N.V., and Mikhailov, N.V. "Study of the vibration assisted deformation of metals", Soviet Material Sci., 1966, 2(4), 346.

(45) Golubev, T.M., and Yavorovskii, V.N. "Distribution of plastic strain during vibrational upsetting with

plane parallel plates", Izvest V.U.Z. Chernaya Metall., 1967, (2), 69.

(46) Golubev, T.M., and Yarorovskii, V.N. "The influence of vibrational load on the distribution of plastic deformation during hot upsetting", "Izvest. V.U.Z. Chernaya. Metall., 1968, (8), 93.

(47) Zaleskii, V.I., and Volkov, I.P. "Upsetting with vibratory loading", Izvest. V.U.Z. Chernaya Metall., 1965, (4), 98.

(48) Lee, D., Sata, T., and Bakofen, W.A. "The reduction of compressive deformation resistance by cyclic loading", Jnl. Inst. Metals., 1964-65, 23, 416.

(49) Severdenko, V.P., and Klubovich, V.V. "Metal strain in an ultrasonic field" Doklady Akad. Nauk. B.S.S.R., 1961, 5, 15.

(50) Severdenko, V.P., and Klubovich, V.V. "Distribution of the deformation in the height of the specimen placed in an ultrasonic field", Izv. V.U.Z. Charnaya Metall., 1965, (1), 61.

(51) Severdenko, V.P., Klubovich, V.V., and Kharitonovich, M.V., "Investigation of the non-uniformity of deformation on upsetting with ultrasonics", Plasticichnost i Obrabotka Metallov Davleniem, Nauka i Tekhnika, Minsk, 1966, p 179.

(52) Severdenko, V.P., Klubovich, V.V., and Kharitonovich, M.V. "A study of the microhardness distribution throughout a test-piece deformed in an ultrasonic

field", 'Plastichnost i Obrabotka Metallov Davleniem Nauka i Tekhnika, Minsk, 1966, p.186.

(53) Severdenko, V.R., Klubovich, V.V., and Kharitonovich, "Residual stresses of the second kind in Armco iron worked in an ultrasonic field", Metallov. i Term. Obrabotka Metallov, 1966, (9), 11.

(54) Severdenko, V.P., and Labunov, V.A. "New system for applying vibrations in apparatus for the pressure treatment of metals with superimposed ultrasonic vibrations", Doklady Akad. Nauk. B.S.S.R., 1966, 10(8), 558.

(55) Zhadan, V.T. "Effect of ultrasonics in the upsetting of steels which are difficult to work", Izvest. V.U.Z. Chernaya Metall., 1966, (11) 93.

(56) Severdenko, V.P., and Petrenko, V.V. "The effect of ultrasonics on the resistance to deformation of steels", Izv. Akad. Nauk. B.S.S.R., 1968, (4), 12.

(57) Balamuth, L., "Ultrasonic motors fabricate metals and plastics, S.A.E. Jnl., 1966, 74 (6), 72.

(58) Kristoffy, I., "Metal forming with vibrating tools, Trans. A.S.M.E. Jnl. Eng. Ind., Nov. 1969, p 1168.

(59) Izumi, O., et al., "Effect of superimposed ultrasonic vibrations on the compressive deformation of metals", Japan Inst. of Metals; Trans., 1966, 7(3) 158.

(60) Severdenko, V.P., and Petrenko, V.V., "The temperature conditions during open die upsetting of steel in an ultrasonic field", Izv. Akad. Nauk. B.S.S.R., 1969, (1), 87.

(61) Severdenko, V.P., and Klubovich, V.V., "Drawing a copper wire in an ultrasonic field", Doklady Akad. Nauk. B.S.S.R., 1963, 7(2), 95.

(62) Boyd, C.A., and Maropis, N., "The application of ultrasonic energy in the deformation of metals", Defence Metals Information Centre, Batelle Memorial Inst., Columbus, Ohio, Rep. 187, Aug. 1963, Ed. A.R. Rosenfield.

(63) Robinson, A.T., et al., "Study of the application of ultrasonic energy to wire drawing of metals", U.S. Naval Ordnance Station, China Lake, California. Quarterly tech. progress reports, April 1963 to Sept. 1965.

(64) Robinson, A.T. "The application of ultrasonic energy to metal wire drawing", Wire and Wire Prods., 1964, 39(12), 1925.

(65) The Steel Co. of Canada File 780 Research and Development Dept. March 1965.

(66) Maropis, N., and Clement, J.C., "Transition between theory and practice in ultrasonic metal deformation processing", A.S.M. Tech. Rept.

No. C6-26, 3, 1966, A.S.M. Metals Park, Ohio.

(67) Jones, J.B., "Ultrasonic metal deformation processing", International conference on manufacturing technology, 1967, p. 983.

(68) Lehfeldt, E., "Wire drawing with superimposed ultrasonic vibrations", Wire, Aug. 1969, (102), 205.

(69) Winsper, C.E., and Sansome, D.H., "Fundamentals of ultrasonic wire drawing", Jnl. Inst. Metals, 1969, 97, 274.

(70) Winsper, C.E., and Sansome, D.H. "A study of the mechanics of wire drawing with superimposed ultrasonic stress", Proc. 10th Machine Tool Design and Research Conference, Manchester, Sept. 1969, p 553.

(71) Winsper, C.E. "An investigation of the mechanics of wire drawing with the superposition of an oscillatory drawing stress", Ph.D. Thesis, University of Aston, 1966.

(72) Solkowsky, T., and Vilain, A., "Wire drawing with vibrating stock", A.T.B. Metallurgie, 1968, 8(4), 145.

(73) Oelschlagel, D., and Weiss. B., "Improved efficiency in wire drawing with ultrasound", Trans. A.S.M. 1966, 59, 685.

(74) Vatrushin, L.S., "Efficiency of drawing in an ultrasonic field", Tsvet. Metally, 1967, (6), 75.

(75) Golubev, T.M., Dyadechko, G.P. and Khokhryakov, B.D. "A study of the vibrational drawing process" and Effect of vibration drawing on the quality of wire", Sb. Metallurgy i Gornorud. Prom. 1962 No. 3 pp 71-74 and No. 6 pp 56-59.

(76) Tarpley, W.B., and Kartluke, H. "Ultrasonic tube drawing. Niobium, Zircaloy-2, and copper", Rep. NYO 10008. Aeroprojects Inc., West Chester, Pa. Contract AT (30-1)-1836. Dec. 1961.

(77) Boyd, C.A., and Kartluke, H. "The application of ultrasonic energy in the deformation of metals", Defence Metals Information Centre, Battelle Memorial Institute, Columbus, Ohio, Rep. 187, Aug. 1963. Ed. A.R. Rosenfield.

(78) Severdenko, V.P., and Rexnikov, Yu. N. "Heating of pipes during drawing in an ultrasonic field", Doklady Akad, Nauk. B.S.S.R., 1966, 10(6), 388.

(79) Clauser, G.E., "Production tube drawing of metals using ultrasonic energy applied to the mandrel", A.S.M. Rep. No. C6-26, 4 (1966).

(80) Jones, J.B., "Ultrasonic Metal Deformation Processing", International Conference Manufacturing Tech. 1967, p. 983.

(81) Winsper, C.E., and Sansome, D.H., "Application of ultrasonic vibrations to the plug drawing of tube". Metal Forming, March 1971, 71.

(82) Jones, J.B. et al., "Ultrasonic energy applied to the aluminium cladding of tubes", Rep.

No. DP 418. Cont. No. AT(07-2)-1, Nov. 1959. Aeroprojects Inc. West Chester, Pa.

(83) Tarpley, W.B., "The application of ultrasonic energy in the deformation of metals", Defence Metals Information Centre, Battelle Memorial Inst., Colombus, Ohio, Rep. 187, Aug. 1963. Ed. A.R. Rosenfield.

(84) Tursunov, D.A. "Metal extrusion in an ultrasonic field", Kuznechno Shtamp. Proizv., 1964, (5), 10.

(85) Zalesskii, V.I. and Mishchenkov, Yu.I. "Choice of vibrational system for extrusion of lead in an ultrasonic field", Izv. V.U.Z. Chern. Met. 1969, 12(1), 116.

(86) Zalesskii, V.I., and Mendybaev, O.S. "Vibration extrusion using a hydroscrew vibrator", Izv. V.U.Z., Chern. Met., 1965, (1), 88.

(87) Zalesskii, V.I. and Mendybaev, O.S., "Extrusion based on forward flow with vibration", V.U.Z. Chern. Met., 1967, (11), 98.

(88) Spiers, R.M., et al., "Direct extrusion of metal with applied oscillatory energy", Metal Forming, Oct. 1969, p 271.

(89) McKaig, H.L., "The application of ultrasonic energy in the deformation of metals", Defence Metals Information Centre, Battelle Memorial Institute, Colombus, Ohio, Rep. 187, Aug. 1963, Ed. A.R.

Rosenfield.

(90) Cunningham, J.W., Westinghouse Elec. Corp. Pittsburg, Pa. Final Rep. Contract No. NOW64-0294-j, March 1966. (CFSTI AD-612-480P)

(91) Sorokin, N., "Certain aspects of sheet metal forming by stretching with vibrations", Nuznechno Shtamp. Prozv., 1966, 8(4), 23. Abs. in Machinery, 1967, 73(5), 143.

(92) Peacock, J. "Forming goes ultrasonic", Am. Machinist/Metalworking Manfn., Nov., 1961, 105, 83.

(93) Langenecker, B. et al., "Ultrasonics - an aid to metal forming, Metal Progress, April 1964, 85, 97.

(94) Kolsky, H., and Douch, L.S., "Experimental studies in plastic wave propogation", Jnl. Mech. Phys. Solids, 1962, 10, 195.

(95) A.I. Mikhenl'man, and Mashchinov, A.N. "Effect of ultrasonic vibrations on friction between solids", Russian Engineering Jnl., Vol. XLIX No. 1. pp 41-2, 1969.

(96) Petrenko, V.V. "Increasing the effectiveness of lubricants in the deformation of metals on an ultrasonic field". "Vopr. Porchnosti i Plastichn. Metallov". (Russian collection). pub. Nauka i Tekhn., Minsk 1968.

(97) Inoue, M., and Mori, E., "Ultrasonic metal wire drawing", 6th International congress on Acoustics, Tokyo, Japan, Aug. 21-28, 1968, pp k105-k108.

(98) Severdenko, V.P., and Reznikov, Yu. N. "A study of tube drawing in an ultrasonic field", Sbornik. Nauchn. Trudy Beloruss. Politekhn. Inst. 1968, (2) pp 183-184.

(99) Severdenko, V.P., and Reznikov, Yu. N. "How metal drawing is influenced by ultrasonic oscillation in different directions", Plast. i Obrabotka Met. Davelniem, 1966, pp 247-256.

(100) Verderevskii, V.A. et al. "Reduction of drawing force in the presence of ultrasound", Ul'trazvuk tekhn., 5, pp 18-21, 1964.

(101) Zartsev, V.S., Pavlov, I.M., and Burkhanov, S.F. "Geometrical conditions for vibrational rolling", Izvestiay V.U.Z. Chernaya Met. 1969, (5) pp 67-70.

(102) Burkhanov, S.F., Zaitsev, U.S., and Pavlov, I.M., "Specific pressure and torque on shafts of mill in vibrational rolling", Fizika i Khim. Obrobot. Mat. 1969, (6) pp 142-146.

(103) Rozner, A.G., "Effect of ultrasound on stresses during strip drawing", Rept. NOLTR 70-45, U.S. Naval Ordnance Laboratory, White Oak, Maryland, 6th March 1970.

(104) Young, M.J.R., Ph.D. Thesis. University of Aston in Birmingham, Dept. of Mech. Eng., 1972.

(105) Buckley, J. T., and Freeman, M. K. "Ultrasonic tube drawing", Ultrasonics, july 1970, pp pp152-158.

(106) Hoffman, O., and Sachs, G. "Introduction to the theory of plasticity for engineers". McGraw-Hill, New York, 1953.

(107) Baron, H.G., and Thompson, F.C. "Friction in wire drawing". Jnl. Inst. Metals, 1950-51, Vol. 78, p. 415.